EFFECT OF GLUTAMINE LIMITATION ON THE BEHAVIOR OF SP2/0-AG14 MOUSE HYBRIDOMA CELLS

by

Andréane Simone Chénier

A thesis submitted in partial fulfillment
of the requirements for the degree of
Doctor of Philosophy (PhD) in Biomolecular Sciences

The Faculty of Graduate Studies
Laurentian University
Sudbury, Ontario, Canada

© Andréane Simone Chénier, 2014

THESIS DEFENCE COMMITTEE/COMITÉ DE SOUTENANCE DE THÈSE
Laurentian Université/Université Laurentienne
Faculty of Graduate Studies/Faculté des études supérieures

Title of Thesis Titre de la thèse	EFFECT OF GLUTAMINE LIMITATION ON THE BEHAVIOR OF SP2/0-AG14 MOUSE HYBRIDOMA CELLS
Name of Candidate Nom du candidat	Chénier, Andréane Simone
Degree Diplôme	Doctor of Philosophy
Department/Program Département/Programme	Biomolecular Sciences
Date of Defence Date de la soutenance	December 16, 2014

APPROVED/APPROUVÉ

Thesis Examiners/Examinateurs de thèse:

Dr. Eric Gauthier
(Supervisor/Directeur de thèse)

Dr. Amadeo Parissenti
(Committee member/Membre du comité)

Dr. Tom Kovala
(Committee member/Membre du comité)

Dr. Richard Mosser
(External Examiner/Examinateur externe)

Dr. Crestina Beites
(Internal Examiner/Examinateur interne)

Approved for the Faculty of Graduate Studies
Approuvé pour la Faculté des études supérieures
Dr. David Lesbarrères
M. David Lesbarrères
Acting Dean, Faculty of Graduate Studies
Doyen intérimaire, Faculté des études supérieures

ACCESSIBILITY CLAUSE AND PERMISSION TO USE

I, **Andréane Simone Chénier**, hereby grant to Laurentian University and/or its agents the non-exclusive license to archive and make accessible my thesis, dissertation, or project report in whole or in part in all forms of media, now or for the duration of my copyright ownership. I retain all other ownership rights to the copyright of the thesis, dissertation or project report. I also reserve the right to use in future works (such as articles or books) all or part of this thesis, dissertation, or project report. I further agree that permission for copying of this thesis in any manner, in whole or in part, for scholarly purposes may be granted by the professor or professors who supervised my thesis work or, in their absence, by the Head of the Department in which my thesis work was done. It is understood that any copying or publication or use of this thesis or parts thereof for financial gain shall not be allowed without my written permission. It is also understood that this copy is being made available in this form by the authority of the copyright owner solely for the purpose of private study and research and may not be copied or reproduced except as permitted by the copyright laws without written authority from the copyright owner.

ABSTRACT

Cancer cells often display a dependence toward the amino acid L-glutamine for their survival, a phenomenon termed glutamine addiction. The mouse hybridoma Sp2/0-Ag14 (Sp2/0) undergoes rapid apoptotic cell death upon glutamine deprivation, making it a useful model for uncovering the molecular and cellular processes through which glutamine controls cell survival. This work was aimed at gaining a better understanding of the molecular and cellular events triggered when Sp2/0 cells are exposed to limiting amounts of glutamine.

First, the effect of glutamine limitation on Sp2/0 cell behavior was investigated. We found that a threshold concentration of 100 μM glutamine exists where Sp2/0 cell density does not increase, but cells remain viable. Under this threshold, Sp2/0 cells underwent apoptosis, but in a more protracted fashion than under conditions of acute glutamine deprivation. Unexpectedly, I found that exposure of Sp2/0 cells to 25μM glutamine triggered a biphasic activation of caspase-3. Interestingly, glutamine limitation, but not acute glutamine deprivation, was sufficient to maintain intact mitochondria for several hours and to trigger the expression of the stress-related transcription factor GADD-153. My results raise the possibility that glutamine limitation triggers a stress response which could enable Sp2/0 cells to adapt to its environment.

Using microscopic and biochemical techniques, I also provided evidence for a reduction in autophagic processes in Sp2/0 cells exposed to glutamine-limiting conditions. Chemical inhibitors of autophagy caused Sp2/0 cell death even in the presence of adequate supply of glutamine. On the other hand, rapamycin, a known activator of autophagy, improved Sp2/0 viability under glutamine limitation conditions. Therefore, the loss of Sp2/0 cell viability when

exposed to limiting amounts of glutamine could be the result, at least in part, of a reduction in the cell's autophagic capabilities.

Finally, I explored the effect of ammonium ions, a product of glutamine metabolism, on the behavior of Sp2/0 cells exposed to limiting amounts of glutamine. Ammonium ions treatment rescued Sp2/0 cell viability and proliferation in Sp2/0 cells cultured in glutamine-limiting conditions. Interestingly, ammonium acetate, but not ammonium chloride, caused a reduction in caspase-3 activity in Sp2/0 cells maintained under limiting glutamine conditions. Finally, my data suggest that ammonium salts led to a partial restoration of the autophagy process in Sp2/0 cells exposed to limiting amounts of glutamine, providing a potential explanation for the beneficial effect of ammonium ions on cell viability.

All together, the results obtained in the course my studies argue in favor of a mechanistic link between autophagy and ammonium ions in the modulation of the viability of a Sp2/0 cells exposed to glutamine-limiting conditions.

Keywords

Macroautophagy, autophagy, apoptosis, glutamine, cell signalling, survival, adaptation, molecular biology, ammonium.

CO-AUTHORSHIP STATEMENT

This thesis was written in its entirety by the author. Figures 3.4, 3.5. 3.7, 3.9, 3.11, 3.13 and 3.17 were contributed by Matt Mallory and figures 3.2 and 3.15 were contributed by Curtis C. Harnett.

ACKNOWLEDGMENTS

This work would not have been completed without the help of several people. Many thanks to my supervisor, Dr. Eric Gauthier for sharing his knowledge and expertise in all things scientific, and for providing guidance when experiments were not proceeding as planned. Thanks to Dr. Robert Lafrenie, for guidance and assistance with flow cytometry and microscopy. I would also acknowledge the assistance of my labmates in the Gauthier lab, Curtis Harnett, Abdelmuhsen Abusneina and Jenna Woodley as well as the labmates in the Lafrenie lab, Carly and Alison Buckner, without which much of this work would not have been possible.

TABLE OF CONTENTS

LIST OF FIGURES

LIST OF TABLES

LIST OF APPENDICES

LIST OF ABBREVIATIONS

AA: ammonium acetate

ACl: ammonium chloride

Acetyl-CoA: acetyl co-enzyme A

α-KG: α-ketoglutarate

ADP: adenosine 5' diphosphate

AMP: adenosine 5' monophosphate

AMPK: AMP-activated protein kinase

APAF-1: apoptosis protease-activating factor 1

APS: ammonium persulfate

ASK1: apoptosis signal-regulating kinase 1

Atg: autophagy related genes

ATP: adenosine 5' triphosphate

Bad: Bcl-2 antagonist of cell death

Bax: Bcl-2 associated X protein

Bak: Bcl-2 antagonist killer 1

Bcl-2: B-cell lymphoma 2

Bcl-x_L: Bcl-2-related gene, long isoform

BH: Bcl-2homology domain

BID: BH3-interacting domain

CB1: cannabinoid receptor 1

CDK1: cyclin-dependent kinase 1

DAPk: death-associated protein kinase 1

DISC: death-inducing signalling complex

DMSO: dimethyl sulfoxide

DNA: deoxyribonucleic acid

ER: endoplasmic reticulum

ERK: extracellular signal-regulated kinases

FADD: fas-associated death domain

FOXO: forkhead box O

GADD-153: growth arrest and DNA damage-inducible gene 153 (also known as CHOP-10 and DDIT-3)

GFAT: glutamine-fructose-6-phosphate amidotransferase

GlcNAc: N-acetylglucosamine

Gln: glutamine

GLS: glutaminase

GLS2: glutaminase-2

GOT1: cytoplasmic aspartate transaminase

GOT2: mitochondrial aspartate transaminase

GSH: glutathione

HSF-1: heat shock transcription factor-1

HSP70: heat shock protein 70

JNK: c-Jun N-terminal kinases

IκBα: inhibitor of NFκB

IL-2: interleukin-2

IMDM: Iscove's modified Dulbecco's medium

LC3: microtubule-associated light chain 3, also known as Atg-8

LDHA : lactose dehydrogenase A

LPS: lipopolysaccharide

MAP1B : microtubule-associated protein 1B

MAPK: mitogen activated protein kinase

MCL-1: myeloid cell leukemia 1

MnSOD: manganese superoxide dismutase

MOMP: mitochondrial outer membrane permeabilization

mTOR: mammalian target of rapamycin

mTORC1: mammalian target of rapamycin complex 1

mTORC2: mammalian target of rapamycin complex 2

NaA: sodium acetate

NAC: N-acetyl-L-cysteine

NAD^+: nicotinamide adenine dinucleotide oxidized

NADH: nicotinamide adenine dinucleotide, reduced

$NADP^+$: nicotinamide adenine dinucleotide phosphate, oxidized

NADPH: nicotinamide adenine dinucleotide phosphate, reduced

NFκB: nuclear factor κB

O-GlcNAc: O-linked β-N-acetyl-glucosamine

OMM: outer mitochondrial membrane

PDAC: pancreatic ductal adenocarcinoma

PERK: pancreatic eIF2α kinase

PI3K: phosphatidylinositol 3-kinase

PUMA: p53 upregulated modulator of apoptosis

Q: glutamine

Rheb: ras homologue enriched in brain

RNA: ribonucleic acid

ROS: reactive oxygen species

SCO2: synthesis of cytochrome C oxidase

SDS: sodium dodecyl sulfate

SIRT4: sirtuin-4

SMAC/Diablo: second mitochondria-derived activator of caspases/direct IAP binding protein with low pI

TCA: tricarboxylic acid cycle or citric acid cycle

Ulk1: serine/threonine-protein kinase encoded by *ULK1* gene, also known as Atg-1

Vps34: vacuolar protein sorting-34, Class III PI 3-kinase

Units of Measure

°C: degree Celcius

µg: microgram

µL: microlitre

µM: micromolar

x g: centrifugal force

h: hour

kDa: kilodalton

M: molar

mA: milliampere

MFI: mean fluorescence intensity

min: minute

mg: milligram

mL: millilitre

mM: millimolar

nm: nanometre

SD: standard deviation

U: International Unit of Enzyme Activity

1.0 — INTRODUCTION

1.1 — The Warburg Effect and Metabolic Reprogramming

In 1927, Otto Heinrich Warburg published "The metabolism of Tumors in the Body" describing the use of glucose fermentation to produce energy in cancer cells when compared to normal cells (1). The fermentation reaction was described as the formation of lactate from glucose in the presence of oxygen, a process we now call aerobic glycolysis. In 1956, his "On the Origins of Cancers" in the journal Science proposed that the underlying cause of cancers was defects in respiration and the increase in glucose fermentation which has since been dubbed the Warburg effect (2).

The Warburg effect can be defined as a preferential use of glycolysis to produce adenosine 5'-triphosphate (ATP) over oxidative phosphorylation, even under aerobic conditions. This increase in glycolysis is accompanied by higher glucose uptake, a high lactate production and a suppression of respiration (3). Warburg attributed impaired respiration to defective mitochondria. Contrary to the Warburg's speculations that cancer arose from a decrease or defect in mitochondrial metabolism, some cancers have normal or even increased mitochondrial function (4-6). Recent studies indicate that inactivating mutations in mitochondrial DNA or in Krebs cycle enzymes (encoded by the nuclear genome) could be in part responsible for the effect described by Warburg (7). One of the main reasons to increase glucose uptake in tumour genesis is its ability to generate biosynthetic precursors through glycolysis and the pentose phosphate shunt.

1.2 — Generation of Biosynthetic Precursors from Glucose

In resting differentiated cells, glucose metabolism is shuttled through the glycolytic pathway to produce 2 molecules of pyruvate per molecule of glucose in the cytoplasm. The produced pyruvate enters mitochondria and is shuttled through the tricarboxylic acid (TCA) cycle and oxidative phosphorylation to produce ATP, H_2O and CO_2 molecules. The cellular business of proliferation requires the duplication of the entire cellular contents, and glucose metabolism shifts accordingly. In these conditions, most of the pyruvate is kept in the cytosol and converted to lactate by the activity of lactate dehydrogenase (allowing the formation of NAD^+, which is essential to glycolysis), while a limited amount of pyruvate is converted to acetyl CoA and shuttled into the TCA to produce citrate, enabling its use in fatty acid synthesis in the cytosol (4, 8).

The produced lactate can be excreted from the cell, transported to the liver or kidneys where it can be reconverted into glucose, to the heart and skeletal muscle to be used as an oxidative metabolite, or be reconverted to pyruvate by vascular endothelial cells (9, 10). In proliferating cells, the production of lactate is essential. Interestingly, a study of the effects of lactate on cytotoxic T lymphocyte function reported that lactate in culture media could suppress proliferation and cytokine production by up to 95%, and decrease cytotoxic activity by 50%. This outcome would be desirable for tumour proliferation (11). Additionally, it was reported that lactate is used by glucose-deprived cancer cells as fuel and contributed to tumour angiogenesis by promoting the activation of the nuclear factor κB (NF-kB) pathway (12).

When a growth factor binds to its cognate tyrosine kinase receptor, it activates the PI3K-AKT pathway. This activation leads to an increase in glucose uptake by stimulation of glucose

transporters, stimulation of hexokinase to produce more glucose-6-phosphate, and stimulates phosphofructokinase to produce more glyceraldehyde-3-phosphate. Moreover, tyrosine kinase phosphorylation of pyruvate kinase inhibits this enzyme, preventing progression through the mitochondrial steps of glucose metabolism, and allows for the channelling of glucose metabolites into other pathways (see figure 1.1) (4, 13).

During anaerobic glycolysis, glucose metabolites are channelled to the pentose phosphate pathway in order to produce ribose-5-phosphate, a crucial precursor for nucleotide synthesis. In the oxidative arm of the pathway, 2 molecules of $NADP^+$ are reduced to NADPH, which provides the cell with the reductive potential essential for biosynthetic reactions. Ribose-5-phosphate is produced through the non-oxidative arm by combination of glyceraldehyde-3-phosphate, a glycolysis metabolite, to fructose-6-phosphate. Alternatively, fructose-6-phosphate is shuttled into the hexosamine pathway in order to produce UDP-N-acetylglucosamine, which is used to modify proteins by N-linked and O-linked glycosylation, allowing for proper folding of peptides (13-15).

In a study of several interleukin-3-dependent hematopoietic cell types, glucose deprivation led to a downregulation of growth factor receptor expression, decreased glutamine uptake, a depletion of TCA and cellular atrophy. The observed downregulation was reversed by restoration of the hexosamine biosynthetic pathway through addition of N-acetylglucosamine (GlcNAc), which permitted proper receptor folding, resulting in increased glutamine consumption and restored mitochondrial function (15).

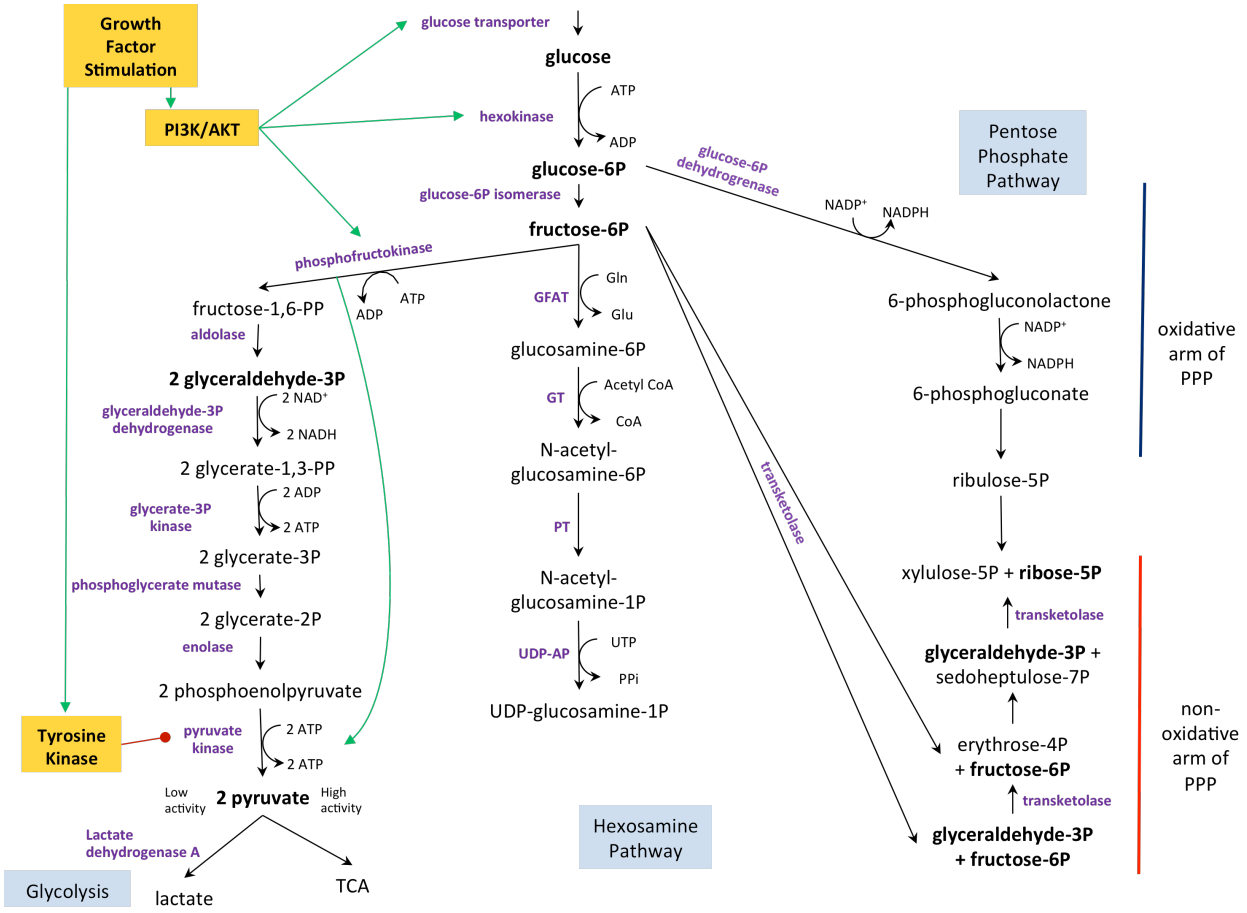

Figure 1.1 - Glucose Metabolism to Generate Metabolic Precursors

Glucose can be used to generate biosynthetic precursors and energy. In proliferating cells, glucose metabolites are diverted from glycolysis to the pentose phosphate pathway to generate ribose-5-phosphate, a critical molecule in the synthesis of nucleotides. Alternatively, glucose metabolites can be diverted to the hexosamine pathway which provides glycosylation molecules for post-translational modifications of proteins. The proliferative signals transduced (yellow box) are represented to indicate where their influence is directed in the glycolytic pathway. Enzymes appear in purple. A red arrow indicates an inhibitory effect while a green arrow indicates stimulation. Blue boxes indicate the metabolic pathway. Metabolites that are used in different metabolic pathways of glucose are represented in bold type. P: phosphate, GFAT: glutamine-fructose-6-phosphate aminotransferase, GT: glucosamine-6-phosphate N-acetyltransferase, PT: phosphoacetylglucosamine mutase, UDP: UDP-N-acetylglucosamine pyrophosphorylase.[1]

[1] Figure 1.1 adapted from Vander Heiden *et al* (4)

Over the last few decades, many reports have described the metabolic reprogramming responsible for the increase in the rate of conversion of glucose to lactate. Ras and Src cellular transformation are both associated with increases in glucose uptake, direct activation of lactose dehydrogenase A (LDHA), AKT-dependent increases in glucose uptake via the mobilization to the plasma membrane of glucose transporter and activation of hexokinase-2 to trap intracellular glucose (5, 16-21). The p53 tumour suppressor transactivates the SCO2 gene to allow the formation of the cytochrome c oxidase complex, a necessary component of oxidative phosphorylation. If either p53 or SCO2 function is lost, as observed in many tumour types, the cell is reprogrammed to use aerobic glycolysis (22).

While glycolytic metabolites are being diverted away from the TCA, there is another substrate that can also be used to fuel proliferation and provide macromolecule building blocks: glutamine.

1.3 — Glutamine

Glutamine is one of the 20 standard amino acids used for protein synthesis and has many diverse functions in the cell. The intracellular concentration of glutamine varies by cell type and ranges from 2 to 20 mM. Its serum concentration in humans averages 0.7 mM. At a neutral pH, it is found in its zwitterion form (23). As skeletal muscles can synthesize glutamine, it is not an essential amino acid. However, in times of stress, such as illness, surgery and exercise, glutamine becomes conditionally essential (24, 25). It has been postulated that the release of glutamine into the extracellular space could act as a stress signal, activating signalling pathways necessary for cellular protection and immune regulation (26).

Glutamine uptake into cells triggers swelling, a process that has been linked to the presence of ammonium ions generated during glutaminolysis (discussed below) (27). This may be the trigger to regulate some anabolic pathways, such as the synthesis of proteins, of DNA and RNA(28). Cell swelling has also been linked to pro-inflammatory cytokines IL-6 and TNF-α (29), two cytokines known to be affected by glutamine levels (23, 30-32). In these reports, the presence of glutamine decreased the secretion of these cytokines. Conversely, glutamine deprivation has been reported to cause cell shrinking, which was followed by apoptosis (33, 34).

1.4 — Glutamine as an Energy Source

Glutamine can be used as a source of energy in many different cell types (35, 36). While glucose metabolites are being redirected to the synthesis of membranes, nucleotides and amino acids, which require more carbon and NADPH than ATP, glutamine can be used to supplement the TCA cycle (4) (see figure 1.2).

Glutamine enters the cell via glutamine transporters and can enter the TCA cycle after deamination to glutamate by glutaminase (GLS) before being shuttled into mitochondria, where glutamate is converted into α-ketoglutarate (α-KG) by glutamate dehydrogenase. The released amine groups are protonated to form ammonium ions (37). Once in the TCA cycle, glutamine (as α-KG) can have different metabolic fates. In enterocytes, it is metabolized to L-alanine by its conversion to malate which is used by malic enzyme to form pyruvate. The latter is then used in transamination reactions to synthesize L-alanine. There are alternatives in other cell types or cell states: the produced pyruvate can be converted to lactate and released from mitochondria as waste, glutamine can be shuttled into the TCA cycle to produce citrate for lipid synthesis, to

produce acetyl-coA for amino acid synthesis or for complete oxidation (23). In the cytosol, glutamine can also be used to generate glycosylation molecules through the hexosamine pathway (see figure 1.1) (10).

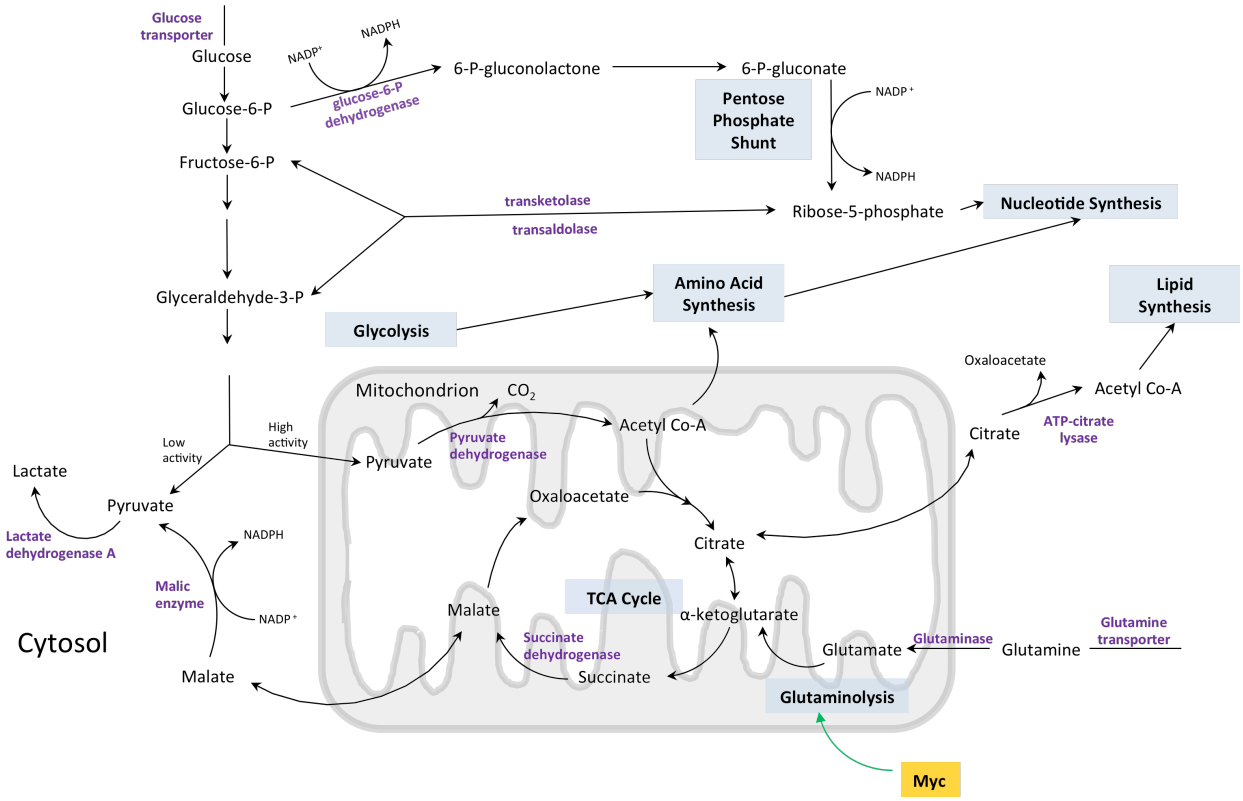

Figure 1.2 - Interplay of Metabolic Pathways in Proliferating Cells

This schematic illustrates the interplay between glucose and glutamine metabolism by depicting their interactions in various cellular pathways necessary to proliferating cells including glycolysis, oxidative phosphorylation, the pentose phosphate pathway and glutaminolysis as currently understood. The Myc oncogene (yellow box) increases the rate of glutaminolysis. Important metabolic processes are in blue boxes, and critical enzymes controlling them in purple[2].

Therefore, both glucose and glutamine can be converted into lactate and used to generate biosynthetic precursors. A recent report showed that the glutamine consumed by proliferating cells was metabolized and accounted for as much 90% of the lactate and 60% of the alanine

[2] Figure 1.2 adapted from Vander Heiden *et al* (4).

produced (38). This research group reported that glutamine metabolism alone was sufficient to fulfill the metabolic requirements for NADPH for fatty acid synthesis and to sustain the levels of oxaloacetate needed to fuel the TCA cycle. They also concluded that since ammonium ions and alanine, along with lactate, were secreted from the cell as waste, the rate of glutamine catabolism was not driven solely by the need to synthesize nucleotides or amino acids. Rather, glutamine metabolism was used as a carbon source (38). It must be considered that cells that are producing lactate and excreting it stimulate the expression of CD44 and the production of its glycosaminoglycan ligand, hyaluronan. Upon ligand binding to CD44, cells decrease their attachment to the extracellular matrix, allowing them to move (39). Also, the excretion of lactate to the extracellular matrix suppresses cytotoxic T cell proliferation and cytokine production and is therefore immune suppressive (11, 40).

1.5 — Glutamine in Proliferating Cells

The importance of L-glutamine in the process of cell proliferation has been known since Harry Eagle's seminal work was published in 1955 in the journal *Science* (41). Glutamine intake is high in cells with a high rate of division such as enterocytes, lymphocytes in clonal expansion and some types of tumour cells (42-46). Glutamine has also been shown to activate protein kinase A (PKA) and mammalian target of rapamycin (mTOR), two kinases that are important in cell proliferation (47). mTOR, when combined with Raptor and mLST8, form the mammalian target of rapamycin complex 1 (mTORC1); this complex controls cells growth and the uptake of nutrients. The activation of mTORC1 is a molecular switch, turning on anabolic processes like glucose uptake, glycolysis, the pentose phosphate pathway and *de novo* synthesis of lipids, while

turning off catabolic processes, including autophagy. A deregulation in mTORC1 activation is frequently observed in cancer and would result in the observed Warburg effect (48).

Glutamine is utilized as a precursor for the synthesis of molecules such as proteins, nucleic acids, amino sugars, and GSH (23, 28). In one study, the supplementation of Caco-2 cells with glutamine but not glutamate stimulated proliferation and nucleotide synthesis. Interestingly, these investigators also showed that this effect was not the result of the use of glutamine as an energy source (28). Another report specifically followed the metabolism of glutamine in proliferation. They also concluded that glutamine was used as a carbon source as ammonia and alanine were excreted from the cell as waste; the rate of glutamine catabolism was not driven solely by the need to synthesize nucleotides or amino acids (38). When one compares the chemical structures of glutamine and glutamate, one can notice that deamination of glutamine yields glutamate; therefore, the amine group of glutamine appeared to be critical.

There is growing evidence that glutamine is a key molecule in several types of tumours, many with quite dismal prognoses, and withdrawal of this amino acid induced apoptosis in intestinal epithelial, neuronal and lymphoid cells (6, 34, 49-53). One proposed mechanism for this glutamine dependence has been linked to the overexpression of the oncogene c-Myc (aka Myc) (50, 52, 54).

Myc expression is associated with the modulation of diverse cellular processes, including cell growth, proliferation and energy metabolism, stimulating cell growth while inhibiting the arrest of the cell cycle (55). Myc is a transcription factor driving proliferation first discovered in Burkitt's lymphoma (56). Activation of Myc in a human B cell model resulted in increased mitochondrial respiration and biogenesis, and when Myc activity is sustained at an elevated rate,

it is associated with increases in reactive oxygen species (ROS) levels (19, 22, 57, 58). In a recent report examining the different gene products expressed between Myc-high and Myc-low B cell lines, mitochondrial GLS as well as glutamine transporters were highly expressed in the Myc-high B cell line (52, 54, 59). In myeloma cell lines, the myc gene is found to be translocated to the immunoglobulin locus, making it highly expressed (60). Myc-driven proliferation has been shown to render cells extremely sensitive to the levels of available glutamine, rendering them "addicted" to this amino acid. Glutamine withdrawal in Myc-transformed cells has been reported to result in rapid cell death (50, 52, 54, 59).

Recently, it was reported that mTORC1 could stimulate glutamine metabolism by repressing mitochondrial sirtuin-4 (SIRT4). SIRT4 represses glutamine metabolism by inhibiting the activity of glutamate dehydrogenase by ADP-ribosylation (61). SIRT4 has also been linked to the DNA damage response by inhibiting glutamine metabolism, and loss of SIRT4 has been linked to tumour development, particularly in tumour types that are reprogrammed to glutamine addiction, such as Myc-transformed cells (61-63).

Proliferating cells need to synthesize lipids to form the plasma membrane. While convention holds that acetyl-CoA generated from glucose-produced pyruvate is the primary source of carbon for lipid synthesis (64, 65), other reports have shown that glutamine, via α-KG and malate, can produce pyruvate to be used for lipogenesis, or that reductive glutamine metabolism by isocitrate dehydrogenase-1 can generate the required acetyl-CoA (38, 66-70).

Glutamine has traditionally been seen as a building block for the production of macromolecules or as fuel, but its importance in normal cell function goes beyond these narrowly defined roles: the presence of glutamine and its metabolites can signal the cell to alter

its behaviour. Conversely, the absence of glutamine can also have profound effects: glutamine's absence can trigger cell death.

1.6 — Glutamine Metabolism Can Modulate Signalling Pathways

The presence or absence of available glutamine can influence cell behaviour, which will vary according to cell type and function (its pro-survival role will be discussed further in a separate section). For example, it has been reported that glutamine can stimulate or inhibit autophagy depending on the cell type. Interestingly, in co-culture experiments with fibroblasts and MCF7 cells, glutamine increased autophagy markers in the fibroblasts, but downregulated those same markers in MCF-7 cells while protecting them from apoptosis (71). In a recent report on human pancreatic ductal adenocarcinoma (PDAC) cells where KRAS reprogrammed metabolism, a non-canonical metabolism of glutamine was described. PDAC tumours are very aggressive, resistant to therapy and respond to changes in the levels of glutamine. In PDAC cells, ^{13}C-labelled glutamine was traced through its metabolism. Interestingly, the majority of aspartate (50-75%) was labelled indicating that glutamine was the carbon source. In PDAC cells deprived of glutamine, an accumulation of ROS, of GSH disulfide and a concomitant loss of growth were observed. α-KG supplementation alone did not rescue growth in PDAC cells deprived of glutamine, but a mixture of α-KG and non-essential amino acids derived from glutamine metabolism did. Inhibition of either cytoplasmic aspartate transaminase (GOT1) or the mitochondrial aspartate transaminase (GOT2) was identified as being critical to glutamine metabolism, rather than glutamate dehydrogenase (see figure 1.3). GOT1 catalyzes the conversion of aspartate and α-KG into oxaloacetate and glutamine in the cytoplasm. The reverse

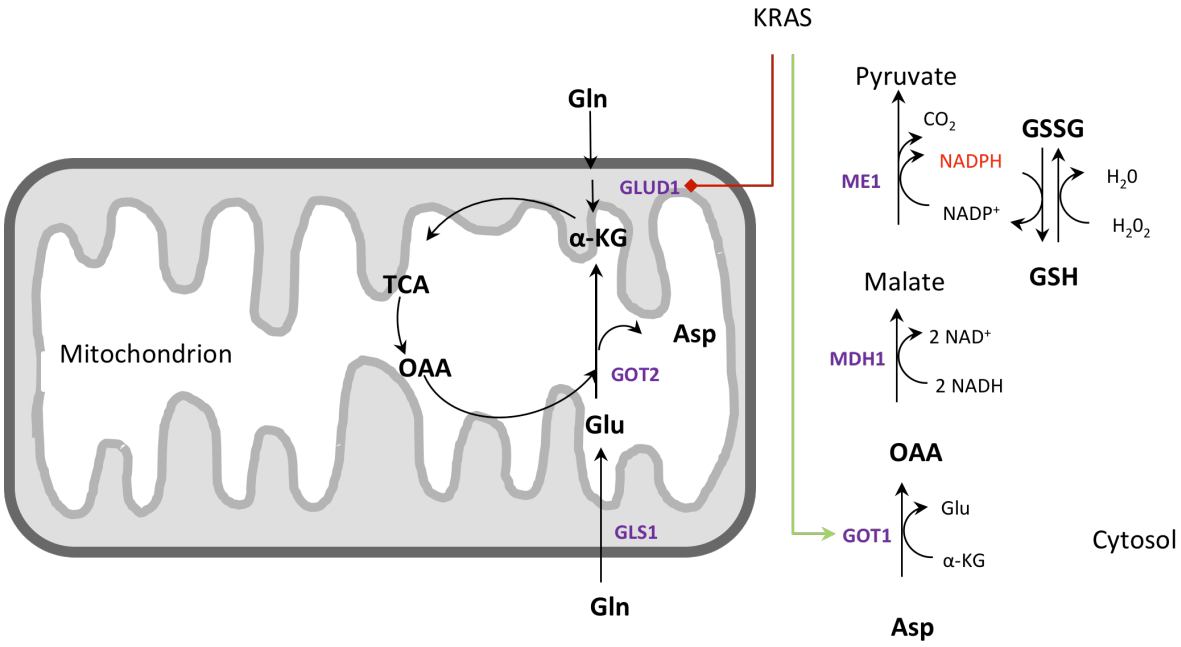

Figure 1.3 - Non-Canonical Metabolism of Glutamine by KRAS Reprogramming

This figure depicts the reprogramming of glutamine metabolism by KRAS in PDAC cells to render them sensitive to glutamine levels. In these aggressive tumour cells, glutamine is converted to aspartate in the mitochondrion, exported to the cytoplasm and then metabolized to pyruvate to produce redox potential and remove reactive oxygen species. KRAS reprogramming stimulates the need for aspartate by upregulating the expression of GOT1 and downregulating the expression of GLUD1. Enzymes are depicted in purple. GLS1: glutaminase, GOT1 cytoplasmic aspartate deaminase 1, GOT2: mitochondrial aspartate deaminase 2, GLUD1: glutamate dehydrogenase, MDH1: malate dehydrogenase, ME1: malic enzyme, GSH: glutathione, GSSG: glutathione disulfide, OAA: oxaloacetate, α-KG: α-ketoglutarate[3].

reaction is catalyzed by GOT2. KRAS reprogramming of glutamine metabolism saw glutamine being converted into aspartate, exported to the cytoplasm, reconverted to glutamine and metabolized to pyruvate to produce NADPH, thus providing PDAC cells with redox potential to deal with ROS via GSH (72). Glutamine also contributes to the redox potential of cells in the synthesis of GSH. GSH is a tri-peptide formed from glutamine-derived glutamate, glycine and cysteine which is oxidized by hydrogen peroxide to form water and glutathione disulfide (73).

[3] Figure 1.3 adapted from Son *et al* (72).

Glutamine can also modulate inflammatory responses. NF-κB is a transcription factor that is involved in the expression of genes in inflammatory responses and glutamine's anti-inflammatory effects in intestinal mucosa had been reported to be mediated via this transcription factor. In intestinal cells, glutamine has been shown to reduce protein degradation mediated by the ubiquitin-proteasome system. Ubiquitin is a small protein that is used to modify proteins after translation and can have differential effects, from tagging proteins for degradation by the proteasome to modulating intracellular sorting. The outcome of ubiquitylation is dictated by the location of ubiquitylation, the length of the ubiquitin chain, and the level of its branching (74). In a study of intestinal cell lines, glutamine treatment was associated with a decrease in the ubiquitylation of the inhibitor of NF-κB (IκBα) leading to a decrease in the expression of pro-inflammatory interleukin-8 in HCT-8 cells without affecting ubiquitin levels or proteasomal activity (31). Conversely, glutamine treatment of Caco-2 cells lead to the proteasomal degradation of NF-κB via activation of the p38 MAPK (75). In a study performed on biopsies taken from human duodenal mucosa, an infusion of glutamine was shown to have affected the ubiquitylation of proteins, among them Grp75, involved in anti-inflammatory responses, and of heat shock protein 74, a protein indirectly regulating cell survival and proliferation in periods of stress (76).

Glutamine can provide cells with the ability to respond to stress. Heat shock proteins are a group of conserved proteins that are expressed to allow cells to adapt to stress conditions such as heat shock. They mediate this adaptation response by aiding in protein refolding and by preventing the aggregation of proteins in the cytoplasm. The transcription of key heat shock proteins is regulated by heat shock transcription factor-1 (HSF1). Glutamine has been reported to

upregulate the expression of HSF1, increase its transactivation and heat shock protein expression (77).

One of two glutaminase isoforms, glutaminase-2 (GLS2), is regulated by p53 in response to oxidative stress or DNA damage. In response to DNA damage caused by DNA oxidation, p53 upregulated the expression of GLS2, to facilitate glutamine metabolism and the synthesis of GSH to allow cells to recover from repairable genotoxic stress (78). In neuronal differentiation, glutaminase has been shown to play a crucial role in neuronal differentiation. A p53 family member, p73, was shown to be essential to GLS2 expression during neuronal differentiation, with GLS2 playing a part in the regulation of glutamate synthesis, a crucial neurotransmitter (79). This fact is made relevant when one considers reports that glutamine, not glutamate, can stimulate proliferation and nucleotide synthesis. That effect does not depend on glutamine being used strictly for the generation of energy or nucleotide synthesis, since alanine and ammonia were excreted. This indicates that the amine moiety had a specific role (28) and that glutamine was used as the main carbon source (38). Additionally, cell death in long-standing glutamine free cultures could be rescued with the addition of ammonia by stimulating anabolic pathways and that glutamine's amine moiety was required for proliferation of tumour cells, not just as a source of carbon (80).

The enzyme glutamate dehydrogenase, which catalyzes the conversion of glutamate to α-KG, has been shown to inhibit autophagy by stimulation of mTOR in HeLa cells (81). Leucine, which is taken up by cells when glutamine is effluxed, is a most potent stimulator of mTORC1 and autophagy inhibitor in HeLa, U2OS and MCF-7 cells (82-84). As glutamine is a non-essential amino acid, its accumulation within the cell acts as a signal that nutrients are plentiful and that proliferation can be sustained, signalling the cell to take up essential amino acids such as

leucine. The predominant model states that mTORC1 activity in nutrient-rich conditions is recruited to the lysosomal membrane where it interacts with Rheb to form a complex with RAG GTPases that are activated by the presence of amino acids. This complex allows the activation of mTORC1 and prevents the autophagy initiation complex from being formed by phosphorylating ULK1 on S757 (83, 85-87). During amino acid starvation, mTORC1 activity is inhibited by phosphorylation by several kinases, such as AKT, AMPK, and results in cell cycle arrest in G1 (86, 88, 89). In the presence of ROS, phosphatase 2A associates with its B55α subunit to activate p53 and inhibit mTOR, promoting cell survival and proliferation in low glutamine concentrations (90). In rapidly proliferating cells that are increasing their uptake of glutamine from the extracellular space (like in Myc-transformed cells), it is possible that glutamine is deaminated before it can be effluxed as it would be in nutrient-rich conditions of non-proliferating cells. This mTOR-independent pathway may be more important in cell populations that are rapidly undergoing proliferation and cannot be solely dependent on *de novo* synthesis of macromolecules. There is evidence for this with the observation that amino acid deprivation induced autophagy in an ULK1/2-dependent manner, but that rising levels of ammonia arising from increased glutaminolysis in glucose deprivation was ULK1/2 independent (91, 92).

In illness, such as sepsis or bacterial infections, the administration of glutamine was shown to improve clinical outcomes (26, 93, 94). In rat macrophages treated with lipopolysaccharide (LPS), a bacterial product known to induce inflammatory responses in septic shock, glutamine treatment minimized the inflammatory response by dephosphorylating p38 and JNK both *in vitro* and *in vivo*. Glutamine elicited this response in a matter of minutes, and effected the response in an ERK-dependent activation of MAP kinase phosphatase-1 (95). In rat cardiomyocytes treated with LPS, glutamine treatment attenuated LPS-induced LDH

upregulation and upregulated the levels of O-linked β-N-acetylglucosamine (O-GlcNAc), a post-translational modification involved in stress response and signal transduction. Glutamine, flowing through the hexosamine pathway (see figure 1.1), provides the amino moiety in the formation of glucosamine-6-phosphate, which is then metabolised to UDP-N-acetyl-glucosamine, the obligatory substrate for O-GlcAc (96). Glutamine treatment increased the endonuclear HSF-1 expression and transcription activity, which increases the expression of heat shock proteins (77). Furthermore, glutamine induced heat shock protein 70 (HSP70) and glutathione (GSH) expression to alleviate damage to cardiomyocytes and preserve cardiac function in LPS-treated rats (96-99). The successful clearance of infection requires that an inflammatory response be activated and robust. However, sepsis tells us that too much inflammation can cause more damage than the initial infection, leading to the death of the patient (26, 94). The inflammatory response must be kept in balance to ensure that there is enough response to be effective, but not so robust as to cause damage. Glutamine provides that balance by activating signalling pathways responsible for the attenuation of the inflammatory response.

1.7 —Apoptosis and Its Regulation by Glutamine

1.7.1 — Apoptosis

Apoptosis is a form of programmed cell death mediated by caspases and characterized by the orderly dismantling of the cellular content, cleavage of DNA and formation of apoptotic bodies which are cleared by neighbouring cells without triggering inflammatory responses (100). Apoptosis can be triggered by signals external to the cell (extrinsic pathway) or by cellular signalling from within (intrinsic pathway) (see figure 1.4).

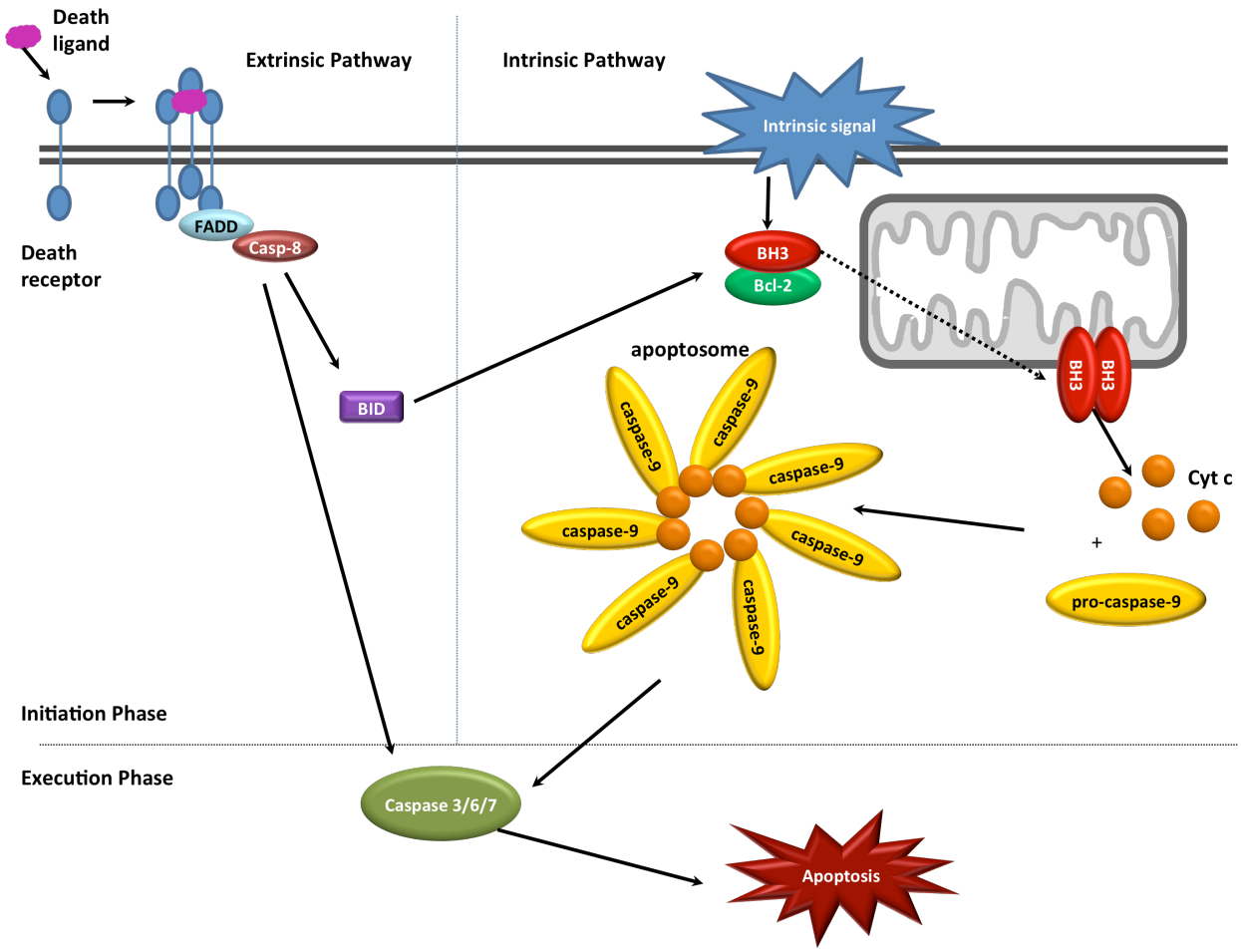

Figure 1.4 - The Apoptotic Pathways

Basic depiction of the apoptotic pathways. On the right is the intrinsic apoptotic pathway. Upon receiving a distress signal from within the cell, for example GADD-153, pro-apoptotic Bcl-2 family members (BH3, red) are dissociated from their anti-apoptotic Bcl-2 family members (Bcl-2, green), and permeabilize the mitochondrial outer membrane, allowing factors like cytochrome c (Cyt c, green) to escape into the cytoplasm. Cytochrome c associates with pro-caspase-9 (initiator caspase, yellow) to form the apoptosome. Once activated, the apoptosome can cleave and activate effector caspases (caspase 3/6/7, grey) to effect the apoptotic phenotype. On the left is the extrinsic apoptotic pathway. This pathway is typically triggered by a death ligand (fushia) binding to its cognate death receptor (blue), causing receptor clustering and recruitment of adaptor proteins (FADD, light blue) and caspase-8 (initiator caspase, orange). Once activated, caspase-8 can activate effector caspases and can cleave BID, to initiate the intrinsic pathway of apoptosis[4].

[4] Figure 1.4 adapted from Franco *et al* (73).

In a brief description of the extrinsic pathway, a death ligand will bind to its cognate death receptor and trigger receptor oligomerization, which in turn recruits adapter proteins such Fas-associated protein with death domain (FADD). The adapter proteins in turn recruit the pro-caspase-8. At this point, the death-inducing signalling complex (DISC) is formed, which auto-catalytically activates caspase-8. Activated caspase-8 will then cleave and activate caspase-3 and BH3-interacting domain (BID). BID cleavage will activate the intrinsic apoptotic pathway (101).

The intrinsic pathway of apoptosis receives stress signals such as DNA damage from within the cell and is triggered at the mitochondria. These stress signals induce mitochondrial outer-membrane permeabilization (MOMP) which allows the release of cytochrome c and SMAC/Diablo from the intermembrane space to the cytoplasm. Cytochrome c associates with apoptosis protease-activating factor 1 (APAF-1) causing oligomerization to form the apoptosome, which binds and activates caspase-9. Activated caspase-9 in turn cleaves and activates the effector caspase-3 and -7 which elicit the apoptotic phenotype by proteolytic cleavage of their targets (102).

The B-cell lymphoma 2 (Bcl-2) family of proteins plays a central role in apoptosis regulation. Bcl-2 family members can be either pro- or anti-apoptotic, and are characterized by the presence of at least one of four Bcl-2 homology (BH) domains (see table 1) (103). The anti-apoptotic members of the Bcl-2 family contain four BH domains (BH1-4). Major members of the anti-apoptotic group include Bcl-2, Bcl-2-related gene, long isoform (Bcl-x_L), and myeloid cell leukemia 1 (MCL-1). The anti-apoptotic Bcl-2 proteins preserve the integrity of the outer-member of the mitochondria by inhibiting the activity of some of the pro-apoptotic Bcl-2 proteins. The pro-apoptosis members of the Bcl-2 family can be subdivided into 2 groups: 1) the effector proteins that oligomerize at the mitochondrial outer membrane to cause MOMP, and

which include Bcl-2 antagonist killer 1 (BAK) and Bcl-2-associated x protein (Bax), and 2) the BH3-only proteins which can interact with the anti-apoptotic proteins and sensitize cells to apoptosis, like Bcl-2 antagonist of cell death (Bad), and those that can interact with either the anti-apoptotic and the effector Bcl-2 family proteins to induce apoptosis, such as Bcl-2-interacting mediator of cell death (BIM) (102, 104). Some of these Bcl-2 proteins (Mcl-1 and Bcl-x_L) have a proline, glutamic acid, serine and threonine-rich (PEST) sequence, which targets proteins for degradation either by caspases or by proteosomal degradation (105). In the case of Bcl-x_L, the PEST sequence is revealed by deamination (106). However, a recent report in Mcl-1, which contains BH1-3 domains, identified the F3 peptide sequence within the BH1 domain as being required for protein degradation, not the PEST sequence (107).

Table 1 – Comparison of Bcl-2 Protein Structures

	Domains Present	**Protein Name**
Anti-Apoptotic, multi-domain	BH4, BH3 BH1, BH2, TM (PEST•)	Bcl-2, Bcl-x_L•, MCL-1•, Bcl-w, Bfl-1, Bcl-B, A1
Pro-Apoptotic, multi-domain,	BH3, BH1, BH2, TM	Bax, Bak, Bok
Pro-Apoptotic, BH3-only	BH3 (TM*)	Bad, BID, Bim, Puma, Gad, Noxa, Hrk, Bik, Bfm, Bcl-G, Spike, Bcl-X_S

•PEST domain-containing protein* Some BH3-only proteins do not have trans-membrane domains. TM: trans-membrane domain. BH: Bcl-2homology domain, MOM: mitochondrial outer membrane, PEST: proline, glutamic acid, serine, threonine-rich sequence. [5]

The translocation of Bax to mitochondria, the release of cytochrome c and SMAC/Diablo to the cytosol and the subsequent caspase-9 activation are cardinal events of the intrinsic apoptotic pathway, which can be triggered by glutamine deprivation (52, 53, 109-111).

[5] Table 1 adapted from Yip *et al*, Chipuk *et al*, Dho *et al* and Garcia-Saez *et al* (102, 104, 106, 108).

1.7.2 — Glutamine Regulation of Apoptosis

Glutamine has been shown to act as a signalling molecule in the regulation of apoptosis. As nutrients are being metabolized within a cell, ROS are being generated as a by-product. In order to counter the noxious effects of these reactive molecules, antioxidants are found within the cell to reduce ROS. Some of these antioxidants, such as GSH, which are regulated by the availability of glutamine. Another such molecule is manganese superoxide dismutase (MnSOD), which resides in the mitochondrial matrix. MnSOD catalyzed the conversion of superoxide (O_2^-) to peroxide (H_2O_2), which can then be reduced to water by GSH (112). In a recent report, Aiken et al showed that in essential amino acid deprivation, histidine depletion induced MnSOD expression, but only in the presence of millimolar levels of glutamine. They further demonstrated that these amino acids mediated their effects by signalling through the mTOR and MEK/ERK pathways and metabolic flux through the TCA was required, as was mitochondrial membrane potential, but that ATP was not concomitantly required, indicating that the requirement for these amino acids was not strictly based on the production of energy (109).

In periods of stress, glutamine can have protective effects against stress-induced apoptosis. In rats after a 1h session of exercise, collected neutrophils had increased expression of p53 and caspase-3, and a higher level of phosphorylated p38 MAPK and JNK were detected when compared to controls. However, if the rats were fed glutamine prior to that session of exercise, there was only a partial upregulation of p38 and JNK phosphorylation and p53 expression, and no increase in caspase-3 expression, indicating that glutamine provided some protection to exercise-induced apoptosis (113).

In HeLa cells deprived of glutamine, apoptosis could be induced by Fas ligation of its cognate receptor via the extrinsic apoptotic pathway (see figure 1.4), but not in normal cells. Fas ligation triggered apoptosis by activating apoptosis signal-regulating kinase 1 (ASK1) and JNK. Mechanistically, the suppression of Fas-mediated apoptosis by glutamine was mediated by the binding and inhibition of ASK1 by glutaminyl-tRNA synthetase. The interaction between ASK1 by glutaminyl-tRNA synthetase was increased by the availability of glutamine (114). Interestingly, in leukemia-derived HL-60 and CEM cells deprived of glutamine, the resulting cell shrinkage caused the clustering of CD95 receptors, activating the extrinsic pathway in the absence of ligand binding (34).

In brain tissues, there exists a delicate balance between glutamine and glutamate. Excess glutamate or ammonium (derived from glutaminolysis) have been shown to induce apoptosis, so synthesis of glutamine to remove these metabolites from the extracellular space is desirable (115). However, excess glutaminolysis within mitochondria leads to the induction of the intrinsic apoptotic pathway, caspase-9 and -3 activation and nuclear fragmentation (116).

1.8 — Autophagy and Its Regulation by Glutamine

1.8.1 — The Molecular and Cellular Basis of Autophagy

Autophagy is a process whereby cellular components are delivered to lysosomes to be degraded into their basic constituents (amino acids, nucleotides, etc.), which are recycled by the cell. There are 3 types of autophagy which can be differentiated by the substrates they degrade: chaperon-mediated autophagy (proteins that contain a KFERQ motif), microautophagy (using lysosomal membranes, targets specific organelles and portions of the cytosol) and

macroautophagy (using autolysomal membranes, targets mitochondria, ER, lipids, carbohydrates, ribosomes, peroxisomes and protein aggregates) (117, 118). The latter is the focus of this section and will be hereafter referred to as autophagy.

While autophagy was originally classified as a type of cell death, it is now regarded as a survival response which can sometimes lead to cell death (119). Autophagy has been implicated in a wide range of cellular processes, from the degradation of bacteria, protein aggregates or aberrant organelles to homeostasis maintenance to anti-tumourigenesis (120-123). The degradation products are shuttled back to the cytoplasm and recycled into other macromolecules or metabolized; this is especially useful when cells are under conditions of stress from infection, hypoxia or starvation (124).

The molecular machinery used in autophagy was identified in yeast using mutations of the autophagy related genes (Atg). There are 31 Atg genes, which are highly conserved in eukaryotes. Of those 31 Atg genes, 18 are considered to encode core proteins of the autophagic machinery, and they can be further subdivided into four different groups: the Atg1/unc51-like kinases (ULK) with their regulators, Vps34/class III PI3K complex I; the Atg9/mAtg9 cycling complex; and the ubiquitin-like systems of Atg12 and Atg8 (124). For clarity, the mammalian autophagy nomenclature will be used from this point on.

The current model of autophagy can be described in five steps which are depicted in figure 1.5: 1) the initiation of phagophore formation (Vps34-Beclin-1 and Atg-13, Atg-17 and Atg-1 kinase/Ulk1) at or near the ER (125, 126); 2) the ubiquitin-like conjugation of Atg-5 to Atg-12; 3) the ubiquitin-like conjugation of phosphatidylethanolamine (PE) to LC3B-I to form

LC3B-II; 4) cargo selection; and 5) the fusion of the autophagosome to lysosomes and the degradation of its content (119, 127, 128).

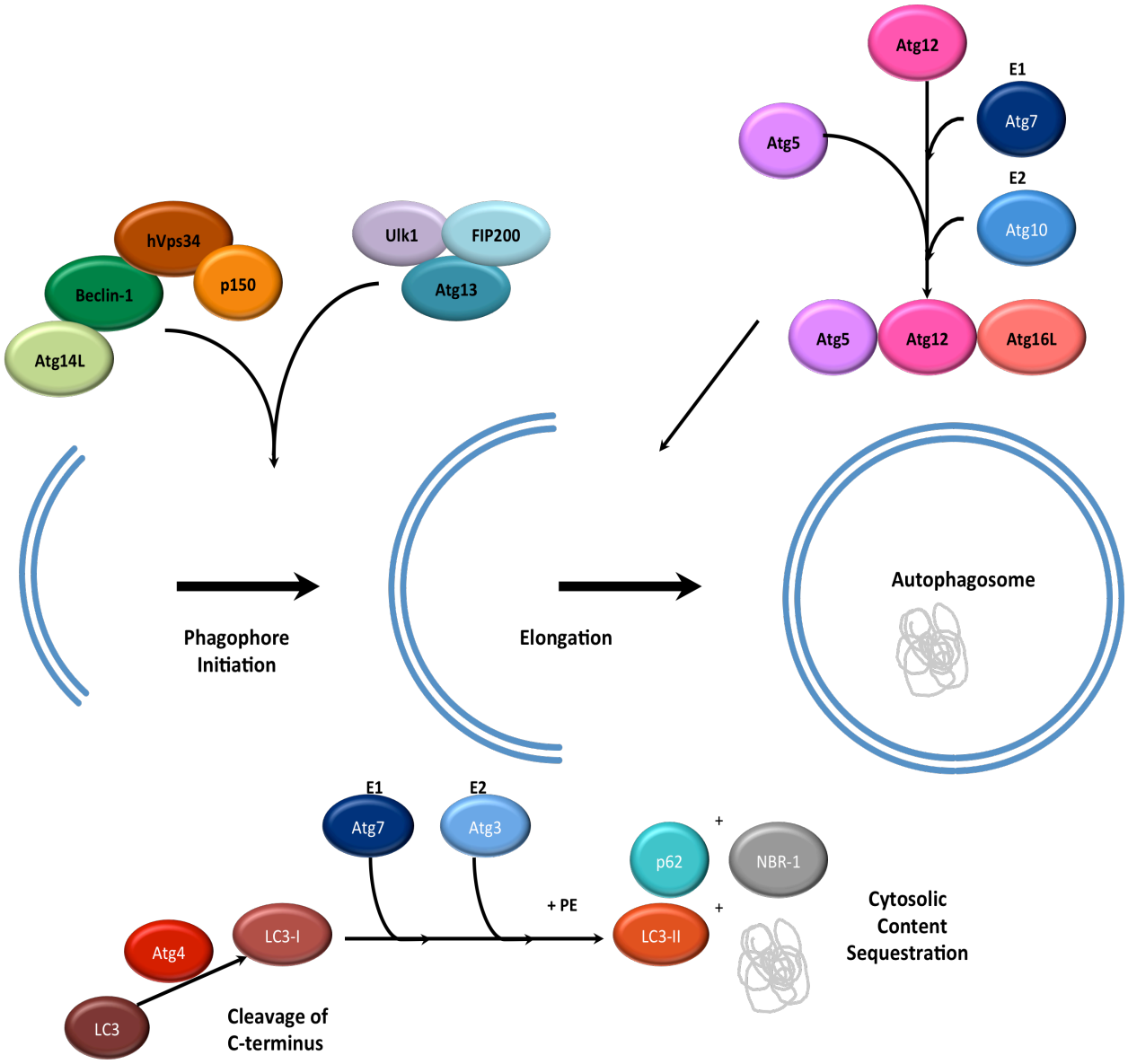

Figure 1.5 - Autophagosome Formation

This figure provides a visual representation of the autophagosome formation, closed and loaded with cargo. The molecular pathways are presented in the context of their place in the autophagosome formation[6].

[6] Figure 1.5 adapted from Glick *et al* (119).

Since the first identification of autophagosomal structures in the 1960s, there has been much debate as to the origins of the membranes used to construct autophagosomes with no definitive answer to date. There are two current models: the first model postulates that the membranes are sourced from pre-existing organelle membranes (129), while the second model postulates *de novo* formation of autophagosomal membranes (130). Some of the organelles that have been reported to provide membranes for the formation of autophagosomes are the ER, mitochondria, endosomes, the plasma membrane and the Golgi apparatus (129-134).

In order for cargo included in autophagosomes to be degraded, the latter must fuse to lysosomes or endosomes to produce the degradative autolysosomes. Once in the autolysosomes, the cargo is degraded by proteolysis and acidification (135). The presence of proteases such as cathepsins L, B and D, is critical to the proper turnover of autolysosomal contents and termination of autophagy. In mouse models deficient in either cathepsin D or L/B, severe neurodegenerative diseases were observed (136).

1.8.2 — Autophagy Regulation by Amino Acid Availability

Cells exist in a delicate balance of signals, and are continuously monitoring their environment. Growth and proliferation will occur when the extracellular environment contains the appropriate conditions to sustain proliferation, but in a restrictive environment, cells will forgo proliferation to favour maintenance.

Protein Kinase A (PKA) is part of a nutrient-sensing pathway which responds to cytoplasmic levels of cyclic AMP (cAMP). When cAMP is elevated in response to the presence of glutamine (137), it increases the activity of glutamine-fructose-6-phosphate amidotransferase

(GFAT), the rate-limiting step of the hexosamine pathway in a PKA-dependent manner (see figure 1.1) (138). PKA can directly phosphorylate LC3 to inhibit autophagy induction. A recent study in neuronal cells demonstrated that a pool of PKA-phosphorylated LC3 was readily available, enabling cells to rapidly mediate the induction of autophagy in response to stresses like nutrient deprivation or injury, but had no effect on vacuoles that were already formed. This PKA LC3 phosphorylation site was not observed in the yeast or *Drosophila melanogaster*, was present in all mammalian forms of LC3, but not on Atg8 homologues GABARAP and GATE16 (139).

In favourable conditions (i.e., when nutrients are plentiful), class I PI3Ks are activated, along with Ras, by growth factor binding to their cognate tyrosine kinase receptor to initiate cell growth and proliferation (see figure 1.6). PI3Ks catalyse the phosphorylation of phosphatidylinositol 4,5 biphosphate (PIP2) to phosphatidylinositol 3,4,5 triphosphate (PIP3) (140). This activity at the lipid membrane creates docking sites for both AKT and its activator, phosphoinositide-dependent protein kinase-1 (PDK-1).

The activation of AKT can be prevented by the activity of phosphatase and tensin homolog (PTEN), which dephosphorylates PI3P into PI2P. Active mTOR inhibits the initiation of autophagy by phosphorylating Atg-13 to prevent its interaction with Atg-1, thereby blocking phagophore formation and providing a link between autophagy and the energy status or growth signals (119, 128, 141). AKT can inhibit autophagy by both activating mTORC1 through phosphorylation and by directly decreasing UVRAG expression in a kinase-independent manner (142). Ras activation leads to activation of extracellular signal-regulated kinase (ERK), which phosphorylates and destabilizes the tuberous sclerosis complex 1/2 (TSC1/TSC2), allowing

mTORC1 catalytic activation by phosphorylating the mTOR activator Ras homologue enriched in brain (Rheb) (143-147).

In many tumours, autophagic activity is decreased. This can be attributed to the fact that many oncogenes, like AKT, PI3K (type I) and pro-survival Bcl-2 family members such as Bcl-2, which can bind Beclin-1 to prevent autophagy initiation, are autophagic suppressors. Conversely, tumour suppressors like PTEN, tuberous sclerosis protein 2 (TSC2), p53 and death-associated protein kinase (DAPk), which are autophagy activators, are silenced (see figure 1.6) (6, 121, 148-150).

In primary liver cells of weaned calves, glutamine infusion increased the levels of autophagy in a dose-dependent fashion. Recent reports highlight the role of the PI3K-AKT-Forkhead Box O (FOXO) module and glutamine metabolism in the regulation of autophagy. Upon growth factor removal, FOXO1, -3 and -4 transcription factors increased the expression and the activity of glutamine synthetase to repress mTOR activity and increase autophagy (see figure 1.6) (151-153).

In unfavourable conditions, such as amino acid withdrawal, the binding of Rheb to mTORC1 is inhibited, preventing its activation (see figure 1.6) (147, 154). In order to be fully active, AKT must be phosphorylated in 2 sites; Ser473 by PDK-1 and Thr308 by mammalian target of rapamycin complex 2 (mTORC2) and DNA-dependent protein kinase (DNA-PK). Phosphorylation of AKT has been reported to be inhibited by several different stressors, including the unfolded protein response (via GRP78) (153), and thereby allowing autophagy to occur. Constitutive activation of the Ras pathway has been reported to bypass mTORC1 inhibition in amino acid deprivation in a melanoma cell line and to have abnormal autophagy

signalling (155). Additionally, Ras-transformed cells, like myc-transformed cells, have an increased dependence on glutamine for growth and survival and activate and rely on autophagy to provide with biosynthetic precursors for proliferation, growth and survival (156-160). However, autophagy triggered by amino acid deprivation is dependent on the ULK1/2 for initiation (92).

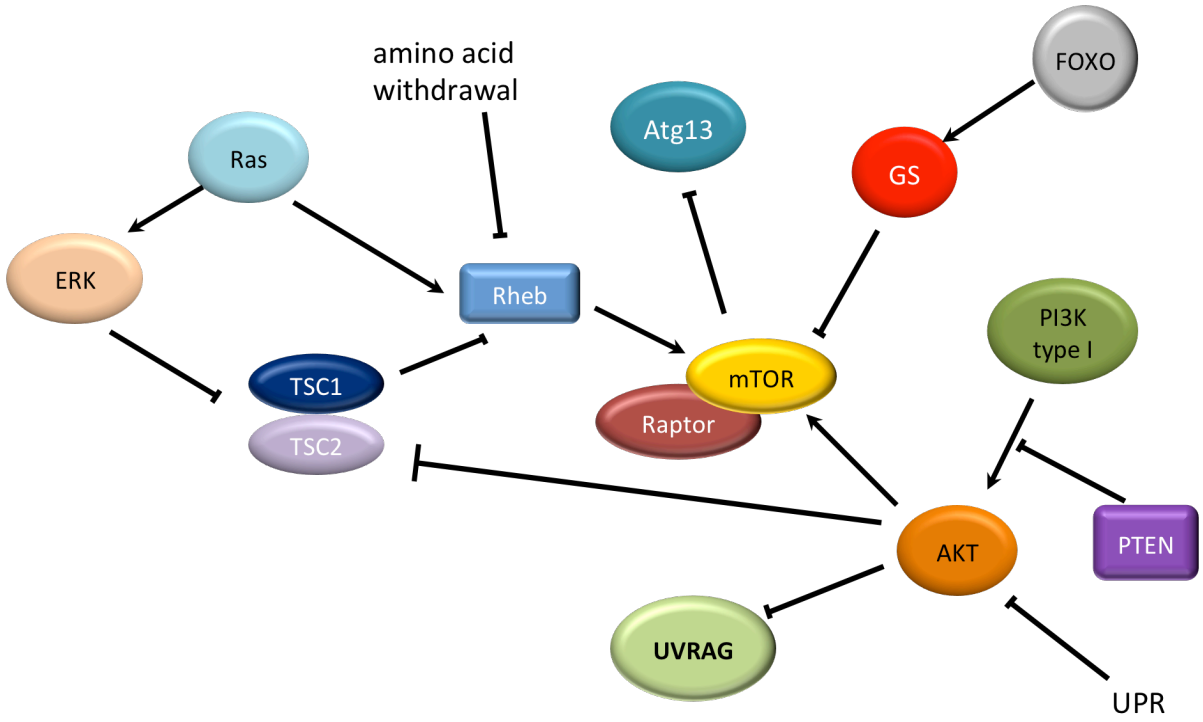

Figure 1.6 - Extracellular Signals Regulate mTOR

The activity of mTOR is affected by signals received to indicate the availalility of nutrients for growth and proliferation Signalling molecules that transduce the signal to proliferate, such as AKT or Ras, will activate mTOR, whereas in unfavourable conditions, like amino acid withdrawal or the unfolded protein response (UPR), PTEN and TSC2 will prevent mTOR activation[7].

A recent report described the role of DAPk in cells under oxidative stress in the activation of the serine/threonine kinase protein kinase D1 (PKD), which in turn binds and phosphorylates Vps34 to activate autophagy (123). The ectopic presence of PKD alone was

[7] Figure 1.6 adapted from Kim *et al,* Demetriades *et al* and Avruch *et al* (87, 147, 154).

sufficient to trigger autophagosome formation, and the activation of PKD by DAPk was independent of PKC (123, 161). This ability of ROS to induce autophagy may be critical in the tumour environment where cells at the center of a mass do not have access to all the nutrients available to the cells on the tumour periphery.

In intestinal epithelial cell lines, glutamine increased the formation of autophagosomes and led to an inhibition of mTOR and p38 MAP kinase. Upon glutamine deprivation, the ability of intestinal epithelial cells to recover from heat shock was severely impaired and apoptosis was induced (162). In a heat stress model, glutamine conferred a protective effect by signalling through the PI3K-AKT pathway to increase heat shock protein 70, prevent the expression of fibronectin-integrin and desphosphorylate p38 MAPK, a downstream effector of fibronectin-integrin signalling (163, 164). Under nutrient-limiting or starvation conditions, the high AMP:ATP ratio leads to the activation of AMP-activated protein kinase (AMPK) activity, which will inhibit cell growth and proliferation and allow autophagy to occur by acting as metabolic checkpoint (see figure 1.7). This occurs in part through the inhibition of mTORC1. This is accomplished by phosphorylation of both Raptor and TSC2, blocking the kinase activity of mTORC1 (165). In addition to removing the inhibitory activity of Raptor and TSC2 on mTORC1, AMPK can directly phosphorylate and activate ULK1 and Beclin-1 (166, 167). Direct AMPK phosphorylation of Vps34 will inhibit its activity. However, Atg14L inhibits AMPK phosphorylation of Vps34 and stimulates AMPK phosphorylation of Beclin-1 (168). Combined, these effects would inhibit the activities of other, non-autophagy related Vps34 complexes while promoting the activity of complex I during autophagy initiation.

1.8.3 — Ammonium Ion Signalling in Autophagy Regulation

There has been much speculation as to how glutamine could affect autophagy. A by-product of glutaminolysis is the release of ammonium ions (6). Recently, a report described the

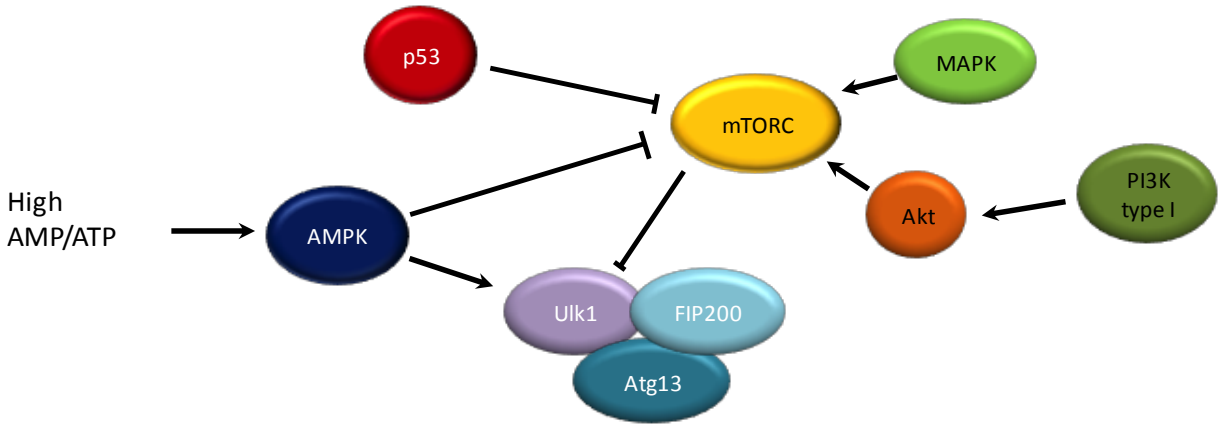

Figure 1.7 - mTORC is an Autophagy Molecular Switch

The regulation of autophagy is highly dependent on the activity of mTORC. Signalling molecules that transduce the signal to proliferate, such as AKT or MAPK will activate mTORC and suppress autophagy initiation. Signalling molecules that are activated in times of cellular stress, like AMPK (low energy) and p53 (DNA damage), suppress the autophagy inhibitory activity of mTORC to allow autophagy to proceed.

importance of glutamine-derived ammonium ions as a regulator of autophagy (169). In this report, cells cultured in glutamine-supplemented medium for more than 48h displayed increases in autophagy. Conditioned medium from this cell culture was then added to a fresh culture and an increase in autophagy was also observed. The autophagy-stimulating compound was identified as ammonium ions and conferred a protective effect against nutrient deprivation and TNF-α induced apoptosis (169). The effect observed was not induced by a pH change and was thought to be significant in tumour microenvironments where nutrient deprivation could occur and confer resistance to apoptosis brought on by nutrient deprivation, metabolic stress, hypoxia

or chemotherapy (6, 169). Eng *et al.* collected and analyzed the interstitial fluids of human tumours xenografts and found the concentration of ammonium ions, in the millimolar range, to be significantly elevated when compared to the plasma levels of the murine host (169). Because of their size and chemical properties, ammonium ions are easily diffusible. This is particularly noteworthy when one considers that the tumour microenvironment can vary drastically. Cells exposed on the outer layer of the tumour may be in a nutrient rich environment, consuming glutamine and excreting ammonium ions, which could diffuse to the inner reaches of the tumour where nutrients may not be as plentiful due to poor vascularisation to stimulate autophagy as a pro-survival mechanism.

While the induction of autophagy by rapamycin is mTOR-dependent, autophagy induced by ammonium ions is mTOR-independent. In double-knockout ULK1/2($^{-/-}$) mouse embryonic fibroblasts, the induction of autophagy in response to amino acid deprivation was inhibited, but not in response to glucose deprivation or to inhibition of glucose metabolism. In this model, autophagy induction in response to glucose deprivation was associated with an increase in the ammonium ions concentration arising from an increase in amino acid catabolism in an Atg-5-dependent manner (92). This would indicate that autophagy provides cells with an adaptation response to both excess (ULK1/2-independent) and deprivation (ULK-1/2 dependent) of nitrogen sources.

In a recent report, quantitative phosphoproteomics was used to assess the signalling pathways that are modulated by ammonium ion-stimulated autophagy, using rapamycin as a comparator, in MCF-7 breast cancer cells. This report confirmed that mTOR was not affected by the induction of autophagy by ammonium ions, and pointed to the upregulation of AMPK and the unfolded protein response as the primary driver of autophagy. Ras signalling, more

specifically MAPK3 activity, was increased (170). Ammonium ion-induced elevation in MAPK1/3 activity had been previously reported in rat astrocytes (171, 172). Furthermore, ammonium ion treatment stimulated Rho GTPase protein signal transduction, which is crucial to the actin cytoskeleton plasticity and is involved in processes such as proliferation, motility and apoptosis. The ability of ammonium pre-treatment to stimulate cell motility was assessed in a wound closure experiment and was found to require MAPK3 activity (170).

1.9 — Cross-talk Between Apoptosis and Autophagy

The balance between autophagy and apoptosis is not as clear as was once believed but there is evidence of crosstalk between the two processes (173, 174). For example, the Vps34-Beclin-1 interaction is inhibited by the binding of anti-apoptotic proteins Bcl-2 family members to Beclin-1 through their BH3 domain (175). In response to anticancer treatment, calpain cleaves Atg-5 to inhibit autophagy, but the cleavage product translocates to mitochondria to interact with Bcl-x_L, allowing cytochrome c release and the initiation of apoptosis (176). Moreover, Vps34, Beclin-1 and Atg4 have been reported to be substrates of caspases (177). p53 is another link between apoptosis and autophagy: in response to adverse cellular conditions such as DNA damage and hypoxia, nuclear p53, a known modulator of apoptosis (178), transactivates the β1 and β2 subunits of AMP-activated protein kinase (AMPK) which inhibits mTOR, which in turn promotes autophagy (179). The relocation of p53 from the nucleus to the cytoplasm has been shown to induce mitochondrial outer membrane permeabilization, allowing cytochrome c release and the induction of apoptosis (150, 180). In a recent report, Rovetta *et al* explored the roles of autophagy and apoptosis in renal toxicity to cisplatin. At low doses of cisplatin, autophagy was cytoprotective, and its inhibition resulted in increased apoptosis. A high-dose of cisplatin

induced apoptosis unless cells were pre-treated with an autophagy inducer which protected cells against death (181).

Autophagy is inhibited by Bcl-2 binding to Beclin-1 monomers or dimers (see figure 1.8) and any protein modifications that weakens this interaction stimulates the progression of the autophagic process. DAPk can phosphorylate Beclin-1 in its BH3 domain to promote dissociation of Bcl-2 (182, 183). Bcl-2 can be phosphorylated by c-Jun N-terminal kinase 1 (JNK1) and ERK, both mitogen-activated protein kinases (MAPK), to destabilize its interaction with Bcl-2/Bcl-$x_{L,}$ allowing phagophore formation (182, 183). As both of these kinases are stress-activated kinases, their role in mediating the starvation-induced stress signal is not surprising (131, 161, 184).

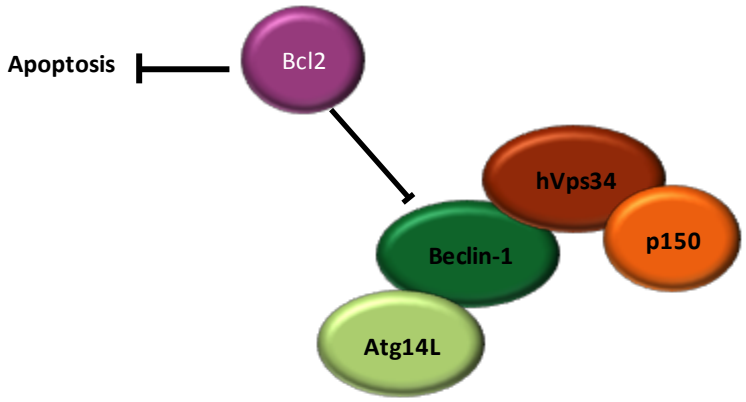

Figure 1.8 - Bcl-2 Family Members Play a Role in Autophagy Regulation

Beclin-1 contains a BH3 domain which allows the binding of Bcl-2 family members. This association will inhibit the ability of Beclin-1 to form interaction in Complex I or II. The ability of Bcl-2 to bind and inhibit Beclin-1 activity is impaired by stress signals such as those transduced by DAPk and MAPK.

DAPk is one of the few regulators of autophagy that seems to be restricted to the induction of autophagic cell death. Because it is also implicated in apoptotic membrane blebbing and necrotic death, emerging models view it as the molecular switch between survival and death

(185). DAPk also interacts with microtubule-associated protein 1B (MAP1B) to allow LC3 processing. DAPk has been reported to allow the stabilization of p53 via p19 (ARF). Since this causes the nuclear accumulation of p53, and p53 transactivates genes for apoptosis, continued signalling via DAPk may tip the balance from autophagy to apoptosis. Many of the pro-apoptotic Bcl-2 family members, such as Bad, Bax and PUMA, have been implicated in the induction of autophagy. It is hypothesized that this induction is mediated by destabilizing the Beclin-1 and Bcl-2 or Bcl-x_L interactions (148).

GADD-153 has recently been implicated in autophagy, even though it is typically associated with apoptosis in response to ER stress. GADD-153 is a transcription factor that was first identified in models of growth arrest or DNA damage; GADD-153 is highly upregulated in stress conditions, particularly in ER stress and nutrient starvation such as glutamine and glucose deprivation (186-190). Proteins that are destined for secretion or shuttled to other cellular compartments such as lysosomes, the Golgi apparatus or the cell membrane are folded in the ER. The accumulation of unfolded proteins signal ER stress and activates UPR pathways. The UPR can downregulate protein synthesis, activate transcription factors to upregulate chaperones, such as GRP78, to allow for the proper folding of proteins. If this response is not sufficient to relieve the ER stress, then other factors, such as GADD-153 expression, are activated or upregulated. This upregulation has been reported to downregulate the expression of Bcl-2 and GSH and lead to apoptosis (181, 191). In models for atherosclerosis, diabetes, Alzheimer's and Parkinson, upregulation of GADD-153-induced apoptosis was suggested as being a contributing factor to disease progression (186, 192-194). One report using chemotherapeutic agents known to induce either autophagy or apoptosis describes the upregulation of GADD-153 in both phenomena. In both cases, the cell viability decreased with GADD-153 expression. The functional contribution

of GADD-153 was confirmed using gene-silencing and overexpression studies. Exogenous expression of GADD-153 in their cell model of human gliomas induced apoptosis and autophagy in the absence of any other form of stimulation (195). In a study of embryonic stem cells, the authors support GADD-153 as being an intermediary between autophagy and apoptosis by increasing the expression of Bax/Bak and decreasing the expression of Bcl-2 and Bcl-x_L. This alone would allow autophagy to occur by releasing Beclin-1 from its inhibitory interactions with anti-apoptotic Bcl-2 family members (196).

1.10 — A Cellular Model to Study Glutamine Signalling

The overall conclusion that can be gleaned from the literature is that glutamine is more than just an amino acid. It is a signalling molecule that plays an important role in cell survival, allowing cells an opportunity to adapt to stressful conditions though the activation of essential pathways. As such, the availability of glutamine is an important determinant to cell fate.

Previous work in the Sp2/0 hybridoma cell line has shown that these cells respond to the levels of glutamine available in the culture medium (110, 197). In order to assess whether that sensitivity was general to all amino acids or specific to glutamine, Sp2/0 cells were cultured in medium containing all but 1 of the 20 amino acids and cell viability was assessed at 4h and 24h. The withdrawal of glutamine for 4h was enough to induce rapid apoptosis along the intrinsic pathway (53). This effect was specific to glutamine, as the withdrawal of any of the other 19 amino acids did not significantly affect cell survival. The induction of the intrinsic pathways of apoptosis was confirmed by translocation of Bax from the cytosol to the mitochondria, cytosolic release of cytochrome c and SMAC/Diablo after 60 min, and activation of caspase-9, and caspase-3 (53, 110). Other types of cells typically require longer culture periods in the absence of

glutamine before cell death is induced, such as human neuroblastoma cells where cell death was observed at 48h, or human leukemia or lymphoma cell lines, CEM (lymphoblastic leukemia), Namalwa (Burkitt's lymphoma), U937 (histiocytic lymphoma) and HL-60 (pro-myelocytic leukemia), where death was observed between 24 to 48h (50, 198). This rapid induction of apoptosis made the Sp2/0 cell line a singularly suitable model to study intracellular signalling induced by modulations of glutamine levels and supported the role of glutamine as a survival signal.

Interestingly, the Sp2/0 cell line expresses few of the anti-apoptotic members of the Bcl-2 family members (Bcl-2, Bcl-W, Mcl-1 and Bfl-1) and with the exception of Mcl-1, expresses them at low levels (111) while expressing many pro-apoptotic family members (Bax, Puma, Bim and Bad), and these at higher levels (figure 1.9). Because of the higher ratio of pro-apoptotic members to anti-apoptotic members, Sp2/0 are poised to undergo apoptosis. This also means that there are few anti-apoptotic members to inhibit autophagy inhibition by binding Beclin-1. The ectopic presence of Bcl-x_L was shown to be sufficient to prevent apoptosis (199), but had the effect of decreasing Sp2/0 cell proliferation, even in the presence of glutamine (110).

In the Sp2/0 cell cultures, glutamine withdrawal leads to an increased production of reactive oxygen species (ROS) and a concurrent decrease in GSH levels, causing oxidative stress as seen in other cell lines, such as mouse embryonic fibroblasts, human glioblastoma, breast and colon epithelial cells (90, 200, 201). However, this oxidative stress was not sufficient to cause cell death. The use of the antioxidant *N*-acetyl-L-cysteine (NAC) did not prevent the activation of apoptosis in glutamine withdrawal, as caspase-3 was activated and cell viability was lost. Interestingly, the number of apoptotic bodies was decreased in the presence of NAC. NAC

decreased the phosphorylation of p38, indicating that ROS were involved in the formation of apoptotic bodies by the activation of p38 MAPK (199, 200).

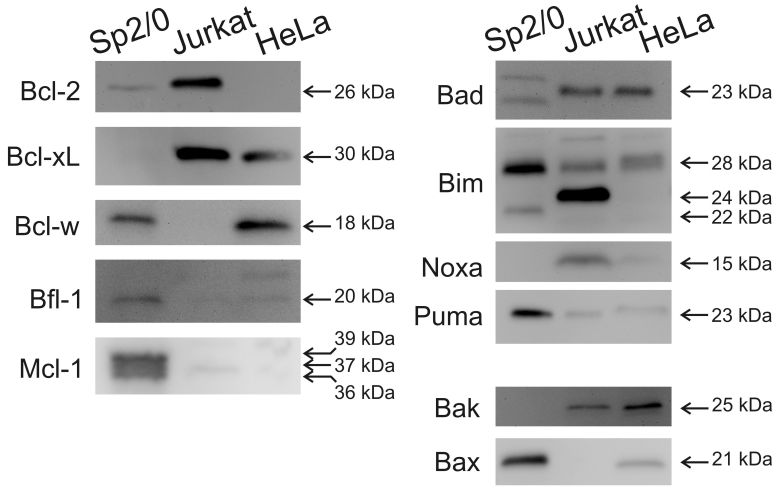

Figure 1.9 - Expression of Bcl-2 Family Proteins in Sp2/0 Cells

This Western blot panel depicts the expression of the various Bcl-2 family members as expressed in the Sp2/0 cell line (Jurkat lymphoid T cell line and HeLa fibroblast cell line were used comparison purposes). The left panel contains the anti-apoptotic Bcl-2 family members, and the right panel contains the pro-apoptotic Bcl-2 family members. Figure courtesy of CC Harnett and ER Gauthier.

In Sp2/0 cells that ectopically expressed Bcl-x_L, p38 phosphorylation was inhibited during glutamine starvation. This would indicate that this phosphorylation event is induced after the mitochondria exhibit signs of dysfunction. Additionally, the inhibition of caspase activity using the pan-caspase inhibitor Z-VAD-fmk did not prevent p38 phosphorylation, indicating that this event is caspase-independent. The activation of p38 MAPK was involved in the induction of late apoptotic features, but not in the initiation of apoptosis in glutamine starved Sp2/0 cell cultures (199).

The Sp2/0 cell line expresses AKT1 and AKT3, but also expresses PTEN, a PI3K pathway inhibitor. Fully active AKT is phosphorylated at 2 critical sites, T308 and S473. When

assessed in Sp2/0 cells under normal culture conditions, AKT was found to remain unphosphorylated at those sites (see figure 1.10). Moreover, Sp2/0 cells exhibit high levels of deregulated c-myc (60). Since c-Myc drives glutaminolysis by increasing the expression of glutamine transporters and GLS to provide fuel for the TCA cycle and biosynthetic precursors while releasing ammonium ions (section 1.8.3), these cells are dependent on glutamine for survival (52, 54, 59). As the presence of activated AKT would also stimulate glucose import and the Sp2/0 cells are AKT-deficient, these two factors combined may in part explain the glutamine dependence of the Sp2/0 cell line (4, 53, 110).

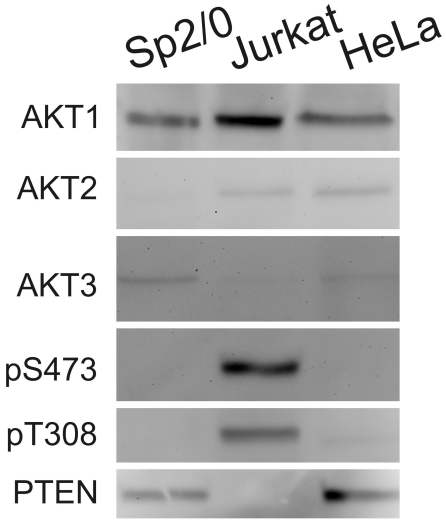

Figure 1.10 - Expression and Phosphorylation Levels of AKT in Sp2/0 cells

This Western blot panel depicts the expression levels of the different AKT isoforms in the Sp2/0 cell line and in Jurkat lymphoid T cell line and HeLa fibroblast cell line as a comparison. The Western blot also assessed the phosphorylation states at 2 critical phosphorylation sites on AKT (S473 and T308). Figure courtesy of CC Harnett and ER Gauthier.

1.11 — Project Hypothesis

The Sp2/0 cell line expresses many pro-apoptotic and fewer anti-apoptotic Bcl-2 proteins and is constantly poised on the brink of apoptosis and will undergo apoptotic death rapidly upon

induction (53). The lack of Bcl-xL expression and relatively low expression of Bcl-2 also provides fewer avenues of autophagy inhibition (202). It is myc-transformed and highly proliferative, making it dependent on glutamine for cell survival (203). Using this cellular model, this body of work was focused on elucidating the relationship between glutamine, proliferation and survival. The project hypothesis is that the presence of glutamine acts as a signalling molecule and is necessary for survival and proliferation in Sp2/0 cells. It is postulated that Sp2/0 cell survival requires autophagy, which will be modulated by glutamine availability.

The study had 3 main objectives: 1) to evaluate the effects of glutamine limitation, rather than deprivation, on Sp2/0 cell behaviour, including cell survival, apoptosis and the effects on the cell cycle both as an endpoint and over a 24h period, 2) to evaluate the presence of autophagy in the Sp2/0 cell line in glutamine-rich and glutamine limiting conditions and 3) to evaluate the effects of ammonium, the by-product of glutaminolysis, on cell behaviour in glutamine-limiting conditions.

2.0 — MATERIALS AND METHODS

2.1 — Reagents and Antibodies

Unless stated otherwise, all reagents were obtained from Sigma-Aldrich Canada (Oakville, ON). Glutamine solutions were freshly prepared as a 200 mM stock in phosphate buffered saline with the pH adjusted to 7.4. (PBS; 9.1 μM Na_2HPO_4, 1.7 mM NaH_2PO_4, 150 mM NaCl, pH 7.4).

Propidium iodide was prepared at a concentration of 1mg/mL for flow cytometry staining. 3-methyladenine (3-MA) was prepared in double distilled water (ddH_2O) as a 100 mM stock solution. Stock solutions for rapamycin (100 μM) and bafilomycin A1 (100 μM) (both from Cell Signaling Technology, Danvers, MA) and caspase inhibitor Z-VAD-fmk (10 mM) (EMD Chemicals, San Diego, CA) were prepared in DMSO.

DMSO was used as the treatment control in experiments using Bafilomycin A1, rapamycin and Z-VAD-fmk, and ddH_2O was used as the treatment control for the 3-MA experiments.

Antibodies raised against the following proteins were from Santa Cruz Biotechnologies Inc. (Santa Cruz, CA): cytochrome c, GADD-153 (clone B3), GRP78, PARP and HSP60. Antibodies against cleaved caspase-3, Atg12, β-actin, LC3B and PTEN were from Cell Signaling Technology (Danvers, MA).

2.2 — Cell Culture

The Sp2/0-Ag14 (Sp2/0) mouse hybridoma cell line was obtained from the American Type Culture Collection (ATCC, Rockville MD) and maintained in Iscove's Modified Dulbecco's Medium (IMDM) supplemented with 5% Fetalclone I (Hyclone, Logan UT), 100U/mL penicillin, 100 µg/mL streptomycin and 4 mM L-glutamine (Q) (hereafter designated as complete IMDM) in 37^{o}C, 5% CO_2 humidified atmosphere. The generation of Sp2/0 cells transfected with Bcl-xL and the control vector pTEj8 was described earlier, and Sp2/0 cells transfected with Bcl-xL or the pTEJ8 vector were maintained in complete IMDM containing 750 µg/mL G-418 (110, 111).

All assays were performed using Sp2/0 cells in the exponential growth phase which were washed twice in warm (37^{o}C) IMDM containing 5% Fetalclone, 100U/mL penicillin and 100 µg/mL streptomycin, but not supplemented with L-glutamine (hereafter referred to as glutamine-free IMDM). The cells were then seeded at 4x10^{5} cells/mL in glutamine-free IMDM medium, supplemented with selected drugs (or their solvent control) and cultured for the indicated period of time. Corresponding controls supplemented with 4 mM L-glutamine were also prepared in parallel.

2.3 — Cell Viability Assays

Cell viability was assessed using the trypan blue exclusion assay. In a trypan blue staining assay, cells that do not maintain their membrane integrity will stain blue and can be visualized by light microscopy. The staining occurs because the chromophore is negatively charged and cannot interact with the cell membrane unless there is damage (204). The

percentage of cells that do not stain gives an indication of cell viability. Cell suspensions were stained with 0.4% trypan blue solution for 5 min at room temperature, then 10 µL were loaded into the chamber of a Neubauer haemocytometer (Fisher Scientific, Ottawa, Ontario) and placed on an inverted microscope under a 10X objective, using phase contrast. The number of unstained and stained (blue) cells was determined and cell viability was expressed as the percentage of white cells (viable) to the total number of cells (white + blue). Cell density was determined using the white cell counts multiplied by $1x10^4$ to estimate the number of cells/mL, as per the manufacturer's instructions. An average of 4 counts were taken for each sample or condition.

As a complementary approach to determine Sp2/0 cell viability, treated cells were subjected to a clonogenic assay. After subjecting the cells to glutamine starvation or limitation, the cell density was adjusted to 5 cells/mL in complete IMDM before 100 µL of this dilution was seeded in a 96 well plate. Cells were allowed to grow for 7 to 10 days, and the number of wells containing colonies of at least 50 cells was counted.

2.4 — Flow Cytometry

To analyse cell cycle distribution, cultured Sp2/0 cells were collected, incubated on ice for 10 min, washed twice with ice cold PBS before being permeabilized in ice-cold 70% ethanol. Cells were stained with propidium iodide (0.1mg/mL propidium iodide, 0.3% IGEPAL, 0.1% sodium citrate and 0.04 µg/mL RNAse A) for 1h at room temperature before flow cytometry analysis.

Detection of early apoptosis was performed using the Annexin V/propidium iodide (PI) assay kit as per the manufacturer's instructions (BioVision, Mountain View, California) or with

Annexin V-FITC (BioVision) and 7-aminoactinomycin D (7-AAD, 0.25 µg/test, eBiosciences, San Diego, CA) incubated in the dark at room temperature for 5 min before analysis by flow cytometry.

Flow cytometry experiments were performed using a BD FACSCanto II instrument and the BD FACSDiva flow and analysis software (BD Biosciences, Mississauga, On) with an argon ion laser, using the FL1 filter for Annexin V, the FL2 filter for propidium iodide and the FL4 filter for 7-AAD. All experiments were performed after single colour compensation.

2.5 — Determination of Caspase Activity

Sp2/0 cells were treated as indicated and collected by centrifugation at 300 x g for 5 min at room temperature. Protein extracts were prepared and subjected to caspase-3 colorimetric enzymatic cleavage assay of a synthetic peptide (DEVD-pNA) as per the manufacturer's instructions (BioVision Inc. Mountain View, CA). This peptide contains a sequence, DEVD, which is preferentially recognized and cleaved by caspase-3 releasing p-nitroaniline (pNA) which can be measured by spectrophotometry at 405 nm. Optical density readings were obtained using a PowerWave X microplate spectrophotometer (BioTek Instruments Inc., Winooski, VT).

2.6 — Western Blot Analysis

Whole cell protein extracts for Western blot analysis were prepared using RIPA buffer (1 % IGEPAL, sodium deoxycholate (12.1 µM), sodium dodecyl sulfate (3.45 mM), Halt protease inhibitor cocktail (1X) (Fisher Scientific), sodium fluoride (50 mM), sodium orthovanadate (0.2 mM), phenyl methyl sulfonyl fluoride (0.1mg/mL) in PBS) (53). Briefly, 10-20x10^6 cells were

washed in PBS and centrifuged twice for 10 min at 300 x g at 4°C. Supernatants were discarded, the cell pellets were resuspended in 100 µL RIPA buffer and incubated on ice for 30 min. The cell pellets were then subjected to 3 freeze (-80°C for 5 min) and thaw (room temperature water bath) cycles. The cell pellets were further incubated on ice for 30 min, then centrifuged at 15 000 x g for 20 min at 4°C. The total cell lysate contained in the supernatants were transferred to a clean tube and stored at -80°C until needed.

For PARP and GADD-153, whole cell proteins extracts were obtained using a urea lysis buffer (205). Briefly, cells were washed in ice-cold PBS twice, then $5x10^5$ cells were resuspended in urea lysis buffer (62.5 mM Tris-HCl, pH 8.6, 6 M urea, 10% glycerol, 2% sodium dodecyl sulfate, freshly added 5% β-mercaptoethanol, 0.00125% bromophenol blue). Cells were then lysed by sonication on ice for 15 s using a Model 50 Sonic Dismembrator (Fisher Scientific) and incubated for 15 min at 65°C before fractionation by SDS-PAGE.

For cytosolic protein extracts, $5x10^7$ Sp2/0 cells were collected by centrifugation (500 x g, 5 min) and incubated on ice for 15 min, washed twice in cold PBS, permeabilized with 250 µL of buffer A (KCl (75 mM), NaH_2PO_4 (1 mM), Na_2HPO_4 (8 mM), sucrose (250 mM), digitonin (230 µg/mL)) and incubated on ice for 10 min (206). An aliquot was taken and permeabilization was assessed by trypan blue exclusion assay. Cells were then centrifuged at 15 000 x g, 4°C for 5 min. The supernatants (cytosolic fraction) were collected and centrifuged at 15 000 x g, 4°C for 5 min, then mixed with an equal volume of 2X RIPA buffer for storage at -80°C.

Proteins were fractionated by SDS-PAGE on a 12% mini-gel (separating gel: 12% acrylamide, 0.375M Tris-HCl, 0.1% SDS, pH 8.8, polymerized with 28.9 mM APS and 40 µL TEMED; stacking gel: 3.9 % acrylamide, 0.125M Tris-HCl, 0.1% SDS, pH 6.8, polymerized

with 14.45 mM APS and 20 µL TEMED) in an SDS electrophoresis buffer (Tris-HCl (0.125 M), glycine (0.96 M), 0.5% SDS, pH 8.3) for 60 min at 75mA (207).

For the analysis of Cytochrome c and LC3B, proteins were fractionated by SDS-PAGE (separating gel: 12% acrylamide, 1 M Tris-HCl with 0.1% SDS, pH 8.45, and 13% glycerol, polymerized with 28.9 mM APS and 40 µL TEMED; stacking gel: 3.89% acrylamide, 0.31 M Tris-HCl with 0.07% SDS, pH 8.45, polymerized with 14.45 mM APS and 20 µL TEMED) using a tris-tricine buffer system (anode buffer: 0.04M Tris-HCl, pH 8.9; cathode buffer: 0.01M Tris-HCl, 0.1M Tricine, 3.47 mM SDS) (208) for 210 min at 30mA.

After fractionation, proteins were transferred onto Immobilon PVDF membranes (Millipore Corporation, Billerica, MA) with a Tris-glycine transfer buffer (48 mM Tris-HCl, 39 mM glycine with 20% methanol) using the Trans-Blot Semi-Dry Transfer Cell system (Bio-Rad Laboratories). To assess transfer efficiency, membranes were stained with Ponceau S (5% Ponceau S, 2% glacial acetic acid) for 15 min at room temperature followed by de-staining in distilled water prior to blocking. Membranes were blocked for 1h at room temperature with 5% non-fat dry milk or 5% bovine serum albumin, in TTBS buffer (0.02 M Tris-HCl, 0.14 M NaCl, 0.1 % Tween 20, pH 7.6). Membranes were then incubated with mouse or rabbit primary antibodies following the conditions shown in Table 2. After three 5 min washes in TTBS, the membranes were incubated with anti-rabbit or anti-mouse IgG secondary antibodies coupled to horseradish peroxidase (HRP) diluted in TTBS containing 5% milk or BSA, and subjected again to three 5 min washes in TTBS. Detection was done by chemiluminescence using the Immobilon Western HRP Substrate Luminol reagent (Millipore). All images were captured using the Fluorchem 8000 imaging system and AlphaEase software (Alpha Innotech, San Leandro, CA).

Table 2 – Experimental Conditions Used for Each Antibody

Antibody	Product	Source	Dilution factor	Blocking solution
Anti-mouse secondary	#7076 Cell Signaling	Horse	1:3000	non-fat milk
Anti-rabbit secondary	#7074 Cell Signaling	Goat	1:3000	non-fat milk
β-actin	#4967 Cell Signaling	Rabbit	1:1000	Bovine serum albumin
Caspase-3	#9662 Cell Signaling	Rabbit	1:1000	non-fat milk
Cytochrome c	#4272 Cell Signaling	Rabbit	1:200	non-fat milk
GADD-153	#sc-7351 Santa Cruz Biotech	Mouse	1:200	non-fat milk
GRP78	#sc-13968 Santa Cruz Biotech	Rabbit	1:200	non-fat milk
HSP60	#sc-13966 Santa Cruz Biotech	Rabbit	1:2000	non-fat milk
LC3B	#2775 Cell Signaling	Rabbit	1:1000	Bovine serum albumin
PARP-1	#9542 Cell Signaling	Rabbit	1:1500	non-fat milk
PTEN	#9552 Cell Signaling	Rabbit	1:1000	non-fat milk

To assess protein loading into SDS-PAGE, mini-gels were stained for 1h with Coomassie Brillant Blue solution (0.1% Coomassie Brillant Blue, 40% methanol, 10% glacial acetic acid) then placed in de-staining buffer (50% methanol, 10% glacial acetic acid) at room temperature overnight. Protein extracts prepared in urea buffer were equalized following examination of Coomassie Blue-stained gels. All other proteins concentrations were assessed using the DC Protein Assay kit as per the manufacturer's instructions (Bio-Rad Laboratories, Mississauga, ON).

2.7 — Microscopy

2.7.1 — Fluorescence Microscopy

Acridine orange (AO) is a hydrophobic dye that is membrane permeable and intercalates DNA and RNA molecules. When excited by blue light, acridine orange emits a green light (525nm filter) when complexed with DNA. In an acidic environment, acridine orange is protonated and forms aggregates, shifting the emitted wavelength into the bright red light (620nm filter). Ethidium bromide (EtBr) is not membrane permeable but also intercalates DNA, and emits light in the red-orange range (595 nm). In cells co-stained with AO/EtBr, co-localization of both dyes (yellow) will indicate cells having lost membrane integrity and can be presumed dead. Therefore, AO/EtBr staining can be used to reveal changes in cell morphology (such as the formation of apoptotic bodies) and to analyse the acidity of intracellular organelles, such as the lysosomes.

For the analysis of the morphology of apoptotic cells, Sp2/0 cells were collected and placed on ice for 10 min, washed twice and stained for 1 min at room temperature in a staining buffer (acridine orange 6 μg/mL, ethidium bromide 6 μg/mL in PBS) and analyzed using a Leitz Diaplan microscope (Leica Microsystems, Richmond Hill, ON).

The presence of acidic vacuoles was assessed by AO staining using the 620nm filter by fluorescence microscopy. Sp2/0 cells were stained in culture at a final acridine orange concentration of 1mg/mL for 20 min (209). Cell culture was collected by pipette and washed twice in PBS, mixed with an equal volume of VectaShield Mounting Medium (Vector Laboratories Inc., Burlington, Ontario) before mounting the samples on slides. Images were

captured by a Zeiss Axiovert 200M fluorescence microscope with 546nm excitation and 590nm emission and analyzed using the Carl Zeiss AxioVision Axio VS40 software, version 4.5.0.0 (210). Quantitation was done by assessing the percentage of brightly stained cells versus the overall number of cells counted across all captured fields. Brightly stained cells were defined as cell with intense colouring comparable to the indicated control condition.

2.7.2 — Analysis of Mitochondrial Transmembrane Potential

The mitochondrial transmembrane potential was assessed by confocal microscopy. Cultured Sp2/0 cells were stained in the dark at 37°C, 5% CO_2 in a humidified atmosphere with Mitotracker Red CM-H2XRos (50nM, Invitrogen, Burlington ON.) 30 min prior to the end of treatments. Cells were collected, washed twice in PBS and fixed for 5 min at room temperature in 1mL of a 4% paraformaldehyde solution. Cells were washed twice in PBS and resuspended in equal volumes of an 80% glycerol solution. Images were captured using a Zeiss LSM 510 Meta confocal microscope (Carl Zeiss Canada, Toronto, ON) with an argon laser at 578nm absorbance and 599nm emission maxima, with 63X magnification and analyzed using Carl Zeiss Laser Scanning Microscope LMS 510 version 3.2 software.

2.7.3 — Transmission Electron Microscopy

Transmission electron microscopy (TEM) analysis was performed at the Electron Microscopy Laboratory, University of New Brunswick (Fredericton, NB). Cultured Sp2/0 cells ($1x10^7$) were collected, washed twice in PBS and fixed for 2-4h in 3% glutaraldehyde in 0.1 M sodium cacodylate buffer, pH 7.4. After primary fixation the cells were washed in the same buffer twice and stored at 4°C before processing. Processing occurred as previously described

(211). Briefly, 1% (v/v) OsO4 post-fixed cells were dehydrated through a series of acetone washes. Samples were infiltrated with an Epon-Araldite resin/acetone mixture and embedded in resin in gelatin capsules and flat-embedding moulds. Sections (100nm) were collected onto uncoated copper grids, double stained with uranyl acetate and Teynolds lead citrate, and observed under a Philips 400T transmission electron microscope. Images were exposed onto negative film (Kodak Electron Microscope film 4489).

2.8 — Statistical Analysis

Statistical analyses were performed using paired t-test or one-way ANOVA with Scheffé's post hoc test, using the statistical software Analyse-it version 2.24 for Microsoft Excel 2007. Statistical significance was assessed with a confidence of 95%.

3.0 — RESULTS

3.1 — EFFECT OF GLUTAMINE LIMITATION ON CELL BEHAVIOUR

Our research group has established that glutamine can affect Sp2/0 cell fate, at least in part by affecting mitochondrial function. Upon glutamine starvation, Sp2/0 cells rapidly undergo apoptosis via the intrinsic apoptotic cascade which is initiated at the mitochondria (53). The lack of available glutamine is accompanied by oxidative stress characterized by the accumulation of reactive oxygen species, protein carbonyl groups and a decrease in glutathione. The oxidative stress activates the p38 MAPK and is associated with the formation of apoptotic bodies, but not with the apoptosis induction (199, 200). Also, in a stationary batch culture system, GADD-153 expression increases as the viability of Sp2/0 cells decreases, though supplementation of glutamine into the batch culture is sufficient to keep GADD-153 expression low, indicating that glutamine can modulate the expression of GADD-153 (212). Our research group has also shown that overexpression of the anti-apoptotic Bcl-2 family member Bcl-xL protects Sp2/0 cells: when overexpressed, Bcl-xL increases viability and decreased the dependence of Sp2/0 on glutamine, and delayed the expression of GADD-153, though it could not prevent GADD-153 expression in the later stages of batch culture (110, 197, 212).

The demonstration by our research group that Gln deprivation triggers a rapid apoptotic response in Sp2/0 cells allowed us to raise the following questions: 1) Is there a critical threshold of Gln concentration required for the maintenance cell survival? 2) If so, are the biochemical apoptotic events triggered at Gln concentrations under this minimal threshold (i.e. *limiting* Gln concentrations) identical to those already described upon *acute* Gln starvation (where extracellular Gln is not available to the cells). 3) Finally, are other basic cellular processes, such

as proliferation, also regulated by this critical threshold of Gln concentrations, or do they require a different minimal concentration of the amino acid? The first part of my thesis aimed at providing some answers to these questions by evaluating the effects of glutamine limitation on cell behaviour, including cell survival, apoptosis and cell cycle progression.

To address these questions, two experimental approaches were used. Firstly, the effect of different glutamine concentrations on the viability and proliferation of Sp2/0 cells was studied. Secondly, the effect of glutamine limitation was studied by exposing Sp2/0 cells to a limiting concentration of glutamine of 25 μM. Several parameters related to cell viability, death, proliferation were then examined.

The reader will note that several of the figures shown in this chapter (specifically, Figs. 3.4, 3.5, 3.7, 3.9, 3.11, 3.13 and 3.17) were originally published as part of the Master's thesis of another student of the Gauthier laboratory (213). Figures 3.2 and 3.15 were contributed by Curtis C. Harnett. In consultation with my supervisor, I have chosen to include them here in order to provide context to my own contribution to this study.

3.1.1 — Glutamine Limitation

As a first step in characterizing the response of Sp2/0 cells to limiting amounts of glutamine, we cultured this cell line for 24h in the presence of a range of glutamine concentrations. The range of glutamine concentration was selected using previously unpublished data (213). It must be noted that this range includes the normal serum level of 0.5-0.7 mM found in humans (214).

We first examined the effect of glutamine concentration on the total number of cells (figure 3.1). At glutamine levels of 100 µM or less, the total cell number did not change significantly from the seeded concentration over the 24h period, indicating that the glutamine levels were insufficient to sustain an increase in cell number.

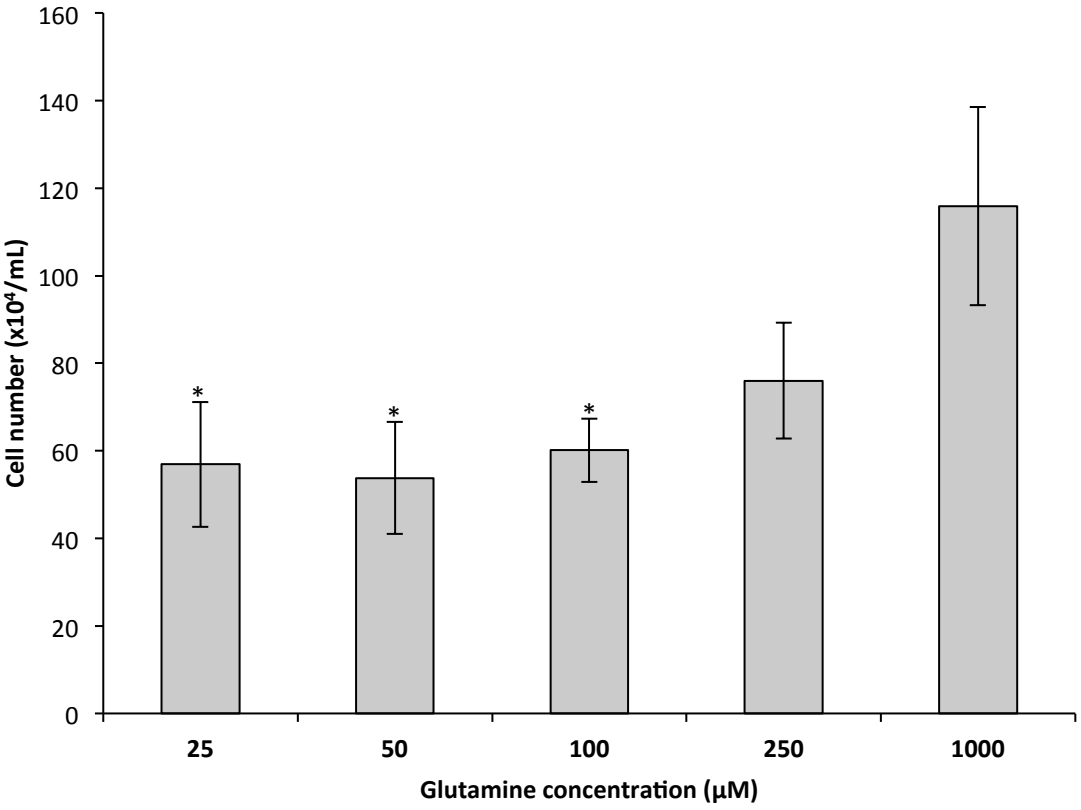

Figure 3.1 - Glutamine Availability Modulates Cell Density

Cells were cultured for 24h in medium supplemented with the indicated glutamine concentrations. Cell number was then determined using a trypan blue assay. Data are the average ± SD of three independent experiments. Statistical significance was assessed by one-way ANOVA with Scheffé's post hoc test, and * indicates $p<0.05$ compared to 1000 µM.

When the glutamine concentration was greater than 100 µM, a progressive increase in the total cell number was observed. The results in figure 3.1 show that glutamine availability in the culture medium modulates the total number of cells collected at 24h.

In order to confirm the data obtained using the trypan blue assay, we used flow cytometry to assess the effect of glutamine availability on cell cycle progression. Figure 3.2 is a representative panel showing the effects of glutamine concentration on the distribution of cells in the cell cycle.

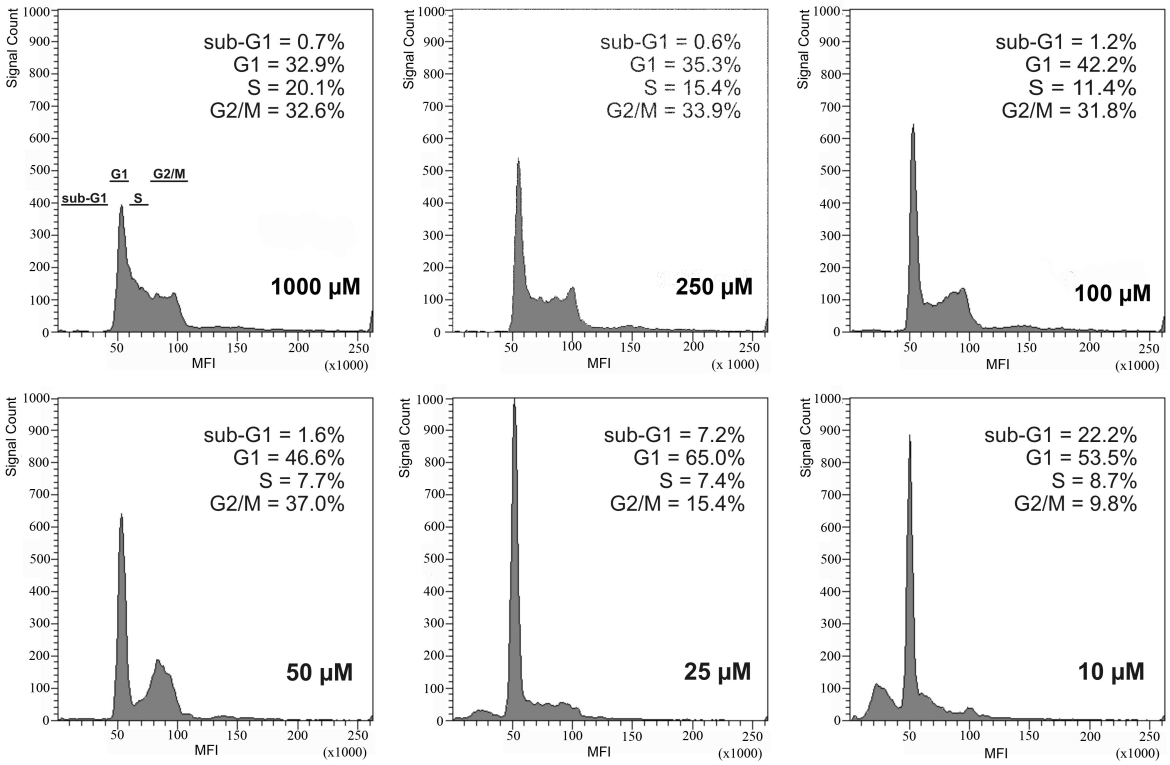

Figure 3.2 - Glutamine Limitation Prevents Cell Cycle Progression

Cells were cultured for 24h in the indicated glutamine concentrations before collection. Cells were then processed for propidium iodide staining and flow cytometry analysis. The x axis of these panels is the mean fluorescence intensity (MFI) of the signal received, and the y axis records the number of events that occur at that particular MFI. Data are representative of 3 independent experiments. Figure courtesy of CC Harnett.

The 1000 µM panel depicts typical cell cycle distribution for the Sp2/0 cell line. The peak over 50 MFI represents the G_0/G_1 peak (1 copy of the diploid DNA content), the peak over 100 MFI is the G_2/M peak (2 copies of the diploid DNA content), and the region between the

two is the S phase (between 1 and 2 copies of the diploid DNA content). Cells found below the 50 MFI peak are classified as sub-G_1 and considered dead by virtue of containing less than the normal diploid DNA content. When cells were cultured in medium containing less than 1000 μM glutamine, we observed that the number of events decreased in the S and G_2/M phases and increased in the G_1 phase. A sub-G_1 peak is also observed at glutamine concentrations under 50 μM. These data indicate a decrease in proliferative capacity, likely due to a block in G_1, and an increase in cell death after 24h of culture in glutamine limiting conditions.

The next experiment was designed to assess whether a critical threshold of glutamine concentration was required for the maintenance of cell viability. Cells were seeded at a density of $4x10^5$ cells/mL in medium containing a range of glutamine concentrations, cultured for 24h, and the number of membrane-intact cells was determined using the trypan blue dye exclusion assay. As shown in figure 3.3, the percentage of viable cells decreased drastically when the glutamine concentration in the medium was below 100 μM.

These results show that a concentration of glutamine of at least 100 μM in the culture medium is required to ensure optimal cell viability under our experimental conditions.

To confirm the effect of Gln concentrations on cell viability, we first examined cell morphology. To this end, cells were stained with acridine orange and with ethidium bromide (figure 3.4, panel A). When cells were cultured in medium containing 1000 μM or 100 μM glutamine, the majority of cells stained green, had the circular shape expected from viable B cells (215) and excluded ethidium bromide, indicating that they have maintained membrane integrity. However, when the glutamine concentration in the medium was less than 100 μM (25 μM and 8 μM), cells stained red (single stain) or yellow (colocalization of green and red),

indicating that they have lost their membrane integrity, they lost the regular circular shape, and demonstrated the characteristic "popcorn" shape of apoptotic cells (216).

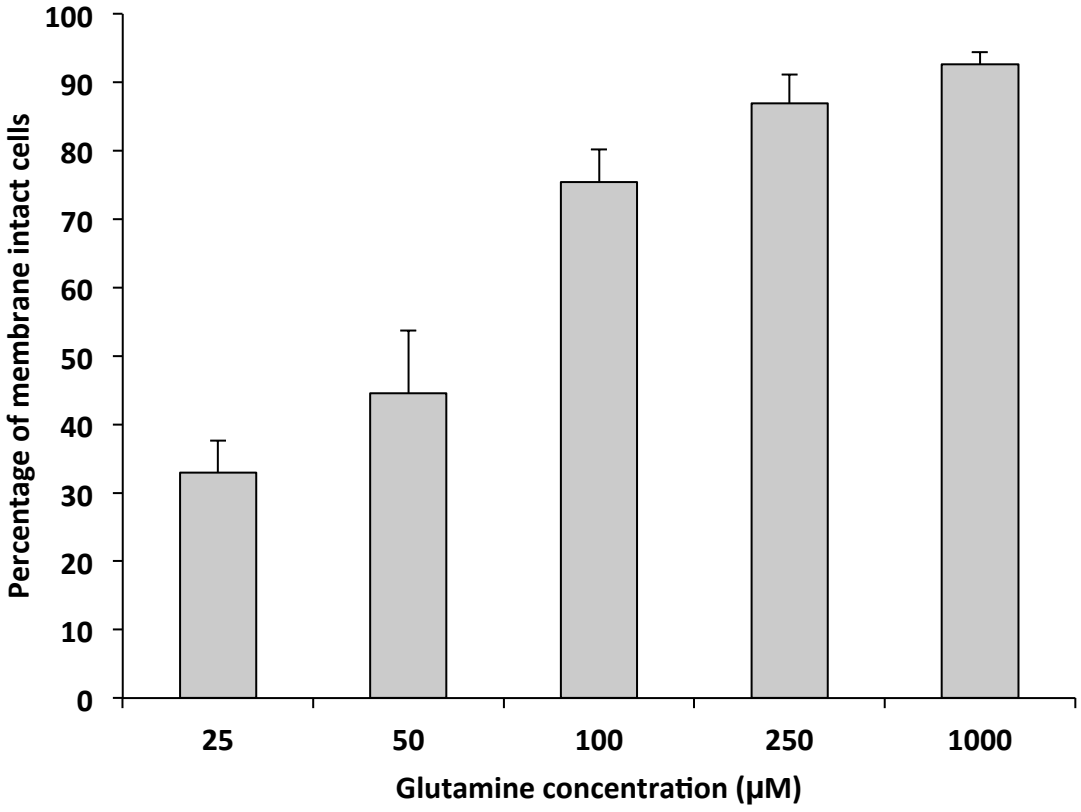

Figure 3.3 - Glutamine Concentration Affects Cell Viability

Sp2/0 cells were cultured for 24h in indicated glutamine concentrations. The data are the average percentage of membrane intact cells ± standard deviation of 5 independent experiments. Statistical significance was assessed by paired two-tailed t-test, and all groups are statistically different from each other with a confidence of $p<0.01$. Statistical analysis by one-way ANOVA showed statistical significance of all groups with the exception of 1000 μM vs 250 μM, with a $p<0.05$.

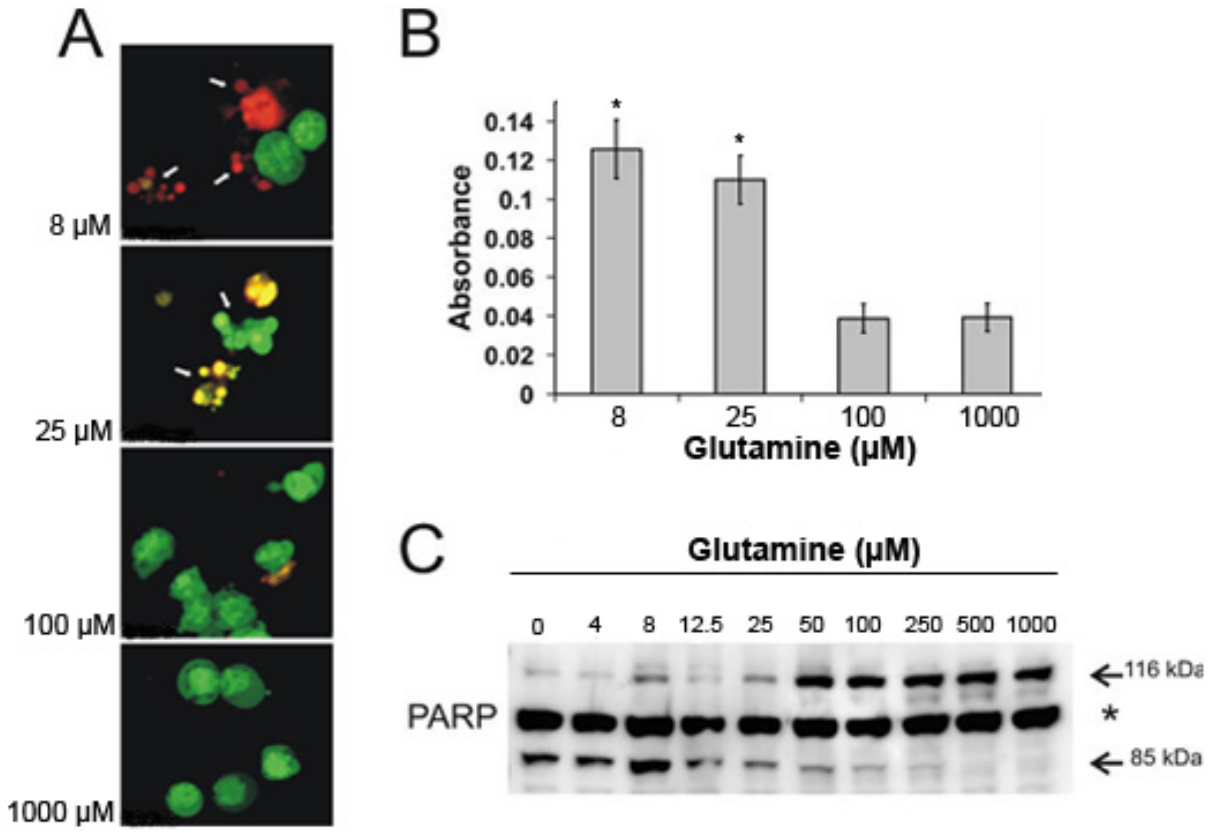

Figure 3.4 - Micromolar Levels of Glutamine Trigger Apoptosis

Cells were cultured in medium supplemented with the indicated glutamine concentrations for 24h. A) Cells were stained with acridine orange (green) and ethidium bromide (red). The arrows show apoptotic cells. Panels are representatives of 3 independent experiments. B) Protein extracts were used in an *in vitro* caspase-3 peptide cleavage assay. Data is the average ± SD of 3 independent experiments. Statistical analysis was done by one-way ANOVA with Scheffé's *ad hoc* test with * $p<0.05$ C) Picture of a Western blot performed on protein extracts using a PARP-1 antibody. Panel is representative of 3 independent experiments; * indicates an unknown protein cross-reacting with the antibody. Figure courtesy of M. Mallory.

One defining aspect of apoptosis is the activation of caspase-3, a protease playing an important role in the limited proteolysis of cellular proteins that in turn leads to the morphological changes characteristic of this type of cell death. The activity of caspase-3 was assayed using a colorimetric peptide cleavage assay. As shown in figure 3.4B, low caspase activity levels were measured in cells cultured in medium supplemented with 100 and 1000 µM

glutamine. This is consistent with our prior observations that the majority of the cells remain viable under these conditions (figure. 3.1). When available glutamine dropped below the threshold concentration of 100 μM, as shown in the 8 μM and 25 μM conditions, the level of caspase activity increased sharply. This was expected since we observed an abundance of apoptotic cells under these conditions (figure 3.4, panel A).

Enzyme activity seen *in vitro* is not always translated *in vivo*. The next experiment was designed to assess whether *in vivo* markers for apoptosis were present under glutamine limiting conditions. PARP-1 was the first identified caspase target (217), has been reported to be cleaved *in vivo* by caspase-3/7 and PARP-1 cleavage is considered a hallmark of apoptosis (218). Proteins extracted from cells cultured for 24h in the indicated concentration of glutamine were processed for Western blot analysis, the results of which are presented in figure 3.4C. When the glutamine concentration is high (1000 μM), the full length 116 kDa form of PARP-1 was present with little to no presence of the 86 kDa cleaved form of PARP-1. The cleaved form appeared faintly in the 250 μM condition. This cleaved band became progressively more intense as the concentration of glutamine decreased and the full-length 116 kDa band concurrently became less intense. The 86 kDa band appeared in the same glutamine concentrations where the percentage of viable cells began to decrease (figure 3.1) suggesting an inverse dose-dependent relationship between glutamine concentration and PARP-1 cleavage.

When the results of figures 3.1, 3.2 and 3.3 are examined jointly, they indicate that there is a threshold concentration of glutamine which modulates Sp2/0 cell behaviour. At 100 μM, cells are not proliferating, but viable. Below this concentration, cells are not viable and glutamine is limited for survival. Above this threshold, cells are viable and proliferating. It should be noted that while there is no increase in cell density at 100 μM, it is possible that cells

have experienced a delay in proliferation that could have been detected at a later time point. However, this is unlikely without glutamine supplementation as Sp2/0 cells utilize glutamine rapidly and would likely exhaust the available glutamine and eventually undergo apoptosis.

The morphology, loss of membrane integrity and *in vitro* and *in vivo* caspase-3 activity assays results presented in figure 3.4 are sufficient to support the conclusion that glutamine limitation triggers apoptotic cell death.

3.1.2 — Glutamine Limitation and Starvation Trigger Distinct Signalling Pathways

GADD-153 is transcription factor expressed in times of amino acid starvation, mitochondrial and endoplasmic reticulum stress (186, 219-222). GRP78 is a chaperone protein which contributes to the ER stress response and is co-expressed with GADD-153 in the unfolded protein stress response (223, 224) GADD-153 was previously shown to be upregulated under conditions of glutamine deprivation (188). To get a better understanding of the response elicited by glutamine limitation, Western blot analysis was used to determine the effect of glutamine concentration on the levels of GADD-153 and GRP78 (figure 3.5).

There was no significant change in the levels of GRP-78 protein in glutamine limitation by Western blotting, suggesting that the cells did not undergo ER stress (figure 3.5). On the other hand, glutamine limitation caused a dramatic increase in GADD-153 levels. GADD-153 was expressed in a range of glutamine concentration of 0.004 to 250 μM. GADD-153 was not expressed when cells were cultured in medium which was not supplemented with glutamine, nor was it expressed when the culture medium contained glutamine at concentrations of 0.5 mM or

more. These findings indicated that, in Sp2/0 cells, the induction of GADD-153 requires the presence of a limited amount of glutamine. At higher glutamine concentrations, GADD-153 is repressed, in accordance with previous studies (188, 212, 213). On the other hand, a 24h glutamine starvation does not lead to GADD-153 expression. When cultured in medium not supplemented with glutamine, Sp2/0 cells would undergo apoptosis before the upregulation of GADD-153 could occur (53). Interestingly, the range of glutamine concentrations where GADD-153 is expressed is also the range of concentrations of glutamine that have been previously shown to either limit proliferation or to lead to apoptosis (figures 3.1 to 3.4).

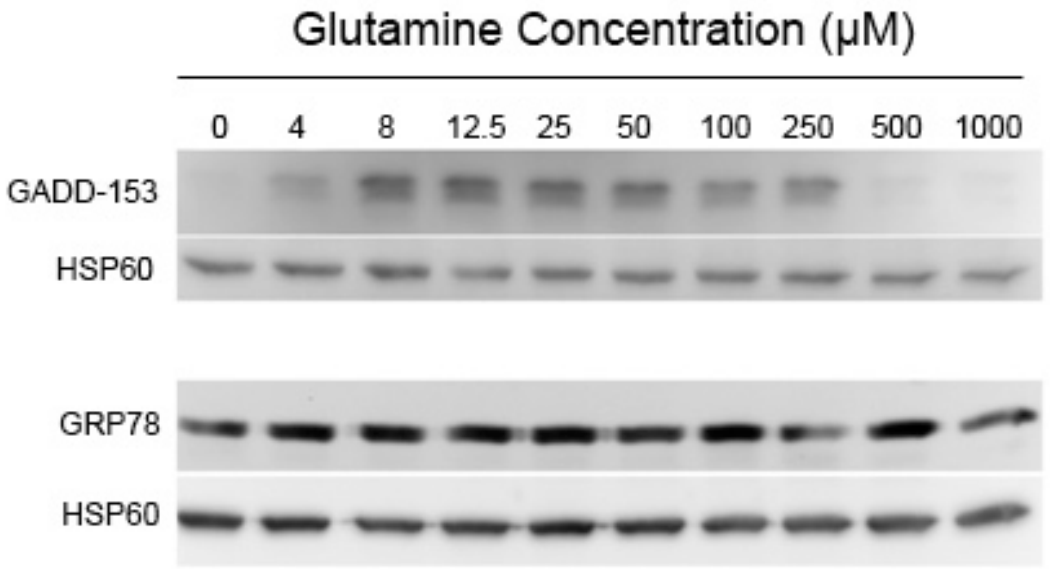

Figure 3.5 - Glutamine Availability Modulates GADD-153 Expression

Protein extracts from cells cultured for 24h in the indicated glutamine concentrations were processed for Western blot analysis and probed with the indicated antibodies. Data are representative of 3 independent experiments. Figure courtesy of M. Mallory.

Previous work from our laboratory has shown that, in Sp2/0 cells, apoptosis is triggered within 30 min of glutamine starvation, as measured by cytochrome c and SMAC release into the cytosol and caspase-3 activity (53). Therefore, we reasoned that the rapid cell death program triggered in these cells upon glutamine starvation may have prevented the initiation of a full stress response, including the induction of GADD-153 expression. If this were the case, then simply blocking the apoptotic program with a caspase inhibitor should restore the stress response and GADD-153 expression. To test this idea, Sp2/0 cells were cultured for 24h in medium not supplemented with glutamine (starvation group), in medium containing 25 μM glutamine (glutamine limited group), and in medium containing 4 mM glutamine (control). For each group, cells were either supplemented with the caspase inhibitor Z-VAD-fmk or an equivalent amount of DMSO.

When Sp2/0 cells were cultured in medium deprived of glutamine, 4.77 % of the population retained their membrane integrity (figure 3.6). This was not statistically different in the DMSO-treated population, with 5.06 % of cells maintaining integrity. In the Z-VAD-fmk-treated population, 33.75 % of cells were membrane intact. This was expected, since it had already been established that glutamine deprivation triggers caspase activation in Sp2/0 cells (53).

When Sp2/0 cells were cultured in medium containing 25 μM glutamine, cell viability was considerably higher than in the glutamine-starved group. The proportion of viable cells in the Gln-limited and DMSO control was not significantly different: 36.02% in Sp2/0 cells, and 34.32% in DMSO-treated cells. However, in the presence of Z-VAD-fmk, there was a significant increase in viability compared to the two control groups. Since Z-VAD-fmk is a pan-caspase

inhibitor, this finding was expected because of the observation of increased caspase-3 activation in cells cultured in medium containing 25 μM glutamine (figure 3.4B, C).

There was no statistical difference between the treatment groups in the 1000 μM glutamine concentration.

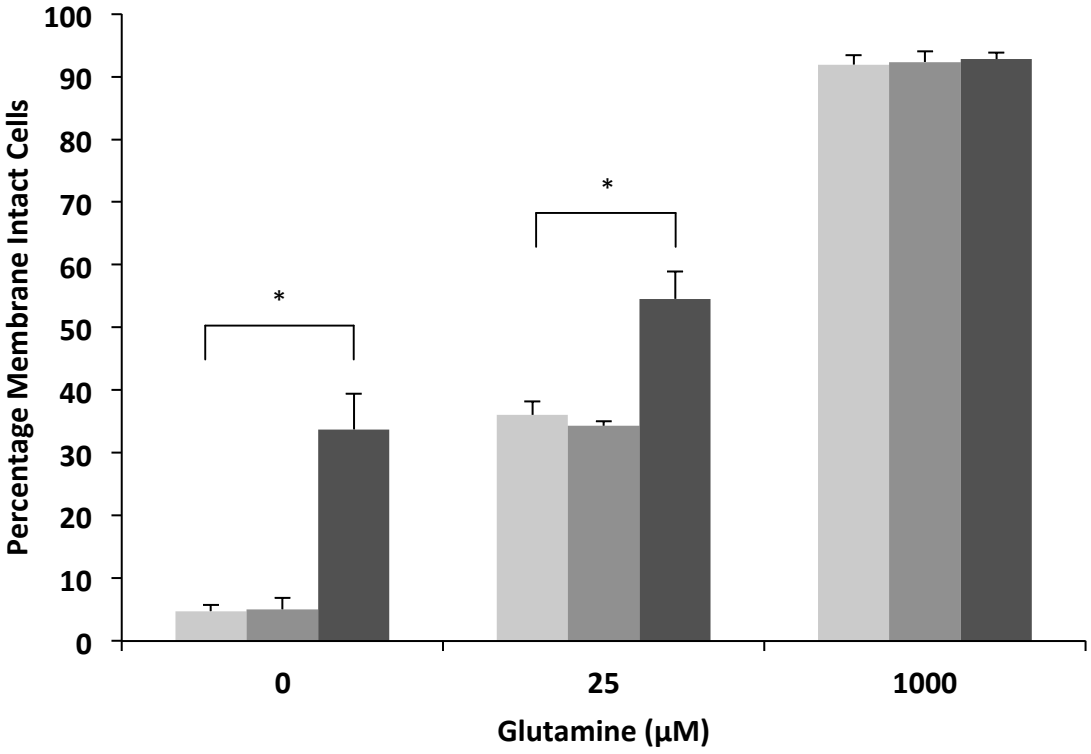

Figure 3.6 - The Additive Effect of Micromolar Glutamine Levels and Caspase Inhibition on Cell Viability

Cells were cultured for 24h in the indicated concentrations of glutamine with or without 10 μM Z-VAD-fmk or the equivalent amount of DMSO. Cells were then counted by trypan blue exclusion assay. Data represents the average ± SD of 3 independent experiments. * Statistical significance of $p<0.01$ by one-way ANOVA with Scheffé's post hoc test. Pale gray are untreated cells, dark grey are DMSO-treated cells and black is Z-VAD-fmk-treated cells.

These results indicated that caspase inhibition in conjunction with a micromolar concentration of glutamine had an additive protective effect and that the protective effect afforded by caspase inhibition alone in glutamine deprivation was similar to that afforded by the 25 μM glutamine concentration. Our previous results (figure 3.5) showed that GADD-153 was expressed at the 25 μM glutamine concentration, and so we investigated whether caspase inhibition would have any effect on the expression of GADD-153.

As shown in figure 3.7 and consistent with the results in figure 3.5, there was little to no expression of GADD-153 without glutamine supplementation of the culture medium or in the 1000 μM glutamine condition, irrespective of whether DMSO or with Z-VAD-fmk had been added to the culture.

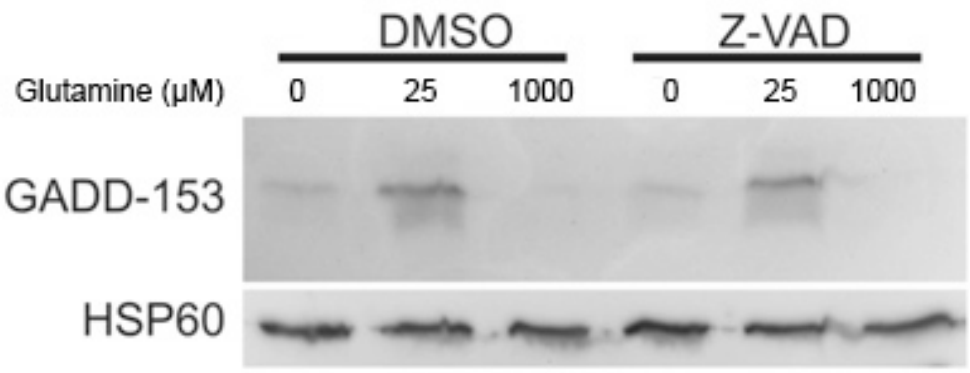

Figure 3.7 - Caspase Inhibition Does Not Influence GADD-153 Expression Following Glutamine Limitation

Western blot analysis performed on protein extracts from cells cultured for 24h in medium containing the indicated glutamine concentrations. Data is representative of 3 independent experiments. Figure courtesy of M. Mallory.

Again in line with results shown in figure 3.5, GADD-153 is expressed in the 25 μM glutamine group treated with DMSO. Interestingly, it is also present in the 25 μM glutamine condition supplemented with Z-VAD-fmk but with no marked increase in intensity when

compared to the corresponding DMSO control. This suggests that caspases are not important for the induction of GADD-153 expression and, by extension, for the stress response triggered in glutamine-starved/limited cells.

The loss of mitochondrial integrity is a major event in several apoptotic pathways, and is subject to regulation by the balance of pro- and anti-apoptotic proteins of the Bcl-2 family (225). Our research group has previously shown that Sp2/0 cells have few anti-apoptotic Bcl-2 family members, with Mcl-1 being expressed at the highest level (figure 1.8). Moreover, the overexpression of the Bcl-2 family member Bcl-xL is sufficient to significantly protect glutamine-starved Sp2/0 cells against the induction of apoptosis (110, 197). We next designed experiments to assess the effect of Bcl-xL overexpression in the stress response triggered by glutamine limitation in Sp2/0 cells.

As shown in figure 3.8, ectopic Bcl-x_L expression is sufficient to protect Sp2/0 cells against cell death caused by glutamine limitation or starvation. In conditions of glutamine deprivation, the control group transfected with the pTEJ8 vector had a proportion of cells with intact membranes of 2.6%, while for the cells transfected with Bcl-x_L, this proportion rose to 33.0%. When transfected cells were cultured in medium containing 25 μM of glutamine, viability was significantly increased in both cases: the percentage of viable cells was 32.34% for pTEJ8-transfected cells and 68.83% for Bcl-x_L-transfected cells. Interestingly, there was no statistically significant difference in cell viability between glutamine-deprived Sp2/0 overexpressing Bcl-x_L and Sp2/0 cells containing the vector control and cultured under glutamine -limited conditions.

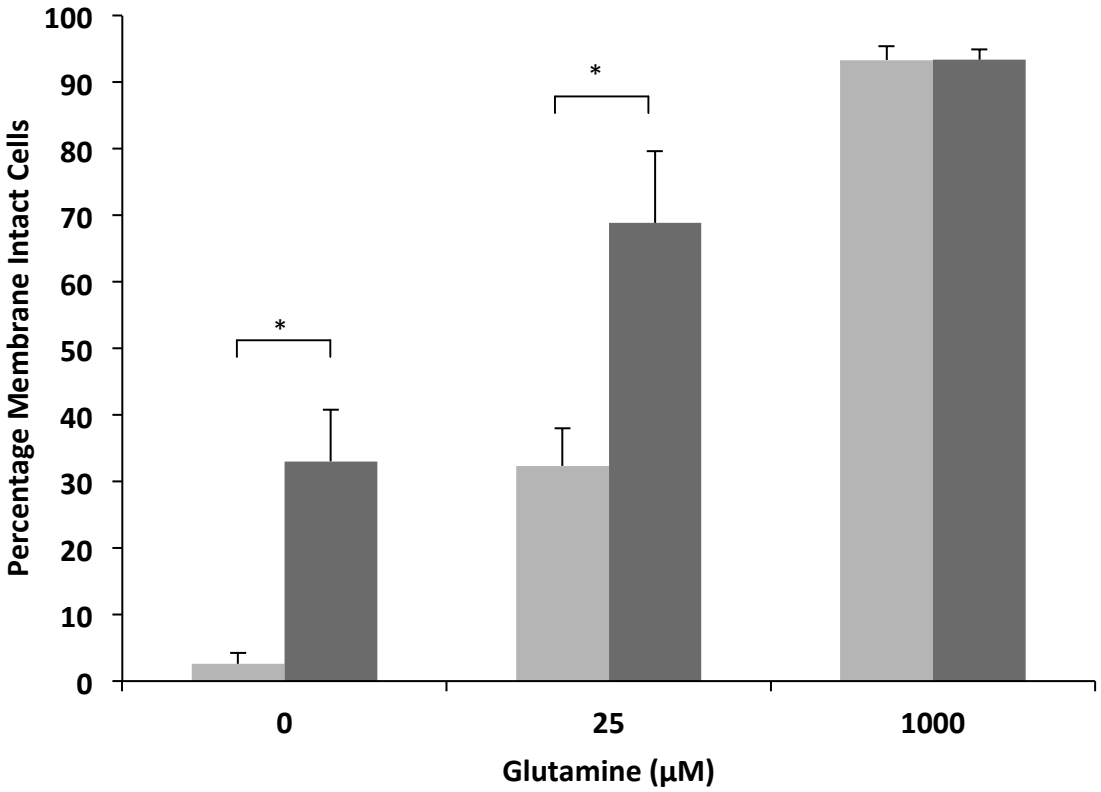

Figure 3.8 - Bcl-X_L Overexpression and Micromolar Amounts of Glutamine Have an Additive Protective Effect

Sp2/0 cells transfected with either the empty vector pTEJ8 or with the vector containing a cDNA encoding Bcl-x_L were cultured for 24h in medium containing the indicated concentrations of glutamine (111). Cells were then counted by trypan blue exclusion assay. Data represents the average ± SD of 3 independent experiments. Statistical significance ($p<0.05$ one-way ANOVA with Scheffé's post hoc test) is indicated by the following symbols for paired concentrations: * pTEJ8 0 mM glutamine vs Bcl-x_L 0 mM glutamine, ¶ pTEJ8 25 µM glutamine vs Bcl-x_L 25 µM glutamine. The pTEJ8 cells are pale grey and the Bcl-x_L are in black.

Protein extracts for each treatment group were analyzed for GADD-153 expression by Western blotting, as shown in figure 3.9. As expected in light of the results presented in figures 3.5 and 3.7, GADD-153 expression was observed in the vector-control Sp2/0 cells cultured in medium containing 25 µM glutamine. Interestingly, GADD-153 expression was detected in both the glutamine-deprived and the 25 µM glutamine treatment groups in Bcl-x_L-transfected cells.

Bcl-x_L is an anti-apoptotic member of the Bcl-2 family of protein that interacts with pro-apoptotic Bcl-2 family members to prevent the formation of pores on the mitochondrial outer membrane. Its presence would serve to prevent the release of cytochrome c and SMAC/Diablo from the mitochondria, preventing intrinsic apoptotic pathway activation (102, 202, 225). The presence of a GADD-153 signal in the glutamine-deprived cells transfected with Bcl-x_L confirms our previous data indicating that mitochondrial integrity is important to the stress response triggered by glutamine limitation (35).

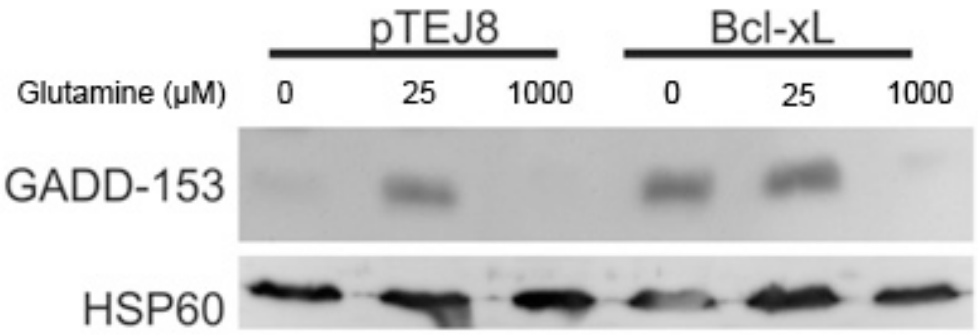

Figure 3.9 - Increased GADD-153 Expression in Glutamine-Deprived Bcl-X_L-Transfected Cells

Western blot analysis performed on protein extracts from cells cultured for 24h in medium containing the indicated glutamine concentrations. Anti-HSP60 was used as loading control. Data are representative of 3 independent experiments. Figure courtesy of M. Mallory.

The results presented thus far indicate that the restriction of glutamine in the culture medium affects cells viability and proliferation in a dose-dependent manner at 24h and that the cells that were not viable underwent apoptosis. During that same time period, a stress response to glutamine limitation was induced, as revealed by the induction of the expression of GADD-153. Additionally, while caspase inhibition in glutamine-starved Sp2/0 cells could increase the number of viable cells to the same amount seen in the glutamine-limited culture, it had no effect

on GADD-153 expression. Finally, Bcl-x_L overexpression did have an effect on GADD-153 expression, allowing for its expression in glutamine-deprived conditions and implicating the mitochondria in the stress response triggered by glutamine limitation in Sp2/0 cells.

3.1.3 — Chronology of Responses to Glutamine Limitation

The data shown so far indicate that a stress response was initiated upon glutamine limitation in Sp2/0 cells. Moreover, this stress response is not seen in glutamine-starved Sp2/0 cells, indicating that a minimal threshold of glutamine is required. Since all of the previous studies were performed at 24h endpoint, we set out to expand our investigation of this phenomenon by performing time-course experiments in which GADD-153 expression as well as various apoptotic markers were examined.

For these experiments, we chose a glutamine concentration of 25 μM because at that concentration, GADD-153 was highly expressed (figure 3.5) and a significant proportion of the cell population was still viable after 24h of culture. This indicated that at that concentration, the stress response had been initiated and had partially succeeded in protecting some cells from apoptotic cell death. The first experiment we devised was to establish the amount of time for which the Sp2/0 cell population could be exposed to 25 μM of glutamine before the activation of the apoptotic death program. Sp2/0 cells cultured for 24h in limiting glutamine concentrations die by apoptosis (figure 3.4). In order to establish the time frame required for the commitment to the death program, Sp2/0 cells were cultured in medium containing 25 μM for set time intervals before the culture medium was supplemented with 4 mM of glutamine. The cells were returned to culture for the remainder of the 24h period then viability was assessed by a trypan blue assay.

The percentage of dead cells at 24h is taken as an estimate of the percentage of cells committed to the death program, at the time of glutamine supplementation.

As shown in figure 3.10, after 4h of culture in 25 μM concentration of glutamine, a progressive increase in the number of non-viable cells was observed, with 19.9% at 8h, 28.0% at 12h, and 65. 9% at 24h. The 4 mM glutamine treatment group was included as a control: as expected, less than 10% of cells in culture (7.1%) had lost their membrane integrity. Even after 12h in culture, the viability of the majority of the cell population could still be rescued. By comparison, 79.6 % of the cells in the control treatment group consisting of cells starved of glutamine for 4h had lost their membrane integrity and is in line with earlier observations made by our research team (53).

It had been previously established that glutamine deprivation triggers cell death via the intrinsic apoptotic pathway (53). We sought to characterize the biochemical events leading to apoptosis in cells cultured in medium containing a limiting amount of glutamine. In several apoptotic pathways, executioner caspases (such as caspase-3) are activated by cleavage by initiator caspases (such as caspase-9) (202, 218, 225).

We first analysed caspase-3 activation. Protein extracts from Sp2/0 cells that were cultured in medium containing 25 μM over a 24h period were probed for the presence of the activated, cleaved form of caspase-3 (figure 3.11). The cleaved form of the protein was detected at the 4h time point, but unexpectedly it was not apparent at the 8h time point. The cleaved form of caspase-3 was not detected again in protein extracts until the 24h time point. The levels of the HSP60 control were constant, indicating that the absence of the cleaved caspase-3 protein at the 8 and 12h time points was not the result of improper sample loading of the gel.

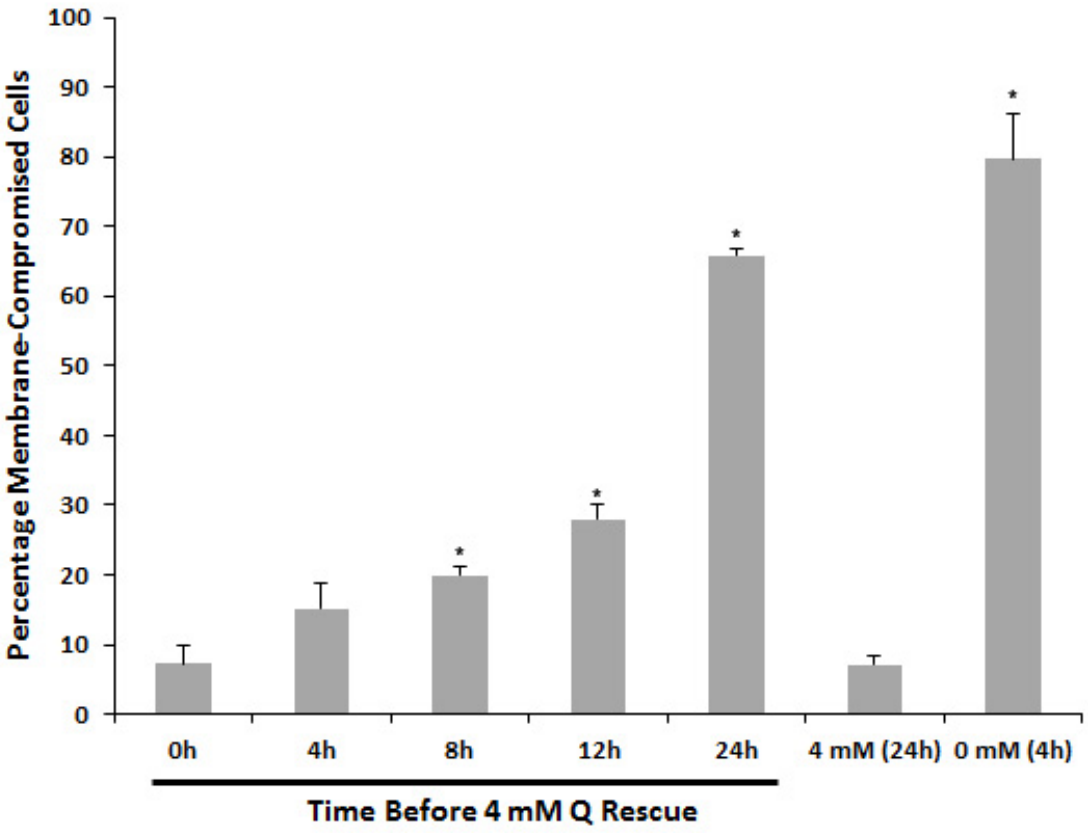

Figure 3.10 - Micromolar Levels of Glutamine Protects Cells From Cell Death

Sp2/0 cells were cultured in 25 µM glutamine for the indicated length of time before the glutamine was adjusted to 4 mM. Cells were counted by trypan blue exclusion assay 24h after the start of the experiment. Data represents the average ± SD of 3 independent experiments. Statistical significance (vs T = 0h) was assessed by ANOVA + Scheffé's *ad hoc* test with * $p<0.05$.

While the cleaved form of caspase-3 has been reported to be the active form of the enzyme, we sought to confirm these results by performing a caspase-3 colorimetric activity assay. Sp2/0 cells were cultured in medium containing 25 µM glutamine over a 24h period and protein extracts were prepared and subjected to an *in vitro* synthetic peptide cleavage assay. The results obtained are shown in figure 3.12. In accordance with previous results (figure 3.5), there was little cleavage of the DEVD peptide in the extracts from cells cultured in medium containing 1000 µM glutamine. We observed a statistically significant increase in caspase-3 activity after 4h

of culture in medium supplemented with 25 µM glutamine. Interestingly, there was a statistically significant decrease in caspase-3 activity after 8h in culture when compared to the 4h time point. Caspase-3 activity remained low for several hours, and was statistically significantly increased at the 24h time point, where the greatest amount of caspase-3 activity was measured. These results confirmed the findings presented in figure 3.11.

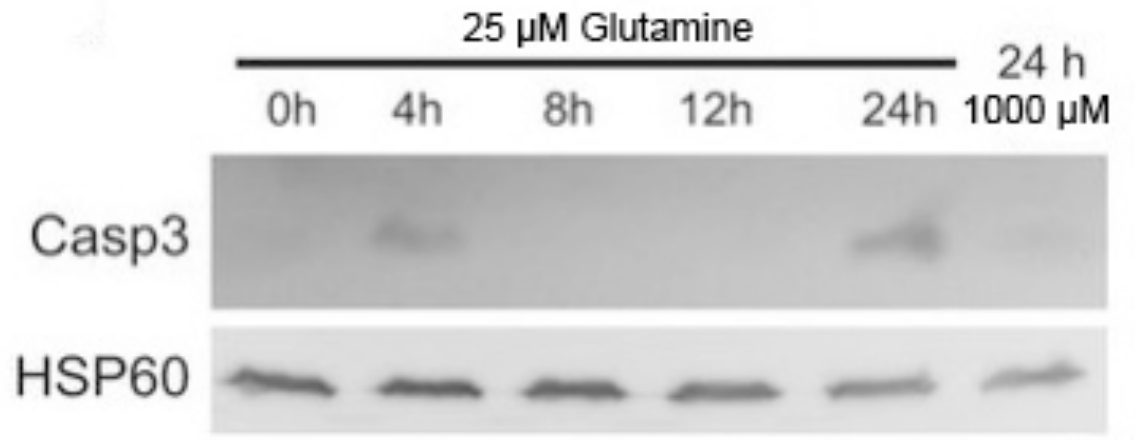

Figure 3.11 - Effect of Micromolar Glutamine Levels on Caspase-3 Cleavage

Western blot analysis of protein extracts from cells cultured over a period of 24h in medium containing 25 µM glutamine and probed with an anti-caspase-3 antibody recognizing the cleaved form of the protease. An anti-HSP60 antibody was used as a loading control. Data are representative of 3 independent experiments. Figure courtesy of M. Mallory.

The *in vitro* activity assay results were confirmed *in vivo* by the analysis of PARP cleavage. In figure 3.13, it can be observed that the cleaved form (85 kDa) of PARP-1 was absent at the beginning of the time course (0h) and in the 1000 µM glutamine condition which is consistent with the low activity of caspase-3 in these samples (figures 3.4, 3.11 and 3.12). The 85 kDa cleavage product was observed at the 4h time point. Interestingly, the intensity of the signal neither increased nor disappeared at the 8h or 12h time points, suggesting that little or no further

cleavage of PARP-1had occurred. A more intense cleaved PARP band was finally seen after 24h, in agreement with a much higher caspase-3 activity in this sample.

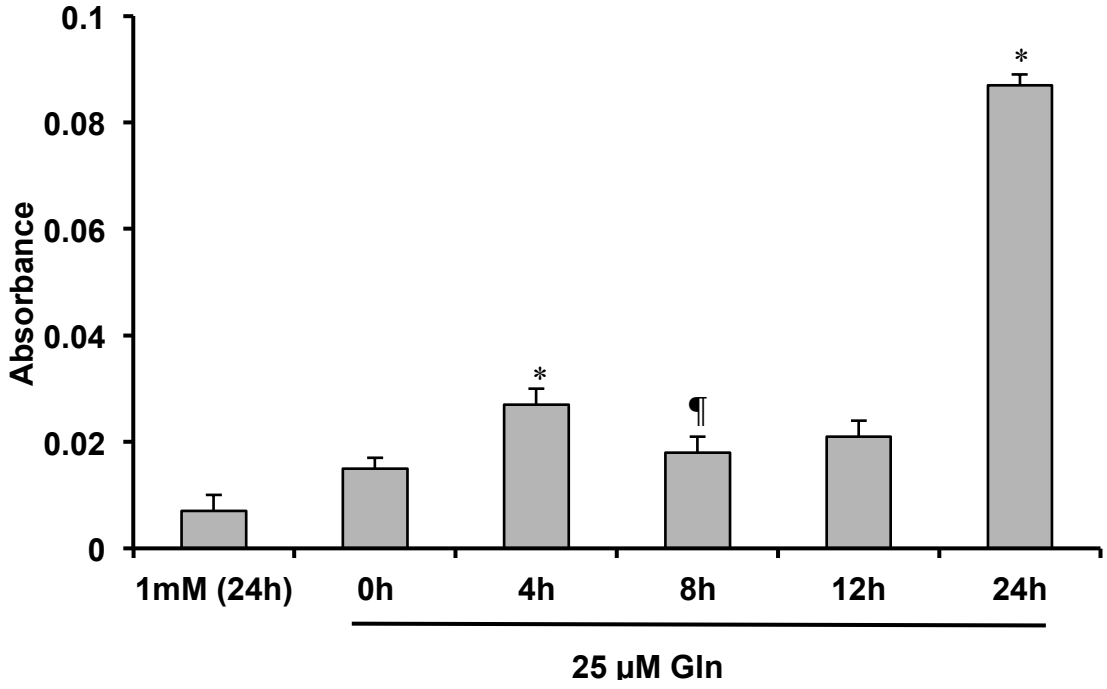

Figure 3.12 - Micromolar Levels of Glutamine Affect Caspase-3 Activity

Protein extracts were used in an *in vitro* caspase-3 peptide cleavage assay. Data are the average ± SD of 3 independent experiments. Statistical analysis was done by one-way ANOVA with Scheffé's *ad hoc* test with * $p<0.01$ compared to T=0h and ¶ $p<0.05$ compared to T=4h.

Figures 3.11 to 3.13 clearly show that caspase-3 is not only in its cleaved form, active both *in vitro* and *in vivo* at the 4h time point, but that the activity is decreased at 8h. In the glutamine deprivation model, caspase-3 activation was induced as early as 30 min after glutamine withdrawal, and inevitably led to cell death by apoptosis by 4h (53). These results show that the presence of limiting amounts of glutamine can limit caspase-3 activity and delay

the onset of death. Alternatively, these results may indicate that there is a subset of the population that is more sensitive to the limited amounts of glutamine present in the culture medium and undergo apoptosis within 4h. In this scenario, the rest of the population would not be affected until approximately 12h in culture.

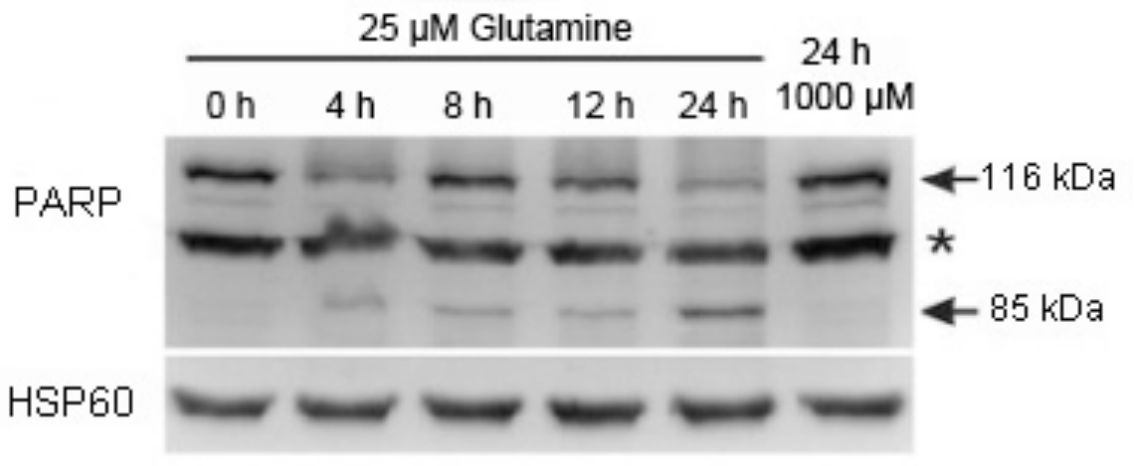

Figure 3.13 - Micromolar Glutamine Levels Delay the Onset of PARP-1 Cleavage

Western blot analysis of protein extracts from cells cultured over a period of 24h in medium containing 25 µM glutamine, and probed with anti-PARP-1 antibody recognizing both the cleaved and uncleaved forms of PARP-1. An Anti-HSP60 antibody was used to control for gel loading. Data are representative of 3 independent experiments. The star (*) indicates an unknown protein which cross-reacted with the PARP antibody. Data are representative of 3 independent experiments. Figure courtesy of M. Mallory.

Work previously done by our research team demonstrated that the intrinsic apoptotic pathway was triggered rapidly in glutamine-deprived Sp2/0 cells (53). We therefore set out to determine whether the induction of apoptosis under glutamine limiting conditions also involves the intrinsic pathway. The first assay performed was to assess the activity of caspase-9, the initiator caspase of the intrinsic pathway (225).

As shown in figure 3.14, there was no detectable increase in caspase-9 activity in the first 12h of culture in 25 μM glutamine. In fact, caspase-9 activation was only detected after 24h of culture, when the majority of Sp2/0 cells were not viable (figure 3.1). Since the caspase-9 activity assay did not provide any insight into the method of apoptosis activation, we assayed other indicators of apoptosis.

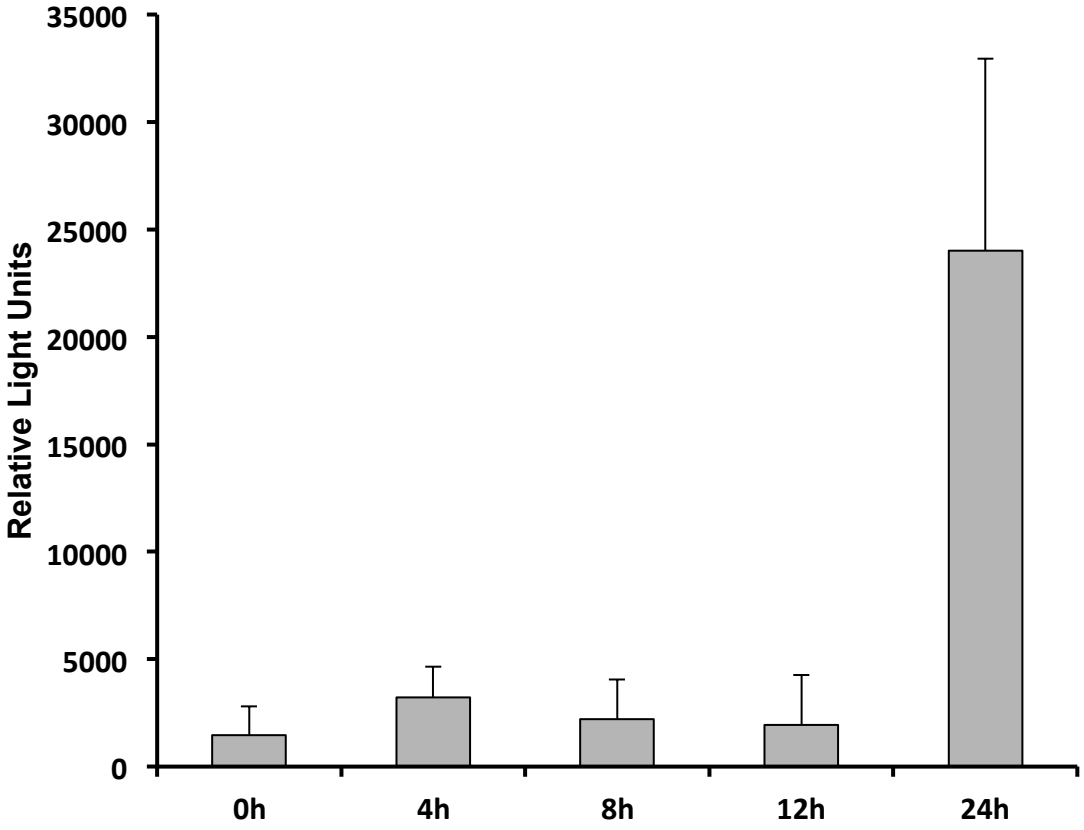

Figure 3.14 - Caspase-9 Is Not Active Early in the Stress Response

Protein extracts from Sp2/0 cells cultured over 24h in 25 μM glutamine were used in an *in vitro* caspase-9 fluorometric peptide cleavage assay. Data are the average ± SD of 3 independent experiments.

One of the upstream events leading to activation of caspase-3 in the intrinsic pathway is the release of cytochrome c from mitochondrial intermembrane space when the mitochondrial outer membrane is permeabilised. Cytosolic cytochrome c contributes to the activation of

caspase-9 via the formation of the apoptosome (53, 225). To determine the kinetics of cytochrome c release from the intermembrane space, cytosolic proteins were extracted from cells cultured for the indicated time intervals in medium containing 25 μM of glutamine, and subjected to Western blotting analysis.

Representative results from these analyses are shown in figure 3.15. There was little cytochrome c in the cytosol at the beginning of the assay, consistent with the low percentage of dead cells in the culture at this point (figures 3.10, 3.12-14). However, there was an appreciable increase in cytosolic cytochrome c at 4h followed by a decrease to baseline levels at 8h. This coincides with the activation profile of caspase-3 during the first 8h of cell culture in glutamine-limiting medium (figures 3.11-12). Interestingly, the levels of cytosolic cytochrome c rose again at 12h and 24h, results consistent with the activation of caspase-9 (figure 3.14).

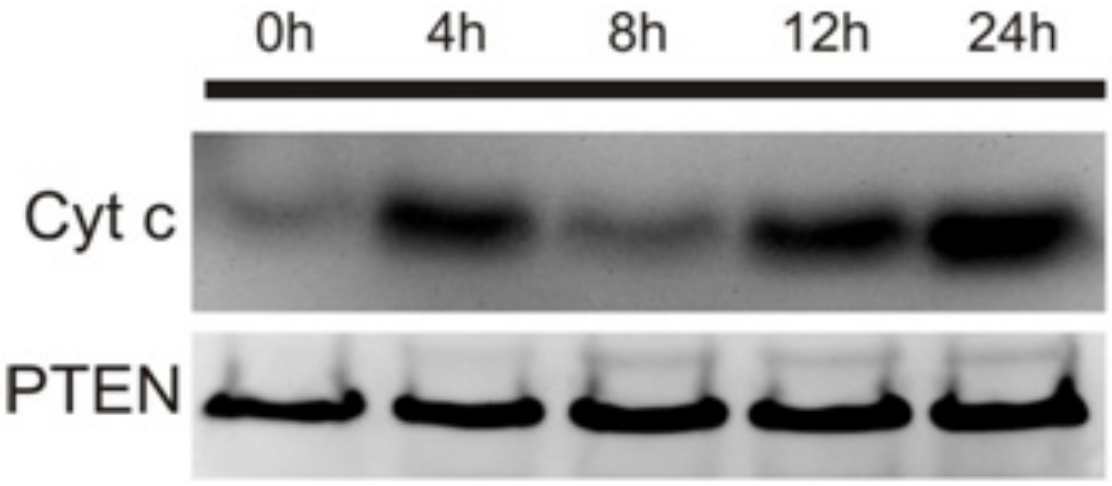

Figure 3.15 - Effect of Micromolar Glutamine Concentrations on the Cytosolic Release of Cytochrome C

Western blot analysis of cytosolic protein extracts from Sp2/0 cells cultured over a period of 24h in medium containing 25 μM glutamine and probed with an anti-cytochrome c antibody. An anti-PTEN antibody was used as loading control. Data are representative of 3 independent experiments. Figure courtesy of CC Harnett.

Because cytochrome c was leaking from the mitochondrial outer membrane, the mitochondrial transmembrane potential was assessed (figure 3.16).

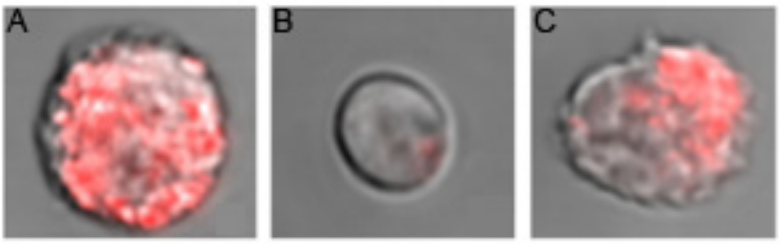

Figure 3.16 - Effect of Glutamine Limitation on the Mitochondrial Transmembrane Potential

Confocal microscopy pictures of cells cultured for 4h in medium containing varying concentrations of glutamine and stained with Mitotracker H_2ROS Red. a) 1000 µM glutamine, b) 0 mM glutamine, c) 25 µM glutamine. Data are representative of 3 independent experiments with on average 25 cells for each sample. Magnification = 630 x. Micrographs taken at lower magnification and showing clusters of cells can be found in Appendix A.1.

After 4h, cells that were cultured in medium containing 1000 µM glutamine were round in shape and had bright MitoTracker Red CM-H_2XRos staining (figure 3.16, panel A), indicating that they possessed healthy mitochondria that are capable of oxidizing the reduced dye. When Sp2/0 cells were deprived of glutamine for 4h, cells were noticeably smaller and were faintly stained with the Mitotracker dye (figure 3.16b). This was expected because previous work from our laboratory showed that Sp2/0 cells exhibit cytochrome c leakage as early as 1h after glutamine deprivation (53). However, as seen in Figure 3.16c, cells cultured for 4h in 25 µM glutamine had morphology and Mitotracker staining similar to those found in cells cultured in medium containing 1000 µM glutamine. This indicates that micromolar amounts of glutamine are sufficient for cells to maintain their mitochondrial membrane potential for several hours. The majority of cells at 4h in 25 µM glutamine maintained their mitochondrial membrane potential as

assessed by Mitotracker Red; considering that caspase-9 and caspase-3 were not highly active at and that the cells were viable at this point, this was to be expected.

Our previous results demonstrated that the induction of GADD-153 expression in Sp2/0 cells only occurs when the glutamine concentration in the culture medium is limiting (figures 3.5, 3.7 and 3.9). To better understand the dynamics of the stress response, GADD-153 expression was evaluated in the 24h time course. As shown in figure 3.17, GADD-153 was first expressed after 4h in culture in medium containing 25 µM of glutamine, and its expression increased over time, with the most intense expression at 24h. GADD-153 expression paralleled the increase in caspase-3 activation (figure 3.12) and the decrease in cell viability (figure 3.10). It is interesting to note that the late increase in caspase-3 activity coincided with the time when GADD-153 was most intense.

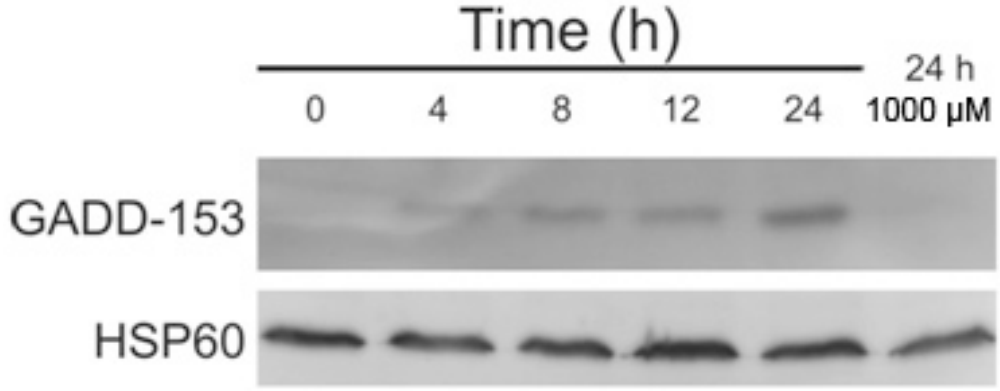

Figure 3.17 - Micromolar Amounts of Glutamine Affect GADD-153 Expression

Western blot analysis of protein extracts from Sp2/0 cells cultured over a period of 24h in medium containing 25 µM of glutamine. HSP60 was used as loading control. Data are representative of 3 independent experiments. Figure courtesy of M. Mallory.

3.1.4 — Distribution in the Cell Cycle

One interpretation of the data shown so far is that there are two separate populations in the culture, which could be distinguished by the caspase-3 activation profile when cultured in medium containing 25 μM glutamine: those with active caspase-3 at 4h and those with caspase activity at 12h. The next series of experiments were designed to assess whether two such populations existed. The first aspect that was considered was whether there were variants within the Sp2/0 cell population which could account for the differences in caspase activation (figure 3.18).

In order make that evaluation, clonal populations of Sp2/0 cells were obtained by limiting dilution and propagated. Each clonal population (A5, B1, B3, B4 and B5) with the parental line (AC1) were cultured for 24h in medium supplemented with 25 μM glutamine, rescued by 4 mM glutamine supplementation at the indicated time interval, and the commitment to death assessed by trypan blue exclusion assay as described previously. The results clearly show that there was no difference in the behaviour of the parental line and any of the clones. Thus, the presence of clonal variants in our original culture does not account for the biphasic induction of apoptosis observed in Sp2/0 cell cultured under conditions of glutamine limitation.

Interestingly, restriction of glutamine has been proposed recently to function as a metabolic checkpoint preventing cell cycle progression (226). Therefore, we assessed another possibility: that progression through a particular phase of the cell cycle could render the Sp2/0 more vulnerable to apoptotic cell death when cultured under limiting glutamine conditions.

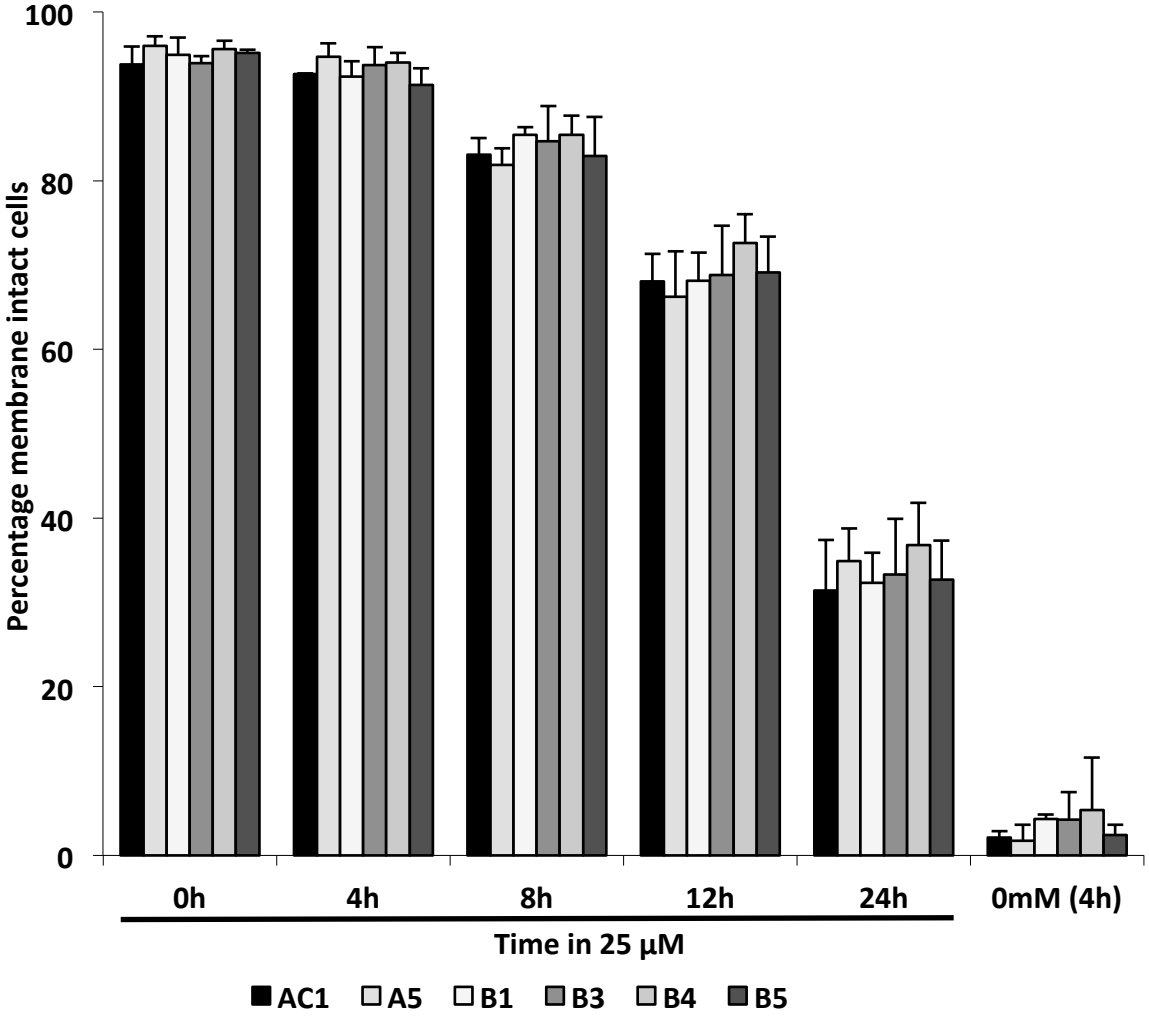

Figure 3.18 - Commitment to Death Is Not an Artefact of Clonal Selection

Cells were cultured in culture medium containing 25 µM glutamine for the indicated period of time before 4 mM glutamine was added to the medium. Mean percentage of cells not committed to death after culture at 400 000cells/mL in 25uMQ, with 4 mM Q added in at specified times. The AC1 is the parental line to which all clones (A5, B1, B3, B4 and B5) are compared. Average of three independent trypan blue exclusion assays.

In order to assess this possibility, cells cultured in medium containing 25 µM glutamine for different time intervals were harvested at the indicated time and processed for cell cycle

distribution analysis. As shown in figure 3.19, the percentage of cells in sub-G_1 increased progressively over time reaching 21.36% after 24h of culture in medium containing 25 µM glutamine. The percentage of cells in sub-G_1 at each of the time points after the start of culture is statistically distinct from the baseline (0h). The percentage of cells in sub-G_1 in the culture control condition, 24h in the presence of 4 mM glutamine, is not statistically distinct from the baseline value.

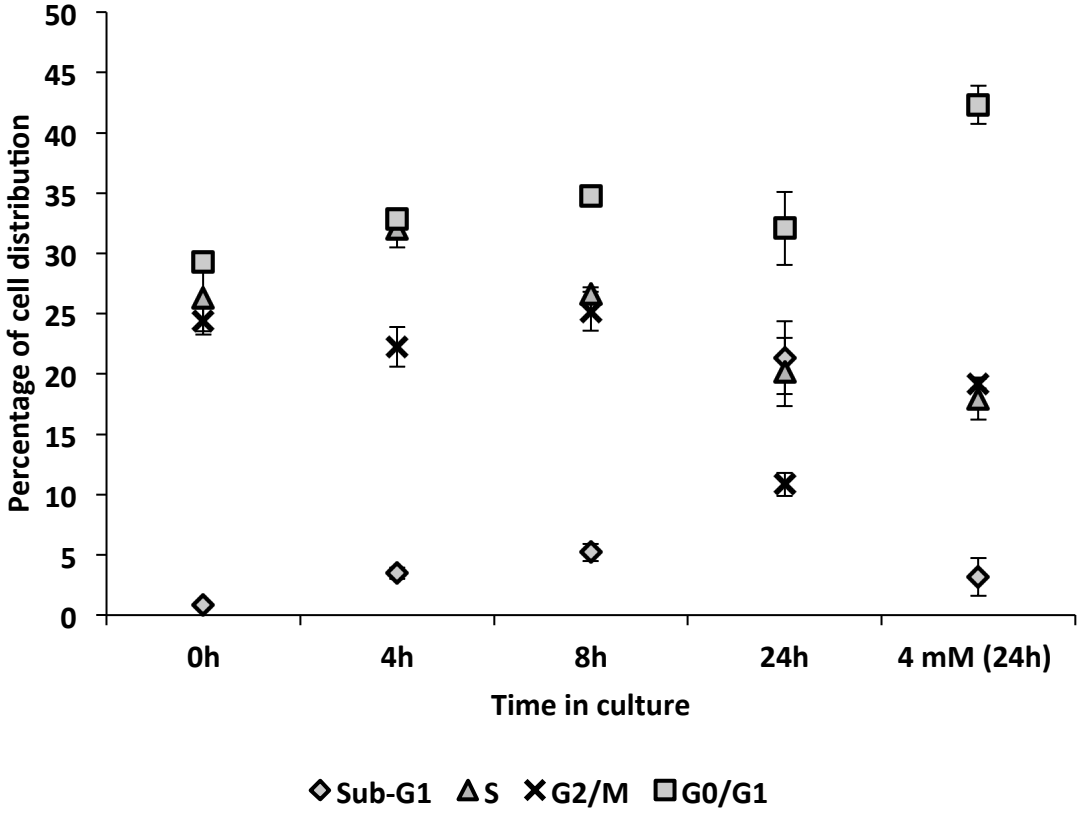

Figure 3.19 - Effect of Micromolar Glutamine on Cell Cycle Distribution

Sp2/0 cells were cultured in medium containing 25 µM glutamine over a period of 24h. Cells were collected at the indicated time points and processed for propidium iodide staining and flow cytometry analysis. Data represent the average ± SD of 3 independent experiments. Statistical significance was assessed by paired t-test presented in Appendix A.2.

At baseline, 29.28% of cells were in the G_0/G_1 phase, 32.86% at 4h, 34.74% at 8h and 32.05% at 24h. In the culture control condition, the proportion of cells in the G_0/G_1 phase is 42.31%. Only the culture control condition is statistically different from the baseline value, indicating that accumulation occurs only in this condition.

Cells that are proliferating will be found in the S phase and progressing into the G_2/M phase. For the S phase, 26.36% of cells are in this phase at baseline, with 32.00% at 4h, 26.58% at 8h and 20.17% at 24h. The difference is statistically significant at 24h compared to baseline and, when compared to the 4h time point, both the 8h and 24h percentages are statistically different. This difference is also observed when comparing the 24h time point to the 8h time point. The conclusion to be drawn is that after 4h of culture in medium containing 25 μM glutamine, fewer cells are progressing into the cell cycle.

For the G_2/M phase, 24.43% of cells are in this phase at baseline, 22.24% at 4h, 25.19% at 8h and 10.83% at 24h. The change at 24h is statistically different from the baseline, the 4h and the 8h time point values. The peak in cell proportion is observed at the 8h time point before a sharp decrease at 24h. Interestingly, the difference in the percentage of cells between the 8h and the 24h time point, 14.81%, is very similar to the difference between the same time points in sub-G_1, 16.17%.

The data presented in figure 3.19 shows that the proportion of cells in sub-G_1 peak gradually increased over the course of the 24h period. This was not surprising as our results indicated that cell viability was slowly decreasing over the 24h period when cultured in medium containing 25 μM of glutamine. While this steady increase in sub-G_1 was occurring, concurrent decreases were observed in the proportion of cells in both S and G_2/M phases; on the other hand,

the proportion of cells in G_0/G_1 was stable. These data suggest that the induction of apoptosis in cells cultured in the presence of 25 μM glutamine occurs preferentially in the cell population in S and G_2/M phases. It should be noted that it is possible that cells may also be completing the cell cycle through G_2/M to G_1 before undergoing apoptosis.

In order to test that hypothesis, several experiments were designed to assess which segment of the cell population was responsible for the increase in the sub-G_1 phase. The first were designed to attempt to synchronize the Sp2/0 cells. This would facilitate the identification of a cell cycle phase in which cells would be more susceptible to undergo apoptosis under stress due to glutamine limitation. Since the Sp2/0 cell line is very sensitive to toxic insults (53, 197, 200, 211), synchronization techniques which did not require the use cell cycle-interfering chemicals were chosen.

The first cell cycle synchronization procedure we chose was growth factor starvation. Preliminary work done by our research group had shown that, while serum withdrawal led to apoptotic cell death, Sp2/0 cells cultured in medium containing 4 mM glutamine and 0.1% serum stopped proliferating but remained viable for at least 24h.

As presented in figure 3.20, after 24h of culture in medium containing 1% serum and 4 mM glutamine (panel A), cells progressed through the cell cycle as expected and did not synchronize. Many different serum concentrations were assayed, as well as different culture times. A range of serum concentrations from 0.1% to 1% in medium containing 4 mM of glutamine were trialed with no accumulation in G_0/G_1 (not shown). The most promising experimental conditions, 48h culture in medium containing 4 mM of glutamine and 0.1% serum, did present an accumulation of cells in the G_0/G_1, had few cells in the S and G_2/M phase with

some cells in sub G_0 (figure 3.20b). However, when released from the synchronizing pressure by a return to normal culture conditions (5% serum/4 mM glutamine) for 24h (figure 3.20, panel C), a high proportion of cells in sub-G_1 was seen, making this experimental approach impractical. Serum starvation over 24h did not yield a synchronized population.

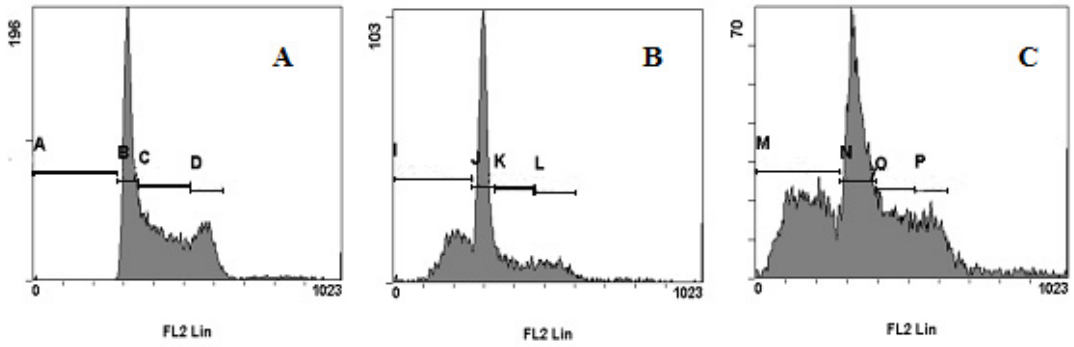

Figure 3.20 - Cell Synchronization by Serum Starvation

Sp2/0 cells were cultured in the indicated conditions for the indicated length of time before collection and subsequent EtOH fixation. Cellular DNA content was stained with propidium iodide and analysed by flow cytometry. Panel A: 24h 1% serum, panel B: 48h 0.1% serum and panel C: 48h 0.1% serum + 24h 5% serum. Gating identification: the sub-G_1 peak: A (1.7%), I (23.6%), M (29.1%), the G_0/G_1 peak: B (37.2%), J (37.5%), N (29.7%), the S phase peak: C (32.8%), K(12.5%), O (10.6%) and the G_2/M peak: D (17.7%), L (14.9%), P (10.7%).

We next tested centrifugal elutriation as a means to obtain synchronized cell cultures. Elutriation is a technique based on the principles of sedimentation to separate objects according to their size. Cells in a typical Sp2/0 culture can be found to be in every phase of the cell cycle; these cells have different physical sizes due to the increase in mass when cells enter the cell cycle in G_1, the differences in their DNA content as the genome is replicated in S phase and whether the two daughter cells have separated at the end of the G_2/M phase.

In centrifugal elutriation, there are two key pieces: the centrifuge to establish the centrifugal force and the counter flow going through the chamber (figure 3.21). The centrifuge is

run at a steady speed and the cells enter through the elutriation chamber with a counter flow of medium and form a gradient: the heaviest cells pellet, and the lightest cells are maintained in suspension by the current of the counter flow. By steadily increasing the counter flow rate, different segments of the population can be removed from the chamber and collected in fractions (227). In Figure 3.21, the white outlined cells would be collected in the first fractions, then by increasing the speed, the grey cells would be collected next, and the black-outlined cells would be collected last, if at all.

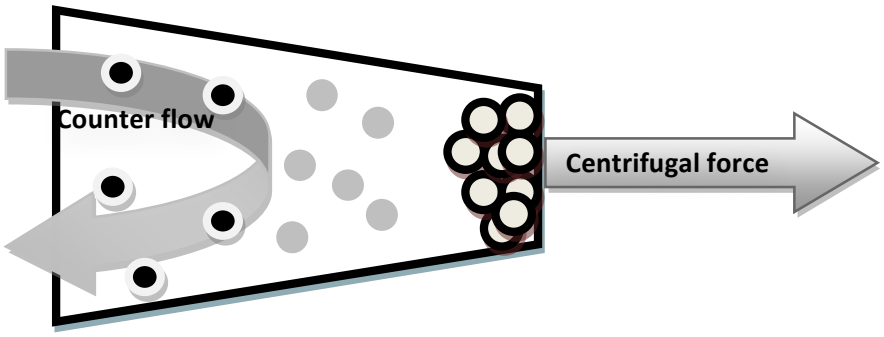

Figure 3.21 - Illustration of Centrifugal Elutriation Principle

The chamber is subjected to centrifugation which allows the cells coming into the chamber through the counter flow to form a gradient and/or pellet (black outline). The speed at which the counter flow is run through the chamber will remove cells according to their differences in mass, first the white-outlined black cells, then the gray cells.

Using this technique, I was successful in purifying Sp2/0 cells residing in the G_0/G_1 phase of the cell cycle, and the result is presented in figure 3.22. When a culture of Sp2/0 cells in the exponential growth phase was subjected to separation by centrifugal elutriation at a speed of 1800 RPM with a counter flow rate of 7mL/min, 72.07% of cells were found in the G_0/G_1 peak, with 8.98% in the S phase, 6.93% in the G_2/M phase and only 7.43% in the sub-G_1 phase. This indicated that centrifugal elutriation could be used as a means to enrich an Sp2/0 population for cells in the G_1 phase, enabling us to test the sensitivity of the cells to the effect of glutamine

limitation. Unfortunately, the experiment could not be performed due to mechanical failure of the centrifugal elutriator and the difficulty in obtaining replacement parts.

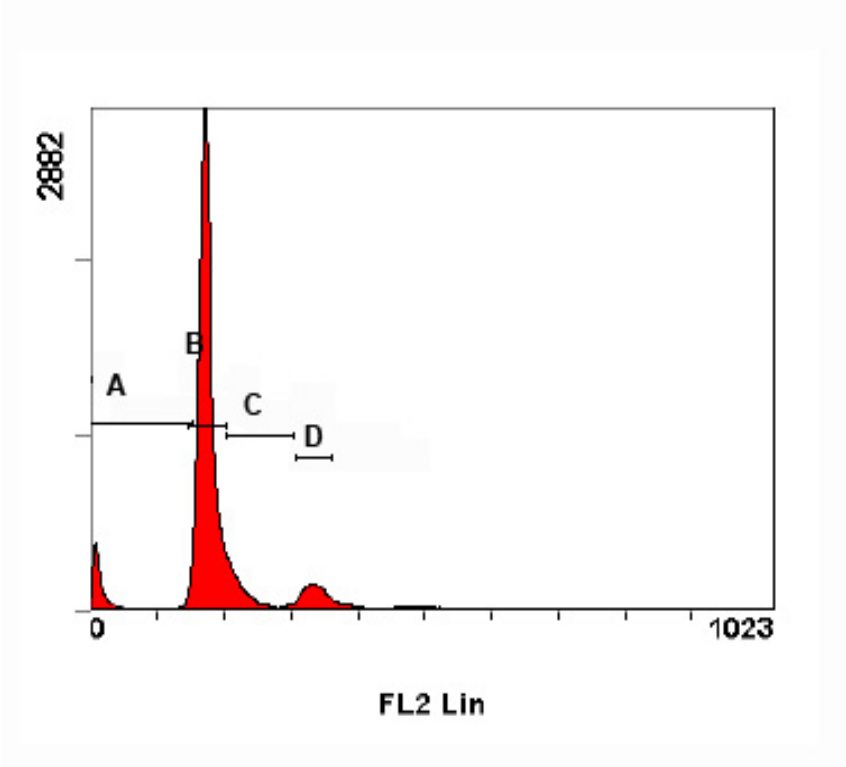

Figure 3.22 - Cell Synchronization by Elutriation

Sp2/0 cells were separated by elutriation at a centrifugal speed of 1800RPM with a flow rate of 7mL/min. A 50mL fraction was collected and processed for propidium iodide and flow cytometry analysis. Gate A; sub-G_1 peak 7.4%, Gate B: G_0/G_1 peak 72.1%, Gate C: S phase peak 9.0% and Gate D: G_2/M peak 6.9%.

3.1.5 — Chapter Summary

The results obtained thus far have shown that variations in glutamine concentration can affect cell behaviour.

The results obtained in section 3.1.1have demonstrated that, under our experimental conditions, there is a threshold concentration of glutamine of 100 μM. Above this threshold, cells

survive and proliferate. At this threshold concentration, cells survive but cannot proliferate and below this threshold, cells die by apoptosis. The results have also demonstrated that a stress response is present: not all cells are dead in micromolar concentrations of glutamine. This stress response may be mediated by GADD-153, which is expressed only when glutamine is limiting; in the absence or abundance of glutamine, GADD-153 is not expressed. The presence of 25 μM of glutamine afforded Sp2/0 cells a measure of protection against apoptosis that was comparable to that afforded by ectopic expression of Bcl-xL or caspase inhibition. Ectopic expression of Bcl-xL, but not caspase inhibition, allowed GADD-153 expression in glutamine-deprived conditions. Bcl-xL is involved in the negative regulation of both apoptosis and autophagy: it prevents the loss of MOMP in the former, and binds Beclin-1 to prevent autophagic initiation in the latter (202). Glutamine withdrawal leads to oxidative stress (199), a stress which is known to induce the expression of GADD-153 (228, 229). It is likely that apoptosis occurs too rapidly in Sp2/0 deprived of glutamine for *de novo* synthesis of GADD-153 to occur without Bcl-xL expression, which affords Sp2/0 a measure of protection (figure 3.8). If this is the case, a study of GADD-153 mRNA expression in Sp2/0 cells deprived of glutamine would address this question. The functional requirement for GADD-153 could also be assessed by performing RNA knockdown experiments or by generating GADD-153 knockout Sp2/0, then assessing the ability of Sp2/0 cells of adapting to glutamine limitation.

In section 3.1.2, a sequence of events was established. The majority of Sp2/0 cells cultured in medium containing 25 μM of glutamine were not irreversibly committed to the apoptotic program until 24h. Even at 12h, only 28.0% of cells had committed to the death program. However, there were two distinct populations: the first population entered into the apoptotic program at 4h in culture in medium containing 25 μM of glutamine as characterized by

caspase-3 activity, cytochrome c release and PARP-1 cleavage. The second population did not readily undergo apoptosis upon exposure to glutamine limitation. This second population likely comprises the cells expressing GADD-153 and showing intact mitochondrial potential. This could be identified by immunofluorescence experiments showing co-localization of GADD-153 and membrane potential. As the stress of glutamine limitation continued, the cells eventually succumbed to apoptosis. Reports have shown that mitochondria regulate the expression of GADD-153 when reactive oxygen species levels in the mitochondria rise, a phenomenon that was associated with apoptosis in adipocyte and leukemia cell lines (228, 229).

Section 3.1.3 presented results showing that, in Sp2/0 cells grown under conditions of glutamine limitation, there was a progressive increase in cells in the sub-G_1 phase and a concomitant decrease in the proportion of cells in S and G_2/M phase. These intriguing results led me to undertake further studies to try and come up with a potential mechanism that could responsible for the observations. These studies are described in sections 3.2 and 3.3 of my thesis.

CHAPTER 3.2 — AUTOPHAGY IN THE SP2/0 MODEL

The results of section 3.1 led to the conclusion that the presence of micromolar concentrations of glutamine in the culture medium affected cellular signalling pathways and changed cellular fate. Even after 24h, a greater proportion of cells remained viable (figure 3.1) when compared to a 4-hour acute glutamine deprivation treatment (53).

This increase in the number of viable cells in culture suggested that some cells may be able to adapt to the stress of limiting nutrients while awaiting more favourable conditions. As expected, inhibition of caspases provided some rescue from death since cells died by apoptosis, but this inhibition was not sufficient to rescue the majority of cells. Also, ectopic expression of Bcl-xL in conjunction with micromolar amounts of glutamine was sufficient to rescue the majority of cells from apoptotic death. Bcl-xL acts at the mitochondria to prevent pro-apoptotic Bcl-2 family members from creating pores in the outer mitochondrial membrane, a key step of the intrinsic apoptotic pathway (230). Interestingly, Bcl-xL can also block autophagy (202).

These results raised the interesting possibility that both glutamine and Bcl-2 family members were involved in an "adaptation" response, blocking key steps of the apoptosis machinery and allowing for the onset of stress-related signalling. In that regard, our results also indicated that during the 24h period when the Sp2/0 cells were adapting to that stress, GADD-153 was being expressed. There is one stress adaption response that has been linked to amino acid deprivation, GADD-153 and Bcl-2 family members: that response is autophagy (196, 202, 231).

Autophagy has not previously been characterized in the Sp2/0 model in the context of glutamine deprivation, though it has been reported in rapidly dividing cells such as those of

immune lineage, and is important to immune cell function, proliferation and development (232-237). As such, I hypothesized that autophagy would be occurring in the Sp2/0 cell line and that the autophagic response would be modulated under conditions of glutamine limitation.

3.2.1 — Visualisation of Acidic Organelles by Acridine Orange Staining

Autophagy is characterized by the presence of acidic vacuoles that occur when lysosomes fuse with autophagosomes to form autophagolysosomes. This is an important step in autophagy; the formation of autophagolysosomes allows for the degradation of the contents of the vacuole into smaller building blocks that can be exported to the cytosol and recycled into different macromolecules without the requirement for *de novo* synthesis (238, 239). These acidic vacuoles can be visualized by the use of pH-dependent dyes such as acridine orange (AO). In low pH conditions, AO becomes protonated and loses its membrane permeability and thus becomes sequestered into acidic vacuoles (240).

It should be noted that Sp2/0 cells are murine lymphoid cells; when compared to epithelial cells, lymphoid cells are characterized by a relatively small size, a large nucleus and small cytosol. Figure 3.23 illustrates the differential staining patterns of AO in Sp2/0 cells; the green AO staining visualized by the FITC filter was centralized and limited to the large nucleus while the orange staining visualized by the rhodamine filter clearly labelled different structures which resided in the cytosol. These data confirm that the AO staining procedure can be used in Sp2/0 cells to visualize acidic cytosolic organelles.

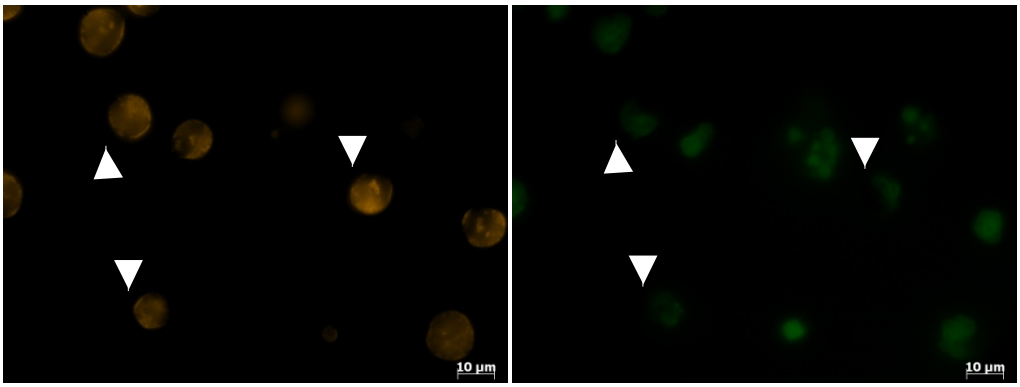

Figure 3.23 - Differential Acridine Orange Staining in Sp2/0 Cells

Representative panel of AO staining in exponentially growing Sp2/0 cells. The image was captured by fluorescence microscopy at 40X magnification using the rhodamine filters on the left (orange, acidic staining) or the FITC filters on the right (green, nuclear staining). The arrows indicate cells which illustrate a differential AO staining obtained with the rhodamine and FITC filters, where the staining are not superimposed.

3.2.2 — Glutamine Restriction Affects Acidic Vacuoles

We next used acridine orange staining to investigate the effect of glutamine limitation on acidic organelles. Sp2/0 cells were cultured for 24h under limiting glutamine conditions, then stained with acridine orange (figure 3.24). Glutamine concentrations spanned the range from 1000 µM (panel A) to 25 µM (panel E). Cells from each sample were then analyzed by fluorescence microscopy. In order to assess any change in intensity of staining and be certain to capture the 25 µM glutamine cell staining, the exposure time was set on that sample and maintained across all samples. In order to compare samples, the intensity of the cells in panel A of figure 3.24 and panel A of figure 3.27 were determined to be "bright" and used as a comparator.

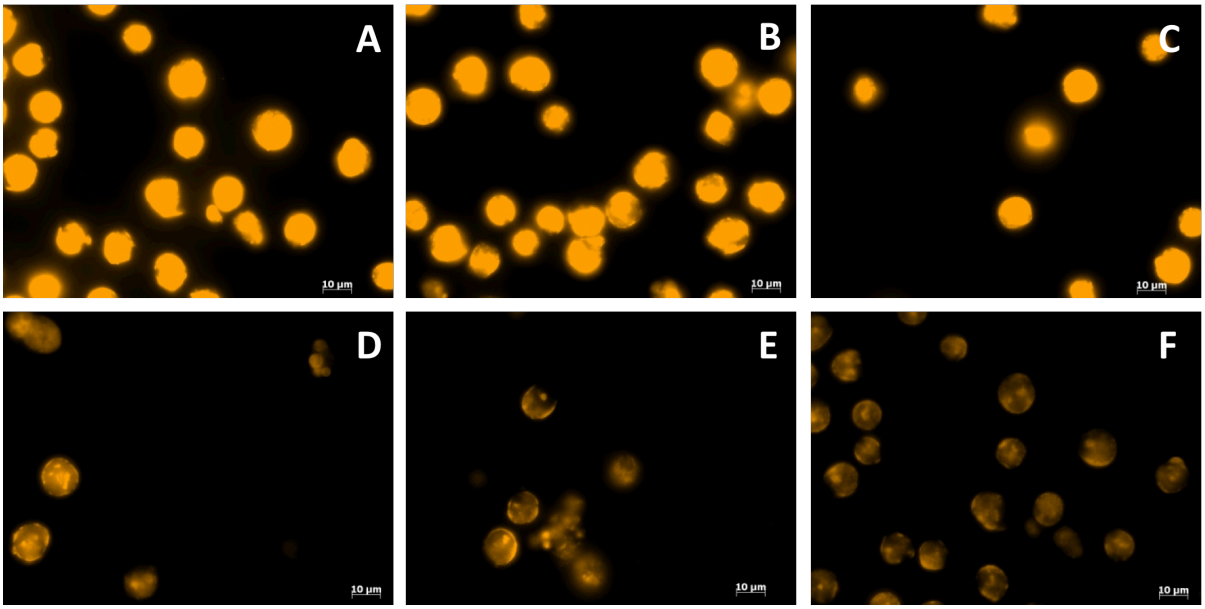

Figure 3.24 - Glutamine Limitation Leads to a Reduction in AO Staining

Sp2/0 cells were cultured for 24h in the indicated concentration of glutamine, and processed for AO staining. An identical exposure time (6 ms) was used for samples A-E. A) 1000 µM glutamine B) 250 µM glutamine C) 100 µM glutamine D) 50 µM glutamine E) 25 µM glutamine. A shorter exposure time (2 ms) was used for panel F (glutamine concentration: 1000 µM). At least 5 fields (totalling at least 50 cells) were captured at 400X magnification for each condition of each experimental group. Each panel is a representative field of 3 independent experiments.

When observing the staining patterns in panels A-E of figure 3.24, the staining is brightest in cells cultured in media supplemented with at least 100 µM of glutamine (panels A-C). This staining was too intense to identify intracellular structures. A shorter exposure time of 2ms was used in panel F to show that the intensity of the signal captured is not due to the dye having saturated the cell, but rather that the signal in the cytosolic structures was very intense The percentage of cells with bright staining was determined and presented in figure 3.25. A noticeable drop in the intensity of signal was observed in stained cells that had been cultured in medium supplemented with 25 µM and 50 µM glutamine. Interestingly, the latter correspond to the glutamine concentrations associated with a decrease in cell viability (figure 3.1).

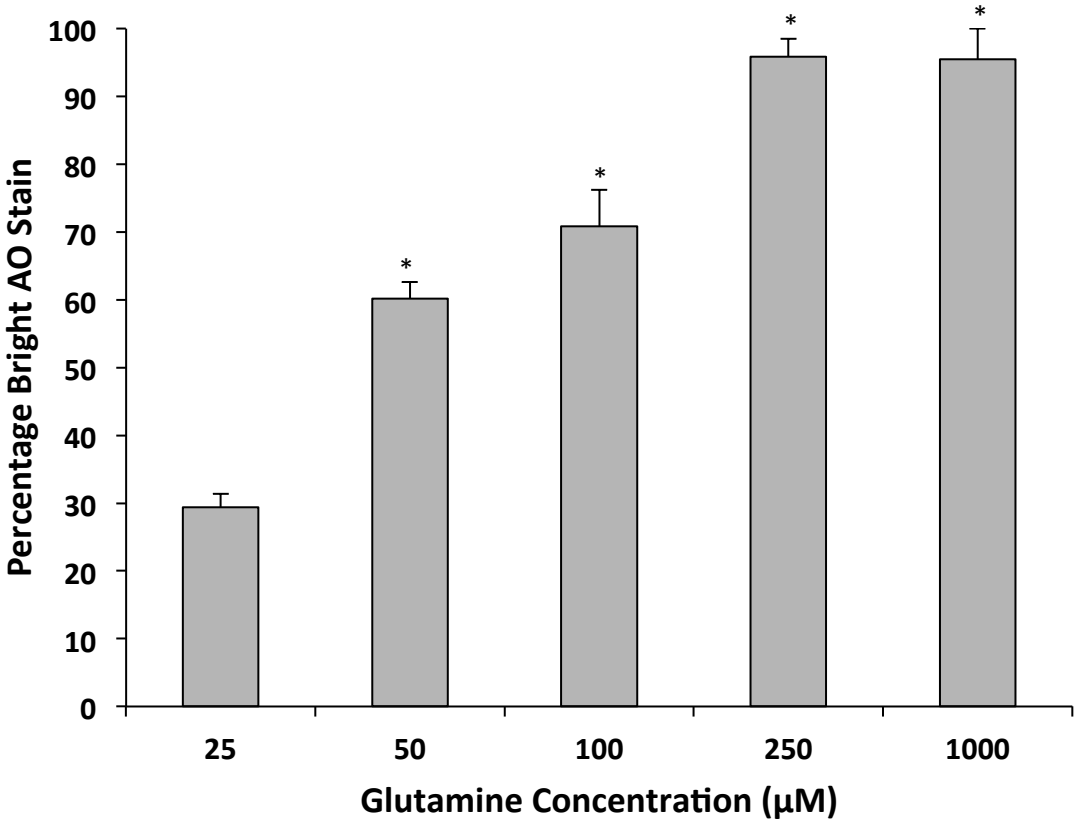

Figure 3.25 - Glutamine Limitation Leads to Reduction of Bright Staining in Acidic Compartments

The Sp2/0 cells presented in figure 3.24 were counted and scored as to intensity relative to the 1000 µM glutamine-supplemented group. Data represent the average ± SD from 3 independent experiments. The statistical significance was assessed by ANOVA + Scheffé's *ad hoc* test where * is $p < 0.05$ compared to the 25 µM glutamine-supplemented group. At least 70 cells were counted for each group.

The results shown in figure 3.25 confirmed that the percentage of cells with bright staining was significantly lower when glutamine concentrations in the culture medium were of 100 µM or less. All together, these data show that the function of acidic cytosolic organelles in Sp2/0 cells is affected when glutamine levels in the medium are decreased below a concentration threshold. This, in turn, suggests that the autophagic machinery might be compromised when cells are maintained in medium containing micromolar levels of glutamine.

The panels in figure 3.26 are presented to show the presence of cells with an abnormal staining pattern in the culture when glutamine was limiting in the medium over a 24h period (yellow arrows); these green-stained bodies were not observed in the red filter, nor were they observed in the culture conditions containing 100 µM or more of glutamine. In order to have the orange staining, cells must be able to maintain an acidic pH; the absence of orange staining while the green staining remains indicates that acridine orange is present and bound to DNA but not acidified. This indicated that the integrity of the acidic organelle was compromised in these cells. Interestingly, the apoptotic body formation, the so-called "popcorn" morphology, was readily observed in the 25 µM glutamine condition.

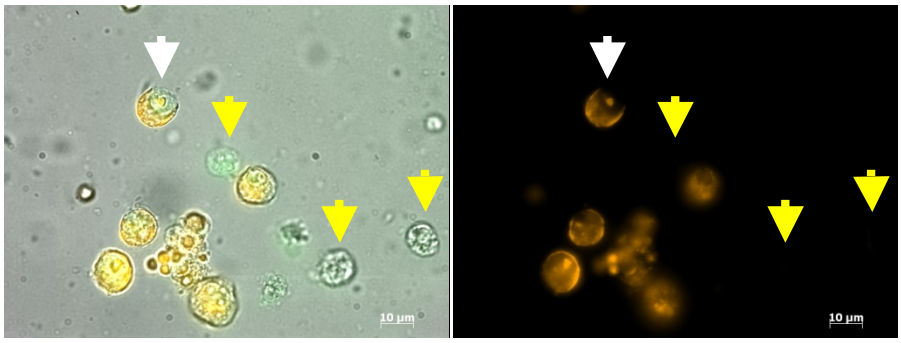

Figure 3.26 - Abnormal Cells in the 25 µM Glutamine Condition

Panels show the acridine orange staining for the DNA (green in merged brightfield on the left panel) and acidic compartment staining (orange in the right panel) of cells cultured in 25 µM glutamine as in figure 3.22. The white arrow points to a cells stained both green and orange, and the yellow arrows point to cells with green staining only.

The results presented in figure 3.24 and 3.25 illustrated that, when grown under glutamine-limiting conditions, Sp2/0 cells had fewer acidic vacuoles that stained intensely with acridine orange. The next experiment was aimed at examining the effects of glutamine limitation over time on the integrity of acidic vacuoles.

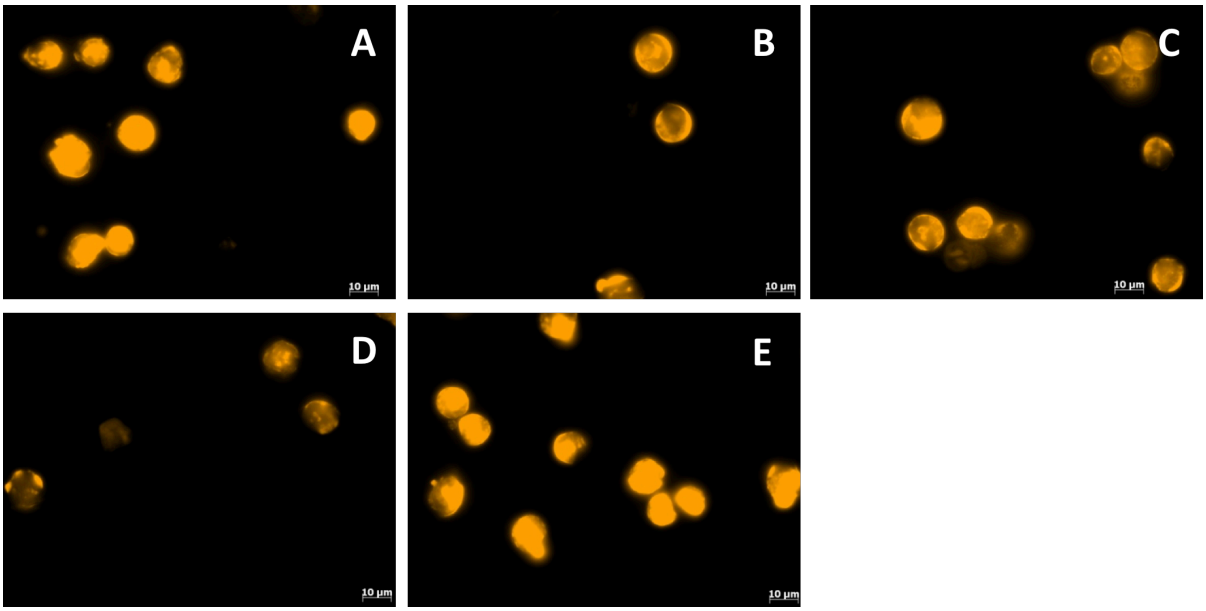

Figure 3.27 - Micromolar Levels of Glutamine Affect Cytosolic Acidic Organelles Over 24h

Sp2/0 cells were cultured over a 24h period in medium containing 25 µM glutamine. At the indicated time points, the cells were collected and stained with AO and the images captured 40X magnification using the same exposure time (6ms) for all groups. A) 0h, B) 4h, C) 8h, D) 24h, E) 24h with 4 mM glutamine control. At least 5 fields (totalling at least 40 cells) were captured for each condition of each experimental group. The panels are representative fields of 3 independent experiments.

The results shown in figure 3.27 were as expected. At the start of the experiment (panel A), the AO stain was intense and the panel resembles panels A- C of figure 3.24. Likewise, cells that were cultured in 1000 µM glutamine (panel E) also had intense AO staining. In panels B and C, the AO staining was still intense, though the internal structures of the vacuoles could be distinguished and most cells presented with acidic vacuoles found in the centre of the cytoplasm. At 24h in culture with 25 µM glutamine (panel D), similarly to panel E of figure 3.23, cells had noticeably less intense AO staining, and more of the acidic vacuoles appeared on the periphery of the cell, closer to the cell membrane. The effects observed were quantified as in figure 3.25 and are presented in figure 3.28.

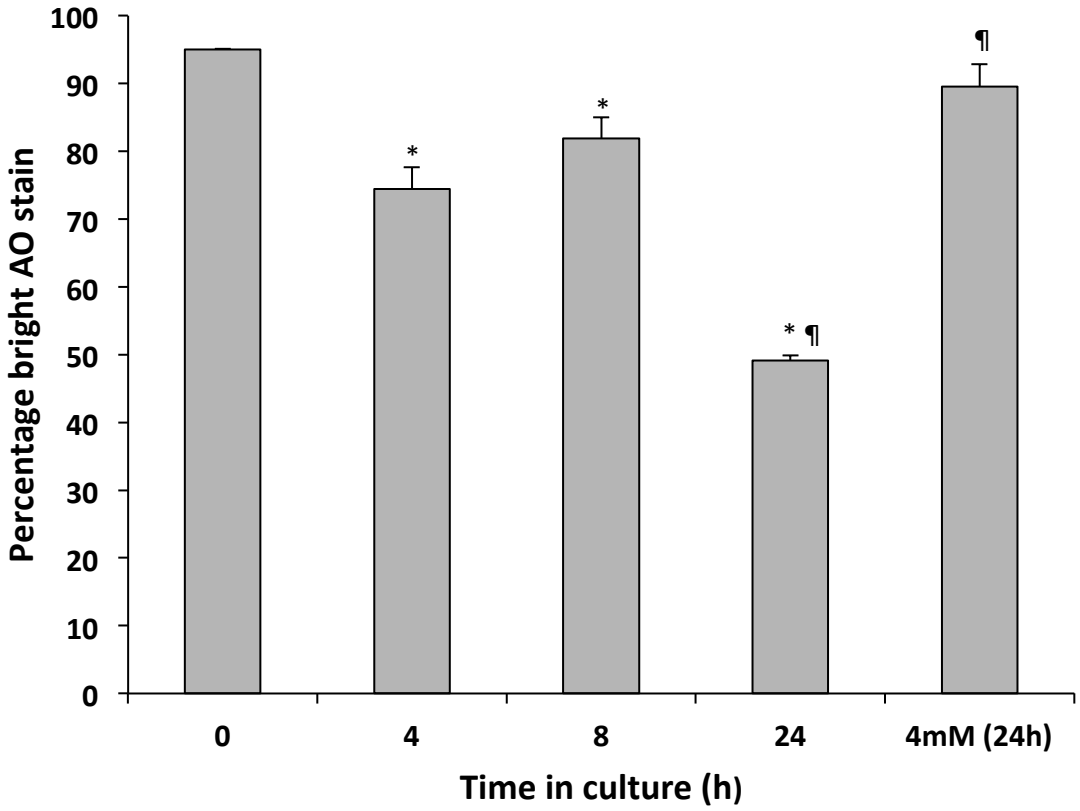

Figure 3.28 - Glutamine Limitation Leads to a Time-dependent Reduction in Brightly Stained Acidic Organelles

The Sp2/0 cells presented in figure 3.26 were counted and scored as to intensity relative to the 0h group. Data represent the average ± SD from 3 independent experiments. Statistical significance was assessed by ANOVA + Scheffé's *ad hoc* test where * is $p < 0.05$ compared to 0h and ¶ is $p < 0.05$ compared to 4h. At least 85 cells were counted for each group.

At the start of the experiment (0h, baseline), 95% of cells counted had bright staining. There was an initial moderate decrease in the percentage of brightly stained cells at the 4h time point (74%) which was similar to that seen after 8h in culture (82%). These two conditions were not significantly different from each other, but were significantly different from the baseline condition. There was a marked decrease at 24h, with only 49% of the cells brightly stained, a difference that was significant when compared to the baseline, 4h and 8h conditions. The cells

cultured in abundant glutamine were not significantly different from baseline, but were significantly different from the 4h condition.

The results presented in figures 3.24, 3.25, 3.27 and 3.28 suggest that glutamine limitation can compromise the integrity of the acidic vacuoles in Sp2/0 cells. Interestingly, the reduction in AO staining intensity occurred in a time frame which is similar to the pattern of caspase-3 activation observed under similar conditions (figure 3.12). This suggests that the loss of function of acidic organelles may be an event which contributes to the induction of cell death under conditions of glutamine limitation.

3.2.3 — Constitutive Autophagy Activity is Critical to Sp2/0 Cell Survival

The presence of acidic vacuoles is a necessary step in the progression of autophagy; the contents of autophagosomes must be degraded. Their presence alone is not definitive proof of autophagy. In order to verify that autophagosomes were present in Sp2/0 cells, cells cultured under varying glutamine conditions were prepared as described and visualized by transmission electron microscopy.

As shown in figure 3.29, Sp2/0 cells cultured in glutamine-rich conditions presented with double-membraned vacuoles within the cytoplasm of the cell. In panel A, the vacuole appears to contain a mitochondrion. In panel B, the vacuoles are less dense. Panels C and D denote forming vesicles (241-243).

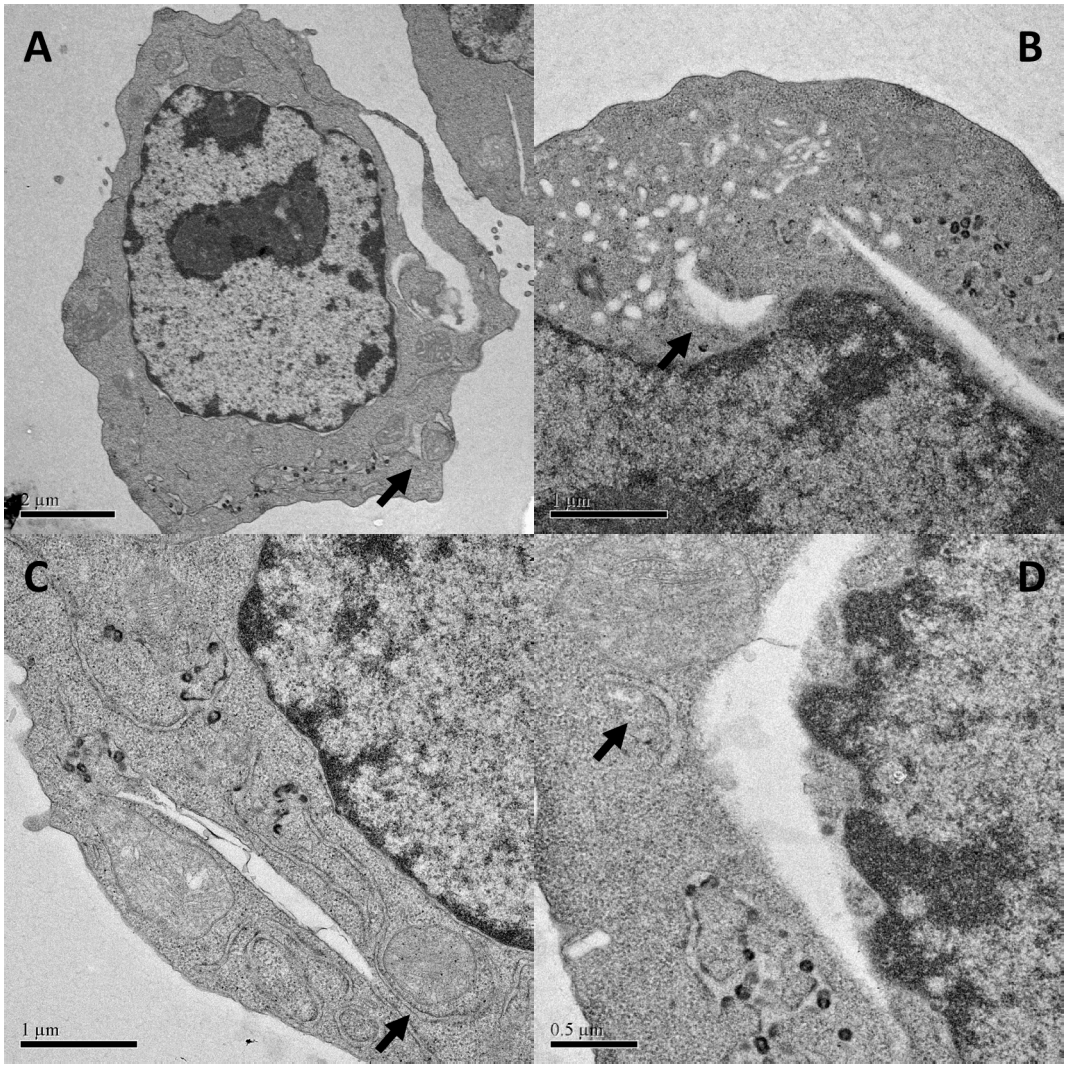

Figure 3.29 - Vacuoles Are Present in Glutamine-Rich conditions

Panel shows a cell cultured for 24h in 1000 µM glutamine. After 24h, cells were collected and 4 for transmission electron microscopy analysis, as described in the Materials and Methods section. Black arrow indicates the presence of vacuoles, some containing cellular materials and others in the process of forming.

When cells were cultured in glutamine limited conditions for 24h (figure 3.30, panels A-D) the vacuoles were more prominent and more of them contained cellular material. Also, the cytoplasm appeared to have more debris accumulated and was not as uniform as the cytoplasm of cells cultured in 1 mM glutamine (figure 3.29). This could be attributed to a failure by the cell

to successfully complete the autophagic process, where the autophagic vacuoles would have encapsulated the cellular materials, but have failed to degrade them.

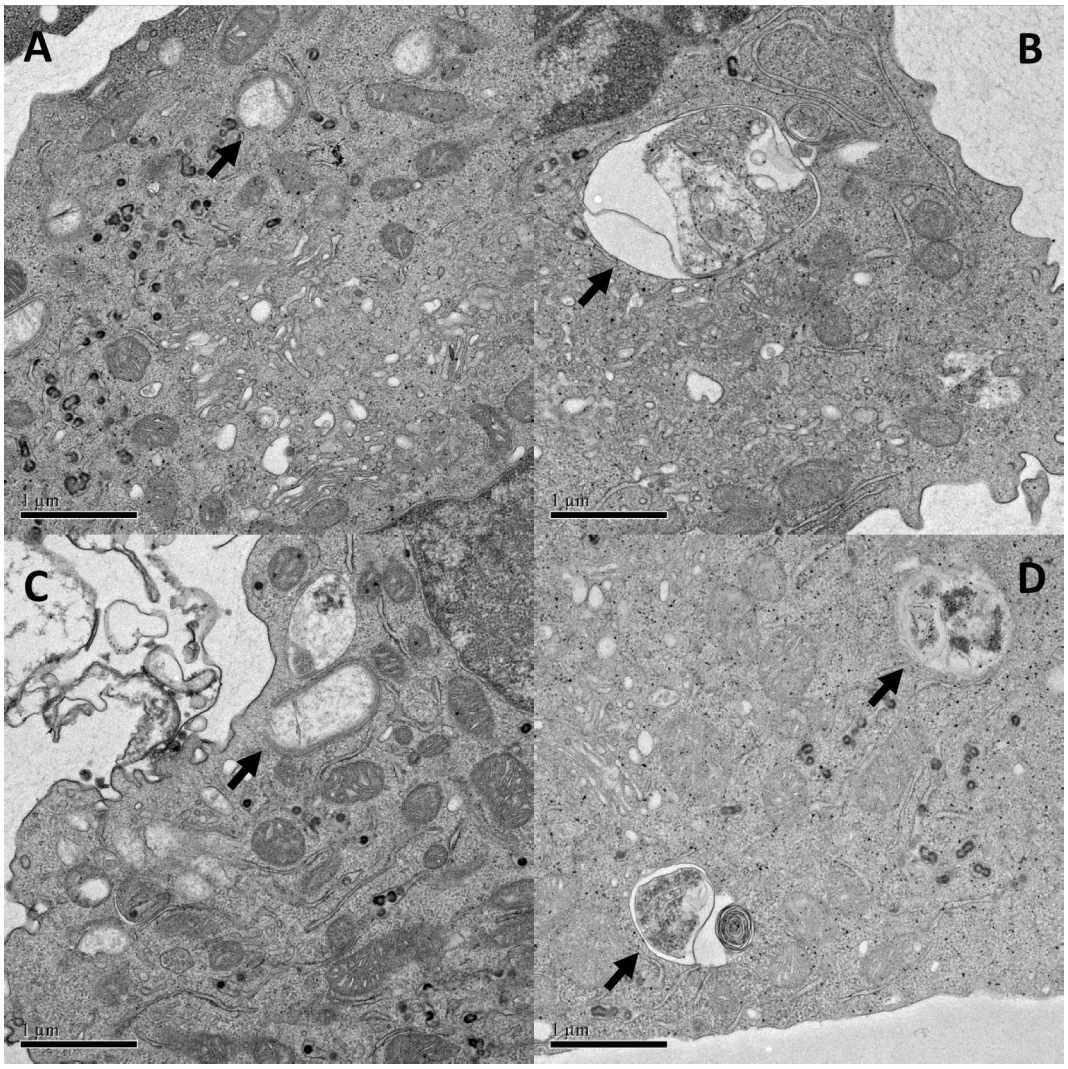

Figure 3.30 - Vacuoles Are Present in Glutamine-Limited Conditions

Panel shows cells cultured for 24h in 25 µM glutamine. After 24h, cells were collected and processed for transmission electron microscopy analysis, as described in the Materials and Methods section. Black arrows indicate the presence of vacuoles.

Our observation of a decrease in the abundance of acidic organelles by acridine orange and the prominence of the vacuoles by TEM led us to consider the possibility of an impairment of autophagy following glutamine limitation. One protein associated to the autophagic pathway

is microtubule-associated light chain 3 (LC3). When the autophagic machinery is not activated, the non-lipidated form of LC3, LC3-I, is the predominant form present.

Upon activation, LC3-I is cleaved to remove a terminal glycine and conjugated to phosphatidylethanolamine, becoming LC3-II (244). The addition of the lipid moiety allows for the insertion of LC3 into the developing autophagosomal membrane to facilitate membrane curvature. The presence of a lipidated form of LC3-II has been reported as being a necessary step of autophagy (139).

Since the results of figures 3.24, 3.25, 3.27 to 3.30 indicated that autophagic vacuoles are present in Sp2/0, and that the AO staining was more intense in cells that were cultured in the presence of non-limiting amounts of glutamine, we next sought to determine whether LC3 was expressed in that cell line, and if so, whether the levels of either LC3 forms would be modulated under conditions of glutamine limitation.

As can be seen from figure 3.31, two forms of LC3 were observed. The LC3-I form was most evident in the 1000 μM and 25 μM conditions, and barely detectable in all other conditions. The LC3-II form was present in all conditions, with greatest quantity in the 1000 μM and 25 μM conditions. To get a better characterization of the increase in expression, the ratio of intensity of LC3-II to LC3-I was calculated. In the 1000 μM condition, the LC3-II band was 2.9 fold more intense than the LC3-I form, 2.6 fold more intense in the 250 μM condition, 2.8 fold more intense in the 100 μM condition, 4.4 fold more intense in 50 μM and 2.8 fold more intense in the 25 μM condition. This observation was similar across all 3 experiments (see appendix A.3 and A.4). The high ratio of LC3-II to LC3-I suggests that autophagy is constitutively activated in Sp2/0 cells, irrespective of the glutamine concentration in the medium.

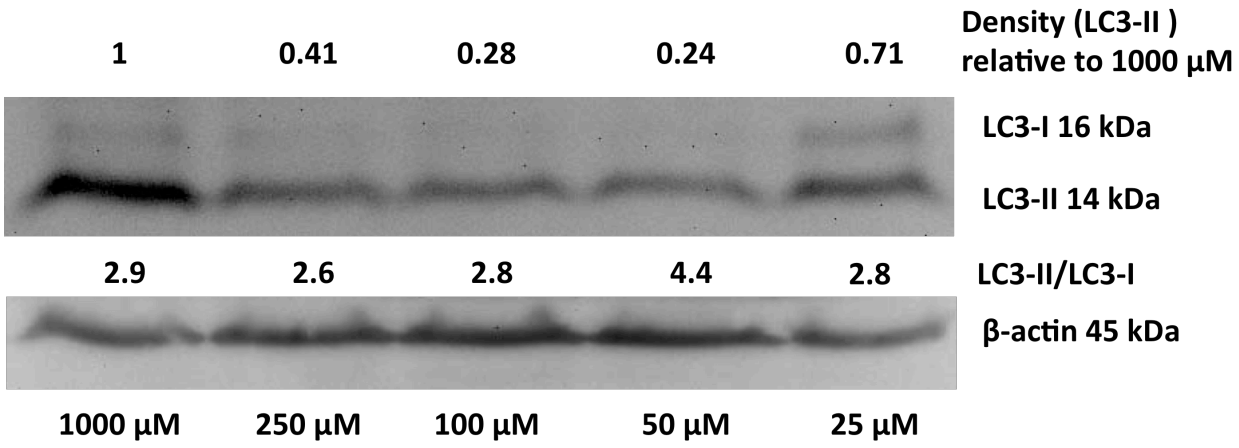

Figure 3.31 - Glutamine Limitation Modulates LC3-II Expression

Western blot analysis of protein extracts from cells cultured for 24h in medium containing the indicated concentration of glutamine and probed with an anti-LC3 antibody. An anti-β-actin antibody was used as loading control. Data are representative of 3 independent experiments (band densities for all 3 experiments are presented in appendix A.3). The density (LC3-II) is the β-actin-normalized densitometry reading of the LC3-II band compared to the 1000 µM condition. The LC3-II/LC3-I indicates the normalized expression ratio for each condition.

We next examined the modulation of LC3-I and -II over time in Sp2/0 cells cultured under glutamine-limiting conditions (figure 3.32). LC3-II expression, when compared to the 0h (baseline) time point, was slightly decreased after 8h of culture in medium containing 25 µM glutamine, only to increase for the 24h time point condition. This trend was consistent across the experiments (see Appendix A.5) while not being statistically different because of the variations in densitometry reading. The LC3-I band was not consistently detectable at the time points before the 24h condition. When evaluating the results presented in figures 3.30-3.32, the evidence suggests that glutamine limitation causes a decrease in autophagic activity, which is proportional to the amount of glutamine in the medium.

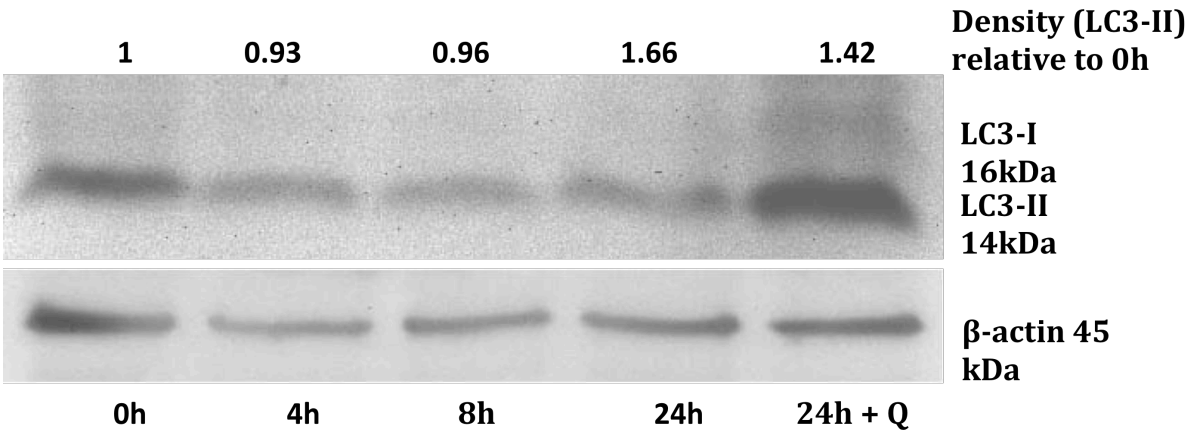

Figure 3.32 - LC3-II Expression in Glutamine-limited Sp2/0 Cells

Western blot analysis of protein extracts from Sp2/0 cells cultured over a period of 24h in medium containing 25 μM of glutamine. At the indicated time, cells were collected and processed for SDS-PAGE electrophoresis and Western blotting using an anti-LC3 antibody. An anti-β-actin antibody used to control for protein loading. Data are representative of 3 independent experiments. The density (LC3II relative to 0h is the β-actin-normalized densitometry reading of the LC3-II band compared to the 25 μM condition.

The presence of acidic vacuoles (figure 3.24) and of the lipidated form of LC3-II when cells were not limited by glutamine (figure 3.31) suggested that autophagy may be a constitutive process in the Sp2/0 cell line. We attempted to detect the presence of the autophagosome marker p62, however this proved to be unsuccessful in the Sp2/0 cell line. This failure could have been technical in nature (such as the quality of the antibody) or because p62 was being degraded in the autophagosomes. We also attempted to transfect Sp2/0 cells with a GFP-LC3 construct in order to use the cleavage of the fusion protein as a reporter for autophagy (245). Unfortunately, while Sp2/0 cells could be readily transfected with a plasmid expressing GFP, the expression of the GFP-LC3 fusion protein proved to be toxic to the cells. To evaluate the importance of autophagy for Sp2/0 cell survival, we tested the effect of chemical inhibitors of autophagy on the behavior of Sp2/0 cells cultured under non-limiting glutamine conditions.

The autophagy inhibitor 3-methyladenine (3-MA) inhibits class I PI3K, a protein kinase that phosphorylates phosphatidylinositol-4,5-bisphosphate (PIP_2) to phosphatidylinositol-3,4,5-trisphosphate (PIP_3) which leads to AKT activation (246). More importantly, 3-MA also inhibits the class III PI3K Vsp34 (247), which produces phosphatidylinositol-3-monophosphate (248) and has been implicated in the regulation of autophagy (249). Therefore, we tested the effect of 3-MA on the behaviour of Sp2/0 cells.

Sp2/0 cells were cultured for 24h in glutamine-rich (4 mM) medium, with or without supplementation with 3-MA. After 24h, the cells were collected and assessed for survival using the trypan blue assay (figure 3.33).

As shown in figure 3.33, the presence of 3-MA in the culture medium resulted in a significant loss of viability even at the lowest dose; 23% trypan blue positive cells were present in the 1 mM 3-MA condition. When the 5 mM 3-MA supplemented the culture medium, 81% of the cell population was trypan blue positive and at the highest concentration (10 mM), 95% of the cell population was stained with trypan blue. The concentrations of 3-MA chosen has been shown block autophagy in previously published work (249, 250).

The results presented in figure 3.33 were confirmed by flow cytometry analysis. 7-aminoactinomycin D (7AAD) is a DNA-binding fluorescent dye that is not membrane permeable; as such, only cells having lost their membrane integrity (i.e. late apoptotic or necrotic cells) will have a positive 7-AAD signal when assessed by flow cytometry. As seen in figure 3.34, 3-MA treatment (blue) caused a significant dose-dependent increase in the number of 7-AAD stained cells when compared to the control (red), confirming that 3-MA treatment triggered Sp2/0 cell death.

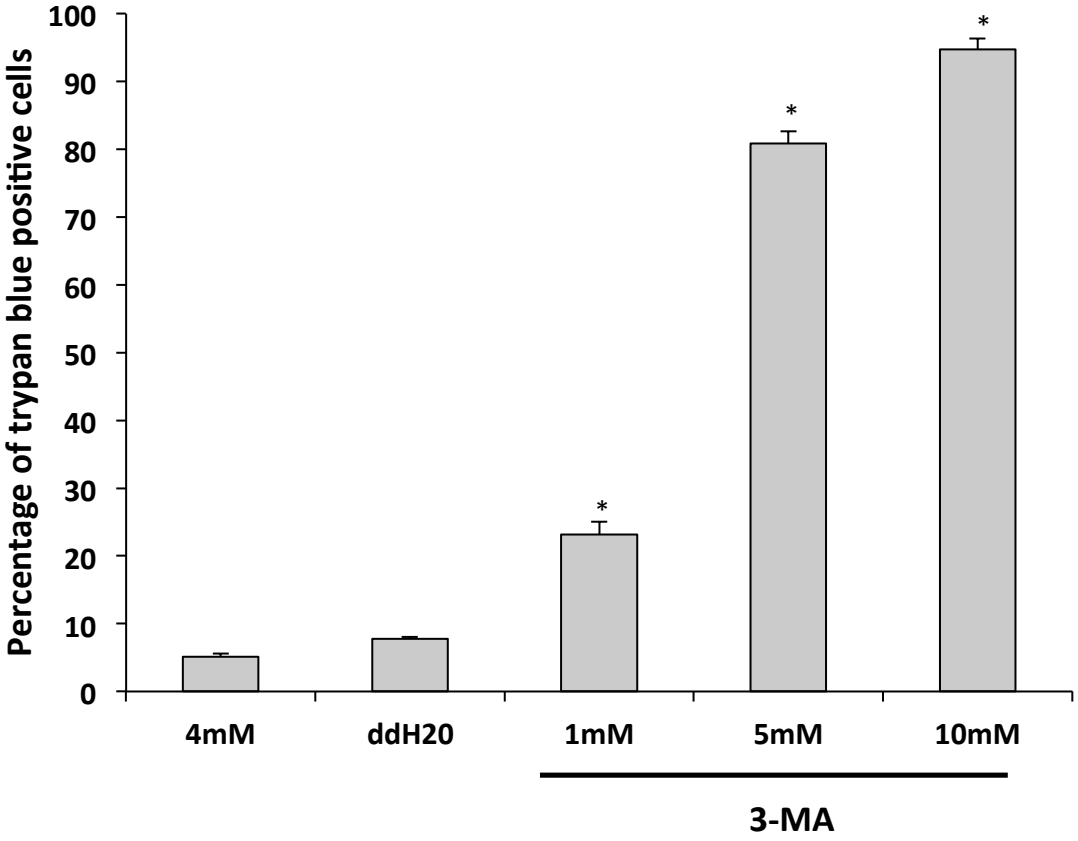

Figure 3.33 - 3-MA Treatment Decreases Cell Viability in Glutamine-Rich Conditions

Sp2/0 cells were cultured in medium containing 4 mM glutamine for a period of 24h in the presence of the indicated concentration of 3-methyladenine, with ddH_20 used as the solvent control. Cell viability was then assessed by trypan blue exclusion assay. Data represent the average ± SD of 3 independent experiments. Statistical significance was assessed by ANOVA + Scheffé's *ad hoc* test with * $p<0.05$ compared to the 4 mM group.

While 3-MA is widely used to study autophagy by virtue of inhibiting the activity of class III PI3Ks, it is not specific to the autophagic pathway because it can also inhibit class I and class III PI3Ks which have been involved in other cellular pathways which include cellular trafficking and nutrient signalling (251). In order to confirm the 3-MA data, we used bafilomycin A1, another chemical frequently used to inhibit autophagy (241, 252). Bafilomycin A1 acts by inhibiting the lysosomal proton pump, preventing the acidification of the organelle. The higher

pH of the organelle decreases the activity of several of its hydrolytic enzymes, and thus hinders the degradation of the contents of the autophagolysosomes.

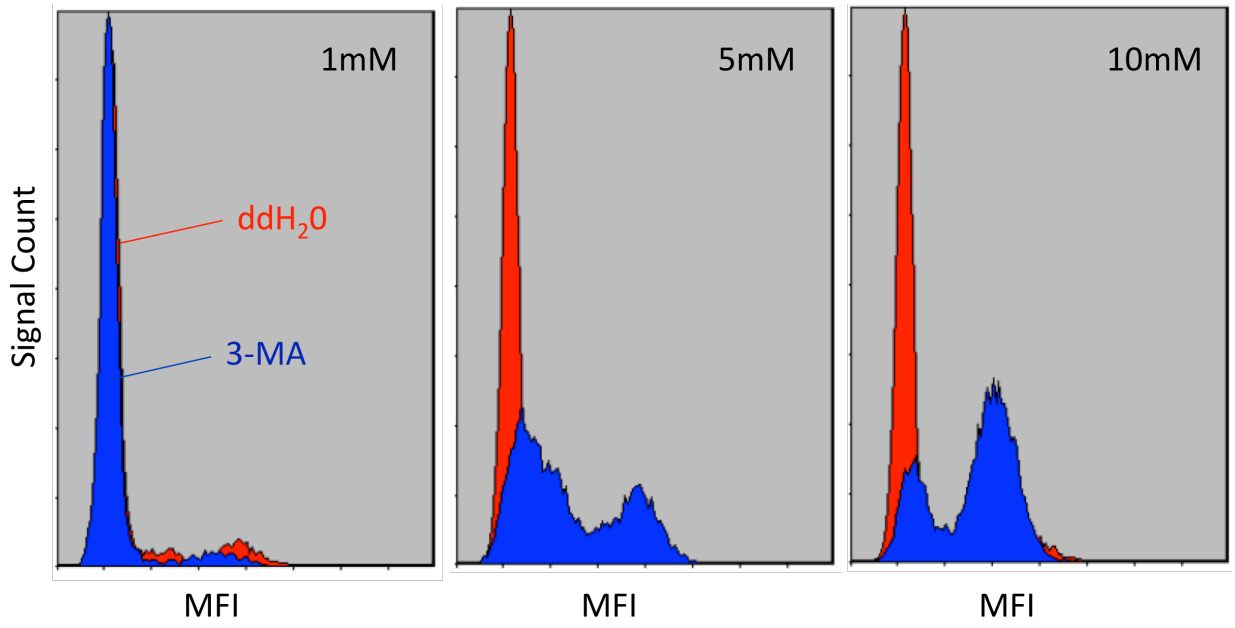

Figure 3.34 - Sp2/0 Cells Treated With 3MA Lose Membrane Integrity

Sp2/0 cells were cultured for 24h in medium containing 4 mM glutamine in the presence of 3MA treatment (blue) or an equivalent volume of ddH_20 (red). The cells were then stained with membrane-impermeable 7AAD and analyzed by flow cytometry. The concentration of 3MA used in the experiment is indicated in the top right corner of each panel. Data are representative of 3 independent experiments. MFI: mean fluorescence intensity.

As shown in figure 3.35, even in glutamine-rich conditions, concentrations of bafilomycin A1 as low as 10 nM caused a dramatic increase in the number of dead cells, as 89% of cells assessed were trypan blue positive compared to 7% in the solvent control. These data were confirmed by the flow cytometry analysis of 7-AAD-stained cells (figure 3.36). The DMSO solvent control shows very little 7-AAD staining, whereas all conditions containing bafilomycin A1 have a strong 7-AAD signal, indicating loss of membrane integrity.

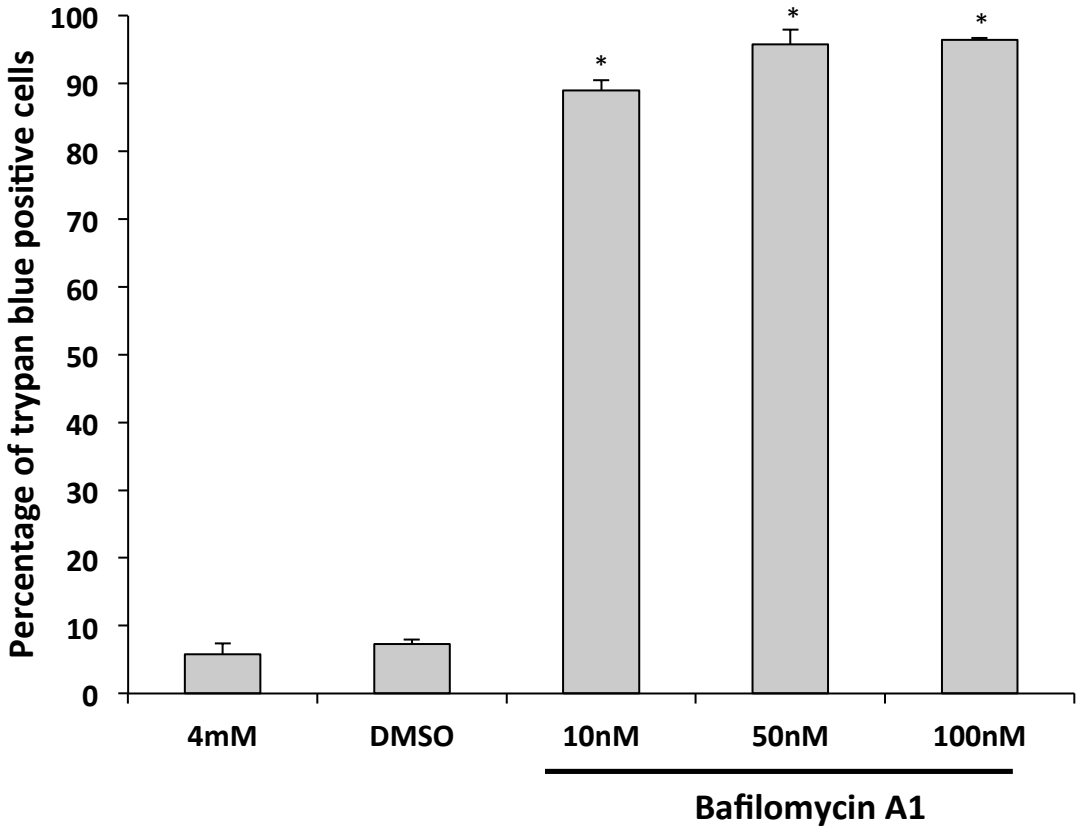

Figure 3.35 - Bafilomycin A1 Decreases Cell Viability in Glutamine-Rich Conditions

Sp2/0 cells were cultured in medium containing 4 mM glutamine for a period of 24h in the presence of the indicated concentrations of bafilomycin A1, with DMSO being used as a solvent control. Cell viability was then assessed by the trypan blue exclusion assay. The data represents the mean ± SD of 3 independent experiments. Statistical significance was assessed by ANOVA + Scheffé's *ad hoc* test with * $p<0.05$ compared to the 4 mM glutamine control group.

The induction of cell death by the addition of 3-MA or bafilomycin A1 confirms the importance of autophagy for the survival of Sp2/0 cells in typical culture conditions. These results also suggest that activation of autophagy may reduce the sensitivity of Sp2/0 cells to apoptosis induction when Sp2/0 cells are cultured in glutamine-limited conditions. To test this possibility, we evaluated the effects of rapamycin (figure 3.37), a known activator of autophagy which acts through its inhibition of the mTOR protein kinase (253).

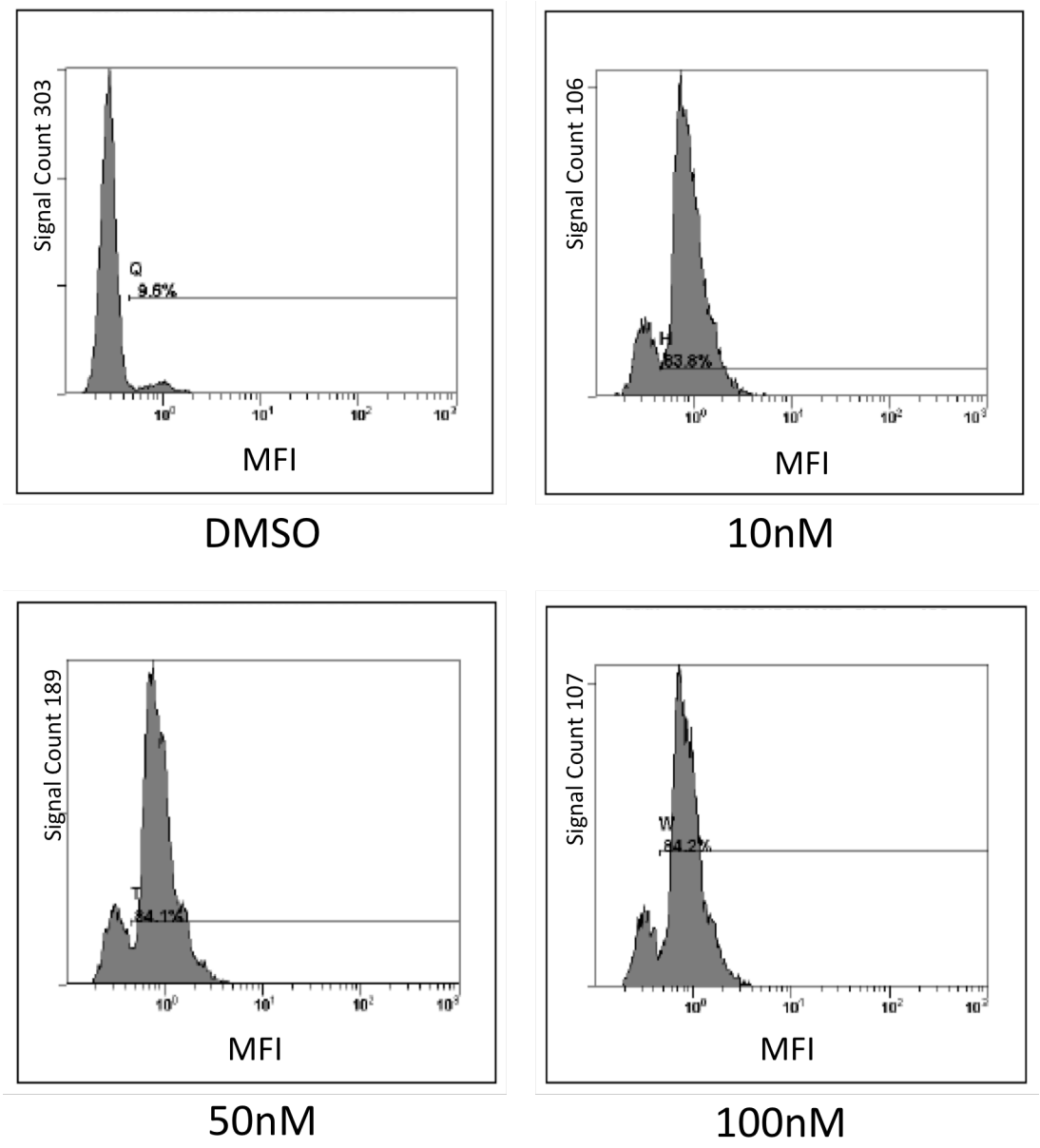

Figure 3.36 - Sp2/0 Cells Treated With Bafilomycin A1 Lose Membrane Integrity

Sp2/0 cells were cultured in medium containing 4 mM glutamine for a period of 24h in the presence of 10 nM bafilomycin A1, with DMSO being used as the solvent control. Cells were then processed for 7-AAD staining and flow cytometry analysis. Data presented is representative of 3 independent experiments. MFI: mean fluorescence intensity.

First, Sp2/0 cells were cultured for 24h in culture medium containing 4 mM glutamine and a range of rapamycin concentrations. DMSO was included as a negative control. As shown

in figure 3.37, rapamycin alone did not reduce cell viability when compared to the 4 mM glutamine control. However, cells cultured in rapamycin did have a statistically significant dose-dependent reduction in cell density. They showed reduced capacity to proliferate when compared to the 4 mM glutamine condition. This was not unexpected considering that mTOR is known to positively regulate proliferation.

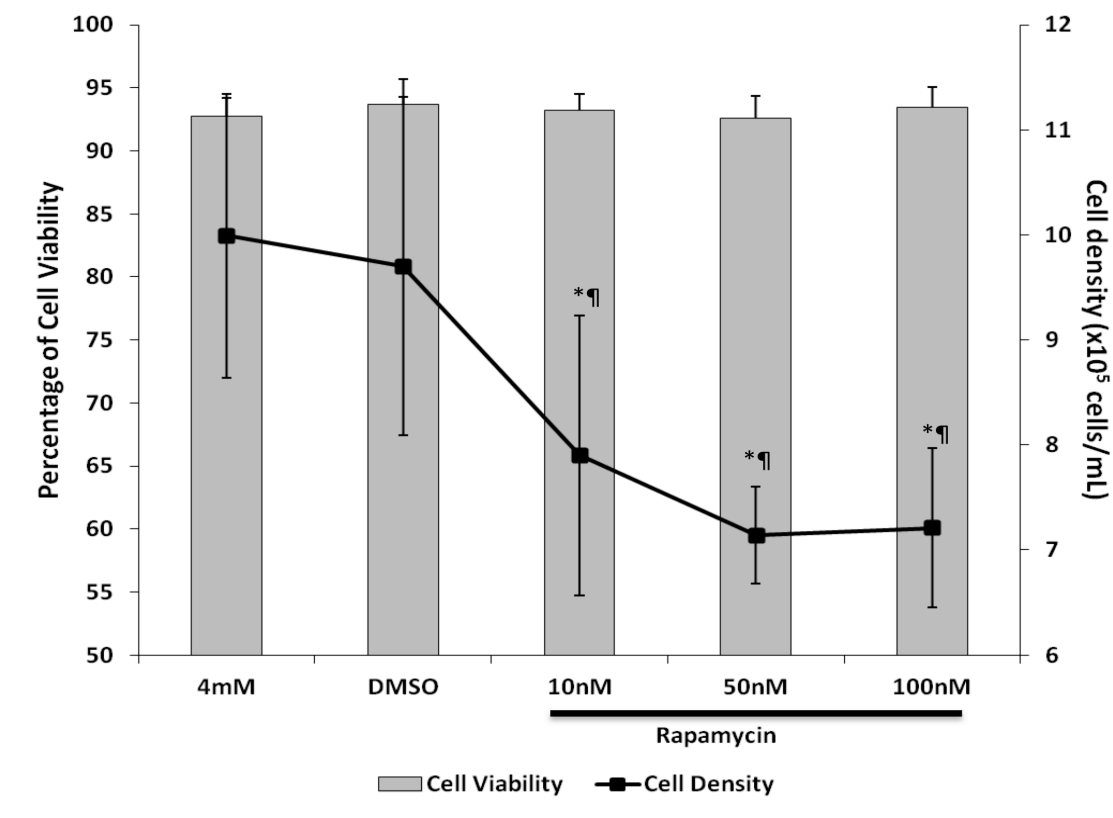

Figure 3.37 - Rapamycin Prevents Increase in Cell Density in Glutamine-Rich Conditions

Sp2/0 cells were cultured in medium supplemented with 4 mM glutamine for a period of 24h in the presence of the indicated concentration of rapamycin, with DMSO as the solvent control. Cell viability and density were then assessed by the trypan blue exclusion assay. Data represent the mean ± SD of 3 independent experiments. Statistical significance for cell density was determined assessed by two tailed paired t-test with * $p<0.05$ compared to 4 mM.

Since rapamycin treatment did not have any toxic effect on Sp2/0 cell cultured in glutamine-rich conditions, we next tested the effects of this autophagy inducer on Sp2/0 cells cultured for 24h under glutamine-limiting conditions. Remarkably, our results showed that, at concentrations of 50 nM and 100 nM, rapamycin treatment markedly improved the viability of Sp2/0 cells cultured in medium supplemented with 25 µM glutamine, with no discernible effect on cell density (figure 3.38).

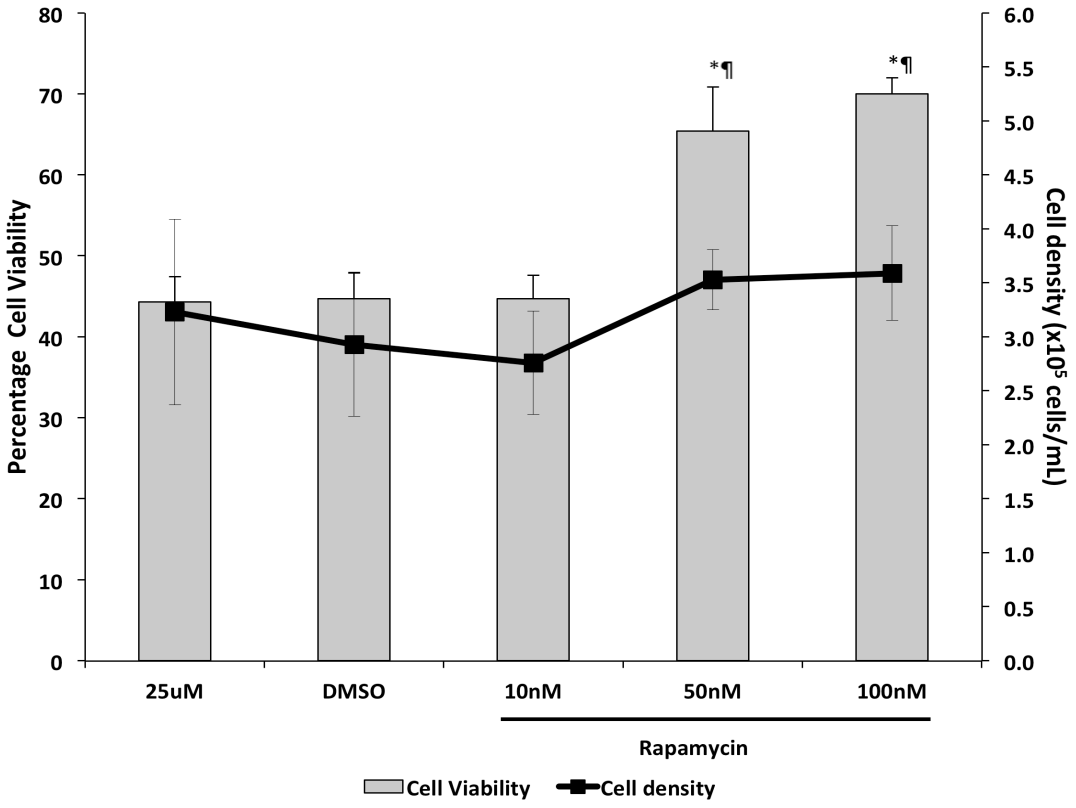

Figure 3.38 - Rapamycin Rescues Cell Viability in Glutamine-Limited Conditions

Sp2/0 cells were cultured in medium containing 25 µM glutamine for a period of 24h in the presence of the indicated concentrations of rapamycin, with DMSO included as the solvent control. Cell viability was then assessed by the trypan blue exclusion assay. Data represent the mean ± SD of 3 independent experiments. Statistical significance was determined by paired two-tailed t-test with * $p<0.05$ compared to the 25 µM glutamine control 25 µM.

3.2.4 — Chapter Summary

Overall, the results presented in Chapter 3.2 show that autophagy is not only present in Sp2/0 cells, but that it is an important mechanism for cellular survival. Autophagy markers were more evident in glutamine-rich conditions than in glutamine-limited conditions. The results presented show that autophagy inhibition either early (with 3-MA) or late in the signalling cascades (with bafilomycin A1) leads to a high proportion of Sp2/0 cell death. In contrast, in glutamine-limited conditions, autophagy activation by the mTOR inhibitor rapamycin increased cell survival but not the capacity to proliferate.

The results suggest a link between glutamine, autophagic activity and cell survival: in glutamine-rich conditions, autophagy is active and cells survive and proliferate while in glutamine-limited conditions, cells do not proliferate, autophagy markers are decreased and cells are apoptotic. If autophagy is stimulated by rapamycin in glutamine-limited conditions, cell viability is rescued though there is no concomitant increase in cell density. If autophagy is inhibited in glutamine-rich conditions, cells are not viable. The next section aims to explore in greater detail the potential relationship between Sp2/0 cell viability, glutamine and autophagy.

CHAPTER 3.3 — GLUTAMINE LINK TO AUTOPHAGY

The Sp2/0 cell line is addicted to glutamine and cannot survive in its absence. The previous sections (3.1 and 3.2) have characterized the response in this cell model to limiting concentration of glutamine and showed the importance of autophagy for Sp2/0 cell survival. The link between glutamine, autophagy and cell survival may reside in the metabolism of glutamine within the cell. When glutamine is metabolized to enter the TCA cycle, it releases an ammonium ion (NH_4^+) via the action of glutaminase (6, 169).

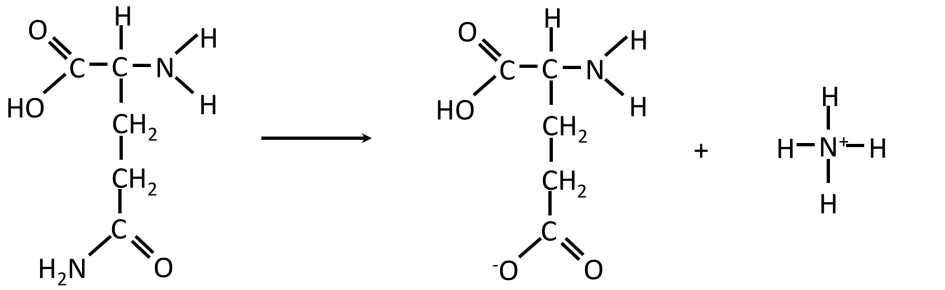

A recent study showed that ammonium ions derived from glutamine metabolism stimulate autophagy. Moreover, this stimulatory effect was correlated to an increase in cell survival in an osteosarcoma cell line (U2OS) and in kidney epithelial cells (iBMK) (169, 231).

The results obtained thus far, and described in sections 3.1 and 3.2 of this thesis, have demonstrated that glutamine is critical to Sp2/0 cell survival and proliferation. Sp2/0 cells grown in medium containing less than 100 μM of glutamine do not proliferate, die by apoptosis, have prominent cytoplasmic vacuoles containing cellular materials, less intense acridine orange staining, and show lower LC3-II expression. Furthermore, when Sp2/0 cells were cultured in

medium containing limiting amounts of glutamine, the inclusion of the mTOR inhibitor rapamycin led to a significant decrease in cell viability.

Considering the information reported by Eng *et al.* (169) in the context of the Sp2/0 cell line, we next assessed whether ammonium ions could be a mechanism by which glutamine promotes Sp2/0 cell survival.

3.3.1 — Ammonium Ions Affect Cell Viability and Proliferation

We first examined whether ammonium ions could modulate the viability of Sp2/0 cells grown under conditions of glutamine limitation. Two different sources of ammonium ions were used: an organic source, ammonium acetate (AA) and an inorganic source, ammonium chloride (ACl). Sodium acetate (NaA) and sodium chloride (NaCl) were used to assess whether the effect observed was due to the ammonium ion or the anion. Sp2/0 cells were cultured for 24h in medium containing 25 μM glutamine and supplemented with either AA, NaA, ACl or NaCl.

The effects of the ammonium salts on Sp2/0 cells were quite striking and could be qualitatively assessed by microscopy (figure 3.39 A-H). While Sp2/0 cells grown for 24h in the presence of 25 μM glutamine were clearly apoptotic (B), the addition of either ammonium salt increased cell density and seemed to increase the number of viable cells (C-D, F-G) to resemble the 4 mM glutamine control, while sodium salts had no such rescue effect (E, H).

The effect of ammonium ions on Sp2/0 cell viability and proliferation was confirmed using the trypan blue exclusion assay. When cells were cultured under limiting glutamine conditions (25 μM), the average percentage of dead cells was 57.39% (figure 3.40). Treatment of cells cultured under glutamine-limited conditions with either ammonium salt significantly

decreased the number of dead cells, with 17.98% when treated with AA and 28.97% when treated with ACl. This effect was specific to ammonium salt treatment as sodium salt treatments had no significant effect on cell viability.

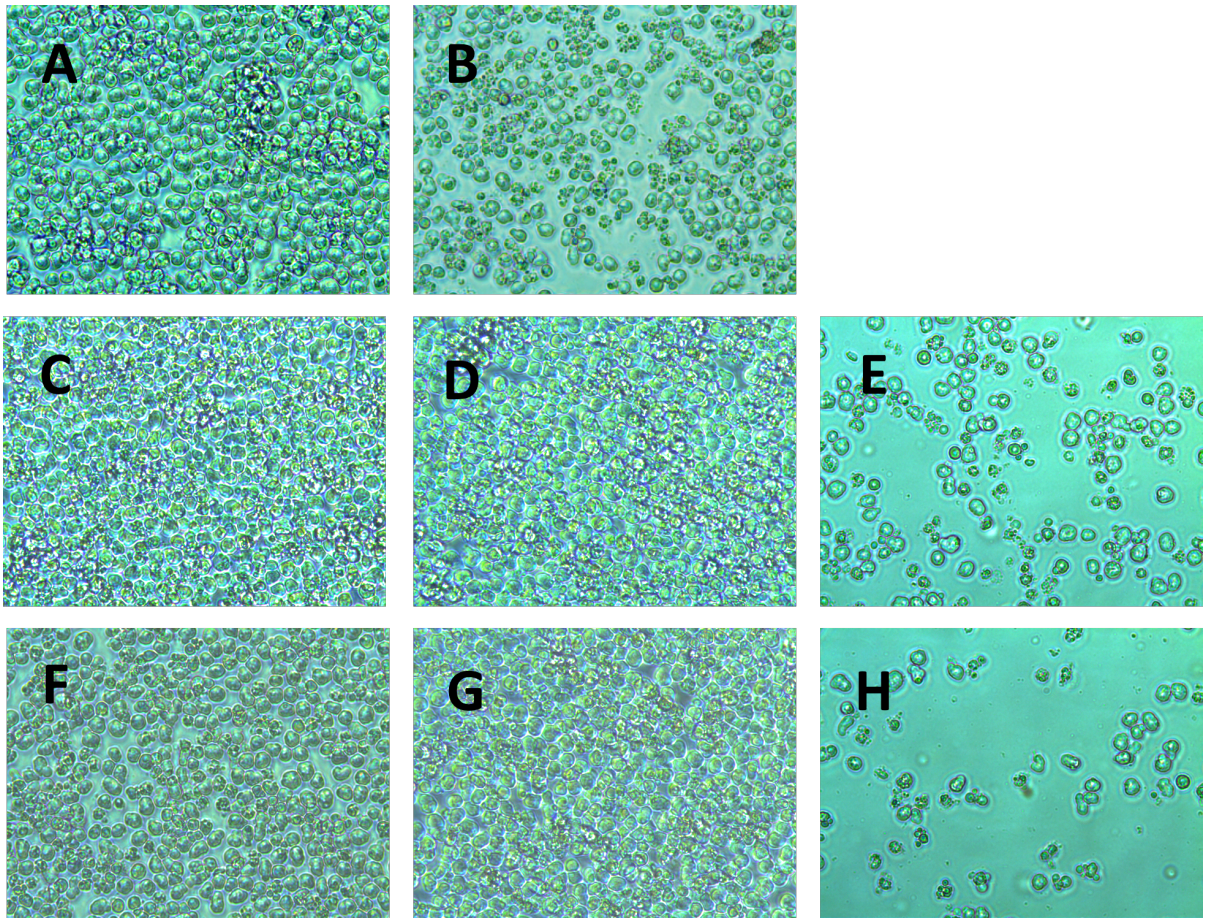

Figure 3.39 - Effect of Ammonium Ions on the Morphology of Sp2/0 Cells Grown Under Conditions of Glutamine Limitation

Pictures taken at 100X magnification in brightfield by light microscopy of Sp2/0 cells cultured in medium containing 25 µM glutamine for a period of 24h. The cultures also included a source of ammonium ions or the corresponding sodium counter-ion control. A) 4 mM glutamine, B) 25 µM glutamine, C) 5 mM ammonium acetate, D) 10 mM ammonium acetate, E) 10 mM sodium acetate, F) 5 mM ammonium chloride, G) 10 mM ammonium chloride, H) 10 mM sodium chloride.

We next assessed the effect of ammonium ions on cell proliferation. AA and ACl both caused a significant increase in cell density compared to the control sample (figure 3.40): while

the 25 µM glutamine control had a cell density of $3.12x10^5$ cells/mL, the cultures treated with AA and ACl reached $1.13x10^6$ and $8.80x10^5$ cells/mL, respectively. The cultures treated with sodium salts showed no significant change in cell density compared to the control. These results suggest that ammonium ions have a protective effect on viability and a potentiating effect on cell proliferation when Sp2/0 cells were cultured in glutamine-limited conditions.

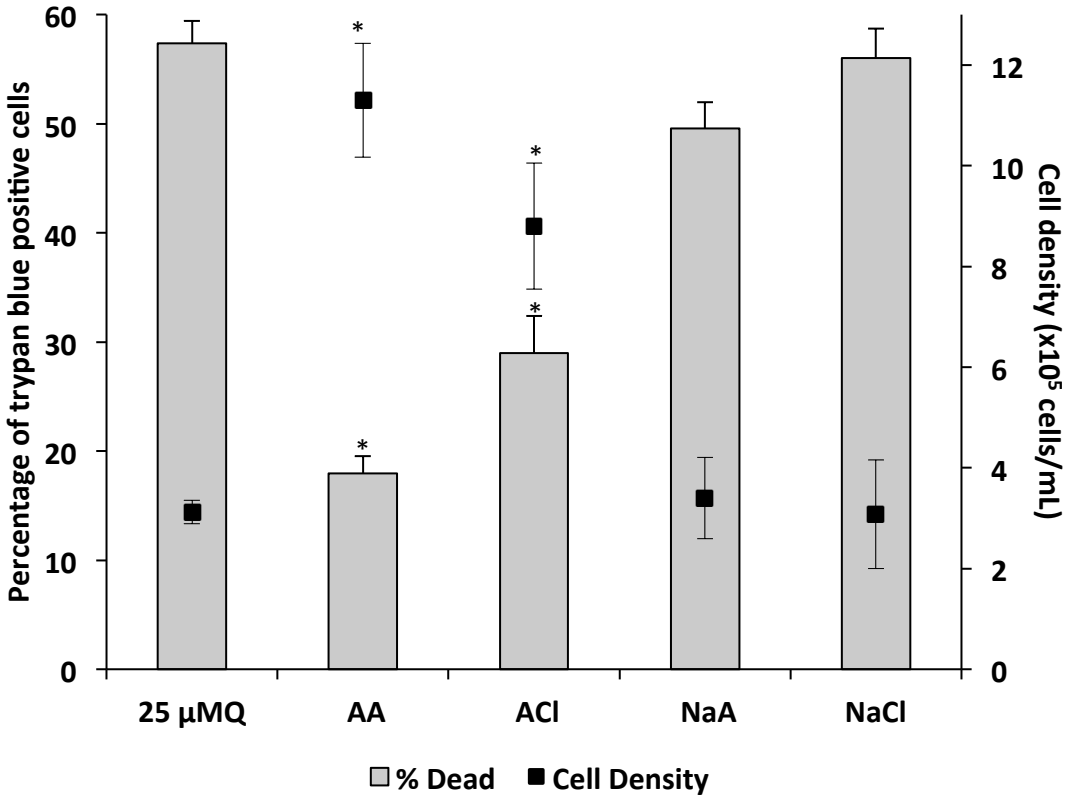

Figure 3.40 - Ammonium Ion Treatment Increases Cell Density and Viability in Glutamine-Limited Conditions

Sp2/0 cells were cultured for a period of 24h in medium containing 25 µM glutamine and supplemented with 5 mM of the indicated salt. Cell density and viability were then determined by the trypan blue staining assay. Data are the average ± SD of 3 independent experiments. * represent $p<0.05$ by ANOVA with Scheffé's *post-hoc* test when compared to the 25 µM glutamine control condition. AA: ammonium acetate, NaA: sodium acetate, ACl: ammonium chloride, NaCl: sodium chloride.

We next sought to confirm these data using a clonogenic assay, which is a more stringent test for measuring cell survival (254). When Sp2/0 cells cultured under glutamine limitation conditions were tested in a clonogenic assay, supplementation with either ammonium salts led to a significant increase in the number of colonies over the untreated control (figure 3.41).

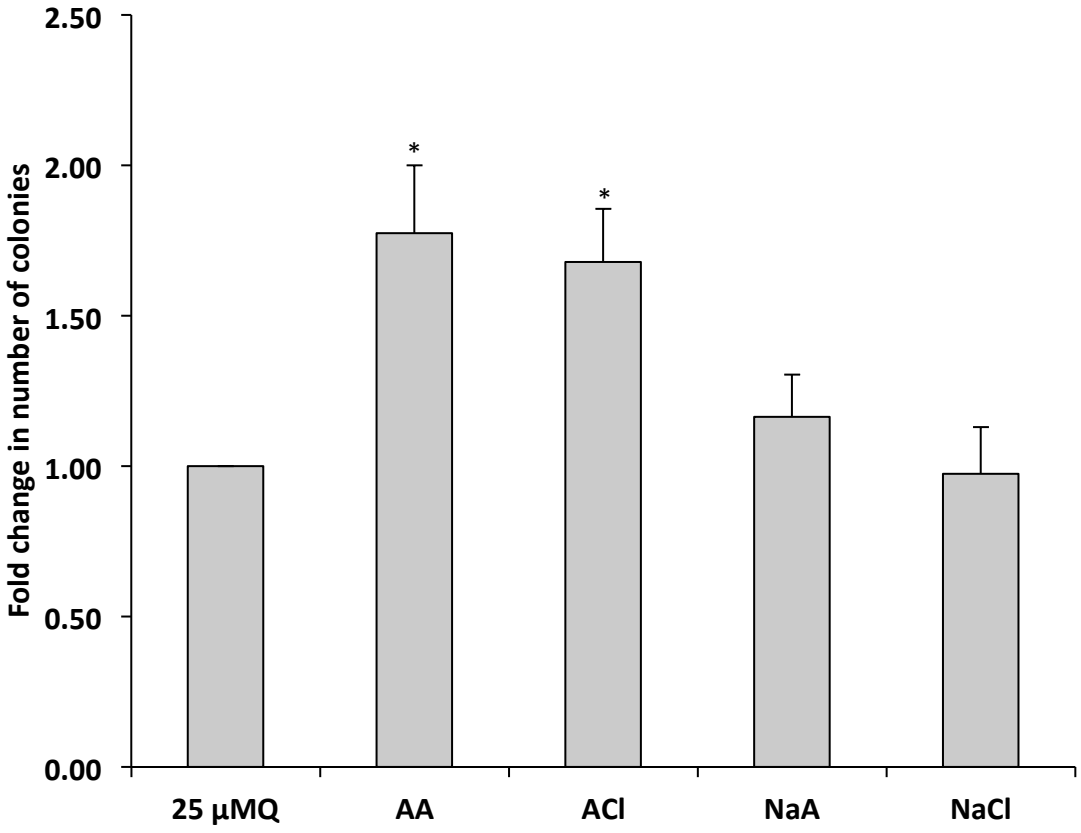

Figure 3.41 - Treatment With Ammonium Ions Increase Sp2/0 Cell Survival in Glutamine-limited Conditions

Sp2/0 cells were cultured for a period of 24h in medium containing 25 µM glutamine in the presence of 5 mM of the indicated ammonium or sodium salts. The cells were then processed for the clonogenic assay, as described in the Material and Methods section. The data presented are the average ± SD of the fold change in the number of colonies compared to the 25 µM glutamine control group (from 3 independent experiments). The star (*) represents $p<0.05$ in a paired two-tailed t-test when compared to the control group. AA: ammonium acetate, NaA: sodium acetate, ACl: ammonium chloride, NaCl: sodium chloride.

Neither sodium salt controls provided a beneficial effect on viability. These results therefore confirm that that ammonium ions can stimulate cell survival of Sp2/0 grown under glutamine-limiting conditions. They also raise the possibility that part of the effect of glutamine on cell viability can be effected by the ammonium ions released following the catabolism of the amino acid.

3.3.2 — Ammonium Salt Treatment Decreases Cell Death

The results shown in figures 3.39-3.41 indicate that Sp2/0 cells are more viable and able to sustain proliferation in glutamine restricted conditions when ammonium salts are supplied in the medium. We next addressed the question of whether ammonium ions acted by interfering with apoptosis. To this aim, we first used the Annexin V/propidium iodide (PI) staining assay. Annexin V is a protein which binds phosphatidylserine (PS), a major phospholipid component of the inner leaflet of the plasma membrane. Propidium iodide is a non cell-permeable, DNA intercalating agent. In apoptotic cells, PS is exposed on the outer leaflet of the plasma membrane, and will be accessible to Annexin V. However, early apoptotic cells still have an intact plasma membrane and will not stain with PI. On the other hand, late apoptotic and necrotic cells have lost membrane integrity, allowing Annexin V to bind PS on the inner leaflet of the plasma membrane, and PI to bind DNA. Thus, this assay can be used to discriminate between viable (Annexin V negative/PI negative), early apoptotic (Annexin V positive/PI negative) and late apoptotic/necrotic cells (Annexin V positive/PI positive).

Figure 3.42 shows the results of an Annexin V/PI staining experiments when Sp2/0 cells were cultured for 24h under glutamine limitation conditions, in the presence of increasing

amounts of ammonium acetate. Cells cultured in medium containing 4 mM glutamine or under glutamine deprivation conditions were used as controls.

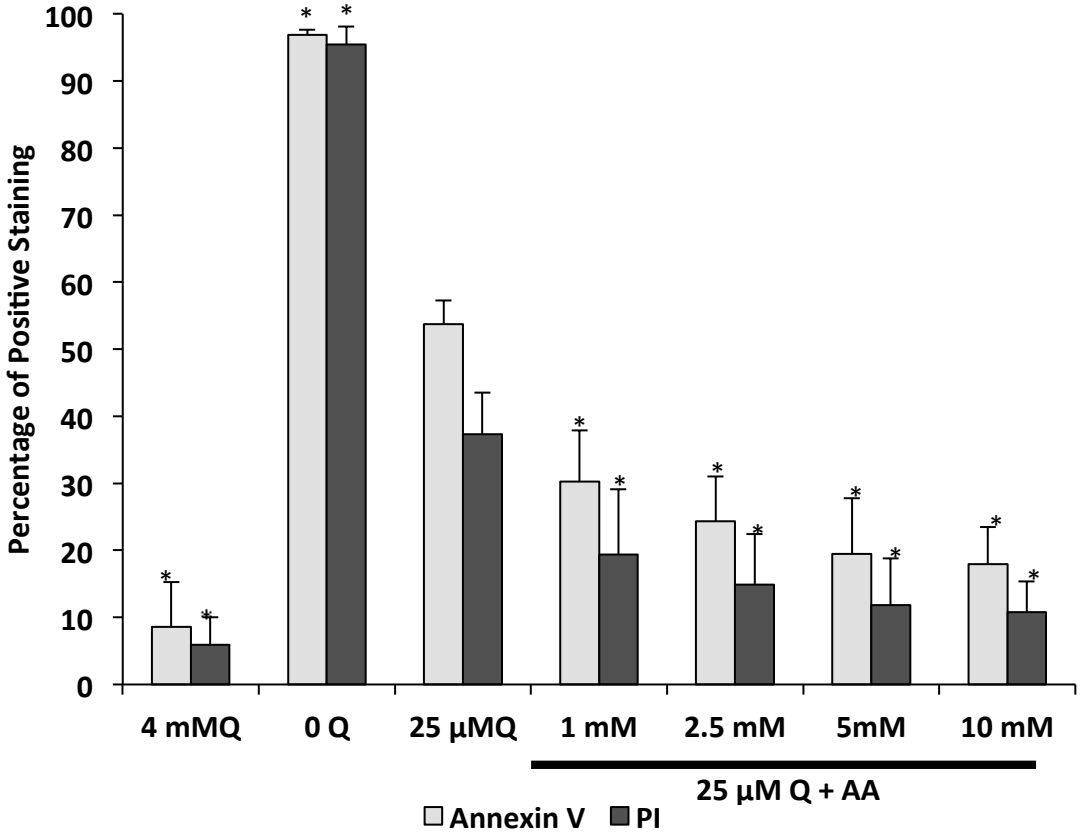

Figure 3.42 - Ammonium Acetate Treatment Protects Against Cell Death in Glutamine-limited Conditions

Sp2/0 cells were cultured for 24h under the indicated conditions before being processed for Annexin V and PI staining and subjected to flow cytometry analysis. Cells cultured in medium containing 4 mM glutamine (4 mM Q), under glutamine deprivation conditions (0 Q), or subjected to glutamine limitation (25 µM Q) were used as controls. Data are the mean ± SD of three independent experiments.* indicates $p<0.05$ in a paired t-test when compared to the 25 µM Q condition. AA: ammonium acetate.

For the control condition, the cells cultured in medium containing 4 mM glutamine had 8.10% of cells that were Annexin V positive, 96.83% of the cells were Annexin V positive when subjected to glutamine deprivation (0 Q) and 53.70% of the cells were positive for Annexin V

staining when cultured under glutamine-limiting conditions. When glutamine-limited Sp2/0 cells were treated with AA, 30.27% of cells were Annexin V positive in the 1000 μM AA condition, 24.33% in the 2.5 mM AA condition, 19.47% in the 5 mM AA condition and 17.90% in the 10 mM AA condition.

For PI staining, the culture control conditions had 5.93% (4 mM glutamine), 95.93% (glutamine-deprived) and 37.30% (glutamine-limited) PI-positive cells respectively. Supplementing the culture medium with AA led to a significant decrease in PI staining, with 19.70% PI-positive cells in the 1000 μM AA condition, 14.87% in the 2.5 mM AA condition, 11.83% in the 5 mM AA condition and 10.77% in the 10 mM AA condition.

The percentage of Annexin V positive or PI positive cells decreased when cells cultured in 25 μM glutamine were treated with AA, and the decrease was more important as the concentration of AA increased, and when compared to the 25 μM glutamine condition. The percentage of cells positive for Annexin V indicate that cells are either apoptotic or necrotic, but does not discriminate between the two. However, cells that are positive of Annexin V staining but negative for PI are apoptotic because they have exposed PS on the outer leaflet of the plasma membrane but have not lost membrane integrity. The percentage of cells that are Annexin V^+/PI^- is shown in figure 3.43. For the culture control conditions 3.54% of the cells were Annexin V^+/PI^- in the 4 mM glutamine group, 2.33% were Annexin V^+/PI^- in the glutamine-deprived group (0Q) and 16.70% were Annexin V^+/PI^- in the glutamine-limited culture. When the glutamine-limited cultures were supplemented with AA, 11.40% of cells were Annexin V^+/PI^- in the 1000 μM AA group, 9.73% in the 2.5 mM AA sample, 8.07% in the 5 mM AA condition and 7.43% in the 10 mM AA group. Therefore, these data show that AA treatment decreases the percentage of cells that are apoptotic when subjected to glutamine-limiting condition.

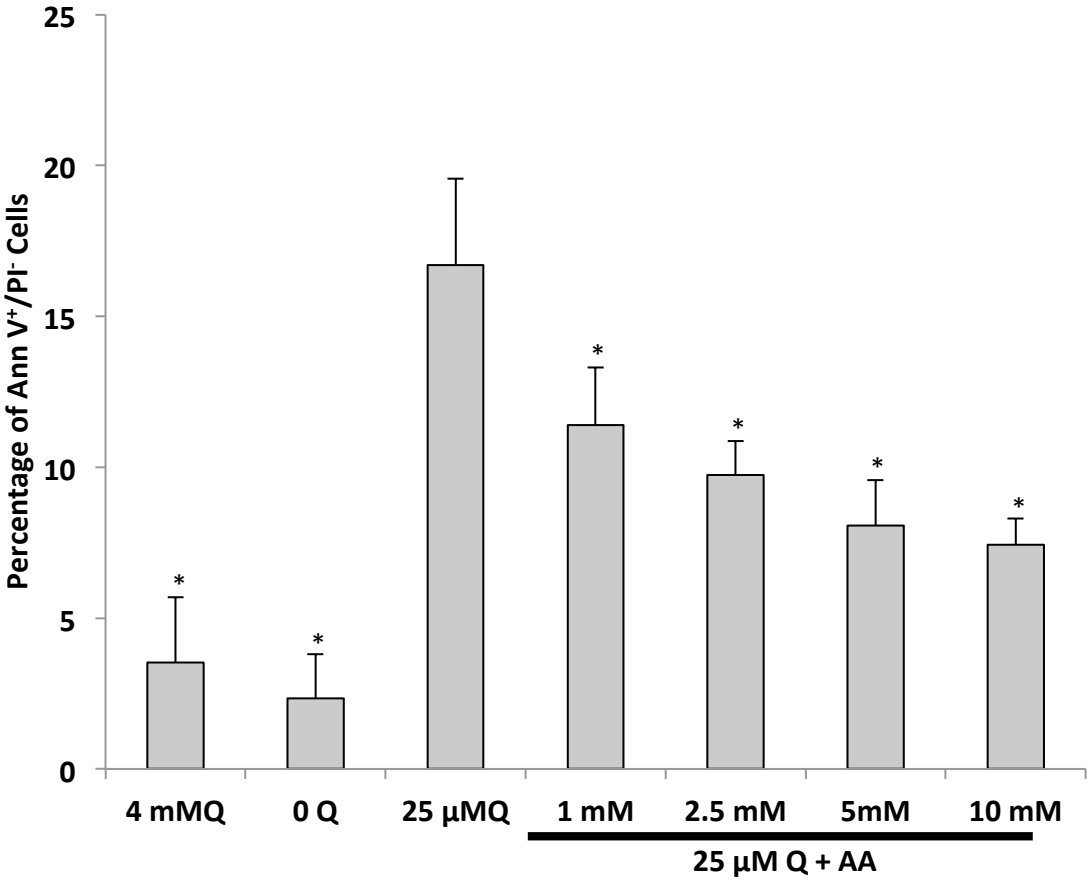

Figure 3.43 - Ammonium Acetate Treatment Prevents Apoptosis

Cells were cultured for 24h in the indicated conditions before being stained and subjected to analysis by flow cytometry with Annexin V and PI. 4 mM glutamine is the culture control condition, and 0 glutamine controls for glutamine-deprivation. Data are the mean of three independent experiments ± standard deviations. * indicates $p<0.05$ in a paired t-test when compared to the 25 µM glutamine condition. Q: glutamine, AA: ammonium acetate.

Unexpectedly, somewhat different results were obtained when the effect of ACl was studied. As shown in Figure 3.44, Sp2/0 cells cultured for 24h under glutamine limitation conditions had 34.73% of cells positive for Annexin V in the 1000 µM ACl group, 31.20% in the 2.5 mM ACl sample, 29.27% in the 5 mM AA condition and 32.52% in the 10 mM AA group (since this experiment was performed at the same time as Figure 3.42, the 3 controls were the same). For the PI staining, 20.71% of glutamine-limited cells were PI positive in the presence of

1000 µM AA condition, 16.87% in the 2.5 mM AA condition, 14.40% in the 5 mM AA condition and 17.40% in the 10 mM AA condition.

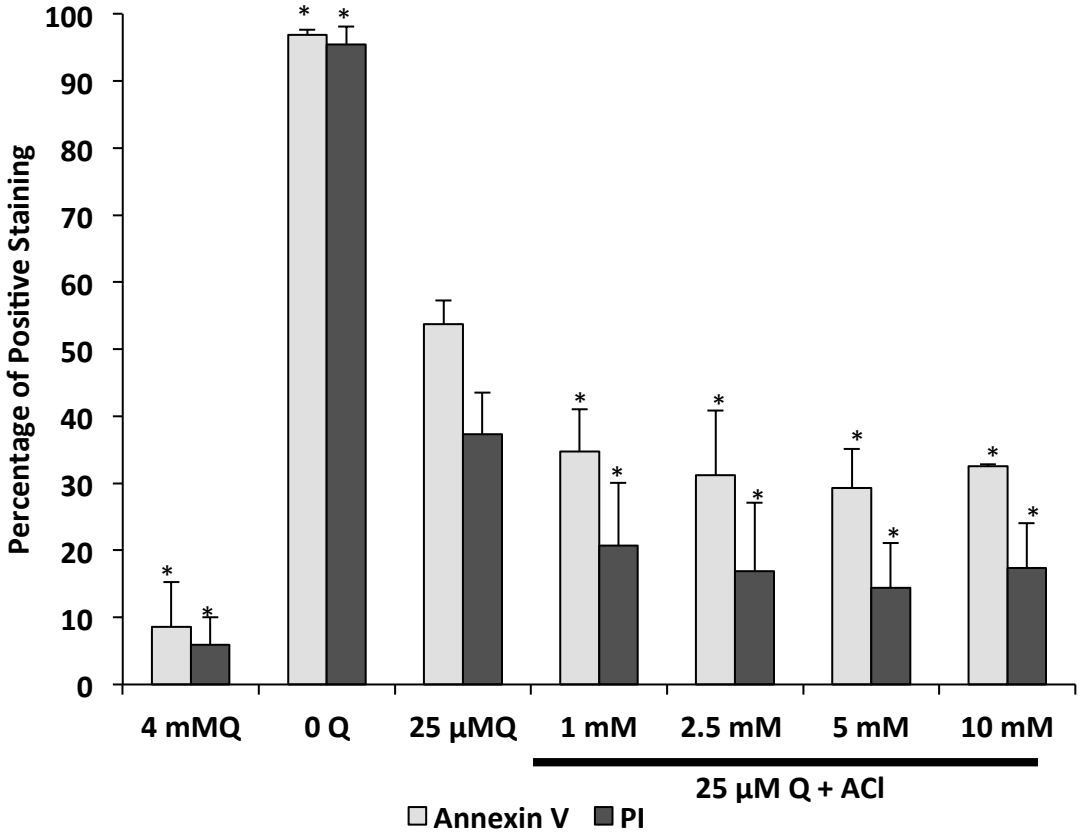

Figure 3.44 - Annexin V and PI Staining With Ammonium Chloride Treatment

Sp2/0 cells were cultured for a period of 24h under the indicated conditions before being processed for Annexin V / PI staining and analysed by flow cytometry. Cells cultured in medium containing 4 mM glutamine (4 mM Q), under glutamine deprivation conditions (0 Q), or subjected to glutamine limitation (25 µM Q) were used as controls. Data are the mean ± SD of three independent experiments. The star (*) denotes $p<0.05$ in a paired t-test when compared to the glutamine-limited (25 µM) for Annexin V staining, ¶ denotes $p<0.05$ in a paired t-test when compared to the glutamine-limited (25 µM) group for PI staining. Q: glutamine, ACl: ammonium chloride.

Therefore, ammonium chloride is not as effective as ammonium acetate in preventing cell death, but the decrease in cell death which we observed is statistically significant across the ACl

treatment groups. The degree of protection from cell death afforded Sp2/0 cells was optimal at 5 mM ACl; there was no statistically significant difference between the results obtained for 5 mM and 10 mM ACl treatments. Figure 3.45 presents the percentage of early apoptotic cells (i.e. Annexin V^+ / PI^-) in the ACl treatment group.

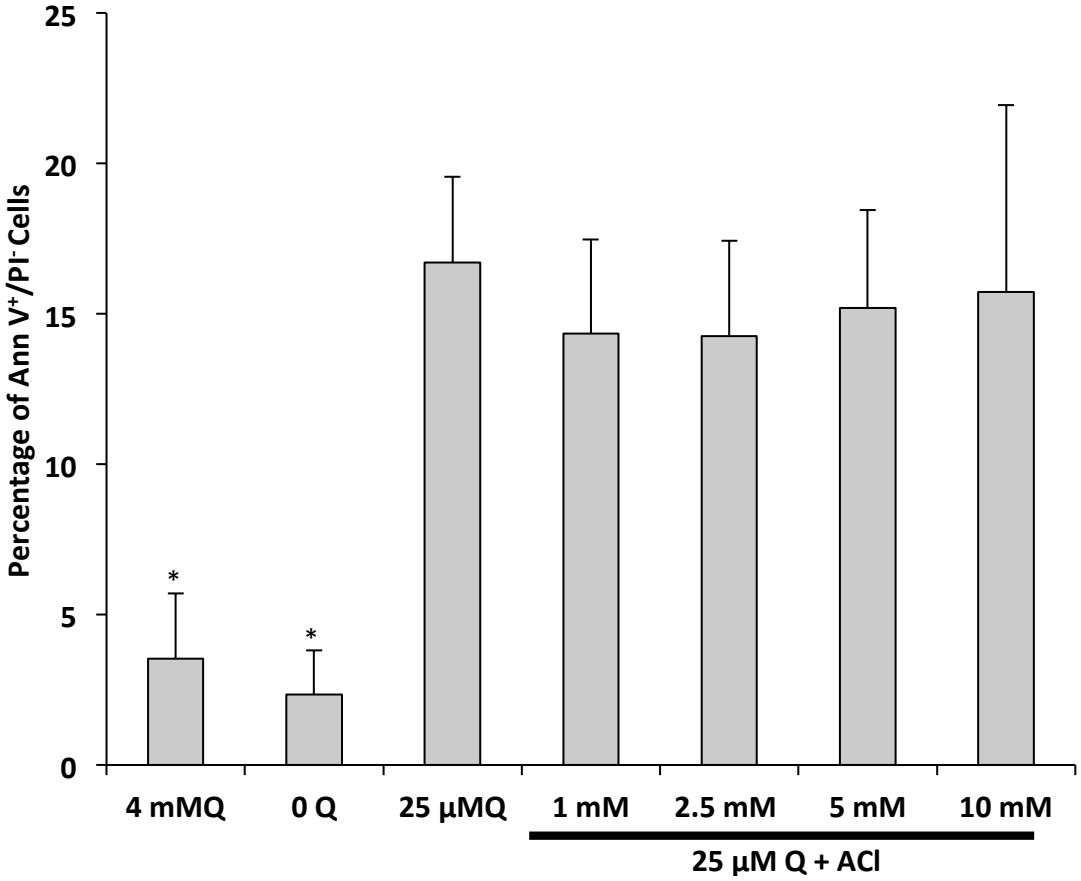

Figure 3.45 - Annexin V^+/PI^- Staining with Ammonium Chloride Treatment

Cells were cultured for 24h in the indicated conditions before being stained and subjected to analysis by flow cytometry with Annexin V and PI. 4 mM glutamine is the culture control condition, and 0 glutamine controls for glutamine-deprivation. Data are the mean of three independent experiments ± standard deviations.* Denotes $p<0.05$ in a paired t-test when compared to the 25 µM glutamine condition. Q: glutamine, ACl: ammonium chloride.

The control conditions were the same as those shown in the figure 3.43, since these experiments were performed at the same time. In glutamine-limited Sp2/0 cells treated with ACl,

14.33% of cells were Annexin V^+/PI^- when exposed to 1000 μM ACl, 14.27% in the 2.5 mM ACl condition, 15.20% in the 5 mM ACl group and 15.73% in the 10 mM ACl sample. These data show that ACl treatment does not affect the percentage of early apoptotic cells under glutamine-limiting conditions.

These data thus far (figures 3.39 to 3.45) indicate that cells are protected from death when treated with either ammonium salt in restricted glutamine conditions, but that only ammonium acetate treatment decreases the percentage of early apoptotic cells.

3.3.3 — Caspase-3 Activity

The presence of ammonium salts in the culture medium protected Sp2/0 cells from cell death under glutamine-restricted conditions, but differed in the way they affected apoptosis. In order to better tease out the effects of ammonium salts on apoptosis, the activation state of caspase-3 was assessed in Sp2/0 cell cultured under conditions of glutamine limitation, in the presence of either ammonium acetate, ammonium chloride, or the corresponding sodium salt controls.

The caspase-3 *in vitro* peptide cleavage assay results presented in figure 3.46 confirmed the Annexin V staining observations. The ammonium acetate treatment decreased the caspase-3 activity to 0.46 of the control condition while ammonium chloride treatment increased the activity to 1.51 fold, a statistically significant difference. Caspase-3 activity in cells cultured in the presence of sodium acetate or sodium chloride was was 1.27 and 1.38 fold higher than the control, respectively. Neither of these two treatments was statistically different from either the 25 μM glutamine or the ammonium chloride conditions. The conclusion to be drawn is that sodium

salts did not have an effect on caspase activity, but that both ammonium molecules did have modulatory effect, but the effects observed were opposite. The difference between the molecules rests with the nature of the anion, whether it be organic or inorganic in nature. It is possible that the organic nature of acetate would be more easily absorbable, or that it would provide additional carbons that could be metabolized within the cell.

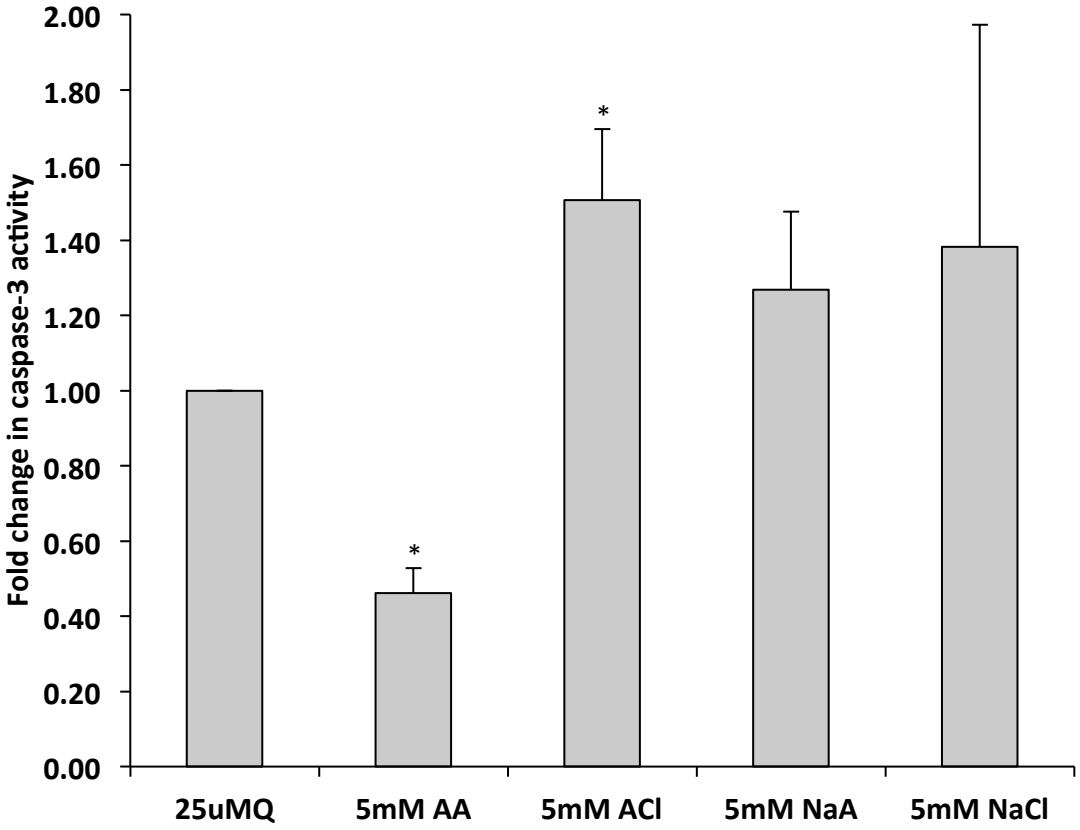

Figure 3.46 - Ammonium Salt Treatment Modulates Caspase-3 Activity

Sp2/0 cells were cultured for 24h in medium containing 25 μM glutamine and the indicated ammonium or sodium salts. The cells were then collected and processed for the caspase-3 activity assay, as described in the Materials and Methods section. Data are the mean fold change of three independent experiments ± standard deviations. The star (*) denotes $p<0.05$ in a paired t-test when compared to the control group. AA: ammonium acetate, NaA: sodium acetate, ACl: ammonium chloride, NaCl: sodium chloride.

3.3.4 — Ammonium Salts Preserve Acidic Vesicles

Ammonium salt treatment has been reported to protect cells from apoptotic death by activating the autophagy pathway (169, 231). In order to assess the effect of ammonium salts on the autophagy pathway, the presence of acidic vesicles was assessed using acridine orange staining. The panel shown in figure 3.47 presents pictures of cells cultured for 24h in medium containing 25 μM glutamine and supplemented with ammonium or sodium salts.

Cells cultured under conditions of glutamine deprivation (0 mM, panel A) or glutamine sufficiency (4 mM, panel B) were used as controls. The cells were then processed for AO staining and observed by fluorescence microscopy. Under conditions of glutamine deprivation, few cells could be observed and they had very diffuse staining. When the cells were cultured in medium containing 4 mM glutamine, the cell density was much greater and the AO staining brighter. Under conditions of glutamine limitation (25 μM, panel C), some of the cells had a uniform shape and were brightly stained, while others have diffuse staining and the presence of apoptotic bodies can be observed (white arrows).

When cells cultured under glutamine-limiting cells were treated with 5 mM AA, they more closely resembled the 4 mM glutamine condition: there were few apoptotic bodies visible, a greater number of cells were present in each field, and the acridine orange staining was of a similar intensity (panels B and D). When Sp2/0 cells cultured in 25 μM Q were treated with 5 mM NaA, the rescue phenomenon disappeared: cells were few, the presence of apoptotic bodies was readily observed and the intensity of the staining was decreased, much like the 25 μM Q condition (panels C and E). Treatment with ammonium chloride had an effect similar to that seen with ammonium acetate, with more cells in each field than the 25 μM Q condition, but not as

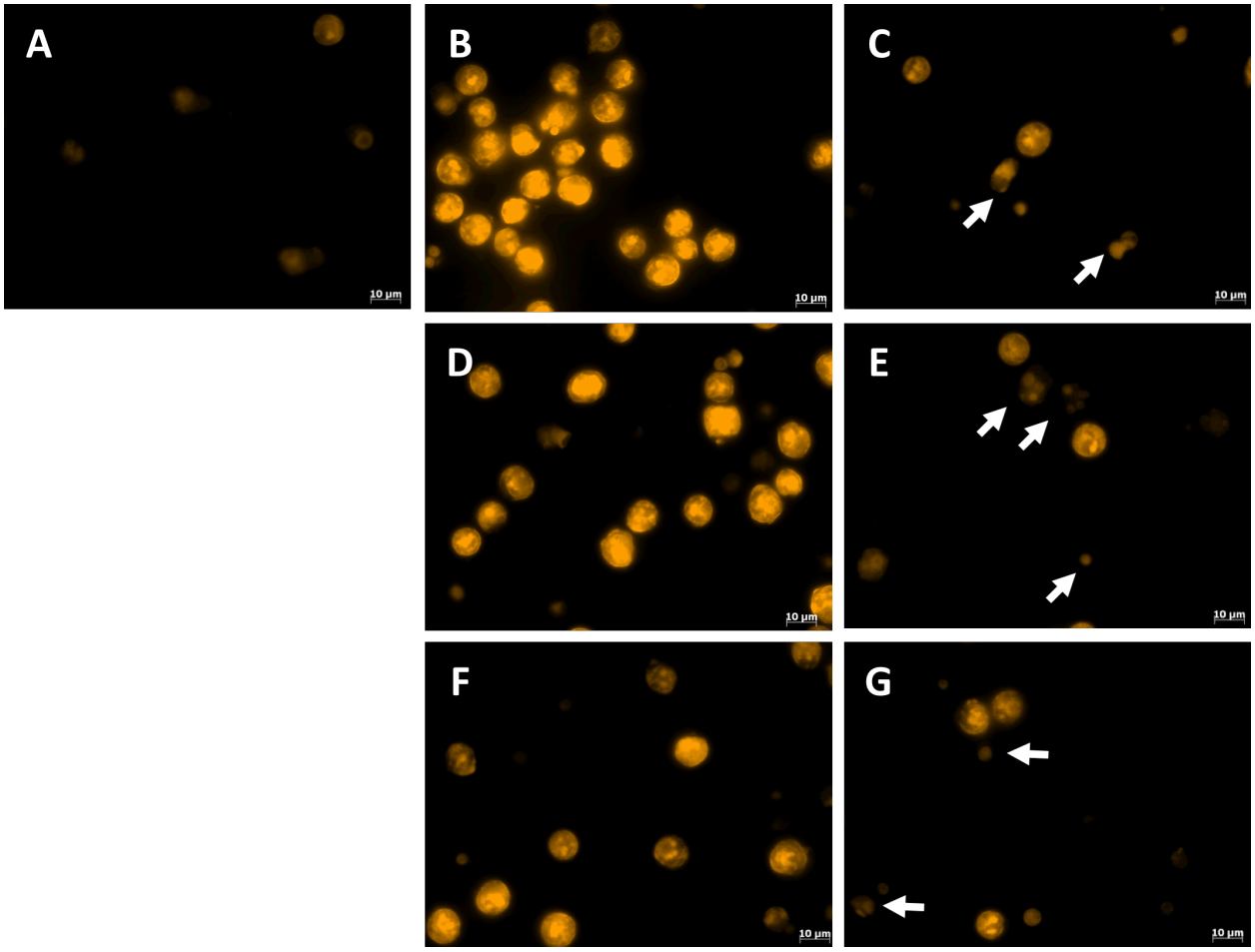

Figure 3.47 - Ammonium Salts Preserve Acidic Vesicles in Glutamine Restriction

Sp2/0 cells were cultured over a 24h period in medium containing 25 µM glutamine, with or without supplementation with ammonium salts or the corresponding sodium salt. After 24h, the cells were collected and stained with AO and the images captured using the same exposure time (6ms) for all groups. A) 0 Q, B) 4 mM Q, C) 25 µM Q, D) 25 µM + 5 mM AA, E) 25 µM Q + 5 mM NaA, F) 25 µM Q + 5 mM ACl, G) 25 µM Q + 5 mM NaCl. At least 5 fields (totalling at least 40 cells) were captured at 40X magnification for each condition of each experimental group. The panels are representative fields of 3 independent experiments. AA: ammonium acetate, NaA: sodium acetate, ACl: ammonium chloride, NaCl: sodium chloride. White arrows indicate the presence of apoptotic bodies.

many as the ammonium acetate condition, intense acridine orange staining and few apoptotic vesicles present in the fields (panel F) and sodium chloride, like sodium acetate, had no protective effect (panel G).

The staining of acidic vesicles with acridine orange presented in figure 3.48 was quantified and is presented in figure 3.49. The intensity of the Sp2/0 cell staining was scored compared to the staining of cells cultured for 24h in medium supplemented 4 mM glutamine condition.

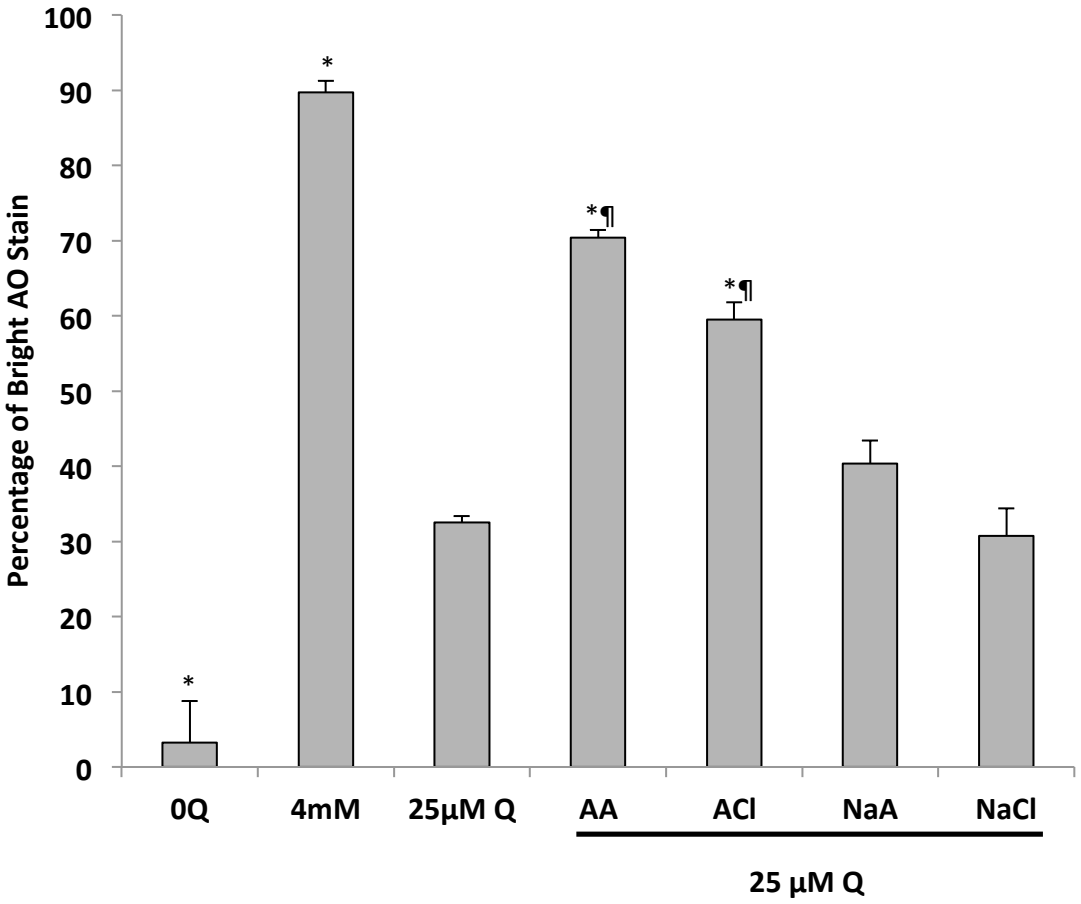

Figure 3.48 - Quantitation of the Rescue Effect of Ammonium Salts

The Sp2/0 cells presented in figure 3.47 were counted and scored as to intensity relative to the 4 mM glutamine group. Data represent the average ± SD from 3 independent experiments. Statistical significance assessed by paired t-test with * $p<0.05$ in a paired t-test when compared to the 25 µM Q condition. ¶ $p<0.05$ in a paired t-test when the AA condition was compared to ACl condition. AA: ammonium acetate, NaA: sodium acetate, ACl: ammonium chloride, NaCl: sodium chloride.

In Sp2/0 cells cultured for 24h in medium supplemented with 4 mM Q, 89.73% of cells had bright AO staining. In the medium not supplemented with glutamine, 3.21% of cells had bright AO staining. In the cells cultured in medium supplemented with 25 μM glutamine, 32.52% of cells had bright AO staining, with 70.40% with AA treatment, 59.54% with ACl treatment, 40.37% with NaA treatment and 30.73% with NaCl. The difference between the 25 μM glutamine control group and those treated with either ammonium salt was statistically significant. It should be noted that the difference between the two ammonium salt treatments was also significant. It should be cautioned that these were not blinded experiments. However, the flow cytometry experiments with Annexin V and PI staining and the Western blot experiments also indicate that there is a differential effect between the ammonium samples and the sodium samples. New techniques would allow for the unbiased quantitation of acidic vesicles by flow cytometry to confirm this observation, and are described in section 4.1 (255).

The acridine orange staining indicated that ammonium salt treatment modulated the ability and number of acidic vacuoles with a rescue effect that resembled that conferred by a culture medium containing a sufficient amount of glutamine. The presence of acidic vacuoles is crucial to the proper degradation of cellular materials during autophagy (133, 210) and so the next experiment was designed to determine the expression of LC3 in Sp2/0 cells treated with glutamine. Cells were cultured for 24h in 25 μM glutamine with or without ammonium salt treatment or the corresponding sodium salt control. A representative image is presented in figure 3.49.

When comparing to the 25 M glutamine, the LC3-II band in the AA condition was 2.04 fold more intense, 1.51 fold more intense in the ACl condition, was less intense (0.6 fold intensity) in the NaA, and relatively similar (1.07 intensity) in the NaCl condition. In all

experiments, the intensity of the LC3-II band was more intense with AA and ACl treatments and either a decrease or similar intensity with NaCl and NaA (see appendix A.6). The presence of the LC3-I form was also more evident in the sodium salt-supplemented cultures and the 25 μM glutamine conditions, but was not consistently present across all experiments. Thus, ammonium salt treatment was associated with increased presence of autophagosome-associated LC3-II, which would suggest a higher rate of autophagy. In the conditions where ammonium ions were not supplied, less autophagosome-associated LC3-II was present and the more evident presence of LC3-I band indicates that autophagy may be present but at a lower rate.

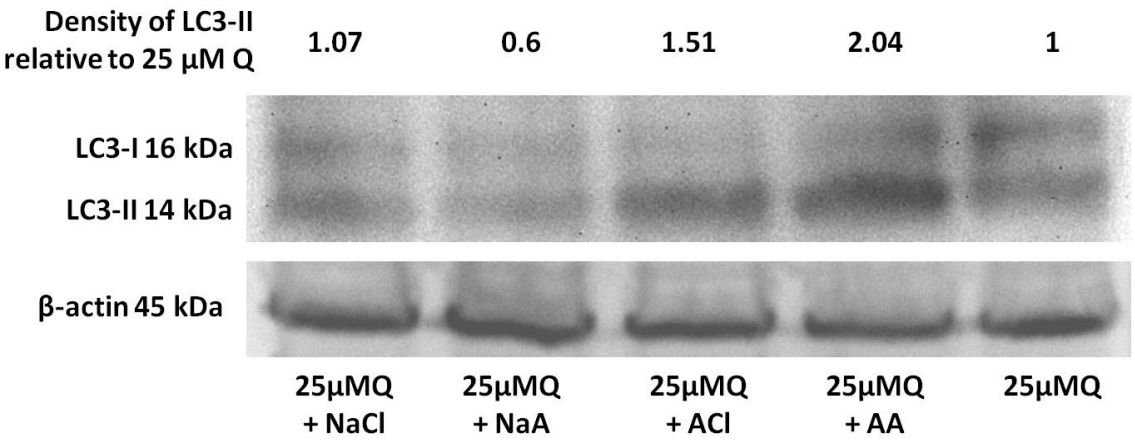

Figure 3.49 - Ammonium Salts Increase LC3-II Expression in Glutamine Limitation

Western blot analysis of protein extracts from Sp2/0 cells cultured over a period of 24h in medium containing 25 μM of glutamine cells. At 24h cells were collected and processed for Western blot analysis with an anti-LC3 antibody. An anti-β-actin antibody used to control for protein loading. Data are representative of 3 independent experiments (see appendix A.5). Density of LC3II relative to the 25 μM Q condition is the β-actin-normalized densitometry reading ratio of the LC3-II band compared to the 25 μM condition. AA: ammonium acetate, NaA: sodium acetate, ACl: ammonium chloride, NaCl: sodium chloride.

In order to confirm the presence of autophagic vacuoles, transmission electron microscopy was also performed (see figure 3.50). When comparing the ammonium salt

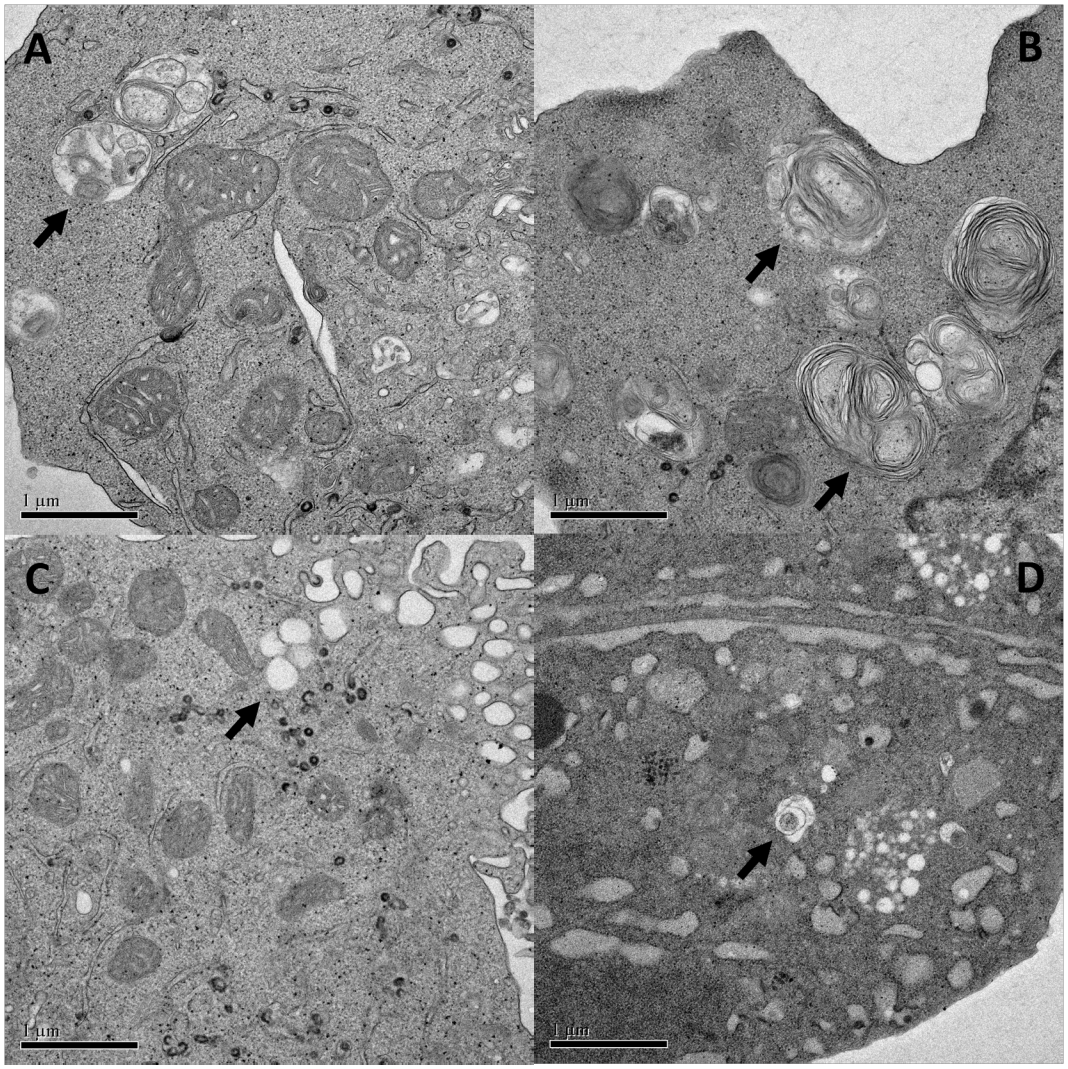

Figure 3.50 - Ammonium and Sodium Salt Treatments

Panel shows cells cultured for 24h in 25 µM glutamine with the following salt treatments: A) ammonium acetate, B) ammonium chloride, C) sodium acetate, D) sodium chloride. After 24h, cells were collected and processed for transmission electron microscopy analysis, as described in the Materials and Methods section. Black arrows indicate the presence of vacuoles.

treatments (panels A and B) to the sodium salt treatments (panels C and D), vacuoles can be observed in all treatments (black arrows). What is striking is the quality of the cytoplasm. The sodium treatments appear to have more vacuoles with less electron density than the ammonium treatments. In fact, the cytoplasm from Sp2/0 cells cultured in 25 µM glutamine and treated with ammonium salt (panels A and B) resemble those observed in the cells culture in glutamine-rich

conditions (see figure 3.29), while those treated with sodium salts resemble cells cultured in 25 μM glutamine (see figure 3.30).

It is noteworthy that more vacuoles containing materials can be observed in panels A and B than can be observed in the panels from Sp2/0 cells cultured in glutamine-rich conditions (figure 3.29). The structures resemble whorl-like autophagosomes reported to contain ribosomes. It was hypothesized that the whorl-like appearance of the autophagosome arose because the membranes originated from the Golgi apparatus, a hypothesis supported by the close association of ribosomes with the Golgi apparatus (256). It is possible that this difference is due to the availability of glutamine in culture media. While ammonium salt treatments did increase cell viability and cell density, cells did not survive to the same extent as those cultured in glutamine-rich medium (see figures 3.30, 3.42 and 3.44). The accumulation of empty cytoplasmic vacuoles, as observed in panels C-D, have been reported in nutrient depletion (257).

3.3.5 — Chapter Summary

The results presented in this section of my thesis allow for the conclusion that supplementation with ammonium ions rescues not only cell viability but proliferation in Sp2/0 cells cultured under glutamine-limiting conditions. Glutamine-restricted culture conditions do not allow for cellular proliferation in Sp2/0 cells; yet Sp2/0 cells cultured in glutamine-restricted medium supplemented with ammonium salts proliferated (figure 3.40). Caspase-3 is activated and cells stain with Annexin V when glutamine availability is limited yet ammonium acetate decreased caspase-3 activity, demonstrating a decrease in apoptotic death (figure 3.46). Acridine orange staining and LC3-II expression where increased in cells treated with ammonium salts,

suggesting that the degree of autophagy was increased in these treated cells when compared to untreated cells (figures 3.48 3.49).

4.0 — DISCUSSION

4.1 — Glutamine Limitation, Ammonium and Autophagy

Our research group has previously shown that Sp2/0 cells are "addicted" to glutamine (53), and the results of figure 3.2 and 3.3 show that there exists a critical threshold concentration of glutamine (100 μM) that affects cellular fate. At this critical threshold, cells are viable, but don't proliferate. Above this threshold concentration of glutamine, cells proliferate, and below it, they undergo apoptosis (see figure 3.4). The results of the AO staining shown in Fig, 3.24 confirmed that the percentage of cells with bright staining was significantly lower when glutamine concentrations in the culture medium were of 100 μM or less. At 25 μM, TEM panels show an accumulation of vacuoles containing undegraded structures within the cytoplasm (figure 3.30), and an accumulation of unlipidated LC3-I (figure 3.31). All together, these data show that the function of acidic cytosolic organelles in Sp2/0 cells is affected when glutamine levels in the medium are decreased below the critical threshold. This, in turn, suggests that the autophagic machinery might be compromised when cell culture levels drop below this threshold.

Interestingly, when Sp2/0 cells were cultured in medium containing 25 μM glutamine, we observed the transient activation of caspase 3. While caspase-3 was clearly activated after 4h of culture in medium containing 25 μM glutamine, the activity of this protease was significantly diminished at 8h, and resumed after 12h. That this was accompanied by a transient cytoplasmic release of cytochrome c suggests that the biphasic activation of caspase-3 could originate from the presence of two populations of Sp2/0 cells which differ in their sensitivity to undergo apoptosis. It is interesting to note that a ubiquitin ligase (PARC/CUL9) promoting cell survival

and targeting cytochrome c for degradation has been recently identified (258). Whether or not the expression or activity of PARC/CUL9 is altered in Sp2/0 exposed to limited concentrations of glutamine remains to be determined. It is possible that a subset of the cell population is undergoing apoptosis. The resulting apoptotic bodies could be phagocytosed by adjacent cells to provide them with nutrients, glutamine and ammonia to stimulate autophagy (259). It is also possible that the cell cycle phase in which cells experience nutrient deprivation would render them more susceptible to enter the apoptotic cascade (figure 3.19). Whether this hypothesis is correct could be assessed by investigating the effect of glutamine limitation over time in the presence or absence of autophagy inhibitors 3-MA and bafilomycin A1 or autophagy stimulators rapamycin and ammonium. These experiments would help elucidate whether the stimulation of autophagy is indeed the reason why apoptosis occurs as biphasic process, and whether mTOR is involved in this response.

In addition to ULK-independent autophagy, other pathways for the non-canonical formation of autophagosomes have been described which bypass the canonical nucleation and elongation phases and would therefore not be responsive to 3-MA inhibition (260, 261). However, as these pathways were described in ATG5 null constructs, in infection models or in epithelial cells, it is unlikely to be the major contributing factor in Sp2/0 cells under glutamine-limiting conditions. It should be noted as a comparison that autophagy inhibitors 3-MA and bafilomycin A1have been used in similar concentrations in other bodies of work. In one study using both 3-MA and bafilomycin A1 in HeLa cells, the authors inhibited autophagy with 10 mM 3-MA and 100 nM bafilomycin (262). Another work reports a concentration of 1nM bafilomycin A1 in several human colon cell lines (252). In HeLa cells, when inhibition of PI3K was employed including 3-MA at 5 mM, mitotic cell death was triggered (263, 264).

The results further indicate that in the Sp2/0 cell line, the autophagic machinery is constitutively activated (figures 3.23, 3.30) and that it is required for survival. There is supporting evidence in the literature for these observations both *in vivo* and *in vitro*. In the experiments where autophagy was inhibited by 3-MA (figure 3.32) or bafilomycin A1 (figure 3.34), cell survival was lost even in glutamine-rich conditions. This could be confirmed by ATG5 knockdown experiments. It is expected that successful knockdown of ATG5 would result in a loss of Sp2/0 cell survival as ATG5 is required for the elongation of the autophagosomal membrane (265). Conversely, when autophagy was stimulated, Sp2/0 cells grown in glutamine-limiting conditions could survive (figure 3.36). Alternatively, ROS have been shown to stimulate autophagy, and thus ROS-generating treatments could be used to confirm this phenomenon in the absence of mTOR inhibition (266). Cannabinoid receptor 1 (CB1) inhibitors have also been reported to increase autophagic flux independent of mTOR inhibition and Beclin-1. As lymphomas have been reported to express different levels of CB1, this could also be another potential way of stimulating autophagy in Sp2 cells (267, 268).

The presence of autophagy in tumour cells is not a new discovery. In fact, LC3B has been identified a marker of solid tumour progression, proliferation and metastasis, and the pro-survival or pro-apoptotic role of autophagy in cancer is largely dependent on the tumour type and context (238, 269, 270). In a recent report in kidney cells, a high basal level of autophagy was required for normal kidney function both *in vivo* and *in vitro* (250). Inhibition of autophagy with 3-MA was shown to induce ER stress, as indicated by an elevation of GRP78 and GADD-153 expression, and subsequently induce apoptosis. The authors further demonstrated that the apoptosis induced by autophagy inhibition was mediated by GADD-153, as knock-down of GADD-153 decreased the autophagy inhibition-induced apoptosis (250). In contrast, our studies

show that glutamine limitation did not induce ER stress, as GRP78 expression was unchanged while GADD-153 expression was increased (figure 3.5), indicating that GADD-153 expression in glutamine limitation may have a different function than that seen in ER stress. GADD-153 knock-down experiments in Sp2/0 cells subjected to glutamine-limiting conditions may shed some light on the role of GADD-153 in autophagy, if any. To assess whether GADD-153 contributes to apoptosis or to survival by adaption in this cellular model, the expression of GADD-153 could be assessed in ammonium-supplemented medium and 25 μM glutamine, conditions under which this work has shown Sp2/0 cells survive and proliferate. The expression of GADD-153 is not likely to trigger apoptosis through mitochondrial dysfunction, as its expression was not modulated by caspase inhibition and was not present in the absence of glutamine unless Bcl-X_L was expressed by transfection (see figures 3.7 and 3.9). Since Bcl-X_L afforded a measure of protection against cell death that was similar to that observed by the addition of micromolar amounts of glutamine (see figure 3.8) or caspase-inhibition (see figure 3.6), it is possible that the up-regulation of GADD-153 may require intact mitochondria, which Bcl-xL would provide, and it may then influence downstream events of the stress response/apoptotic processes. The role of Bcl-X_L or caspase inhibition in autophagy would also need to be elucidated. It would be interesting to investigate whether bafilomycin A1, 3-MA and rapamycin can modulate the expression of GADD-153 in glutamine-limiting conditions, and conversely, whether GADD-153 knockdown experiments would have any effect of autophagy.

Lung adenocarcinoma cells that were epidermal growth-factor independent displayed higher levels of basal autophagy than their growth-factor dependent counterparts (271). The constant activation of autophagy allowed the cells to thrive *in vitro* in hypoxic, reduced-serum conditions, mimicking the tumour microenvironment. Autophagy inhibition by either

chloroquine or ATG5 depletion led to a decrease in cell viability. The authors of this report also report the presence of autophagosomes in lung cancer patient samples with epidermal growth factor receptor mutations (271). In myc-transformed tamoxifen-inducible p53 murine model, lymphoma tumour cells were resistant to apoptosis due to a lack of nuclear p53 (272). The systemic administration of tamoxifen induced the expression of p53, which led to the induction of apoptosis and tumour regression. But while apoptosis was induced in some cells, autophagy was triggered in others which led to tumour recurrence. When apoptosis was induced and autophagy inhibited concurrently, cells then became susceptible to apoptosis (272). In Ras-transformed mouse embryonic fibroblasts and in human transformed cell lines from colon (HCT-116 and DLD-1) and cervical epithelium (HeLa), treatment with Ras inhibitor farnesylthiosalicylic acid induced autophagy and enhanced cell survival. However, in these Ras-transformed cells, autophagy induction by farnesylthiosalicylic acid was also associated with inhibition of tumour growth (273). The differential effect could be linked to Ras transformation as opposed to myc transformation. A recent report indicates that myc-dependent excess cell growth requires autophagy (274). This study performed in *Drosophila melanogaster* identifies myc as being a physiological regulator of autophagy. Under starvation condition, myc was required for the formation of acidic, ATG8-positive puncta, and loss of myc inhibited autophagy. From a mechanistic view, myc overexpression resulted in an increase in the unfolded protein response due to an accumulation of ubiquitinated proteins, which led to phosphorylation of eIF2α by pancreatic eIF2α kinase (PERK) leading to autophagy induction, a process antagonized by GADD-34 (274). Similarly, myc has been reported to be responsible for the metabolic reprogramming required to ensure lymphocyte clonal expansion after activation, a process which is glutamine dependent (275). When combined, these data would suggest that myc

transformation is both capable of reprogramming cells for rapid proliferation but rendering them glutamine-dependent, and to induce autophagy in order to provide building blocks and adaptation capacity.

These reports all support the findings of this study. In addition to the findings that autophagy is a crucial process in Sp2/0 cells is the finding that the levels of available glutamine are capable of modulating autophagy. In Sp2/0 cells cultured at or above the threshold glutamine concentration of 100 μM where cells are viable, the acidic compartments are brightly stained, whereas below this threshold, the intensity of the signal is markedly decreased (figures 3.23, 3.24). From a temporal perspective, the intensity of the acidic compartment staining is significantly decreased as early as 4h after transfer into a medium containing limiting amounts of glutamine (figures 3.26 and 3.27). The ability of glutamine to affect autophagy has been previously reported (276-279). The inhibition of autophagy by ATG5 siRNA or by chloroquine or assaying protein half-life with ^{35}S-labelled methionine could be performed to further confirm the ability of glutamine to affect autophagy in these temporal and glutamine-limiting conditions.

A sufficient amount of glutamine is required for Sp2/0 cell survival. However, its importance is not strictly related to the ability of glutamine to provide fuel to the TCA cycle. This is evidenced by the fact that cells cultured in glutamine-limiting conditions which typically led to reduced viability at 24h were capable of proliferation as long as a source of ammonium ions was supplied (figure 3.40). The by-product of glutamine metabolism, ammonium ion, has been shown to induce autophagy (231). There is an interesting difference in Sp2/0 cell viability and density when autophagy was stimulated by rapamycin or ammonium ions. In figure 3.36, autophagy was stimulated by rapamycin in Sp2/0 cells maintained under glutamine-limiting conditions. Cells had increased survival when compared to the solvent-treated, but cell density

did not increase, a result consistent with mTOR inhibition (280). In figure 3.40, cells cultured under glutamine-limiting conditions were treated with ammonium ions to stimulate autophagy. It should be noted that ammonium ions may have influenced other cellular processes that could also contribute to cell viability. In those conditions, cell viability was partially restored and cell density increased to levels observed in glutamine-rich conditions (see figure 3.1). The stimulation of autophagy can therefore be either mTOR-dependent or mTOR-independent, rapamycin stimulating autophagy by inhibition of mTOR while ammonium ions have been shown to induce autophagy in a mTOR-independent manner (92). It is possible that combining rapamycin and ammonium ion treatments could lead to a synergistic effect on Sp2/0 cell viability when cells are cultured in 25 μM glutamine, potentially rescuing viability to a level as that seen in glutamine-rich conditions. However since rapamycin also inhibits cell proliferation, the synergistic effect may be offset by a lower rate of proliferation.

Sp2/0 cells cultured under glutamine-limiting conditions did not increase the cell density over 24h, but rather underwent apoptosis, leaving approximately 30% of viable cells (figure 3.1). Additionally, Sp2/0 cells cultured in glutamine-rich conditions but in the presence of rapamycin, an mTOR-dependent stimulator of autophagy, cell density was significantly decreased while viability was maintained (see figure 3.37) while rescuing viability but not proliferation in glutamine-limited conditions (see figure 3.38). But when Sp2/0 cells were cultured for 24h in glutamine-limiting conditions in the presence of ammonium ions, viability was increased as was cell density. The ability of ammonium to restore proliferative capacity to Sp2/0 cells in glutamine-limiting conditions could be verified by cell cycle distribution analysis by flow cytometry, using rapamycin as a contrasting autophagic stimulation shown to prevent proliferation in this model. Interestingly, in a recent report, plumbagin, an agent with

anticarcinogenic, antiatherosclerotic and antimicrobial properties, prevents cell proliferation and triggered autophagic cell death by inhibiting the mTOR/Akt pathway, inducing a G_2/M arrest with a concomitant reduction in cyclin B1, cyclin A and cyclin-dependent kinase 1 (Cdk1) (281). In Sp2/0 cells cultured in 25 μM glutamine, there was a decrease in the percentage of cells in G_2/M with a corresponding increase in sub-G_1 cell percentage. Examination of cyclin A, cyclin B1 and Cdk1 when cells are cultured in 25 μM glutamine with ammonium salt treatments may provide further evidence to the ability of ammonium salts to restore proliferative capacity, even in glutamine-limiting conditions.

When considering the cell cycle, the threshold concentration of 100 μM glutamine must be considered. At this concentration, Sp2/0 cells were viable but not proliferating and were arrested in the G_1 phase (figure 3.2). Arrest in the G_1 phase has been induced by downregulation of cyclin D1 in mTOR inhibition by temsirolimus. The ability of temsirolimus to prevent proliferation was augmented by the addition of chloroquine, an autophagy inhibitor (282). In another report, piperine treatment also lead to G_1 cell cycle arrest, downregulation of cyclin D1 and cyclinA, but promoted autophagy induction without inducing apoptosis (283). Examination of cyclin D1 temporally in glutamine limitation with ammonium treatment may also yield interesting information.

It can be postulated that an increase in the rate of autophagy caused by the ammonium salt treatment is the mechanism for the rescue of cell viability and function in glutamine restriction. Unbiased quantitative measure of autophagic flux has been difficult. Most methods require the counting of autophagic vacuoles by microscopy but recently, several flow cytometry-based methods have been described. A new method was recently described using flow cytometry, sonication to release cellular substructures and acridine orange staining (255). The

technique takes advantage of the sensitivity of flow cytometry and the differential staining of acridine orange when excited. Acridine orange emits in the green spectrum when bound to DNA and in the red-orange spectrum when in acidic vacuoles. A high red, low green signal would be indicative of an acidic vacuole (255). Another method would involve LC3-GFP transfection of cells co-stained with monodansylcadeverin, an autofluorescent dye that accumulates in lipid membranes of autophagic vacuoles much like acridine orange, and subjected to flow cytometry. Such staining has been reported to be used to measure autophagic flux (119, 284). In another method reported in *Drosophila* transfected with a UASp-GFP-mCherry-DrAtg8a transgene (285). Once expressed, Atg8, the LC3B homologue, was dual-tagged. When autophagy was not occurring, Atg8 was diffuse in the cytoplasm and fluoresced in the yellow spectrum because of an overlap between the green (GFP) and red (mCherry) signals. When autophagy was triggered and Atg8 was lipidated, the yellow signal would migrate to autophagosomes and form puncta. When the autophagosome fused with lysosomes, hydrolases quenched the GFP signal and only the mCherry signal was detected (285). These investigations could provide interesting results when considering that Sp2/0 cells proliferate at a high rate.

4.2 — Overall Conclusions and Significance

Overall, this body of work shows that glutamine can affect cell behaviour and influence cell signalling to effect cell survival. Moreover, the results suggest that autophagy is a critical mechanism in Sp2/0 cells that allows cells to proliferate even in glutamine-limiting conditions. Autophagy would allow this to occur by recycling non-essential organelles or macromolecules into the building blocks needed for cell replication. What would be required is the signal to do so. As evidenced by this work, this signal could very well be provided by glutamine.

This body of work allows for the conclusion that ammonium ions, likely originating from glutaminolysis, allow the Sp2/0 cells to not only survive in the presence of stress due to nutrient deprivation and protects cells from apoptosis, but also allows for proliferation in times of nutrient restriction. The ability to resist apoptosis, survive in nutrient-restricted conditions and even proliferate could be made possible, at least in part, by the successful induction of the autophagic pathway. As the Sp2/0 cell line is used to commercially manufacture monoclonal antibodies, the discovery that autophagy stimulation via ammonium could allow the Sp2/0 cells to adapt to nutrient-limiting conditions while maintaining the ability to sustain proliferation is a practical way to ensure antibody production without the need for expensive additives to culture media.

Appendix A — Supplementary Figures

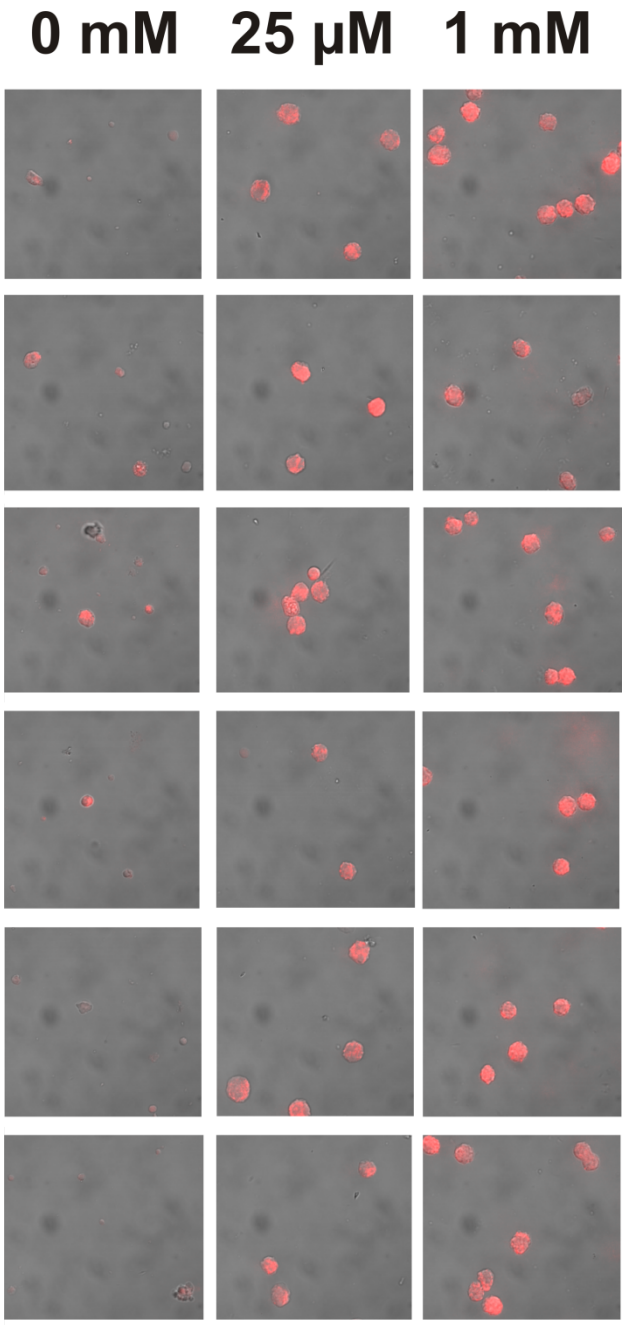

A.1 - Mitotracker Red At 4h

Confocal microscopy picture of cells at 63X magnification, cultured for 4h the indicated concentration of glutamine and stained with Mitotracker H_2ROS Red. Representative of 3 independent experiments (figure 3.16), with at least 5 fields for each sample.

Cell Cycle Stage	0h	4h	8h	24h	24h + Q
Sub G0	0.81	3.46*	5.19*	21.36* ¶ ŧ	3.16
G0/G1	29.28	32.86	34.74¶	32.05	42.31* ¶
S	26.36	32.00	26.58¶	20.17* ¶ ŧ	17.96¶
G2/M	24.43	22.24	25.19	10.83* ¶ ŧ	19.19*

A.2 - Percentage Distribution in the Cell Cycle

Sp2/0 cells were cultured in 25 μM glutamine over 24h for the indicated length of time before collection and subsequent EtOH fixation. Cellular DNA content was stained with propidium iodide and analysed by flow cytometry. Data represents the mean of 3 independent experiments and is presented in figure 3.19. Statistical significance assessed by paired t-test with * $p<0.05$ compared to 0h, ¶ $p<0.05$ compared to 4h and ŧ $p<0.05$ compared to 8h.

Sample	Band	1000 µM Q	250 µM Q	100 µM Q	50 µM Q	25 µM Q
1	LC3-II	1.42	0.58	0.4	0.35	1
	LC3-I	1.35	0.62	0.39	0.22	1
2	LC3-II	2.07	1.67	0.80	0.80	1
	LC3-I	2.54	1.43	0.62	0.36	1
3	LC3-II	1.10	0.86	0.85	0.68	1
	LC3-I	1.11	2.03	1.31	0.19	1

A.3 - β-actin-Normalized Densitometry Expressed Relative to 25 µM Treatment Group in the Gradual Limitation Model

Densitometry values for the LC3-II and LC3-I bands as obtained by Western blotting and presented in figure 3.31. The densitometry readings were normalized to the densitometry reading of β-actin then compared to the 25 µM treatment group.

Sample	Ratio	1000 µM Q	250 µM Q	100 µM Q	50 µM Q	25 µM Q
1	LC3-II / LC3-I	2.9	2.6	2.8	4.4	2.8
2	LC3-II / LC3-I	1.6	2.3	2.5	4.4	1.9
3	LC3-II / LC3-I	17.8	7.6	11.7	64.1	18.0

A.4 - β-actin-Normalized Densitometry of LC3-II:LC3-1 Within Each Treatment Group in the Gradual Limitation Model

Ratio of LC3-II:LC3-I values calculated from the densitometry data presented in A.3. The ratios present the relative densitometry readings of LC3-II when compared to the LC3-I for each condition.

Sample	T=0h	T=4h	T=8h	T=24h	T=24h + Q
1	1	0.72	0.68	1.58	2.43
2	1	0.93	0.96	1.66	1.42
3	1	0.96	0.74	1.20	1.28

A.5 - β-actin-Normalized Densitometry Expressed Relative to Baseline Group in the Time Course Model

Densitometry values for the LC3-II band as obtained by Western blotting and presented in figure 3.31. The densitometry readings for the LC3-II band were normalized to the densitometry reading of β-actin then compared to the baseline (t=0h) treatment group.

Sample	25 µMQ	AA	ACl	NaA	NaCl
1	1	2.04	1.51	0.6	1.07
2	1	16.85	28.51	7.27	8.90
3	1	5.20	6.45	3.65	2.93

A.6 - β-actin-Normalized Densitometry Expressed Relative to 25 µM Treatment Group in the Ammonium Model

Densitometry values for the LC3-II band as obtained by Western blotting and presented in figure 3.49. The densitometry readings for the LC3-II band were normalized to the densitometry reading of β-actin then compared to the 25 µM treatment group.

REFERENCES

1. Warburg, O., Wind, F., and Negelein, E. (1927) The Metabolism of Tumors in the Body. *J.Gen.Physiol.* **8,** 519-530

2. Warburg, O. (1956) On the origin of cancer cells. *Science.* **123,** 309-314

3. Jose, C., Bellance, N., and Rossignol, R. (2011) Choosing between glycolysis and oxidative phosphorylation: a tumor's dilemma?. *Biochim.Biophys.Acta.* **1807,** 552-561

4. Vander Heiden, M.G., Cantley, L.C., and Thompson, C.B. (2009) Understanding the Warburg effect: the metabolic requirements of cell proliferation. *Science.* **324,** 1029-1033

5. Kim, J.W., and Dang, C.V. (2006) Cancer's molecular sweet tooth and the Warburg effect. *Cancer Res.* **66,** 8927-8930

6. Marino, G., and Kroemer, G. (2010) Ammonia: a diffusible factor released by proliferating cells that induces autophagy. *Sci.Signal.* **3,** pe19

7. Gottlieb, E., and Tomlinson, I.P. (2005) Mitochondrial tumour suppressors: a genetic and biochemical update. *Nat.Rev.Cancer.* **5,** 857-866

8. Greiner, E.F., Guppy, M., and Brand, K. (1994) Glucose is essential for proliferation and the glycolytic enzyme induction that provokes a transition to glycolytic energy production. *J.Biol.Chem.* **269,** 31484-31490

9. DeBerardinis, R.J., Lum, J.J., Hatzivassiliou, G., and Thompson, C.B. (2008) The biology of cancer: metabolic reprogramming fuels cell growth and proliferation. *Cell.Metab.* **7,** 11-20

10. Doherty, J.R., and Cleveland, J.L. (2013) Targeting lactate metabolism for cancer therapeutics. *J.Clin.Invest.* **123,** 3685-3692

11. Fischer, K., Hoffmann, P., Voelkl, S., Meidenbauer, N., Ammer, J., Edinger, M., Gottfried, E., Schwarz, S., Rothe, G., Hoves, S., Renner, K., Timischl, B., Mackensen, A., Kunz-Schughart, L., Andreesen, R., Krause, S.W., and Kreutz, M. (2007) Inhibitory effect of tumor cell-derived lactic acid on human T cells. *Blood.* **109,** 3812-3819

12. Polet, F., and Feron, O. (2013) Endothelial cell metabolism and tumour angiogenesis: glucose and glutamine as essential fuels and lactate as the driving force. *J.Intern.Med.* **273,** 156-165

13. Metallo, C.M., and Vander Heiden, M.G. (2010) Metabolism strikes back: metabolic flux regulates cell signaling. *Genes Dev.* **24,** 2717-2722

14. Sutton-McDowall, M.L., Gilchrist, R.B., and Thompson, J.G. (2010) The pivotal role of glucose metabolism in determining oocyte developmental competence. *Reproduction.* **139,** 685-695

15. Wellen, K.E., Lu, C., Mancuso, A., Lemons, J.M., Ryczko, M., Dennis, J.W., Rabinowitz, J.D., Coller, H.A., and Thompson, C.B. (2010) The hexosamine biosynthetic pathway couples growth factor-induced glutamine uptake to glucose metabolism. *Genes Dev.* **24,** 2784-2799

16. Flier, J.S., Mueckler, M.M., Usher, P., and Lodish, H.F. (1987) Elevated levels of glucose transport and transporter messenger RNA are induced by ras or src oncogenes. *Science.* **235,** 1492-1495

17. Shim, H., Dolde, C., Lewis, B.C., Wu, C.S., Dang, G., Jungmann, R.A., Dalla-Favera, R., and Dang, C.V. (1997) c-Myc transactivation of LDH-A: implications for tumor metabolism and growth. *Proc.Natl.Acad.Sci.U.S.A.* **94,** 6658-6663

18. Elstrom, R.L., Bauer, D.E., Buzzai, M., Karnauskas, R., Harris, M.H., Plas, D.R., Zhuang, H., Cinalli, R.M., Alavi, A., Rudin, C.M., and Thompson, C.B. (2004) Akt stimulates aerobic glycolysis in cancer cells. *Cancer Res.* **64,** 3892-3899

19. Fantin, V.R., St-Pierre, J., and Leder, P. (2006) Attenuation of LDH-A expression uncovers a link between glycolysis, mitochondrial physiology, and tumor maintenance. *Cancer.Cell.* **9,** 425-434

20. Gaglio, D., Metallo, C.M., Gameiro, P.A., Hiller, K., Danna, L.S., Balestrieri, C., Alberghina, L., Stephanopoulos, G., and Chiaradonna, F. (2011) Oncogenic K-Ras decouples glucose and glutamine metabolism to support cancer cell growth. *Mol.Syst.Biol.* **7,** 523

21. Chiaradonna, F., Sacco, E., Manzoni, R., Giorgio, M., Vanoni, M., and Alberghina, L. (2006) Ras-dependent carbon metabolism and transformation in mouse fibroblasts. *Oncogene.* **25,** 5391-5404

22. Powers, J.T., Hong, S., Mayhew, C.N., Rogers, P.M., Knudsen, E.S., and Johnson, D.G. (2004) E2F1 uses the ATM signaling pathway to induce p53 and Chk2 phosphorylation and apoptosis. *Mol.Cancer.Res.* **2,** 203-214

23. Curi, R., Lagranha, C.J., Doi, S.Q., Sellitti, D.F., Procopio, J., Pithon-Curi, T.C., Corless, M., and Newsholme, P. (2005) Molecular mechanisms of glutamine action. *J.Cell.Physiol.* **204,** 392-401

24. Newsholme, P., Procopio, J., Lima, M.M., Pithon-Curi, T.C., and Curi, R. (2003) Glutamine and glutamate--their central role in cell metabolism and function. *Cell Biochem.Funct.* **21,** 1-9

25. Kim, H. (2011) Glutamine as an immunonutrient. *Yonsei Med.J.* **52,** 892-897

26. Wischmeyer, P.E. (2007) Glutamine: mode of action in critical illness. *Crit.Care Med.* **35,** S541-4

27. Bodega, G., Suarez, I., Lopez-Fernandez, L.A., Garcia, M.I., Kober, M., Penedo, M., Luna, M., Juarez, S., Ciordia, S., Oria, M., Cordoba, J., and Fernandez, B. (2012) Ammonia induces aquaporin-4 rearrangement in the plasma membrane of cultured astrocytes. *Neurochem.Int.* **61,** 1314-1324

28. Yamauchi, K., Komatsu, T., Kulkarni, A.D., Ohmori, Y., Minami, H., Ushiyama, Y., Nakayama, M., and Yamamoto, S. (2002) Glutamine and arginine affect Caco-2 cell proliferation by promotion of nucleotide synthesis. *Nutrition.* **18,** 329-333

29. Li, L., Zhang, H., Varrin-Doyer, M., Zamvil, S.S., and Verkman, A.S. (2011) Proinflammatory role of aquaporin-4 in autoimmune neuroinflammation. *FASEB J.* **25,** 1556-1566

30. Yeh, C.L., Hsu, C.S., Yeh, S.L., and Chen, W.J. (2005) Dietary glutamine supplementation modulates Th1/Th2 cytokine and interleukin-6 expressions in septic mice. *Cytokine.* **31,** 329-334

31. Hubert-Buron, A., Leblond, J., Jacquot, A., Ducrotte, P., Dechelotte, P., and Coeffier, M. (2006) Glutamine pretreatment reduces IL-8 production in human intestinal epithelial cells by limiting IkappaBalpha ubiquitination. *J.Nutr.* **136,** 1461-1465

32. Coeffier, M., Marion, R., Ducrotte, P., and Dechelotte, P. (2003) Modulating effect of glutamine on IL-1beta-induced cytokine production by human gut. *Clin.Nutr.* **22,** 407-413

33. Bussolati, O., Belletti, S., Uggeri, J., Gatti, R., Orlandini, G., Dall'Asta, V., and Gazzola, G.C. (1995) Characterization of apoptotic phenomena induced by treatment with L-asparaginase in NIH3T3 cells. *Exp.Cell Res.* **220,** 283-291

34. Fumarola, C., Zerbini, A., and Guidotti, G.G. (2001) Glutamine deprivation-mediated cell shrinkage induces ligand-independent CD95 receptor signaling and apoptosis. *Cell Death Differ.* **8,** 1004-1013

35. Mates, J.M., Segura, J.A., Campos-Sandoval, J.A., Lobo, C., Alonso, L., Alonso, F.J., and Marquez, J. (2009) Glutamine homeostasis and mitochondrial dynamics. *Int.J.Biochem.Cell Biol.* **41,** 2051-2061

36. Castell, L., Vance, C., Abbott, R., Marquez, J., and Eggleton, P. (2004) Granule localization of glutaminase in human neutrophils and the consequence of glutamine utilization for neutrophil activity. *J.Biol.Chem.* **279,** 13305-13310

37. Adeva, M.M., Souto, G., Blanco, N., and Donapetry, C. (2012) Ammonium metabolism in humans. *Metabolism.* **61,** 1495-1511

38. DeBerardinis, R.J., Mancuso, A., Daikhin, E., Nissim, I., Yudkoff, M., Wehrli, S., and Thompson, C.B. (2007) Beyond aerobic glycolysis: transformed cells can engage in glutamine metabolism that exceeds the requirement for protein and nucleotide synthesis. *Proc.Natl.Acad.Sci.U.S.A.* **104,** 19345-19350

39. Stern, R., Shuster, S., Neudecker, B.A., and Formby, B. (2002) Lactate stimulates fibroblast expression of hyaluronan and CD44: the Warburg effect revisited. *Exp.Cell Res.* **276,** 24-31

40. Ferreira, L.M. (2010) Cancer metabolism: the Warburg effect today. *Exp.Mol.Pathol.* **89,** 372-380

41. Eagle, H. (1955) Nutrition needs of mammalian cells in tissue culture. *Science.* **122,** 501-514

42. Curi, R., Newsholme, P., Pithon-Curi, T.C., Pires-de-Melo, M., Garcia, C., Homem-de-Bittencourt Junior, P.I., and Guimaraes, A.R. (1999) Metabolic fate of glutamine in lymphocytes, macrophages and neutrophils. *Braz.J.Med.Biol.Res.* **32,** 15-21

43. Mates, J.M., Perez-Gomez, C., Nunez de Castro, I., Asenjo, M., and Marquez, J. (2002) Glutamine and its relationship with intracellular redox status, oxidative stress and cell proliferation/death. *Int.J.Biochem.Cell Biol.* **34,** 439-458

44. Perez-Gomez, C., Campos-Sandoval, J.A., Alonso, F.J., Segura, J.A., Manzanares, E., Ruiz-Sanchez, P., Gonzalez, M.E., Marquez, J., and Mates, J.M. (2005) Co-expression of glutaminase K and L isoenzymes in human tumour cells. *Biochem.J.* **386,** 535-542

45. Mates, J.M., Segura, J.A., Martin-Rufian, M., Campos-Sandoval, J.A., Alonso, F.J., and Marquez, J. (2013) Glutaminase Isoenzymes as Key Regulators in Metabolic and Oxidative Stress against Cancer. *Curr.Mol.Med.* **13,** 514-534

46. Obrador, E., Carretero, J., Esteve, J.M., Pellicer, J.A., Pascual, A., Petschen, I., and Estrela, J.M. (2001) Glutamine potentiates TNF-alpha-induced tumor cytotoxicity. *Free Radic.Biol.Med.* **31,** 642-650

47. Xia, Y., Wen, H.Y., Young, M.E., Guthrie, P.H., Taegtmeyer, H., and Kellems, R.E. (2003) Mammalian target of rapamycin and protein kinase A signaling mediate the cardiac transcriptional response to glutamine. *J.Biol.Chem.* **278,** 13143-13150

48. Yecies, J.L., and Manning, B.D. (2011) mTOR links oncogenic signaling to tumor cell metabolism. *J.Mol.Med.(Berl).* **89,** 221-228

49. Le, A., Lane, A.N., Hamaker, M., Bose, S., Gouw, A., Barbi, J., Tsukamoto, T., Rojas, C.J., Slusher, B.S., Zhang, H., Zimmerman, L.J., Liebler, D.C., Slebos, R.J., Lorkiewicz, P.K., Higashi, R.M., Fan, T.W., and Dang, C.V. (2012) Glucose-independent glutamine metabolism via TCA cycling for proliferation and survival in B cells. *Cell.Metab.* **15,** 110-121

50. Qing, G., Li, B., Vu, A., Skuli, N., Walton, Z.E., Liu, X., Mayes, P.A., Wise, D.R., Thompson, C.B., Maris, J.M., Hogarty, M.D., and Simon, M.C. (2012) ATF4 Regulates MYC-Mediated Neuroblastoma Cell Death upon Glutamine Deprivation. *Cancer.Cell.* **22,** 631-644

51. Motoki, T., Naomoto, Y., Hoshiba, J., Shirakawa, Y., Yamatsuji, T., Matsuoka, J., Takaoka, M., Tomono, Y., Fujiwara, Y., Tsuchita, H., Gunduz, M., Nagatsuka, H., Tanaka, N., and Fujiwara, T. (2011) Glutamine depletion induces murine neonatal melena with increased apoptosis of the intestinal epithelium. *World J.Gastroenterol.* **17,** 717-726

52. Yuneva, M., Zamboni, N., Oefner, P., Sachidanandam, R., and Lazebnik, Y. (2007) Deficiency in glutamine but not glucose induces MYC-dependent apoptosis in human cells. *J.Cell Biol.* **178,** 93-105

53. Paquette, J.C., Guerin, P.J., and Gauthier, E.R. (2005) Rapid induction of the intrinsic apoptotic pathway by L-glutamine starvation. *J.Cell.Physiol.* **202,** 912-921

54. Wise, D.R., DeBerardinis, R.J., Mancuso, A., Sayed, N., Zhang, X.Y., Pfeiffer, H.K., Nissim, I., Daikhin, E., Yudkoff, M., McMahon, S.B., and Thompson, C.B. (2008) Myc regulates a transcriptional program that stimulates mitochondrial glutaminolysis and leads to glutamine addiction. *Proc.Natl.Acad.Sci.U.S.A.* **105,** 18782-18787

55. Eilers, M., and Eisenman, R.N. (2008) Myc's broad reach. *Genes Dev.* **22,** 2755-2766

56. Mbulaiteye, S.M. (2013) Burkitt Lymphoma: beyond discoveries. *Infect.Agent Cancer.* **8,** 35

57. Li, F., Wang, Y., Zeller, K.I., Potter, J.J., Wonsey, D.R., O'Donnell, K.A., Kim, J.W., Yustein, J.T., Lee, L.A., and Dang, C.V. (2005) Myc stimulates nuclearly encoded mitochondrial genes and mitochondrial biogenesis. *Mol.Cell.Biol.* **25,** 6225-6234

58. Soucek, L., Whitfield, J., Martins, C.P., Finch, A.J., Murphy, D.J., Sodir, N.M., Karnezis, A.N., Swigart, L.B., Nasi, S., and Evan, G.I. (2008) Modelling Myc inhibition as a cancer therapy. *Nature.* **455,** 679-683

59. Gao, P., Tchernyshyov, I., Chang, T.C., Lee, Y.S., Kita, K., Ochi, T., Zeller, K.I., De Marzo, A.M., Van Eyk, J.E., Mendell, J.T., and Dang, C.V. (2009) c-Myc suppression of miR-23a/b enhances mitochondrial glutaminase expression and glutamine metabolism. *Nature.* **458,** 762-765

60. Taub, R., Kirsch, I., Morton, C., Lenoir, G., Swan, D., Tronick, S., Aaronson, S., and Leder, P. (1982) Translocation of the c-myc gene into the immunoglobulin heavy chain locus in human Burkitt lymphoma and murine plasmacytoma cells. *Proc.Natl.Acad.Sci.U.S.A.* **79,** 7837-7841

61. Csibi, A., Fendt, S.M., Li, C., Poulogiannis, G., Choo, A.Y., Chapski, D.J., Jeong, S.M., Dempsey, J.M., Parkhitko, A., Morrison, T., Henske, E.P., Haigis, M.C., Cantley, L.C., Stephanopoulos, G., Yu, J., and Blenis, J. (2013) The mTORC1 pathway stimulates glutamine metabolism and cell proliferation by repressing SIRT4. *Cell.* **153,** 840-854

62. Jeong, S.M., Xiao, C., Finley, L.W., Lahusen, T., Souza, A.L., Pierce, K., Li, Y.H., Wang, X., Laurent, G., German, N.J., Xu, X., Li, C., Wang, R.H., Lee, J., Csibi, A., Cerione, R., Blenis, J., Clish, C.B., Kimmelman, A., Deng, C.X., and Haigis, M.C. (2013) SIRT4 has tumor-suppressive activity and regulates the cellular metabolic response to DNA damage by inhibiting mitochondrial glutamine metabolism. *Cancer.Cell.* **23,** 450-463

63. Jeong, S.M., Lee, A., Lee, J., and Haigis, M.C. (2014) SIRT4 protein suppresses tumor formation in genetic models of Myc-induced B cell lymphoma. *J.Biol.Chem.* **289,** 4135-4144

64. Hatzivassiliou, G., Zhao, F., Bauer, D.E., Andreadis, C., Shaw, A.N., Dhanak, D., Hingorani, S.R., Tuveson, D.A., and Thompson, C.B. (2005) ATP citrate lyase inhibition can suppress tumor cell growth. *Cancer.Cell.* **8,** 311-321

65. Wellen, K.E., Hatzivassiliou, G., Sachdeva, U.M., Bui, T.V., Cross, J.R., and Thompson, C.B. (2009) ATP-citrate lyase links cellular metabolism to histone acetylation. *Science.* **324,** 1076-1080

66. Metallo, C.M., Gameiro, P.A., Bell, E.L., Mattaini, K.R., Yang, J., Hiller, K., Jewell, C.M., Johnson, Z.R., Irvine, D.J., Guarente, L., Kelleher, J.K., Vander Heiden, M.G., Iliopoulos, O., and Stephanopoulos, G. (2011) Reductive glutamine metabolism by IDH1 mediates lipogenesis under hypoxia. *Nature.* **481,** 380-384

67. Des Rosiers, C., Di Donato, L., Comte, B., Laplante, A., Marcoux, C., David, F., Fernandez, C.A., and Brunengraber, H. (1995) Isotopomer analysis of citric acid cycle and gluconeogenesis in rat liver. Reversibility of isocitrate dehydrogenase and involvement of ATP-citrate lyase in gluconeogenesis. *J.Biol.Chem.* **270,** 10027-10036

68. Yoo, H., Antoniewicz, M.R., Stephanopoulos, G., and Kelleher, J.K. (2008) Quantifying reductive carboxylation flux of glutamine to lipid in a brown adipocyte cell line. *J.Biol.Chem.* **283,** 20621-20627

69. Lemons, J.M., Feng, X.J., Bennett, B.D., Legesse-Miller, A., Johnson, E.L., Raitman, I., Pollina, E.A., Rabitz, H.A., Rabinowitz, J.D., and Coller, H.A. (2010) Quiescent fibroblasts exhibit high metabolic activity. *PLoS Biol.* **8,** e1000514

70. Ward, P.S., Patel, J., Wise, D.R., Abdel-Wahab, O., Bennett, B.D., Coller, H.A., Cross, J.R., Fantin, V.R., Hedvat, C.V., Perl, A.E., Rabinowitz, J.D., Carroll, M., Su, S.M., Sharp, K.A., Levine, R.L., and Thompson, C.B. (2010) The common feature of leukemia-associated IDH1 and IDH2 mutations is a neomorphic enzyme activity converting alpha-ketoglutarate to 2-hydroxyglutarate. *Cancer.Cell.* **17,** 225-234

71. Ko, Y.H., Lin, Z., Flomenberg, N., Pestell, R.G., Howell, A., Sotgia, F., Lisanti, M.P., and Martinez-Outschoorn, U.E. (2011) Glutamine fuels a vicious cycle of autophagy in the tumor stroma and oxidative mitochondrial metabolism in epithelial cancer cells: implications for preventing chemotherapy resistance. *Cancer.Biol.Ther.* **12,** 1085-1097

72. Son, J., Lyssiotis, C.A., Ying, H., Wang, X., Hua, S., Ligorio, M., Perera, R.M., Ferrone, C.R., Mullarky, E., Shyh-Chang, N., Kang, Y., Fleming, J.B., Bardeesy, N., Asara, J.M., Haigis, M.C., DePinho, R.A., Cantley, L.C., and Kimmelman, A.C. (2013) Glutamine supports pancreatic cancer growth through a KRAS-regulated metabolic pathway. *Nature.* **496,** 101-105

73. Franco, R., and Cidlowski, J.A. (2009) Apoptosis and glutathione: beyond an antioxidant. *Cell Death Differ.* **16,** 1303-1314

74. Myeku, N., and Figueiredo-Pereira, M.E. (2011) Dynamics of the degradation of ubiquitinated proteins by proteasomes and autophagy: association with sequestosome 1/p62. *J.Biol.Chem.* **286,** 22426-22440

75. Lesueur, C., Bole-Feysot, C., Bekri, S., Husson, A., Lavoinne, A., and Brasse-Lagnel, C. (2012) Glutamine induces nuclear degradation of the NF-kappaB p65 subunit in Caco-2/TC7 cells. *Biochimie.* **94,** 806-815

76. Bertrand, J., Goichon, A., Chan, P., Azhar, S., Lecleire, S., Donnadieu, N., Vaudry, D., Cailleux, A.F., Dechelotte, P., and Coeffier, M. (2014) Enteral glutamine infusion modulates ubiquitination of heat shock proteins, Grp-75 and Apg-2, in the human duodenal mucosa. *Amino Acids.* **46,** 1059-1067

77. Xue, H., Slavov, D., and Wischmeyer, P.E. (2012) Glutamine-mediated dual regulation of heat shock transcription factor-1 activation and expression. *J.Biol.Chem.* **287,** 40400-40413

78. Suzuki, S., Tanaka, T., Poyurovsky, M.V., Nagano, H., Mayama, T., Ohkubo, S., Lokshin, M., Hosokawa, H., Nakayama, T., Suzuki, Y., Sugano, S., Sato, E., Nagao, T., Yokote, K., Tatsuno, I., and Prives, C. (2010) Phosphate-activated glutaminase (GLS2), a p53-inducible regulator of glutamine metabolism and reactive oxygen species. *Proc.Natl.Acad.Sci.U.S.A.* **107,** 7461-7466

79. Velletri, T., Romeo, F., Tucci, P., Peschiaroli, A., Annicchiarico-Petruzzelli, M., Niklison-Chirou, M.V., Amelio, I., Knight, R.A., Mak, T.W., Melino, G., and Agostini, M. (2013) GLS2 is transcriptionally regulated by p73 and contributes to neuronal differentiation. *Cell.Cycle.* **12,** 3564-3573

80. Meng, M., Chen, S., Lao, T., Liang, D., and Sang, N. (2010) Nitrogen anabolism underlies the importance of glutaminolysis in proliferating cells. *Cell.Cycle.* **9,** 3921-3932

81. Lorin, S., Tol, M.J., Bauvy, C., Strijland, A., Pous, C., Verhoeven, A.J., Codogno, P., and Meijer, A.J. (2013) Glutamate dehydrogenase contributes to leucine sensing in the regulation of autophagy. *Autophagy.* **9,** 850-860

82. Duran, R.V., Oppliger, W., Robitaille, A.M., Heiserich, L., Skendaj, R., Gottlieb, E., and Hall, M.N. (2012) Glutaminolysis activates Rag-mTORC1 signaling. *Mol.Cell.* **47,** 349-358

83. Nicklin, P., Bergman, P., Zhang, B., Triantafellow, E., Wang, H., Nyfeler, B., Yang, H., Hild, M., Kung, C., Wilson, C., Myer, V.E., MacKeigan, J.P., Porter, J.A., Wang, Y.K., Cantley, L.C., Finan, P.M., and Murphy, L.O. (2009) Bidirectional transport of amino acids regulates mTOR and autophagy. *Cell.* **136,** 521-534

84. Avruch, J., Long, X., Ortiz-Vega, S., Rapley, J., Papageorgiou, A., and Dai, N. (2009) Amino acid regulation of TOR complex 1. *Am.J.Physiol.Endocrinol.Metab.* **296,** E592-602

85. Sengupta, S., Peterson, T.R., and Sabatini, D.M. (2010) Regulation of the mTOR complex 1 pathway by nutrients, growth factors, and stress. *Mol.Cell.* **40,** 310-322

86. Sarkar, S. (2013) Regulation of autophagy by mTOR-dependent and mTOR-independent pathways: autophagy dysfunction in neurodegenerative diseases and therapeutic application of autophagy enhancers. *Biochem.Soc.Trans.* **41,** 1103-1130

87. Kim, J., Kundu, M., Viollet, B., and Guan, K.L. (2011) AMPK and mTOR regulate autophagy through direct phosphorylation of Ulk1. *Nat.Cell Biol.* **13,** 132-141

88. Hosokawa, N., Hara, T., Kaizuka, T., Kishi, C., Takamura, A., Miura, Y., Iemura, S., Natsume, T., Takehana, K., Yamada, N., Guan, J.L., Oshiro, N., and Mizushima, N. (2009) Nutrient-dependent mTORC1 association with the ULK1-Atg13-FIP200 complex required for autophagy. *Mol.Biol.Cell.* **20,** 1981-1991

89. Saqcena, M., Menon, D., Patel, D., Mukhopadhyay, S., Chow, V., and Foster, D.A. (2013) Amino acids and mTOR mediate distinct metabolic checkpoints in mammalian G1 cell cycle. *PLoS One.* **8,** e74157

90. Reid, M.A., Wang, W.I., Rosales, K.R., Welliver, M.X., Pan, M., and Kong, M. (2013) The B55alpha subunit of PP2A drives a p53-dependent metabolic adaptation to glutamine deprivation. *Mol.Cell.* **50,** 200-211

91. Cheong, H., Lindsten, T., and Thompson, C.B. (2012) Autophagy and ammonia. *Autophagy.* **8,** 122-123

92. Cheong, H., Lindsten, T., Wu, J., Lu, C., and Thompson, C.B. (2011) Ammonia-induced autophagy is independent of ULK1/ULK2 kinases. *Proc.Natl.Acad.Sci.U.S.A.* **108,** 11121-11126

93. Kuhn, K.S., Muscaritoli, M., Wischmeyer, P., and Stehle, P. (2010) Glutamine as indispensable nutrient in oncology: experimental and clinical evidence. *Eur.J.Nutr.* **49,** 197-210

94. Wischmeyer, P.E. (2008) Glutamine: role in critical illness and ongoing clinical trials. *Curr.Opin.Gastroenterol.* **24,** 190-197

95. Ko, H.M., Oh, S.H., Bang, H.S., Kang, N.I., Cho, B.H., Im, S.Y., and Lee, H.K. (2009) Glutamine protects mice from lethal endotoxic shock via a rapid induction of MAPK phosphatase-1. *J.Immunol.* **182,** 7957-7962

96. Gong, J., and Jing, L. (2011) Glutamine induces heat shock protein 70 expression via O-GlcNAc modification and subsequent increased expression and transcriptional activity of heat shock factor-1. *Minerva Anestesiol.* **77,** 488-495

97. Singleton, K.D., and Wischmeyer, P.E. (2008) Glutamine induces heat shock protein expression via O-glycosylation and phosphorylation of HSF-1 and Sp1. *JPEN J.Parenter.Enteral Nutr.* **32,** 371-376

98. Jing, L., Wu, Q., and Wang, F. (2007) Glutamine induces heat-shock protein and protects against Escherichia coli lipopolysaccharide-induced vascular hyporeactivity in rats. *Crit.Care.* **11,** R34

99. Jang, H.J., Kwak, J.H., Cho, E.Y., We, Y.M., Lee, Y.H., Kim, S.C., and Han, D.J. (2008) Glutamine induces heat-shock protein-70 and glutathione expression and attenuates ischemic damage in rat islets. *Transplant.Proc.* **40,** 2581-2584

100. Poon, I.K., Lucas, C.D., Rossi, A.G., and Ravichandran, K.S. (2014) Apoptotic cell clearance: basic biology and therapeutic potential. *Nat.Rev.Immunol.* **14,** 166-180

101. Elmore, S. (2007) Apoptosis: a review of programmed cell death. *Toxicol.Pathol.* **35,** 495-516

102. Chipuk, J.E., Moldoveanu, T., Llambi, F., Parsons, M.J., and Green, D.R. (2010) The BCL-2 family reunion. *Mol.Cell.* **37,** 299-310

103. Levine, B., Sinha, S., and Kroemer, G. (2008) Bcl-2 family members: dual regulators of apoptosis and autophagy. *Autophagy.* **4,** 600-606

104. Garcia-Saez, A.J. (2012) The secrets of the Bcl-2 family. *Cell Death Differ.* **19,** 1733-1740

105. Belizario, J.E., Alves, J., Garay-Malpartida, M., and Occhiucci, J.M. (2008) Coupling caspase cleavage and proteasomal degradation of proteins carrying PEST motif. *Curr.Protein Pept.Sci.* **9,** 210-220

106. Dho, S.H., Deverman, B.E., Lapid, C., Manson, S.R., Gan, L., Riehm, J.J., Aurora, R., Kwon, K.S., and Weintraub, S.J. (2013) Control of cellular Bcl-xL levels by deamidation-regulated degradation. *PLoS Biol.* **11,** e1001588

107. Xiao, K., Chen, P., and Chang, D.C. (2014) The VTLISFG motif in the BH1 domain plays a significant role in regulating the degradation of Mcl-1. *FEBS Open Bio.* **4,** 147-152

108. Yip, K.W., and Reed, J.C. (2008) Bcl-2 family proteins and cancer. *Oncogene.* **27,** 6398-6406

109. Aiken, K.J., Bickford, J.S., Kilberg, M.S., and Nick, H.S. (2008) Metabolic regulation of manganese superoxide dismutase expression via essential amino acid deprivation. *J.Biol.Chem.* **283,** 10252-10263

110. Charbonneau, J.R., Furtak, T., Lefebvre, J., and Gauthier, E.R. (2003) Bcl-xL expression interferes with the effects of L-glutamine supplementation on hybridoma cultures. *Biotechnol.Bioeng.* **81,** 279-290

111. Gauthier, E.R., Piche, L., Lemieux, G., and Lemieux, R. (1996) Role of bcl-X(L) in the control of apoptosis in murine myeloma cells. *Cancer Res.* **56,** 1451-1456

112. Miriyala, S., Spasojevic, I., Tovmasyan, A., Salvemini, D., Vujaskovic, Z., St Clair, D., and Batinic-Haberle, I. (2012) Manganese superoxide dismutase, MnSOD and its mimics. *Biochim.Biophys.Acta.* **1822,** 794-814

113. Lagranha, C.J., Hirabara, S.M., Curi, R., and Pithon-Curi, T.C. (2007) Glutamine supplementation prevents exercise-induced neutrophil apoptosis and reduces p38 MAPK and JNK phosphorylation and p53 and caspase 3 expression. *Cell Biochem.Funct.* **25,** 563-569

114. Ko, Y.G., Kim, E.Y., Kim, T., Park, H., Park, H.S., Choi, E.J., and Kim, S. (2001) Glutamine-dependent antiapoptotic interaction of human glutaminyl-tRNA synthetase with apoptosis signal-regulating kinase 1. *J.Biol.Chem.* **276,** 6030-6036

115. Svoboda, N., Zierler, S., and Kerschbaum, H.H. (2007) cAMP mediates ammonia-induced programmed cell death in the microglial cell line BV-2. *Eur.J.Neurosci.* **25,** 2285-2295

116. Svoboda, N., and Kerschbaum, H.H. (2009) L-Glutamine-induced apoptosis in microglia is mediated by mitochondrial dysfunction. *Eur.J.Neurosci.* **30,** 196-206

117. Mijaljica, D., Prescott, M., and Devenish, R.J. (2011) Microautophagy in mammalian cells: revisiting a 40-year-old conundrum. *Autophagy.* **7,** 673-682

118. Kaminskyy, V., and Zhivotovsky, B. (2012) Proteases in autophagy. *Biochim.Biophys.Acta.* **1824,** 44-50

119. Glick, D., Barth, S., and Macleod, K.F. (2010) Autophagy: cellular and molecular mechanisms. *J.Pathol.* **221,** 3-12

120. Levine, B., and Yuan, J. (2005) Autophagy in cell death: an innocent convict?. *J.Clin.Invest.* **115,** 2679-2688

121. Mizushima, N., Levine, B., Cuervo, A.M., and Klionsky, D.J. (2008) Autophagy fights disease through cellular self-digestion. *Nature.* **451,** 1069-1075

122. Eisenberg-Lerner, A., Bialik, S., Simon, H.U., and Kimchi, A. (2009) Life and death partners: apoptosis, autophagy and the cross-talk between them. *Cell Death Differ.* **16,** 966-975

123. Eisenberg-Lerner, A., and Kimchi, A. (2012) PKD is a kinase of Vps34 that mediates ROS-induced autophagy downstream of DAPk. *Cell Death Differ.* **19,** 788-797

124. Simonsen, A., and Tooze, S.A. (2009) Coordination of membrane events during autophagy by multiple class III PI3-kinase complexes. *J.Cell Biol.* **186,** 773-782

125. Yla-Anttila, P., Vihinen, H., Jokitalo, E., and Eskelinen, E.L. (2009) 3D tomography reveals connections between the phagophore and endoplasmic reticulum. *Autophagy.* **5,** 1180-1185

126. Hayashi-Nishino, M., Fujita, N., Noda, T., Yamaguchi, A., Yoshimori, T., and Yamamoto, A. (2009) A subdomain of the endoplasmic reticulum forms a cradle for autophagosome formation. *Nat.Cell Biol.* **11,** 1433-1437

127. Martinet, W., and De Meyer, G.R. (2009) Autophagy in atherosclerosis: a cell survival and death phenomenon with therapeutic potential. *Circ.Res.* **104,** 304-317

128. Martinet, W., and De Meyer, G.R. (2008) Autophagy in atherosclerosis. *Curr.Atheroscler.Rep.* **10,** 216-223

129. Axe, E.L., Walker, S.A., Manifava, M., Chandra, P., Roderick, H.L., Habermann, A., Griffiths, G., and Ktistakis, N.T. (2008) Autophagosome formation from membrane compartments enriched in phosphatidylinositol 3-phosphate and dynamically connected to the endoplasmic reticulum. *J.Cell Biol.* **182,** 685-701

130. Girardi, J.P., Pereira, L., and Bakovic, M. (2011) De novo synthesis of phospholipids is coupled with autophagosome formation. *Med.Hypotheses.* **77,** 1083-1087

131. Kang, R., Zeh, H.J., Lotze, M.T., and Tang, D. (2011) The Beclin 1 network regulates autophagy and apoptosis. *Cell Death Differ.* **18,** 571-580

132. Popovic, D., Akutsu, M., Novak, I., Harper, J.W., Behrends, C., and Dikic, I. (2012) Rab GTPase-activating proteins in autophagy: regulation of endocytic and autophagy pathways by direct binding to human ATG8 modifiers. *Mol.Cell.Biol.* **32,** 1733-1744

133. Ravikumar, B., Imarisio, S., Sarkar, S., O'Kane, C.J., and Rubinsztein, D.C. (2008) Rab5 modulates aggregation and toxicity of mutant huntingtin through macroautophagy in cell and fly models of Huntington disease. *J.Cell.Sci.* **121,** 1649-1660

134. Young, A.R., Chan, E.Y., Hu, X.W., Kochl, R., Crawshaw, S.G., High, S., Hailey, D.W., Lippincott-Schwartz, J., and Tooze, S.A. (2006) Starvation and ULK1-dependent cycling of mammalian Atg9 between the TGN and endosomes. *J.Cell.Sci.* **119,** 3888-3900

135. Chang, C.P., Su, Y.C., Hu, C.W., and Lei, H.Y. (2013) TLR2-dependent selective autophagy regulates NF-kappaB lysosomal degradation in hepatoma-derived M2 macrophage differentiation. *Cell Death Differ.* **20,** 515-523

136. Muller, S., Dennemarker, J., and Reinheckel, T. (2012) Specific functions of lysosomal proteases in endocytic and autophagic pathways. *Biochim.Biophys.Acta.* **1824,** 34-43

137. Tolhurst, G., Zheng, Y., Parker, H.E., Habib, A.M., Reimann, F., and Gribble, F.M. (2011) Glutamine triggers and potentiates glucagon-like peptide-1 secretion by raising cytosolic Ca2+ and cAMP. *Endocrinology.* **152,** 405-413

138. Hu, Y., Riesland, L., Paterson, A.J., and Kudlow, J.E. (2004) Phosphorylation of mouse glutamine-fructose-6-phosphate amidotransferase 2 (GFAT2) by cAMP-dependent protein kinase increases the enzyme activity. *J.Biol.Chem.* **279,** 29988-29993

139. Cherra, S.J.,3rd, Kulich, S.M., Uechi, G., Balasubramani, M., Mountzouris, J., Day, B.W., and Chu, C.T. (2010) Regulation of the autophagy protein LC3 by phosphorylation. *J.Cell Biol.* **190,** 533-539

140. Saini, K.S., Loi, S., de Azambuja, E., Metzger-Filho, O., Saini, M.L., Ignatiadis, M., Dancey, J.E., and Piccart-Gebhart, M.J. (2013) Targeting the PI3K/AKT/mTOR and Raf/MEK/ERK pathways in the treatment of breast cancer. *Cancer Treat.Rev.* **39,** 935-946

141. Diaz-Troya, S., Perez-Perez, M.E., Florencio, F.J., and Crespo, J.L. (2008) The role of TOR in autophagy regulation from yeast to plants and mammals. *Autophagy.* **4,** 851-865

142. Yang, W., Ju, J.H., Lee, K.M., Nam, K., Oh, S., and Shin, I. (2013) Protein kinase B/Akt1 inhibits autophagy by down-regulating UVRAG expression. *Exp.Cell Res.* **319,** 122-133

143. Alexander, A., Cai, S.L., Kim, J., Nanez, A., Sahin, M., MacLean, K.H., Inoki, K., Guan, K.L., Shen, J., Person, M.D., Kusewitt, D., Mills, G.B., Kastan, M.B., and Walker, C.L. (2010) ATM signals to TSC2 in the cytoplasm to regulate mTORC1 in response to ROS. *Proc.Natl.Acad.Sci.U.S.A.* **107,** 4153-4158

144. Ma, L., Chen, Z., Erdjument-Bromage, H., Tempst, P., and Pandolfi, P.P. (2005) Phosphorylation and functional inactivation of TSC2 by Erk implications for tuberous sclerosis and cancer pathogenesis. *Cell.* **121,** 179-193

145. Inoki, K., Li, Y., Zhu, T., Wu, J., and Guan, K.L. (2002) TSC2 is phosphorylated and inhibited by Akt and suppresses mTOR signalling. *Nat.Cell Biol.* **4,** 648-657

146. Yang, Z., and Klionsky, D.J. (2010) Mammalian autophagy: core molecular machinery and signaling regulation. *Curr.Opin.Cell Biol.* **22,** 124-131

147. Avruch, J., Long, X., Lin, Y., Ortiz-Vega, S., Rapley, J., Papageorgiou, A., Oshiro, N., and Kikkawa, U. (2009) Activation of mTORC1 in two steps: Rheb-GTP activation of catalytic function and increased binding of substrates to raptor. *Biochem.Soc.Trans.* **37,** 223-226

148. Maiuri, M.C., Galluzzi, L., Morselli, E., Kepp, O., Malik, S.A., and Kroemer, G. (2010) Autophagy regulation by p53. *Curr.Opin.Cell Biol.* **22,** 181-185

149. Maiuri, M.C., Tasdemir, E., Criollo, A., Morselli, E., Vicencio, J.M., Carnuccio, R., and Kroemer, G. (2009) Control of autophagy by oncogenes and tumor suppressor genes. *Cell Death Differ.* **16,** 87-93

150. Tasdemir, E., Maiuri, M.C., Galluzzi, L., Vitale, I., Djavaheri-Mergny, M., D'Amelio, M., Criollo, A., Morselli, E., Zhu, C., Harper, F., Nannmark, U., Samara, C., Pinton, P., Vicencio, J.M., Carnuccio, R., Moll, U.M., Madeo, F., Paterlini-Brechot, P., Rizzuto, R., Szabadkai, G., Pierron, G., Blomgren, K., Tavernarakis, N., Codogno, P., Cecconi, F., and Kroemer, G. (2008) Regulation of autophagy by cytoplasmic p53. *Nat.Cell Biol.* **10,** 676-687

151. van der Vos, K.E., and Coffer, P.J. (2012) Glutamine metabolism links growth factor signaling to the regulation of autophagy. *Autophagy.* **8,** 1862-1864

152. van der Vos, K.E., Eliasson, P., Proikas-Cezanne, T., Vervoort, S.J., van Boxtel, R., Putker, M., van Zutphen, I.J., Mauthe, M., Zellmer, S., Pals, C., Verhagen, L.P., Groot Koerkamp, M.J., Braat, A.K.,

Dansen, T.B., Holstege, F.C., Gebhardt, R., Burgering, B.M., and Coffer, P.J. (2012) Modulation of glutamine metabolism by the PI(3)K-PKB-FOXO network regulates autophagy. *Nat.Cell Biol.* **14,** 829-837

153. Yung, H.W., Charnock-Jones, D.S., and Burton, G.J. (2011) Regulation of AKT phosphorylation at Ser473 and Thr308 by endoplasmic reticulum stress modulates substrate specificity in a severity dependent manner. *PLoS One.* **6,** e17894

154. Demetriades, C., Doumpas, N., and Teleman, A.A. (2014) Regulation of TORC1 in response to amino acid starvation via lysosomal recruitment of TSC2. *Cell.* **156,** 786-799

155. Sheen, J.H., Zoncu, R., Kim, D., and Sabatini, D.M. (2011) Defective regulation of autophagy upon leucine deprivation reveals a targetable liability of human melanoma cells in vitro and in vivo. *Cancer.Cell.* **19,** 613-628

156. White, E. (2012) Deconvoluting the context-dependent role for autophagy in cancer. *Nat.Rev.Cancer.* **12,** 401-410

157. White, E. (2013) Exploiting the bad eating habits of Ras-driven cancers. *Genes Dev.* **27,** 2065-2071

158. Guo, J.Y., Chen, H.Y., Mathew, R., Fan, J., Strohecker, A.M., Karsli-Uzunbas, G., Kamphorst, J.J., Chen, G., Lemons, J.M., Karantza, V., Coller, H.A., Dipaola, R.S., Gelinas, C., Rabinowitz, J.D., and White, E. (2011) Activated Ras requires autophagy to maintain oxidative metabolism and tumorigenesis. *Genes Dev.* **25,** 460-470

159. Lock, R., Roy, S., Kenific, C.M., Su, J.S., Salas, E., Ronen, S.M., and Debnath, J. (2011) Autophagy facilitates glycolysis during Ras-mediated oncogenic transformation. *Mol.Biol.Cell.* **22,** 165-178

160. Yang, S., Wang, X., Contino, G., Liesa, M., Sahin, E., Ying, H., Bause, A., Li, Y., Stommel, J.M., Dell'antonio, G., Mautner, J., Tonon, G., Haigis, M., Shirihai, O.S., Doglioni, C., Bardeesy, N., and Kimmelman, A.C. (2011) Pancreatic cancers require autophagy for tumor growth. *Genes Dev.* **25,** 717-729

161. Eisenberg-Lerner, A., and Kimchi, A. (2007) DAP kinase regulates JNK signaling by binding and activating protein kinase D under oxidative stress. *Cell Death Differ.* **14,** 1908-1915

162. Sakiyama, T., Musch, M.W., Ropeleski, M.J., Tsubouchi, H., and Chang, E.B. (2009) Glutamine increases autophagy under basal and stressed conditions in intestinal epithelial cells. *Gastroenterology.* **136,** 924-932

163. Niederlechner, S., Klawitter, J., Baird, C., Kallweit, A.R., Christians, U., and Wischmeyer, P.E. (2012) Fibronectin-integrin signaling is required for L-glutamine's protection against gut injury. *PLoS One.* **7,** e50185

164. Niederlechner, S., Baird, C., and Wischmeyer, P.E. (2013) P38MAP kinase, but not phosphoinositol-3 kinase, signal downstream of glutamine-mediated fibronectin-integrin signaling after intestinal injury. *Nutr.J.* **12,** 88-96

165. Zang, M., Xu, S., Maitland-Toolan, K.A., Zuccollo, A., Hou, X., Jiang, B., Wierzbicki, M., Verbeuren, T.J., and Cohen, R.A. (2006) Polyphenols stimulate AMP-activated protein kinase, lower lipids, and inhibit accelerated atherosclerosis in diabetic LDL receptor-deficient mice. *Diabetes.* **55,** 2180-2191

166. Mihaylova, M.M., and Shaw, R.J. (2011) The AMPK signalling pathway coordinates cell growth, autophagy and metabolism. *Nat.Cell Biol.* **13,** 1016-1023

167. Mao, K., and Klionsky, D.J. (2011) AMPK activates autophagy by phosphorylating ULK1. *Circ.Res.* **108,** 787-788

168. Kim, J., Kim, Y.C., Fang, C., Russell, R.C., Kim, J.H., Fan, W., Liu, R., Zhong, Q., and Guan, K.L. (2013) Differential regulation of distinct Vps34 complexes by AMPK in nutrient stress and autophagy. *Cell.* **152,** 290-303

169. Eng, C.H., Yu, K., Lucas, J., White, E., and Abraham, R.T. (2010) Ammonia derived from glutaminolysis is a diffusible regulator of autophagy. *Sci.Signal.* **3,** ra31

170. Harder, L.M., Bunkenborg, J., and Andersen, J.S. (2014) Inducing autophagy: a comparative phosphoproteomic study of the cellular response to ammonia and rapamycin. *Autophagy.* **10,** 339-355

171. Jayakumar, A.R., Panickar, K.S., Murthy, C., and Norenberg, M.D. (2006) Oxidative stress and mitogen-activated protein kinase phosphorylation mediate ammonia-induced cell swelling and glutamate uptake inhibition in cultured astrocytes. *J.Neurosci.* **26,** 4774-4784

172. Moriyama, M., Jayakumar, A.R., Tong, X.Y., and Norenberg, M.D. (2010) Role of mitogen-activated protein kinases in the mechanism of oxidant-induced cell swelling in cultured astrocytes. *J.Neurosci.Res.* **88,** 2450-2458

173. Salazar, M., Carracedo, A., Salanueva, I.J., Hernandez-Tiedra, S., Lorente, M., Egia, A., Vazquez, P., Blazquez, C., Torres, S., Garcia, S., Nowak, J., Fimia, G.M., Piacentini, M., Cecconi, F., Pandolfi, P.P., Gonzalez-Feria, L., Iovanna, J.L., Guzman, M., Boya, P., and Velasco, G. (2009) Cannabinoid action induces autophagy-mediated cell death through stimulation of ER stress in human glioma cells. *J.Clin.Invest.* **119,** 1359-1372

174. Maiuri, M.C., Zalckvar, E., Kimchi, A., and Kroemer, G. (2007) Self-eating and self-killing: crosstalk between autophagy and apoptosis. *Nat.Rev.Mol.Cell Biol.* **8,** 741-752

175. Pattingre, S., Tassa, A., Qu, X., Garuti, R., Liang, X.H., Mizushima, N., Packer, M., Schneider, M.D., and Levine, B. (2005) Bcl-2 antiapoptotic proteins inhibit Beclin 1-dependent autophagy. *Cell.* **122,** 927-939

176. Yousefi, S., Perozzo, R., Schmid, I., Ziemiecki, A., Schaffner, T., Scapozza, L., Brunner, T., and Simon, H.U. (2006) Calpain-mediated cleavage of Atg5 switches autophagy to apoptosis. *Nat.Cell Biol.* **8,** 1124-1132

177. Djavaheri-Mergny, M., Maiuri, M.C., and Kroemer, G. (2010) Cross talk between apoptosis and autophagy by caspase-mediated cleavage of Beclin 1. *Oncogene.* **29,** 1717-1719

178. Speidel, D. (2010) Transcription-independent p53 apoptosis: an alternative route to death. *Trends Cell Biol.* **20,** 14-24

179. Feng, Z., Zhang, H., Levine, A.J., and Jin, S. (2005) The coordinate regulation of the p53 and mTOR pathways in cells. *Proc.Natl.Acad.Sci.U.S.A.* **102,** 8204-8209

180. Morselli, E., Tasdemir, E., Maiuri, M.C., Galluzzi, L., Kepp, O., Criollo, A., Vicencio, J.M., Soussi, T., and Kroemer, G. (2008) Mutant p53 protein localized in the cytoplasm inhibits autophagy. *Cell.Cycle.* **7,** 3056-3061

181. Rovetta, F., Stacchiotti, A., Consiglio, A., Cadei, M., Grigolato, P.G., Lavazza, A., Rezzani, R., and Aleo, M.F. (2012) ER signaling regulation drives the switch between autophagy and apoptosis in NRK-52E cells exposed to cisplatin. *Exp.Cell Res.* **318,** 238-250

182. Zalckvar, E., Berissi, H., Eisenstein, M., and Kimchi, A. (2009) Phosphorylation of Beclin 1 by DAP-kinase promotes autophagy by weakening its interactions with Bcl-2 and Bcl-XL. *Autophagy.* **5,** 720-722

183. Zalckvar, E., Berissi, H., Mizrachy, L., Idelchuk, Y., Koren, I., Eisenstein, M., Sabanay, H., Pinkas-Kramarski, R., and Kimchi, A. (2009) DAP-kinase-mediated phosphorylation on the BH3 domain of beclin 1 promotes dissociation of beclin 1 from Bcl-XL and induction of autophagy. *EMBO Rep.* **10,** 285-292

184. Wei, Y., Pattingre, S., Sinha, S., Bassik, M., and Levine, B. (2008) JNK1-mediated phosphorylation of Bcl-2 regulates starvation-induced autophagy. *Mol.Cell.* **30,** 678-688

185. Bialik, S., and Kimchi, A. (2010) Lethal weapons: DAP-kinase, autophagy and cell death DAP-kinase regulates autophagy. *Curr.Opin.Cell Biol.* **22,** 199-205

186. Oyadomari, S., and Mori, M. (2004) Roles of CHOP/GADD153 in endoplasmic reticulum stress. *Cell Death Differ.* **11,** 381-389

187. Marten, N.W., Burke, E.J., Hayden, J.M., and Straus, D.S. (1994) Effect of amino acid limitation on the expression of 19 genes in rat hepatoma cells. *FASEB J.* **8,** 538-544

188. Abcouwer, S.F., Schwarz, C., and Meguid, R.A. (1999) Glutamine deprivation induces the expression of GADD45 and GADD153 primarily by mRNA stabilization. *J.Biol.Chem.* **274,** 28645-28651

189. Carlson, S.G., Fawcett, T.W., Bartlett, J.D., Bernier, M., and Holbrook, N.J. (1993) Regulation of the C/EBP-related gene gadd153 by glucose deprivation. *Mol.Cell.Biol.* **13,** 4736-4744

190. Huang, Q., Lau, S.S., and Monks, T.J. (1999) Induction of gadd153 mRNA by nutrient deprivation is overcome by glutamine. *Biochem.J.* **341 (Pt 1),** 225-231

191. McCullough, K.D., Martindale, J.L., Klotz, L.O., Aw, T.Y., and Holbrook, N.J. (2001) Gadd153 sensitizes cells to endoplasmic reticulum stress by down-regulating Bcl2 and perturbing the cellular redox state. *Mol.Cell.Biol.* **21,** 1249-1259

192. Ryu, E.J., Harding, H.P., Angelastro, J.M., Vitolo, O.V., Ron, D., and Greene, L.A. (2002) Endoplasmic reticulum stress and the unfolded protein response in cellular models of Parkinson's disease. *J.Neurosci.* **22,** 10690-10698

193. Gao, J., Ishigaki, Y., Yamada, T., Kondo, K., Yamaguchi, S., Imai, J., Uno, K., Hasegawa, Y., Sawada, S., Ishihara, H., Oyadomari, S., Mori, M., Oka, Y., and Katagiri, H. (2011) Involvement of endoplasmic stress protein C/EBP homologous protein in arteriosclerosis acceleration with augmented biological stress responses. *Circulation.* **124,** 830-839

194. Prasanthi, J.R., Larson, T., Schommer, J., and Ghribi, O. (2011) Silencing GADD153/CHOP gene expression protects against Alzheimer's disease-like pathology induced by 27-hydroxycholesterol in rabbit hippocampus. *PLoS One.* **6,** e26420

195. Emdad, L., Qadeer, Z.A., Bederson, L.B., Kothari, H.P., Uzzaman, M., and Germano, I.M. (2011) Is there a common upstream link for autophagic and apoptotic cell death in human high-grade gliomas?. *Neuro Oncol.* **13,** 725-735

196. Germano, I.M., Emdad, L., Qadeer, Z.A., Binello, E., and Uzzaman, M. (2010) Embryonic stem cell (ESC)-mediated transgene delivery induces growth suppression, apoptosis and radiosensitization, and overcomes temozolomide resistance in malignant gliomas. *Cancer Gene Ther.* **17,** 664-674

197. Charbonneau, J.R., and Gauthier, E.R. (2000) Prolongation of murine hybridoma cell survival in stationary batch culture by Bcl-xL expression. *Cytotechnology.* **34,** 131-139

198. Petronini, P.G., Urbani, S., Alfieri, R., Borghetti, A.F., and Guidotti, G.G. (1996) Cell susceptibility to apoptosis by glutamine deprivation and rescue: survival and apoptotic death in cultured lymphoma-leukemia cell lines. *J.Cell.Physiol.* **169,** 175-185

199. Harnett, C.C., Guerin, P.J., Furtak, T., and Gauthier, E.R. (2012) Control of late apoptotic events by the p38 stress kinase in l-glutamine-deprived mouse hybridoma cells. *Cell Biochem.Funct.*

200. Guerin, P.J., Furtak, T., Eng, K., and Gauthier, E.R. (2006) Oxidative stress is not required for the induction of apoptosis upon glutamine starvation of Sp2/0-Ag14 hybridoma cells. *Eur.J.Cell Biol.* **85,** 355-365

201. Kim, M.H., Kim, A., Yu, J.H., Lim, J.W., and Kim, H. (2014) Glutamine deprivation induces interleukin-8 expression in ataxia telangiectasia fibroblasts. *Inflamm.Res.* **63,** 347-356

202. Zhou, F., Yang, Y., and Xing, D. (2011) Bcl-2 and Bcl-xL play important roles in the crosstalk between autophagy and apoptosis. *FEBS J.* **278,** 403-413

203. Dang, C.V. (2010) Rethinking the Warburg effect with Myc micromanaging glutamine metabolism. *Cancer Res.* **70,** 859-862

204. Freshney, R. (1987) Culture of Animal Cells: A Manual of Basic Technique p. 117

205. Shah, G.M., Poirier, D., Duchaine, C., Brochu, G., Desnoyers, S., Lagueux, J., Verreault, A., Hoflack, J.C., Kirkland, J.B., and Poirier, G.G. (1995) Methods for biochemical study of poly(ADP-ribose) metabolism in vitro and in vivo. *Anal.Biochem.* **227,** 1-13

206. Gottlieb, R.A., and Granville, D.J. (2002) Analyzing mitochondrial changes during apoptosis. *Methods.* **26,** 341-347

207. Ausubel F, Brent R, Kingston RE, Moore DD, Seidman JG (2003) Electrophoretic Separation of Proteins 10.2A.1-10.2A.34

208. Schagger, H., and von Jagow, G. (1987) Tricine-sodium dodecyl sulfate-polyacrylamide gel electrophoresis for the separation of proteins in the range from 1 to 100 kDa. *Anal.Biochem.* **166,** 368-379

209. Kanzawa, T., Kondo, Y., Ito, H., Kondo, S., and Germano, I. (2003) Induction of autophagic cell death in malignant glioma cells by arsenic trioxide. *Cancer Res.* **63,** 2103-2108

210. Kanzawa, T., Germano, I.M., Komata, T., Ito, H., Kondo, Y., and Kondo, S. (2004) Role of autophagy in temozolomide-induced cytotoxicity for malignant glioma cells. *Cell Death Differ.* **11,** 448-457

211. Guerin, P.J., and Gauthier, E.R. (2003) Induction of cellular necrosis by the glutathione peroxidase mimetic ebselen. *J.Cell.Biochem.* **89,** 203-211

212. Mallory, M., Chartrand, K., and Gauthier, E.R. (2007) GADD153 expression does not necessarily correlate with changes in culture behavior of hybridoma cells. *BMC Biotechnol.* **7,** 89

213. Mallory, M. (2006) The Regulation of GADD153/CHOP-10 in Sp2/0-Ag14 Mouse Hybridoma Cells Subjected to Different L-Glutamine Limitation Conditions. *M.Sc. Thesis.* Laurentian University. Sudbury (ON) Canada.

214. Hiscock, N., and Pedersen, B.K. (2002) Exercise-induced immunodepression- plasma glutamine is not the link. *J.Appl.Physiol.* **93,** 813-822

215. Anastasi, J., Vardiman, J.W., Rudinsky, R., Patel, M., Nachman, J., Rubin, C.M., and Le Beau, M.M. (1991) Direct correlation of cytogenetic findings with cell morphology using in situ hybridization: an analysis of suspicious cells in bone marrow specimens of two patients completing therapy for acute lymphoblastic leukemia. *Blood.* **77,** 2456-2462

216. Harrison, B., Kraus, M., Burch, L., Stevens, C., Craig, A., Gordon-Weeks, P., and Hupp, T.R. (2008) DAPK-1 binding to a linear peptide motif in MAP1B stimulates autophagy and membrane blebbing. *J.Biol.Chem.* **283,** 9999-10014

217. Tewari, M., Quan, L.T., O'Rourke, K., Desnoyers, S., Zeng, Z., Beidler, D.R., Poirier, G.G., Salvesen, G.S., and Dixit, V.M. (1995) Yama/CPP32 beta, a mammalian homolog of CED-3, is a CrmA-inhibitable protease that cleaves the death substrate poly(ADP-ribose) polymerase. *Cell.* **81,** 801-809

218. Boucher, D., Blais, V., and Denault, J.B. (2012) Caspase-7 uses an exosite to promote poly(ADP ribose) polymerase 1 proteolysis. *Proc.Natl.Acad.Sci.U.S.A.* **109,** 5669-5674

219. Zhong, Y., Liao, Y., Fang, S., Tam, J.P., and Liu, D.X. (2012) Up-regulation of Mcl-1 and Bak by coronavirus infection of human, avian and animal cells modulates apoptosis and viral replication. *PLoS One.* **7,** e30191

220. Reinert, R.B., Oberle, L.M., Wek, S.A., Bunpo, P., Wang, X.P., Mileva, I., Goodwin, L.O., Aldrich, C.J., Durden, D.L., McNurlan, M.A., Wek, R.C., and Anthony, T.G. (2006) Role of glutamine depletion in directing tissue-specific nutrient stress responses to L-asparaginase. *J.Biol.Chem.* **281,** 31222-31233

221. Arrington, D.D., and Schnellmann, R.G. (2008) Targeting of the molecular chaperone oxygen-regulated protein 150 (ORP150) to mitochondria and its induction by cellular stress. *Am.J.Physiol.Cell.Physiol.* **294,** C641-50

222. Zhao, Q., Wang, J., Levichkin, I.V., Stasinopoulos, S., Ryan, M.T., and Hoogenraad, N.J. (2002) A mitochondrial specific stress response in mammalian cells. *EMBO J.* **21,** 4411-4419

223. Liu, K.C., Yen, C.Y., Wu, R.S., Yang, J.S., Lu, H.F., Lu, K.W., Lo, C., Chen, H.Y., Tang, N.Y., Wu, C.C., and Chung, J.G. (2014) The roles of endoplasmic reticulum stress and mitochondrial apoptotic signaling pathway in quercetin-mediated cell death of human prostate cancer PC-3 cells. *Environ.Toxicol.* **29,** 428-439

224. Tiffany-Castiglioni, E., and Qian, Y. (2012) ER chaperone-metal interactions: Links to protein folding disorders. *Neurotoxicology.*

225. Martinou, J.C., and Youle, R.J. (2011) Mitochondria in apoptosis: Bcl-2 family members and mitochondrial dynamics. *Dev.Cell.* **21,** 92-101

226. Kaadige, M.R., Looper, R.E., Kamalanaadhan, S., and Ayer, D.E. (2009) Glutamine-dependent anapleurosis dictates glucose uptake and cell growth by regulating MondoA transcriptional activity. *Proc.Natl.Acad.Sci.U.S.A.* **106,** 14878-14883

227. Banfalvi, G. (2011) Synchronization of mammalian cells and nuclei by centrifugal elutriation. *Methods Mol.Biol.* **761,** 25-45

228. Liu, C.B., Chen, L.H., Cheng, A.C., Chen, W.J., Tsai, M.L., Liu, Y., Ho, C.T., and Pan, M.H. (2011) Hexahydro-beta-acids induce apoptosis through mitochondrial pathway, GADD153 expression, and caspase activation in human leukemia cells. *Food Chem.Toxicol.* **49,** 1033-1042

229. Carriere, A., Carmona, M.C., Fernandez, Y., Rigoulet, M., Wenger, R.H., Penicaud, L., and Casteilla, L. (2004) Mitochondrial reactive oxygen species control the transcription factor CHOP-10/GADD153 and adipocyte differentiation: a mechanism for hypoxia-dependent effect. *J.Biol.Chem.* **279,** 40462-40469

230. Zou, H., Lai, Y., Zhao, X., Yan, G., Ma, D., Cardenes, N., Shiva, S., Liu, Y., Bai, X., Jiang, Y., and Jiang, Y. (2013) Regulation of mammalian target of rapamycin complex 1 by Bcl-2 and Bcl-XL. *J.Biol.Chem.* **288,** 28824-28830

231. Eng, C.H., and Abraham, R.T. (2010) Glutaminolysis yields a metabolic by-product that stimulates autophagy. *Autophagy.* **6,** 968-970

232. Kovacs, J.R., Li, C., Yang, Q., Li, G., Garcia, I.G., Ju, S., Roodman, D.G., Windle, J.J., Zhang, X., and Lu, B. (2012) Autophagy promotes T-cell survival through degradation of proteins of the cell death machinery. *Cell Death Differ.* **19,** 144-152

233. Arsov, I., Adebayo, A., Kucerova-Levisohn, M., Haye, J., MacNeil, M., Papavasiliou, F.N., Yue, Z., and Ortiz, B.D. (2011) A role for autophagic protein beclin 1 early in lymphocyte development. *J.Immunol.* **186,** 2201-2209

234. Hubbard, V.M., Valdor, R., Patel, B., Singh, R., Cuervo, A.M., and Macian, F. (2010) Macroautophagy regulates energy metabolism during effector T cell activation. *J.Immunol.* **185,** 7349-7357

235. Walsh, C.M., and Bell, B.D. (2010) T cell intrinsic roles of autophagy in promoting adaptive immunity. *Curr.Opin.Immunol.*

236. Miller, B.C., Zhao, Z., Stephenson, L.M., Cadwell, K., Pua, H.H., Lee, H.K., Mizushima, N.N., Iwasaki, A., He, Y.W., Swat, W., and Virgin, H.W.,4th (2008) The autophagy gene ATG5 plays an essential role in B lymphocyte development. *Autophagy.* **4,** 309-314

237. Pua, H.H., and He, Y.W. (2007) Maintaining T lymphocyte homeostasis: another duty of autophagy. *Autophagy.* **3,** 266-267

238. Yang, Z.J., Chee, C.E., Huang, S., and Sinicrope, F.A. (2011) The role of autophagy in cancer: therapeutic implications. *Mol.Cancer.Ther.* **10,** 1533-1541

239. Moruno, F., Pérez-Jiménez, E., and Knecht, E. (2012) **Regulation of Autophagy by Glucose in Mammalian Cells**. *Cells.* **1,** 372-395

240. Han, J., and Burgess, K. (2010) Fluorescent indicators for intracellular pH. *Chem.Rev.* **110,** 2709-2728

241. Espert, L., Varbanov, M., Robert-Hebmann, V., Sagnier, S., Robbins, I., Sanchez, F., Lafont, V., and Biard-Piechaczyk, M. (2009) Differential role of autophagy in CD4 T cells and macrophages during X4 and R5 HIV-1 infection. *PLoS One.* **4,** e5787

242. Schneider, E.M., Flacke, S., Liu, F., Lorenz, M.R., Schilling, P., Nass, M.E., Foehr, K.J., Huber-Lang, M., and Weiss, M.E. (2011) Autophagy and ATP-induced anti-apoptosis in antigen presenting cells (APC) follows the cytokine storm in patients after major trauma. *J.Cell.Commun.Signal.* **5,** 145-156

243. Esteve, J.M., and Knecht, E. (2011) Mechanisms of autophagy and apoptosis: Recent developments in breast cancer cells. *World J.Biol.Chem.* **2,** 232-238

244. Tanida, I., Ueno, T., and Kominami, E. (2008) LC3 and Autophagy. *Methods Mol.Biol.* **445,** 77-88

245. Ni, H.M., Bockus, A., Wozniak, A.L., Jones, K., Weinman, S., Yin, X.M., and Ding, W.X. (2011) Dissecting the dynamic turnover of GFP-LC3 in the autolysosome. *Autophagy.* **7,** 188-204

246. Franke, T.F. (2008) PI3K/Akt: getting it right matters. *Oncogene.* **27,** 6473-6488

247. Backer, J.M. (2008) The regulation and function of Class III PI3Ks: novel roles for Vps34. *Biochem.J.* **410,** 1-17

248. Zhao, L., and Vogt, P.K. (2008) Class I PI3K in oncogenic cellular transformation. *Oncogene.* **27,** 5486-5496

249. Wu, Y.T., Tan, H.L., Shui, G., Bauvy, C., Huang, Q., Wenk, M.R., Ong, C.N., Codogno, P., and Shen, H.M. (2010) Dual role of 3-methyladenine in modulation of autophagy via different temporal patterns of inhibition on class I and III phosphoinositide 3-kinase. *J.Biol.Chem.* **285,** 10850-10861

250. Fang, L., Li, X., Luo, Y., He, W., Dai, C., and Yang, J. (2014) Autophagy inhibition induces podocyte apoptosis by activating the pro-apoptotic pathway of endoplasmic reticulum stress. *Exp.Cell Res.* **322,** 290-301

251. Miller, S., Tavshanjian, B., Oleksy, A., Perisic, O., Houseman, B.T., Shokat, K.M., and Williams, R.L. (2010) Shaping development of autophagy inhibitors with the structure of the lipid kinase Vps34. *Science.* **327,** 1638-1642

252. Wu, Y.C., Wu, W.K., Li, Y., Yu, L., Li, Z.J., Wong, C.C., Li, H.T., Sung, J.J., and Cho, C.H. (2009) Inhibition of macroautophagy by bafilomycin A1 lowers proliferation and induces apoptosis in colon cancer cells. *Biochem.Biophys.Res.Commun.* **382,** 451-456

253. De Palma, C., Morisi, F., Cheli, S., Pambianco, S., Cappello, V., Vezzoli, M., Rovere-Querini, P., Moggio, M., Ripolone, M., Francolini, M., Sandri, M., and Clementi, E. (2012) Autophagy as a new therapeutic target in Duchenne muscular dystrophy. *Cell.Death Dis.* **3,** e418

254. Galluzzi, L., Aaronson, S.A., Abrams, J., Alnemri, E.S., Andrews, D.W., Baehrecke, E.H., Bazan, N.G., Blagosklonny, M.V., Blomgren, K., Borner, C., Bredesen, D.E., Brenner, C., Castedo, M., Cidlowski, J.A., Ciechanover, A., Cohen, G.M., De Laurenzi, V., De Maria, R., Deshmukh, M., Dynlacht, B.D., El-Deiry, W.S., Flavell, R.A., Fulda, S., Garrido, C., Golstein, P., Gougeon, M.L., Green, D.R., Gronemeyer, H., Hajnoczky, G., Hardwick, J.M., Hengartner, M.O., Ichijo, H., Jaattela, M., Kepp, O., Kimchi, A., Klionsky, D.J., Knight, R.A., Kornbluth, S., Kumar, S., Levine, B., Lipton, S.A., Lugli, E., Madeo, F., Malomi, W., Marine, J.C., Martin, S.J., Medema, J.P., Mehlen, P., Melino, G., Moll, U.M., Morselli, E., Nagata, S., Nicholson, D.W., Nicotera, P., Nunez, G., Oren, M., Penninger, J., Pervaiz, S., Peter, M.E., Piacentini, M., Prehn, J.H., Puthalakath, H., Rabinovich, G.A., Rizzuto, R., Rodrigues, C.M., Rubinsztein, D.C., Rudel, T., Scorrano, L., Simon, H.U., Steller, H., Tschopp, J., Tsujimoto, Y., Vandenabeele, P., Vitale, I., Vousden, K.H., Youle, R.J., Yuan, J., Zhivotovsky, B., and Kroemer, G. (2009) Guidelines for the use and interpretation of assays for monitoring cell death in higher eukaryotes. *Cell Death Differ.* **16,** 1093-1107

255. Degtyarev, M., Reichelt, M., and Lin, K. (2014) Novel quantitative autophagy analysis by organelle flow cytometry after cell sonication. *PLoS One.* **9,** e87707

256. Yang, D.M., and Chiang, A.S. (1997) Formation of a whorl-like autophagosome by Golgi apparatus engulfing a ribosome-containing vacuole in corpora allata of the cockroach Diploptera punctata. *Cell Tissue Res.* **287,** 385-391

257. Gonzalez-Polo, R.A., Boya, P., Pauleau, A.L., Jalil, A., Larochette, N., Souquere, S., Eskelinen, E.L., Pierron, G., Saftig, P., and Kroemer, G. (2005) The apoptosis/autophagy paradox: autophagic vacuolization before apoptotic death. *J.Cell.Sci.* **118,** 3091-3102

258. Gama, V., Swahari, V., Schafer, J., Kole, A.J., Evans, A., Huang, Y., Cliffe, A., Golitz, B., Sciaky, N., Pei, X.H., Xiong, Y., and Deshmukh, M. (2014) The E3 ligase PARC mediates the degradation of cytosolic cytochrome c to promote survival in neurons and cancer cells. *Sci.Signal.* **7,** ra67

259. Taylor, R.C., Cullen, S.P., and Martin, S.J. (2008) Apoptosis: controlled demolition at the cellular level. *Nat.Rev.Mol.Cell Biol.* **9,** 231-241

260. Codogno, P., Mehrpour, M., and Proikas-Cezanne, T. (2011) Canonical and non-canonical autophagy: variations on a common theme of self-eating?. *Nat.Rev.Mol.Cell Biol.* **13,** 7-12

261. Nakagawa, I., Amano, A., Mizushima, N., Yamamoto, A., Yamaguchi, H., Kamimoto, T., Nara, A., Funao, J., Nakata, M., Tsuda, K., Hamada, S., and Yoshimori, T. (2004) Autophagy defends cells against invading group A Streptococcus. *Science.* **306,** 1037-1040

262. Boya, P., Gonzalez-Polo, R.A., Casares, N., Perfettini, J.L., Dessen, P., Larochette, N., Metivier, D., Meley, D., Souquere, S., Yoshimori, T., Pierron, G., Codogno, P., and Kroemer, G. (2005) Inhibition of macroautophagy triggers apoptosis. *Mol.Cell.Biol.* **25,** 1025-1040

263. Hou, H., Zhang, Y., Huang, Y., Yi, Q., Lv, L., Zhang, T., Chen, D., Hao, Q., and Shi, Q. (2012) Inhibitors of phosphatidylinositol 3'-kinases promote mitotic cell death in HeLa cells. *PLoS One.* **7,** e35665

264. Maskey, D., Yousefi, S., Schmid, I., Zlobec, I., Perren, A., Friis, R., and Simon, H.U. (2013) ATG5 is induced by DNA-damaging agents and promotes mitotic catastrophe independent of autophagy. *Nat.Commun.* **4,** 2130

265. Keil, E., Hocker, R., Schuster, M., Essmann, F., Ueffing, N., Hoffman, B., Liebermann, D.A., Pfeffer, K., Schulze-Osthoff, K., and Schmitz, I. (2013) Phosphorylation of Atg5 by the Gadd45beta-MEKK4-p38 pathway inhibits autophagy. *Cell Death Differ.* **20,** 321-332

266. Dewaele, M., Maes, H., and Agostinis, P. (2010) ROS-mediated mechanisms of autophagy stimulation and their relevance in cancer therapy. *Autophagy.* **6,** 838-854

267. Gustafsson, K., Wang, X., Severa, D., Eriksson, M., Kimby, E., Merup, M., Christensson, B., Flygare, J., and Sander, B. (2008) Expression of cannabinoid receptors type 1 and type 2 in non-Hodgkin lymphoma: growth inhibition by receptor activation. *Int.J.Cancer.* **123,** 1025-1033

268. Hiebel, C., Kromm, T., Stark, M., and Behl, C. (2014) Cannabinoid receptor 1 modulates the autophagic flux independent of mTOR- and BECLIN1-complex. *J.Neurochem.* **131,** 484-497

269. Lazova, R., Camp, R.L., Klump, V., Siddiqui, S.F., Amaravadi, R.K., and Pawelek, J.M. (2012) Punctate LC3B expression is a common feature of solid tumors and associated with proliferation, metastasis, and poor outcome. *Clin.Cancer Res.* **18,** 370-379

270. Nencioni, A., Cea, M., Montecucco, F., Longo, V.D., Patrone, F., Carella, A.M., Holyoake, T.L., and Helgason, G.V. (2013) Autophagy in blood cancers: biological role and therapeutic implications. *Haematologica.* **98,** 1335-1343

271. Sakuma, Y., Matsukuma, S., Nakamura, Y., Yoshihara, M., Koizume, S., Sekiguchi, H., Saito, H., Nakayama, H., Kameda, Y., Yokose, T., Oguni, S., Niki, T., and Miyagi, Y. (2013) Enhanced autophagy is required for survival in EGFR-independent EGFR-mutant lung adenocarcinoma cells. *Lab.Invest.* **93,** 1137-1146

272. Amaravadi, R.K., Yu, D., Lum, J.J., Bui, T., Christophorou, M.A., Evan, G.I., Thomas-Tikhonenko, A., and Thompson, C.B. (2007) Autophagy inhibition enhances therapy-induced apoptosis in a Myc-induced model of lymphoma. *J.Clin.Invest.* **117,** 326-336

273. Schmukler, E., Grinboim, E., Schokoroy, S., Amir, A., Wolfson, E., Kloog, Y., and Pinkas-Kramarski, R. (2013) Ras inhibition enhances autophagy, which partially protects cells from death. *Oncotarget.* **4,** 142-152

274. Nagy, P., Varga, A., Pircs, K., Hegedus, K., and Juhasz, G. (2013) Myc-driven overgrowth requires unfolded protein response-mediated induction of autophagy and antioxidant responses in Drosophila melanogaster. *PLoS Genet.* **9,** e1003664

275. Wang, R., Dillon, C.P., Shi, L.Z., Milasta, S., Carter, R., Finkelstein, D., McCormick, L.L., Fitzgerald, P., Chi, H., Munger, J., and Green, D.R. (2011) The transcription factor Myc controls metabolic reprogramming upon T lymphocyte activation. *Immunity.* **35,** 871-882

276. Hu, Z.Y., Su, H.W., Li, S.L., and Cao, Z.J. (2013) Effect of parenteral administration of glutamine on autophagy of liver cell and immune responses in weaned calves. *J.Anim.Physiol.Anim.Nutr.(Berl).* **97,** 1007-1014

277. Hu, Z.Y., Li, S.L., and Cao, Z.J. (2012) Short communication: Glutamine increases autophagy of liver cells in weaned calves. *J.Dairy Sci.* **95,** 7336-7339

278. Lin, T.C., Chen, Y.R., Kensicki, E., Li, A.Y., Kong, M., Li, Y., Mohney, R.P., Shen, H.M., Stiles, B., Mizushima, N., Lin, L.I., and Ann, D.K. (2012) Autophagy: resetting glutamine-dependent metabolism and oxygen consumption. *Autophagy.* **8,** 1477-1493

279. Jardon, M.A., Sattha, B., Braasch, K., Leung, A.O., Cote, H.C., Butler, M., Gorski, S.M., and Piret, J.M. (2012) Inhibition of glutamine-dependent autophagy increases t-PA production in CHO cell fed-batch processes. *Biotechnol.Bioeng.* **109,** 1228-1238

280. Hansel, D.E., Platt, E., Orloff, M., Harwalker, J., Sethu, S., Hicks, J.L., De Marzo, A., Steinle, R.E., Hsi, E.D., Theodorescu, D., Ching, C.B., and Eng, C. (2010) Mammalian target of rapamycin (mTOR) regulates cellular proliferation and tumor growth in urothelial carcinoma. *Am.J.Pathol.* **176,** 3062-3072

281. Kuo, P.L., Hsu, Y.L., and Cho, C.Y. (2006) Plumbagin induces G2-M arrest and autophagy by inhibiting the AKT/mammalian target of rapamycin pathway in breast cancer cells. *Mol.Cancer.Ther.* **5,** 3209-3221

282. Kaneko, M., Nozawa, H., Hiyoshi, M., Tada, N., Murono, K., Nirei, T., Emoto, S., Kishikawa, J., Iida, Y., Sunami, E., Tsuno, N.H., Kitayama, J., Takahashi, K., and Watanabe, T. (2014) Temsirolimus and chloroquine cooperatively exhibit a potent antitumor effect against colorectal cancer cells. *J.Cancer Res.Clin.Oncol.* **140,** 769-781

283. Ouyang, D.Y., Zeng, L.H., Pan, H., Xu, L.H., Wang, Y., Liu, K.P., and He, X.H. (2013) Piperine inhibits the proliferation of human prostate cancer cells via induction of cell cycle arrest and autophagy. *Food Chem.Toxicol.* **60,** 424-430

284. Iwai-Kanai, E., Yuan, H., Huang, C., Sayen, M.R., Perry-Garza, C.N., Kim, L., and Gottlieb, R.A. (2008) A method to measure cardiac autophagic flux in vivo. *Autophagy.* **4,** 322-329

285. DeVorkin, L., Go, N.E., Hou, Y.C., Moradian, A., Morin, G.B., and Gorski, S.M. (2014) The Drosophila effector caspase Dcp-1 regulates mitochondrial dynamics and autophagic flux via SesB. *J.Cell Biol.* **205,** 477-492